

# Development of Characterization Approaches and a Management Tool for the Groundwater-Surface Water System in the Vicinity of Sutherland Reservoir and Gerald Gentlemen Station Lincoln County, Nebraska

Clint P. Carney  
Eileen P. Poeter

**October 2009**

**Completion Report No. 212**



**Colorado Water Institute**

**Colorado  
State**  
University

## Acknowledgements

This work was supported by the National Institutes for Water Resources (NIWR) through the Colorado Water Institute (CWI), the Nebraska Public Power District (NPPD), and the International Ground Water Modeling Center (IGWMC). Additional supporting data was provided by the U.S. Geological Survey (USGS), the Nebraska Department of Natural Resources (NDNR), and the Twin Platte Natural Resources District (TPNRD). This report benefitted from insightful discussions with and careful review by Dr. Peter McMahon of the USGS. The authors would also like to acknowledge current and former Colorado School of Mines graduate students Sophia Seo, Michael LeFrancois, Kimberly McDugle, JoAnne Huie, and Elizabeth Conover for their assistance with setup and operation of the numerous clusters of personal computers utilized for calibration of the models developed in this study via parallel processing. Also, the authors thank Colorado School of Mines graduate students Kyle Richards and Erich Heydweiller for their assistance with dataset preparation and stratigraphic analysis for development of model layers used in the various conceptualizations of the subsurface at the study site.

This report was financed in part by the U.S. Department of the Interior, Geological Survey, through the Colorado Water Institute. The views and conclusions contained in this document are those of the authors and should not be interpreted as necessarily representing the official policies, either expressed or implied, of the U.S. Government.

Additional copies of this report can be obtained from the Colorado Water Institute, E102 Engineering Building, Colorado State University, Fort Collins, CO 80523-1033 970-491-6308 or email: [cwi@colostate.edu](mailto:cwi@colostate.edu), or downloaded as a PDF file from <http://www.cwi.colostate.edu>.

Colorado State University is an equal opportunity/affirmative action employer and complies with all federal and Colorado laws, regulations, and executive orders regarding affirmative action requirements in all programs. The Office of Equal Opportunity and Diversity is located in 101 Student Services. To assist Colorado State University in meeting its affirmative action responsibilities, ethnic minorities, women and other protected class members are encouraged to apply and to so identify themselves.

**Development of  
Characterization Approaches and a Management Tool  
for the  
Groundwater-Surface Water System  
in the Vicinity of  
Sutherland Reservoir and Gerald Gentlemen Station  
Lincoln County, Nebraska**

By

Clint P. Carney

Eileen P. Poeter

International Groundwater Modeling Center

Colorado School of Mines

COMPLETION REPORT

# Abstract

As competing uses of fresh water continue to stress both quantity and quality of the resource worldwide, water management has become increasingly complex and sometimes contentious for resource managers. This complexity in the High Plains region of the United States has been compounded recently by population growth and multi-year drought. Considering the stresses on already limited water resources, policy makers need the best management tools for prediction of future conditions given alternative management scenarios. Recent advancements in modeling of groundwater include automated (inverse) calibration and multi-model averaging techniques that allow for development of optimized models that provide statistical evaluation of certainty associated with predicted impacts.

The strategy of inversely calibrating multiple conceptual models and selecting the top models with multi-model ranking techniques for predictive analyses was applied to a site in western Nebraska where competing uses (power generation, irrigated agriculture, and critical in-stream flows in the Platte River) rely on the High Plains aquifer. Various representations of the High Plains aquifer were developed, ranging from simplistic (2-D) to complex (multi-layered). Variations emphasized differences in aquifer configuration and recharge with the intent of determining the appropriate level of model complexity for groundwater management. Hydrologic features and stresses in the study area include the 3,000-acre Sutherland Reservoir, a water supply canal, the South Platte River, and high capacity industrial and irrigation wells. These features provided abundant observations (2,574) for calibration of the models. In addition, geochemistry of the groundwater was used to derive flowpath-age observations to improve model calibration.

Automated calibration was performed with UCODE\_2005 to estimate upwards of 15 parameters representing characteristics such as recharge, hydraulic conductivity, and conductance terms for surface water features. Multi-model analysis of 42 different representations of the flow system indicated conceptual model 23 as the top model in the suite of conceptualizations with a probability of 0.99. Model 23 utilized a regional representation of hydraulic conductivity based on the USGS High Plains RASA study, and topographically based recharge zones. Output from UCODE\_2005 indicated the influence of each observation on the calibration. For model 23, a drain flow observation exerted the most influence on calibration. A flowpath-age observation was one of the 30 most influential observations and was important in estimating three parameters for model 23. The top three models were used to provide an example predictive simulation of a possible scenario for pumping the power plant wellfield. Drawdowns were on the order of over 25 feet near the well field and decreased to 6.6 feet at a distance of 2 miles from the wellfield boundary, while depletion of flow in the South Platte River was on the order of 0.5 cubic feet per second. Confidence intervals on drawdowns and reductions of flow were narrow. Predictions and associated confidence intervals from model 23 were nearly identical to the model averaged predictions of the top 3 models. The results indicate that the most complex models of a system do not necessarily make the best models, and that using a variety of observation types is important in the estimation of model parameters and model predictions.

## Keywords

Calibration, High Plains aquifer, Platte River, multi-model analysis, UCODE\_2005, Sutherland Reservoir, predictions, confidence intervals, parsimony, MMA



# Contents

INTRODUCTION	1
MODELING STRATEGY	1
Inverse Modeling	1
Multiple Conceptual Model Strategy	1
FIELD SITE FOR INVESTIGATION	2
PREVIOUS RELEVANT WORK IN THE STUDY AREA	3
STUDY SITE DESCRIPTION	5
Physiography	5
Climate	5
Land and Water Use	5
Agriculture	6
Industrial Water Use	8
Municipal Water Use	9
GEOLOGIC SETTING	9
HYDROLOGY	9
Surface Water	10
Groundwater	11
DATA ACQUISITION AND ANALYSIS	14
Geologic Data	14
Interpretation of Geologic Information	14
Aquifer Characteristics in the Near Site Area	19
Hydrologic Data	24
Surface Water	24
Groundwater	24
Geochemistry	25
Climate Data	25
Land Use Influence on Recharge	25
USE OF DIVERSE DATA AS OBSERVATIONS	26
Groundwater Levels	27
Surface Water Flows	27
Reservoir Stages	29
Water Age	29
MULTIPLE CONCEPTUAL MODEL DEVELOPMENT	31
Concepts of Modeling Natural Systems	31
Conceptual Model Strategy	32
Initial Site Conceptualization	33
Groundwater Movement	34
Recharge	37
Uniform Recharge	38

Topographic Regions of Recharge	38
Land-Use Based Recharge	40
Soil-Based Recharge	41
Combined Land-Use / Topographic Regions Recharge	42
Hydrostratigraphy	42
Outer Study Area Transmissivity Zones	42
Near-Site Transmissivity Zones	43
Initial Aquifer Transmissivities	44
Conceptual Models of the Groundwater Flow System	45
<b>NUMERICAL MODEL OF STUDY AREA</b>	<b>51</b>
Numerical Modeling Concepts	51
Model Construction	51
Software	51
Grid Definition	52
Timeframe of Simulations	52
Boundary Conditions as defined with MODFLOW Packages	55
Surface Water Stresses	56
Wells	56
Layer Representation	57
Sequence of Model Execution and Travel Time Simulation	58
<b>CALIBRATION AND QUALITY OF CALIBRATION AND PREDICTION</b>	<b>58</b>
Calibration Methodology	58
Observation Weighting	60
Confidence Intervals on Optimal Parameters	61
Parameter Correlation	62
Alternative Approach to Minimizing Objective Function	62
Prediction	63
Quality of Calibration	63
<b>MULTI-MODEL ANALYSIS</b>	<b>64</b>
<b>MULTI-MODEL ANALYSIS RESULTS</b>	<b>65</b>
<b>CALIBRATION RESULTS</b>	<b>66</b>
Model Fit Information	66
Parameter Correlation	67
Weighted Residuals and Simulated Values	67
Observed and Simulated Values	67
Evaluation of the Statistical Distribution of Residuals	67
Optimized Parameter Information	76
Composite Scaled Sensitivities	79
Analysis of Influence of Individual Observations on the Regression	81
Spatial Trends in Weighted Residuals	84
Discussion of Calibration Results	84
<b>PREDICTIONS</b>	<b>85</b>
Prediction Scenario	86
Prediction Modeling Tools	87
Prediction Analysis Results	87

Important Information for Predictions	90
DISCUSSION	91
Further Discussion of Model Calibrations	91
Use of Unique Observation Data	92
Sequence of Modeling Process	92
CONCLUSIONS	93
Multi-Model Analysis	93
Observations	94
Representation of the HPA	94
Geochemical Analysis	95
Further Exploration and Recommendations	95
REFERENCES	97
APPENDIX A – Flow Data	103
APPENDIX B – Precipitation Records	109
APPENDIX C – Observation Weights	113
APPENDIX D – Well Construction and Test Data	120
APPENDIX E – Hydrographs	125
APPENDIX F – Borehole Data	127
APPENDIX G – Optimized Model Rankings	131

# Figures

Figure 1	Platte River Basin in Wyoming, Colorado, and Nebraska	3
Figure 2	Map of study area and location within Nebraska	4
Figure 3	Contours of average annual precipitation within the model area	6
Figure 4	Satellite imagery of study area land use in 1997 and 2005	7
Figure 5	Location of irrigation wells in the study area	8
Figure 6	Map of study area showing the saturated thickness of the HPA	11
Figure 7	Generalized raster map of the study area showing depth to water table	12
Figure 8	1995 regional water table elevation contours	13
Figure 9	Fall 2004 water table elevation contours in the near-site area	13
Figure 10	An example of the translation of raw field descriptions of borehole cuttings to keyword descriptors for the test borehole at OW-40	17
Figure 11	An example of the translation of raw field descriptions of borehole cuttings to keyword descriptors for the test borehole at OW-19	18
Figure 12	3-D fence diagram of the near-site area hydrostratigraphy based on the five defined hydrostratigraphic zones from the borehole log keyword descriptors	19
Figure 13	GGs well field showing locations of individually numbered wells	21
Figure 14	Continuously recorded well hydrographs Obs 4, Obs6, and Obs 8	22
Figure 15	Map of study area showing outer-area and near-site locations of groundwater level observations	23
Figure 16	Map of continuous recording water level well nests and geochemical monitoring well nests in the near-site area of the model domain	23
Figure 17	Map of study area showing locations of drain and river flow observations	28
Figure 18	Three graphs showing a linear model fit, a complex model, and the tradeoff between the accuracy in predictive capability and complexity in the model	32
Figure 19	Example of results from a multi-model comparison of simulations using different numbers of hydraulic conductivity parameters to represent an alluvial aquifer setting in Switzerland	33
Figure 20	A graphic conceptualization of major influences on the movement of water through the GGS-SR study area	35
Figure 21	North-south cross-section of the study area indicating general direction of lake seepage and groundwater flow near Sutherland Reservoir	36
Figure 22	Four of the five recharge conceptualizations of the study area	39
Figure 23	Hydraulic conductivity distribution from the High Plains RASA	43
Figure 24	Unique hydraulic conductivity zones of near-site area based on thicknesses of continuous Quaternary-age coarse deposits	44
Figure 25	Unique hydraulic conductivity zones of near-site area based on thicknesses of continuous coarse deposits in the upper Ogallala Group	44
Figure 26	Map of hydraulic conductivity values at all irrigation well and GGS well field test locations	46
Figure 27	Block diagrams and descriptions of the alternative hydrostratigraphic hypotheses considered in the multiple conceptual models of the High Plains aquifer in the study area	47-49

Figure 28	Finite-difference model grid of the GGS-SR study area	52
Figure 29	Cross-section of the MODFLOW 4-layer model grid and the TIN model used to define Sutherland Reservoir	53
Figure 30	Average daily crop evapotranspiration for the summer growing season in Nebraska	57
Figure 31	Weighted residuals versus simulated equivalents	68-70
Figure 32	Observed versus simulated values	71-73
Figure 33	Weighted observed vs. weighted simulated values	74
Figure 34	Normal probability graphs for three highest ranked models	75
Figure 35	Optimal parameter values and confidence intervals	77
Figure 36	Composite scaled sensitivities	80
Figure 37	Cook's D values	82
Figure 38	DFBETAS for travel-time observations	83
Figure 39	Spatial distribution of relative magnitude of weighted residuals	84
Figure 40	Locations of groundwater level prediction points	86
Figure 41	Model averaged predictions and their confidence intervals along with individual predictions for the 2nd and 3rd ranked models	89
Figure 42	Difference in water level declines from GGS well field pumping	90
Figure 43	Results from the prediction scaled sensitivity analysis of CM-23	91

## Tables

Table 1	Summary of observation information used in the calibration of numerical models in the study area	31
Table 2	List of 42 conceptual models for the study area evaluated for the multi-model analysis and ranking	50
Table 3	Timeframe of transient simulation	54-55
Table 4	Ranking of the top ten GGS-SR models	65
Table 5	The CEV and standard error values for CM-23, CM25, and CM-18	66
Table 6	Optimal parameter information from the top 3 conceptual models	76
Table 7	Model-averaged predictions of differences in groundwater level declines with and without the 5-year pumping scenario	88

## Images

Image 1	View of Gerald Gentleman Station	3
Image 2	Outcrop of Ogallala Group near Lake McConaughy	10
Image 3	Zoomed-in view of Ogallala Group outcrop	10
Image 4	Drill site of geochemical monitoring well nest 6 east of GGS	15
Image 5	Drill cutting samples collected from the deep well at geochemical monitoring well nest 5	15
Image 6	A view of GGS well field production well 35 located southwest of Sutherland Reservoir	20
Image 7	Flow measurement location of Fremont Slough	28
Image 8	Geochemistry monitoring well nest 3	30
Image 9	Aerial view of geochemistry monitoring well locations in the near-site area	30
Image 10	Aerial view of the sand dune area south of Sutherland Reservoir	41

# Abbreviation, Acronyms, Unit, and Conversion Guide

## Abbreviations/Acronyms

CALMIT- Center of Advanced Land Management Information Technology

COHYST- Platte River Cooperative Hydrology Study

GGS- Gerald Gentleman Station

GGS-SR – Gerald Gentleman Station-Sutherland Reservoir (study area)

GIS- Geographic information system

HPA- High Plains aquifer

Kh- Hydraulic conductivity in the horizontal orientation

MODFLOW- MODFLOW 2000

MMA- Multi-model analysis

NDNR- Nebraska Department of Natural Resources

NPPD- Nebraska Public Power District

NRD- Natural Resources District

RASA- Regional Aquifer Systems Analysis

TPNRD- Twin Platte Natural Resources District

UNL-CSD- University of Nebraska-Lincoln Conservation and Survey Division

USGS – United States Geological Survey

## Units and Rates

ft	feet
----	------

mi	mile
----	------

in	inch
----	------

yr	year
----	------

d	day
---	-----

ac-ft	acre-feet
-------	-----------

ft <sup>3</sup> /s	cubic-feet per second
--------------------	-----------------------

ft <sup>3</sup> /d	cubic-feet per day
--------------------	--------------------

## **Common Conversions**

1 cubic foot = 7.5 gallons

1 acre-foot = 43,560 cubic feet (the amount of water at a depth of 1 foot covering a single acre)

1 cubic foot per second = 449 gallons per minute

1 square mile = 640 acres

## **Other Comments**

**Sea level:** In this report, “sea level” refers to the National Geodetic Vertical Datum of 1983 – a geodetic datum derived from a general adjustment of the first-order level nets of both the United States and Canada, formerly call Sea Level Datum of 1929.

**Elevation:** In this report, “elevation” refers to distance above sea level in feet.





# Introduction

As competing uses of fresh water continue to stress both quantity and quality of the resource worldwide, allocation and supply management has become increasingly more complex and sometimes contentious for planners and managers ranging from the local to international scale. With these issues facing society, it is of utmost importance for today's policy makers and resource managers to have the best management tools at their disposal for analysis and prediction of future conditions given alternative management scenarios. In terms of groundwater models, advancements in recent years with automated (inverse) calibration and multi-model averaging techniques have allowed for the development of optimized models that provide statistical evaluation of certainty on parameters and predictions. In addition to these advancements the strategy of conceptualizing groundwater flow systems with multiple representations that can vary from simple to complex (parsimony) has recently gained traction in the field of groundwater modeling. Models developed through this process will result in more powerful tools for managers to make sound decisions involving a limited and vital resource.

This report discusses the methodologies and findings of an application of automated calibration techniques using multiple conceptual models to a field site in west-central Nebraska, USA. The objective of this study was to develop a groundwater model with predictive capability for use as a management tool in an area where the competing uses of power generation, irrigated agriculture, and maintenance of critical in-stream flows for habitat protection all rely on the same sources of groundwater and surface water supply. In addition to developing this management tool, other objectives of the study include:

- to examine the importance of diverse types of observations for calibration of the groundwater models;
- with inverse modeling and model ranking, to provide insight into the issue of simple vs. complex models for representing hydrogeologic conditions in heterogeneous and stratified geologic units like those present High Plains aquifer; and
- to provide insight into the influence of alternative recharge conceptualizations on the magnitudes of recharge rates given various land use and topographic patterns.

## Modeling Strategy

A brief description of the inverse modeling process and multiple conceptual model strategy facilitates understanding of the study presented in this report.

### ***Inverse Modeling***

In recent years, inverse modeling has become a more utilized approach for calibration of groundwater models (Tiedeman and others, 1998, D'Agnese and others, 2002, Hunt and others, 2005). Inverse modeling provides many benefits that are unattainable with trial-and-error calibration. The primary advantage of using inverse modeling is the ability to find optimal model parameter values that result in the best fit of observed and simulated water levels and flows. In addition to providing the best statistical fit between observed and simulated values, the process of inverse modeling can provide the user with statistics on the quality of the calibration, assessment of data shortcomings, and confidence intervals in both parameters and predictions. This information is not generated during trial-and-error calibration (Poeter and Hill, 1997).

### ***Multiple Conceptual Model Strategy***

Sparse subsurface data cause hydrologists to be uncertain of the nature of groundwater system structure and components. Consequently it is best, although not always customary, practice to consider multiple representations of the structure of a groundwater system before making predictions of system behavior. To the extent possible, items constituting differences in model structure should be automatically adjusted in the calibration process, but this is difficult to achieve, thus the need to consider a set of alternative models to some extent. The adjustable parameters of each alternative model must be calibrated (i.e. parameter values adjusted to obtain the best fit to the field data, e.g. using nonlinear

regression) before models can be compared (Poeter and Hill 1997). Fortunately, the advent of high speed computing and robust inversion algorithms makes calibration of multiple models feasible.

Often, prediction uncertainty is larger across the range of alternative model structures than arises from the misfit and insensitivity of any one optimized model, even to the extent that confidence intervals on predictions from some of the models may not include the values predicted by others. This issue is addressed by weighting the alternative models and calculating model-averaged predictions and intervals (Poeter and Anderson, 2005). If the model averaged predictions are so uncertain that a reasonable decision is untenable, then additional data should be collected to better constrain the range of reasonable models. Hence the iterative process of model development and data collection.

## **Field Site for Investigation**

The site considered in this study (Image 1) is located within the Platte River basin (Figure 1) in western Lincoln County, Nebraska, (Figure 2) approximately 25 mi. west of the city of North Platte. Near Sutherland is Gerald Gentleman Station (GGS), a 1.4 giga-watt coal-fired power plant that supplies much of the state of Nebraska's electricity. Beginning operations in 1979, GGS utilizes water from nearby Sutherland Reservoir for cooling needs. Sutherland Reservoir is an off-channel reservoir that is supplied with water primarily from the North Platte River (via the Sutherland Supply canal). When flows are conducive for diversion, water is also delivered to the reservoir via Korty Canal from the South Platte River.

The drought afflicting the High Plains and the central Rocky Mountains that began in 2000-2001 has had a profound effect on surface water supplies in the Platte River Basin in Nebraska, Wyoming, and Colorado (Figure 2). Of particular interest to this study was the current shortage of water in Lake McConaughy (Nebraska) and upstream reservoirs on the North Platte River in Wyoming, which are the primary source of inflow to Sutherland Reservoir. By December 2004, nearly every major reservoir in the North Platte River Basin contained less than 30 percent of its capacity for storage of water (Ed Kouma, USBR, personal communication). As of early 2008, the three largest reservoirs of the North Platte River basin in Wyoming averaged 29% of capacity, and Lake McConaughy in Nebraska was at 35% of capacity (accessed online at [www.usbr.gov](http://www.usbr.gov) and [www.cnppid.com](http://www.cnppid.com)). By 2005, the water supply forecast indicated that surface water supplies available to maintain Sutherland Reservoir elevations necessary for operations at GGS would be insufficient by the summer of 2006 barring significant cutbacks in water released from Lake McConaughy for irrigation needs.

To maintain water levels in Sutherland reservoir above the level of intake for the power plant in times of drought, Nebraska Public Power District (NPPD) installed 38 high capacity wells on the GGS property (Figure 2) in the spring of 2004. These wells extract water from the High Plains aquifer and pipe it to Sutherland Reservoir. With irrigation water cutbacks imposed by NPPD and other water holders in the Platte basin, withdrawals from the aquifer for maintenance of the water level in Sutherland Reservoir had not been made by 2008. However, due to the drought resulting in historically low water levels in Lake McConaughy, water temperatures entering the power plant were warmer than under normal conditions, thus causing water temperatures leaving the power plant to be warmer than Nebraska Department of Environmental Quality (NDEQ) standards. This secondary implication of the drought has forced NPPD engineers at GGS to utilize the well field to dilute high temperature water leaving the plant with colder groundwater to meet NDEQ temperature limits. During the summers of 2005, 2006, and 2007; 4,430, 3,450, and 8,194 acre-feet were pumped from the aquifer, respectively. Pumping rates for the wells range from 1,200 to 2,900 gallons per minute. Even if reservoir levels remain sufficiently above the power plant intakes, the same pumping patterns for cooling water will likely occur during future summers until water levels recover to long-term average levels in Lake McConaughy.

With the addition of the NPPD well field to the area surrounding Sutherland Reservoir and GGS, a new stress was created on an aquifer system already highly utilized for irrigation needs. Pre-existing irrigation wells were operating adjacent to and even within NPPD property prior to the well field construction, thus creating a sense of urgency for the development of a reliable management tool to assist NPPD in maintaining and optimizing the regional water levels without adversely affecting neighboring users.



IMAGE 1. View of Gerald Gentleman Station from across the cooling pond on the southeast shore of Sutherland Reservoir.

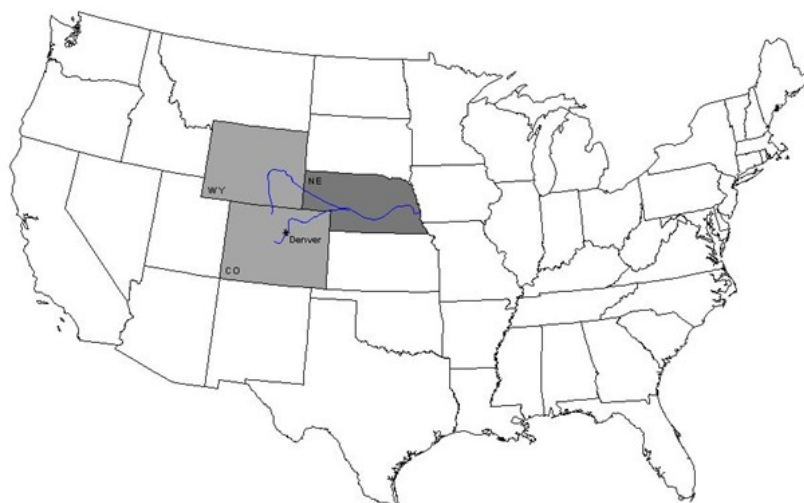


FIGURE 1. Platte River Basin in Wyoming, Colorado, and Nebraska.

## Previous Relevant Work in the Study Area

The earliest studies of groundwater in west-central Nebraska were by Darton (1905). Not long after Darton's work, Condra (1907) investigated groundwater conditions in the Republican River valley. Other studies in the first half of the 20<sup>th</sup> Century within or near the study area include work by Lugn and Wenzel (1938) that focused on geology and groundwater resources of south-central Nebraska. Wenzel and Waite (1941) investigated the groundwater conditions of Keith County (Figure 2).

In the second half of the 20<sup>th</sup> century, a large number of both regional and local investigations were conducted in the region, many of which included numerical simulations of groundwater conditions to address the impacts of the rapidly increasing use of groundwater for irrigation. The first large-scale study of the region began with the Missouri River Basin Commission (1975). This was later followed by the Missouri Basin States Association (1982a and 1982b). A study of the entire High Plains aquifer was reported by Gutentag and others (1984) and Weeks and others (1988). Included in this investigation were

large-scale numerical simulations of the aquifer by Luckey and others (1986, 1988). Pettijohn (1983a and 1983b) published more detailed reports on the Nebraska portion of this study of the High Plains aquifer.

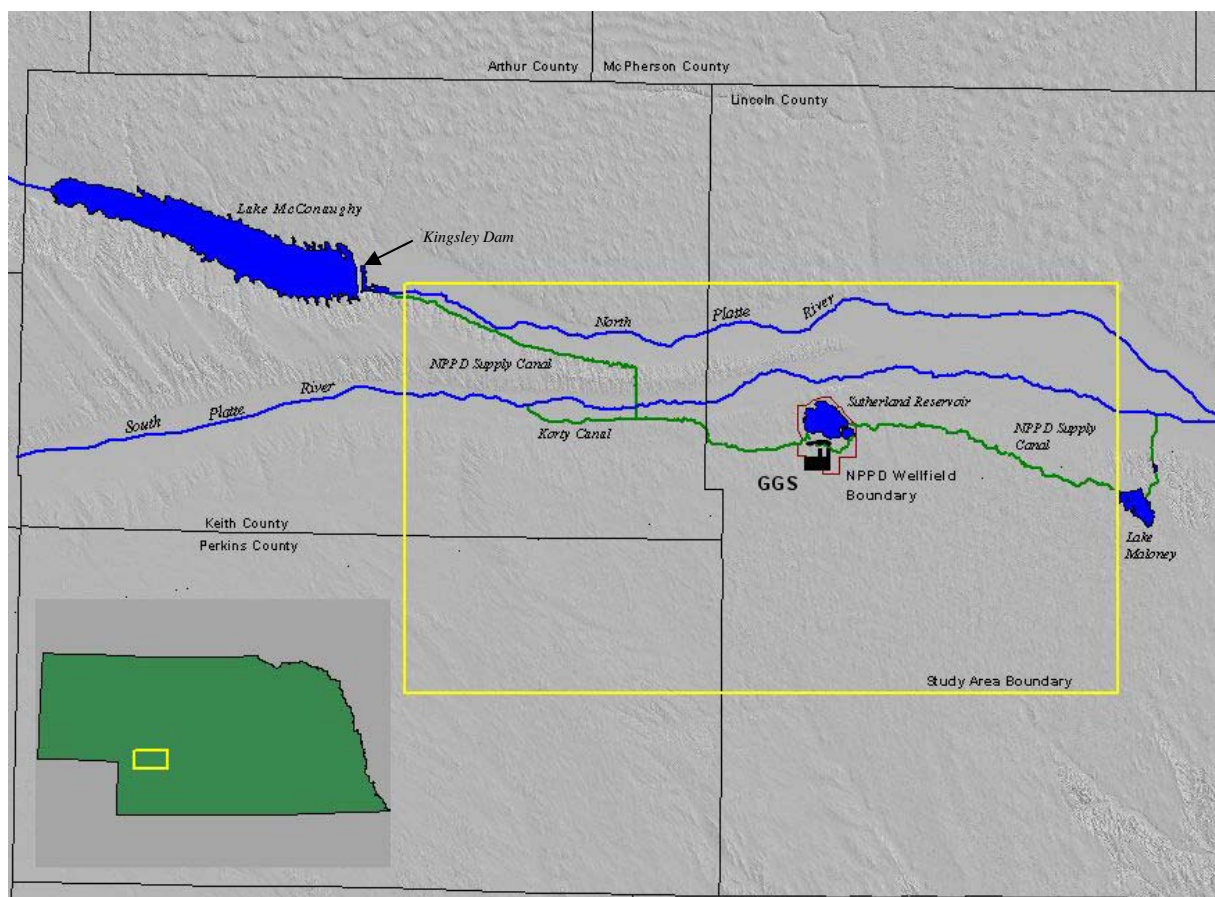


FIGURE 2. Map of study area and location within Nebraska.

On a smaller scale, several studies since 1950 have improved the understanding of the hydrologic system. Bjorklund and Brown (1957) described the hydrogeologic conditions of the South Platte River valley. Lappala (1978) completed a detailed hydrogeologic investigation (with a digital simulation) of Chase and Perkins Counties. Peckenpaugh and others (1995) produced numerical simulations of the same area. Goeke and others (1992) investigated the hydrogeology and surface water conditions of much of the area south of the Platte River system, including most of the GGS study area.

Starting in the late 1990s, the Platte River Cooperative Hydrology Study (COHYST) developed a series of regional groundwater models from the Wyoming-Nebraska border to Columbus, NE, covering an area of over 30,000 square miles (COHYST, 2004). These models were developed initially for assessing and managing impacts of groundwater irrigation on flows in the Platte River system. Data from these models were used to develop an initial local scale model of the GGS well field. Within the same timeframe as the COHYST project, another large scale groundwater modeling project of the Republican River basin was undertaken to address water use issues between the states of Colorado, Nebraska, and Wyoming (Republican River Compact Administration, 2003). The extent of this study area encompasses all of the GGS model area south of the South Platte River.

Some studies attempted to estimate groundwater recharge. Dugan and Zelt (2000) conducted work on soil water conditions of the entire Great Plains area. McMahon and others (2006) examined timing of

flow in thick unsaturated zones on the High Plains aquifer. Test site locations for their study were located just southwest of the GGS model area.

## **Study Site Description**

The GGS model area covers nearly 1,000 square miles in parts of Lincoln, Perkins, and Keith Counties, Nebraska. The GGS well field and Sutherland Reservoir are located slightly north and east of the center of the model area. The population is relatively small and agriculture dominates both the landscape and livelihood of the area. The largest population center is the city of North Platte (24,000) which borders the eastern side of the model area. The remainder of the model area is rural setting with a few small towns and villages.

As a result of the GGS well field installation project, which included test-hole drilling, well performance testing, and installation of nearby monitoring wells, a great concentration of geologic borehole information and groundwater level measurements exist in close proximity to the GGS well field and Sutherland Reservoir. Such information is less abundant in the rest of the model area. Henceforth, in this report the area within 3 miles of the NPPD property boundary (Figure 2) will be called the “near-site” area, and locations beyond this area will be referred to as the “outer study area.”

### ***Physiography***

The model area is located in the northern High Plains and ranges in elevation from approximately 3,400 feet on the west to 3,000 feet above sea level on the east. Most of the model area consists of flat to rolling plains with the exception of the northern third of the model where the North Platte and South Platte River valleys parallel from west to east and eventually merge just east of the town of Sutherland. In the uplands (the area south of the river valleys), gently rolling sand dunes stabilized by grasses are prominent in the southeast quarter of the area, whereas flatter, loess-mantled plains are common in the southwest portion of the model area. From a land use standpoint, the sandy hills contain more areas of open rangeland used for grazing, whereas the southwest part of the study area is predominately used for both irrigated and dryland agriculture. The flatlands of the broad river valleys contain agriculture irrigated by a mixture of surface and groundwater sources, dryland agriculture, and large areas of riparian vegetation.

### ***Climate***

Middle-latitude dry continental climate conditions persist in the study area. This type of climate is characterized by low humidity, high evapotranspiration, abundant sunshine, moderate precipitation, and persistent winds (Gutentag and others, 1984). Average annual precipitation ranges from 18 in/yr on the western boundary to over 20 in/yr in the southeastern corner of the study area (High Plains Regional Climate Center, 2008), Figure 3. Nearly seventy percent of precipitation falls in the active crop-growing months of April through August. Lake evaporation in the area is approximately 47 in/yr (Nebraska Dept. of Environmental Quality, 1981). Average daily high temperature near the center of the study area is 61.7 °F and average daily low temperature is 36.3 °F degrees ([www.worldclimate.com](http://www.worldclimate.com)). The drought afflicting the region since 2000 is quite evident when looking at precipitation records over the first decade of the 21<sup>st</sup> century. For example, at Kingsley Dam, where long-term average precipitation is slightly less than 18.5 in/yr, 6 of the 7 years between 2000 and 2006 experienced below average precipitation, with an average deviation of 3.3 in/yr for the years of less than average precipitation, with the largest difference occurring in 2003 when only 12.6 inches fell at the measurement station.

### ***Land and Water Use***

The study area is located in a region that is heavily dependent on agriculture as its economic engine, despite receiving an average of less than 20 in/yr of precipitation, a rate that falls well short of the water needs for corn, the most prominent grain produced in the study area. The following sections provide a background on the agricultural and water-use trends in the study area.



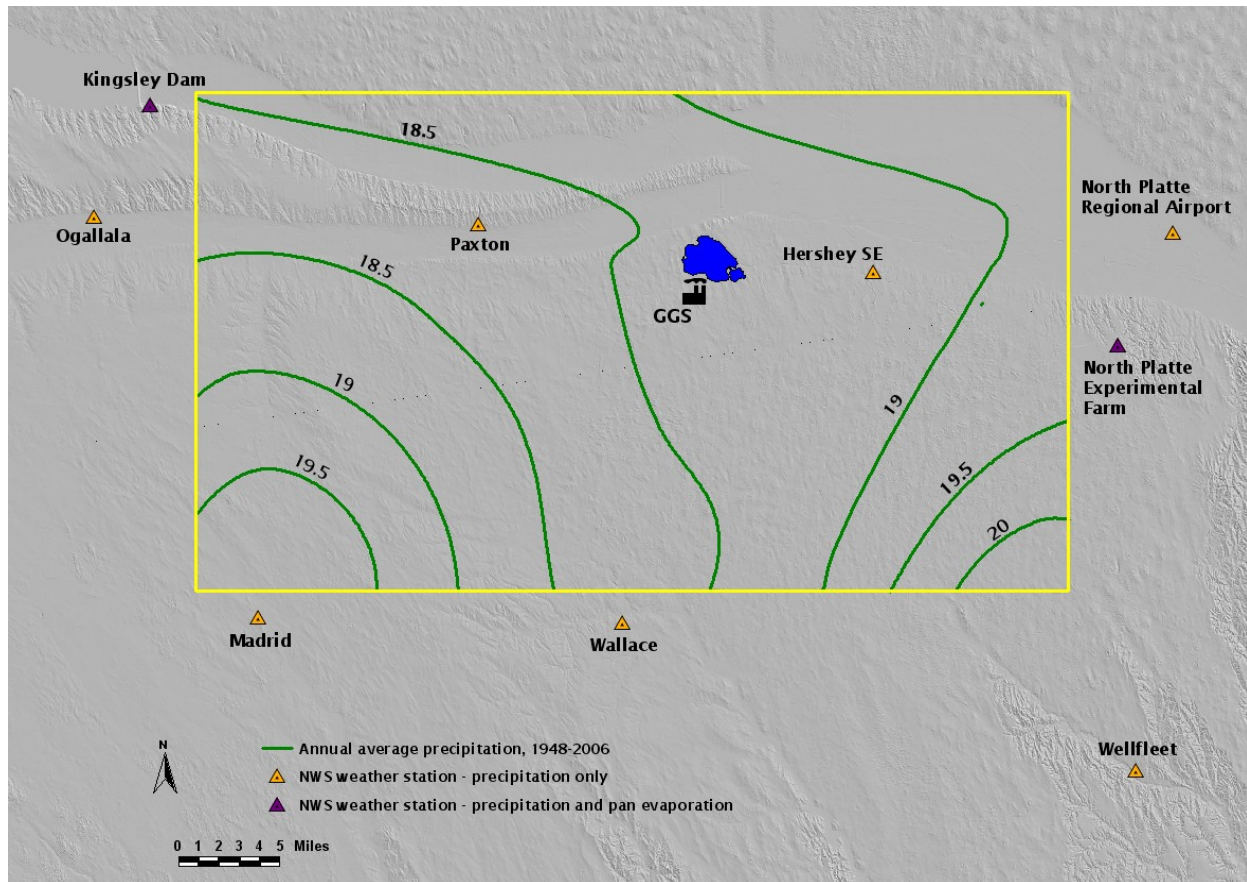


FIGURE 3. Contours of average annual precipitation within the model area (yellow boundary) and National Weather Service weather stations used for interpolating the rates of precipitation to model datasets. Contour interval = 0.5 in.

## Agriculture

As shown in Figure 4, the landscape of the study area is utilized for intensive irrigated and dryland cropping. In 2005, approximately 118,538 acres of center-pivot irrigated corn were planted in the study area, which is nearly 17 percent of the study area. The other major crops planted in 2005 were over 24,700 acres of soybeans, 7,947 acres of alfalfa, 3,060 acres of potatoes, and 3,670 acres of small grains. In total, over 22 percent of the total land in the study area was devoted to center-pivot, groundwater-based irrigation in 2005. The remainder of agricultural lands consisted of dryland-farming for small grains and alfalfa or pasture land for grazing. The land use practices are typical of this area of Nebraska and the amount of irrigated acres and wells in the study area has been relatively stable over the last decade.

Grazing on rangeland is common in areas where soils or land slope make growing row crops unfeasible or uneconomical. In the area surrounding the Sutherland Reservoir and GGS, dark and bright green circles on the map indicate center-pivot plots for soybeans and corn, respectively. Wells that supply these fields with irrigation water tap into the aquifer in close proximity to the GGS well field wells. The irrigation in the eastern half of the study area between the two rivers is sourced by groundwater as well as surface water diverted from the North Platte River. This area is crossed by several canals, ditches, and laterals that have been operating since the start of the 20<sup>th</sup> century. Dryland cropping is more prevalent in the western half of the study area. Figure 5 shows the distribution and pumping capacity of irrigation wells across the study area. The southeast portion of the study area has the lowest concentration of wells because of the abundance of pasture land on the sand dunes. Although most irrigation wells are not screened throughout the entire saturated thickness of the aquifer, the map offers some evidence of the variable permeability of the High Plains aquifer. Small pockets of wells throughout the area have pumping



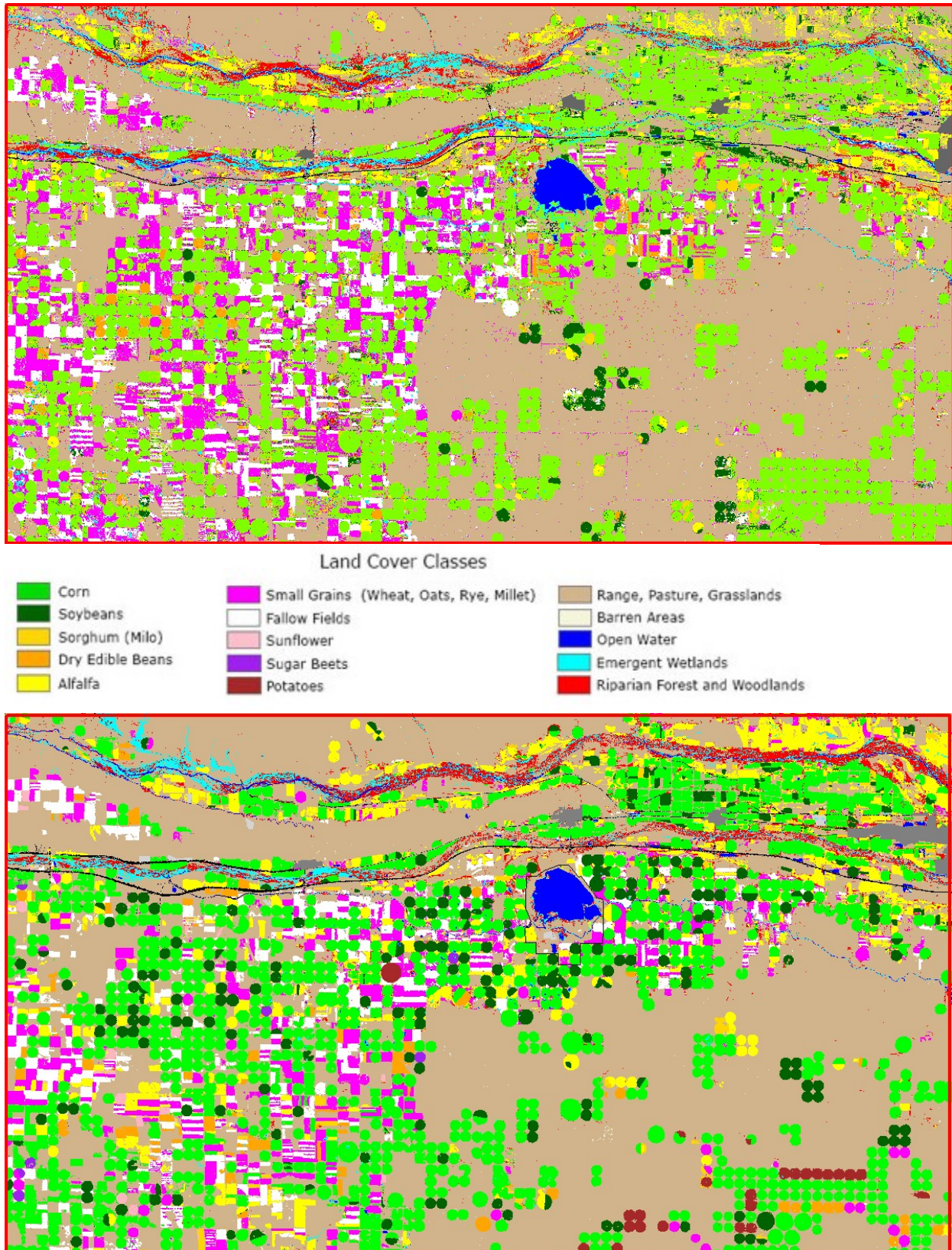


FIGURE 4. Satellite imagery of study area land use in 1997 (top) and 2005 (bottom). (Source: UNL CALMIT).



rates of 2,000 gpm or greater. Although these wells indicate productive zones of the aquifer, productivity can change over short distances as numerous wells that pump less than 1,000 gpm can be found in close proximity to the higher capacity wells. Generally, the southeast quarter of the model area has lower capacity wells with most wells having capacities of 1,500 gpm or less. As described later in the report, these pumping rates were used to estimate aquifer transmissivities for use as an initial estimate for hydraulic conductivity (Kh) values in the numerical simulations.

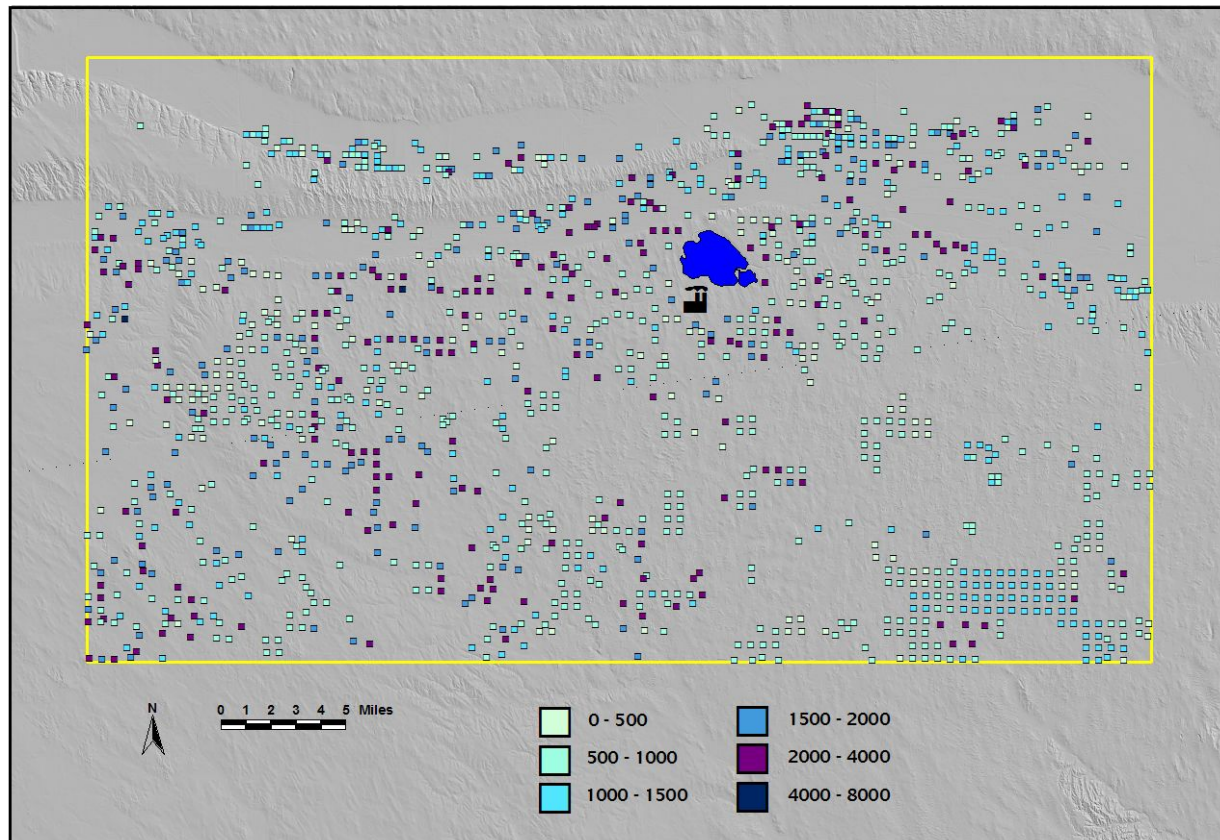


FIGURE 5. Location of irrigation wells in the study area. Color-coded values are in gallons per minute.

## Industrial Water Use

Water use for industrial purposes is relatively limited compared to agricultural needs. The Nebraska Public Power District uses North Platte and South Platte River water for cooling needs at Gerald Gentleman Station. At optimal generation capacity, approximately 1,300 ft<sup>3</sup>/s of water is used for cooling needs at the plant (personal communication, F. Kwapnioski, NPPD, January 2009). Water stored in Sutherland Reservoir is also used at NPPD's North Platte Hydroelectric Plant approximately 5 mi south of the town of North Platte. Aside from evaporative losses, NPPD's diverted water is not consumed and returns to the Platte River drainage system. Processing plants for ethanol are located near the town of Sutherland and three other plants are located just outside of the model boundary at North Platte and Madrid. Although no official records are available on the amount of water pumped by ethanol plants, the operation near Sutherland, owned by Midwest Renewable Energy produces 28 million gallons of ethanol annually. Based on current industrial standards of 3 gallons of water required per 1 gallon of ethanol produced, the plant pumps at least 84 million gallons annually (258 ac-ft).

## ***Municipal Water Use***

Within the study area, municipal and private wells are utilized for domestic needs in the communities of Sutherland (pop. 1,129), Paxton (pop. 614), and Hershey (pop. 572) (US Census Bureau, 2000). Populations were not available for the villages of Keystone or Roscoe. Larger well fields for the cities of North Platte and Ogallala are located just outside the eastern and western boundaries of the model, respectively. Based on average per capita water use of 120 gal/d in Nebraska and the populations of the communities within the study area (NDNR, 1998), over 101 million gallons (311 ac-ft) of water are pumped for municipal use in the study area on an annual basis. The rest of the rural residences rely on private domestic wells for household use and stock wells for livestock.

## **Geologic Setting**

The geologic units in the study area consist of unconsolidated Quaternary-age deposits and the Tertiary-age Ogallala Group. The High Plains aquifer is comprised of the saturated portion of both the Ogallala Group and the overlying younger deposits. Quaternary-age deposits consist of Pleistocene-age alluvial deposits, Pleistocene-age and Holocene-age loess, Holocene-age dune sand, and Holocene-age valley-fill deposits. The alluvial and valley-fill deposits, which typically yield large amounts of water to wells, are present under the North and South Platte valleys. These deposits are primarily sand and gravel, with inter-layered silts and clays. Alluvial deposits also are present in considerable thicknesses (approaching 100 ft) along a narrow zone paralleling the modern day South Platte River valley. These deposits pinch out southward and are not present beyond 5 miles south of the river valley. Mantling the Pleistocene alluvial deposits, Quaternary loess is found in varying thicknesses across the study area. In the southeast quarter of the model, the land surface is primarily Holocene dune sand deposits stabilized by grasses rooted in sandy-loamy soils. These deposits and dunes are significantly thinner than the famous Nebraska sand hills to the north of the study area. Due to the permeability of the sandy soils, this portion of the study area has the potential for elevated rates of groundwater recharge relative to other parts of the study area.

The Ogallala Group consists of a heterogeneous mixture of gravel, sand, silt, clay, sandstone, siltstone, and caliche (Images 2 and 3). The sandstone and siltstones present in the group have varying degrees of consolidation, from loosely friable (sandstone) to very competent (siltstone/caliche). Deposited during the Miocene Epoch, the group is comprised of sediments carried eastward from the uplifting modern Rocky Mountains (Laramide Orogeny) that began near the end of the Cretaceous Period. The extremely heterogeneous nature of the Ogallala Group is due to many of the east flowing, sediment-loaded, braided drainages that resulted in high variability of depositional patterns. The group is subdivided into individual formations in Nebraska, but not in other states underlain by the High Plains aquifer. The Group is not subdivided by formation name for this study. Wells tapping the group typically yield large amounts of water, but due to the heterogeneous depositional patterns, pumping yields can vary greatly between wells located short distances from one another (Figure 5). The Ogallala Group thickens eastward across the study area, from just over 200 ft on the western boundary to over 400 ft near the eastern boundary. The group is thin to absent in a small area of the northwest corner of the model underlying the North Platte River valley. The Ogallala Group can be viewed in outcrops in limited areas of the topographically high ridge that divides the North and South Platte Rivers. The Brule and Pierre formations comprise the base of the High Plains aquifer in the study area. Although some zones within the Brule formation can yield small amounts of water to wells from fractures, it is relatively impermeable when compared to the Ogallala Group. The Brule formation is of Oligocene age and consists primarily of siltstone and volcanic ash deposits. The Pierre Formation of late-Cretaceous age is marine shale that formed when a shallow intercontinental seaway covered much of the North American interior.

## **Hydrology**

Both surface and groundwater components are important to the hydrologic system in the GGS-SR study area. They are discussed in separate sections below.

## Surface Water

Draining the Rocky Mountains of Colorado and Wyoming, the North and South Platte River systems are the lifeblood of the region. Irrigated agriculture began in the region in the late 19<sup>th</sup> century and is still one of the vital parts of rural Nebraska's economy today. In addition to agriculture, water from the Platte River system (both North and South Platte Rivers) is used for power generation at hydroelectric and coal-fired stream-turbine plants. In the 1930s, the predecessor to NPPD, the Platte Valley Public Power and Irrigation District, constructed the Sutherland Project, a system of canals that divert and transport North Platte River water over 50 miles to gain enough head to operate a hydroelectric plant near the end of the system at the city of North Platte. Along the system, two storage reservoirs were constructed to regulate



IMAGES 2. and 3. Outcrop (above) of the Ogallala Group near Lake McConaughy showing the stratigraphic variability within the group. To the right is a close-up photograph of the above outcrop showing sand and fine gravel, semi-cemented sand and silt, and siltstone all within an interval of approximately 1 ft.





flow for hydroelectric power generation and storage for surface water irrigators downstream of the system. One of these storage reservoirs, Sutherland, filled in the early 1940s. However, due to non-ideal subsurface conditions, the new reservoir never filled to the design capacity because of greater than estimated seepage losses. This seepage loss over the last 65 years has created a large mound of groundwater in the underlying High Plains aquifer that extends over 30 miles to the south and east of the reservoir. In response to the groundwater mounding, several artificial drains were constructed in areas west, north, and east of the reservoir to alleviate excessively high water tables that resulted from the reservoir seepage. In addition to North Platte River water supplying the Sutherland Project with water, the Korty canal also diverts South Platte River water in the system when flows in the river are adequate for diversion.

## Groundwater

The High Plains aquifer (HPA) is comprised of the Tertiary-age Ogallala Group and overlying Quaternary-age alluvial deposits, and underlies the entire model area. The Ogallala Group was formed primarily by sediment deposition from braided streams that drained the uplifting Rocky Mountains to the west. The group is a highly heterogeneous mix of sandstone, siltstone, sand, silt, gravel, clay, and caliche. The erratic depositional pattern of the braided streams created discontinuous zones of varying thickness of each of these materials. Within close proximity of the GGS well field, typically fine sandstones/siltstones and fine sands form the lower 100-150 feet of the Ogallala Group, whereas the upper 100-150 feet has considerable thicknesses of coarse sand and gravel inter-layered with sandstone. The overlying Quaternary deposits are typically very coarse and are extensive in the present-day valleys of the North Platte and South Platte Rivers. A considerable thickness of these deposits underlies Sutherland Reservoir but become discontinuous less than two miles south of the reservoir. Saturated thicknesses of these deposits range from less than 100 ft in the northwest to over 300 ft in much of the southern half of the study area. Overall, the aquifer saturated thickness (Figure 6) ranges from approximately 200 ft in the western extent of the study area to over 500 ft south and east of the well field. The aquifer approaches 700 ft. in thickness in the northeast corner of the model domain. The aquifer is considered unconfined (water table is the upper boundary of the aquifer), although localized areas of semi-confined conditions are known to exist in the HPA. Figure 7 shows a generalized depth to water ranging from nearly 0 to over 200 ft in the study area.

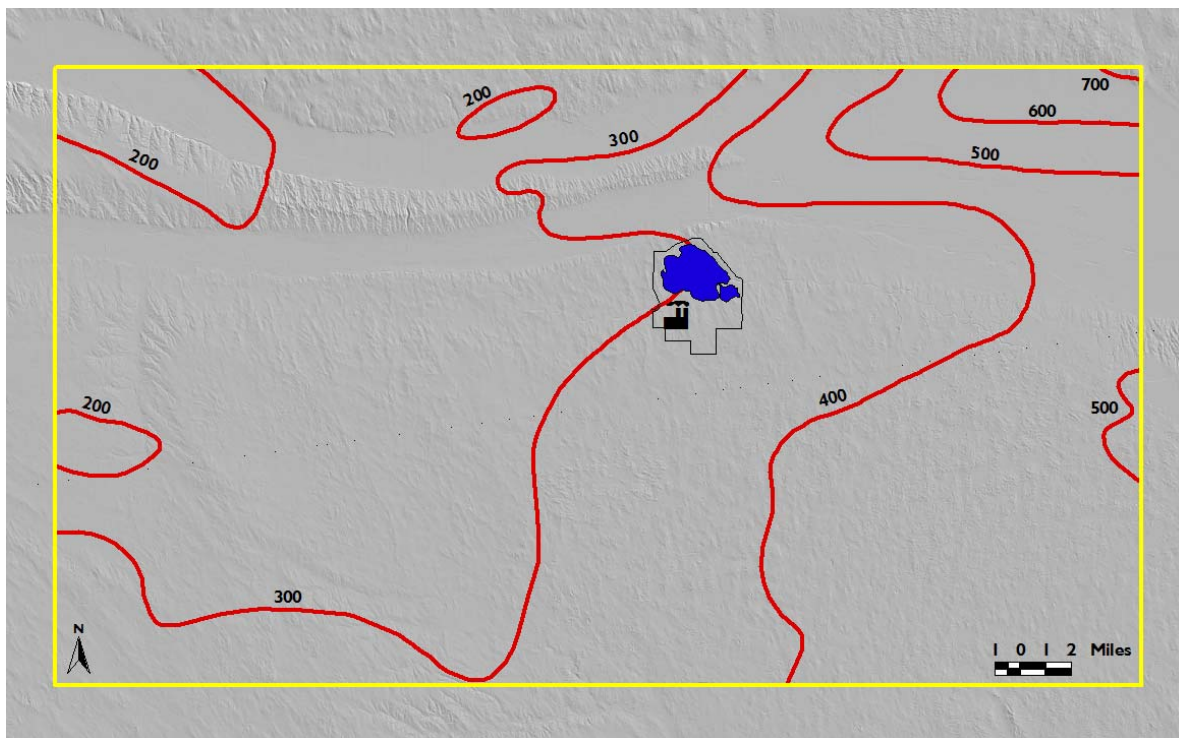


FIGURE 6. Map of the study area showing the saturated thickness of the HPA (Gutentag and others, 1984).

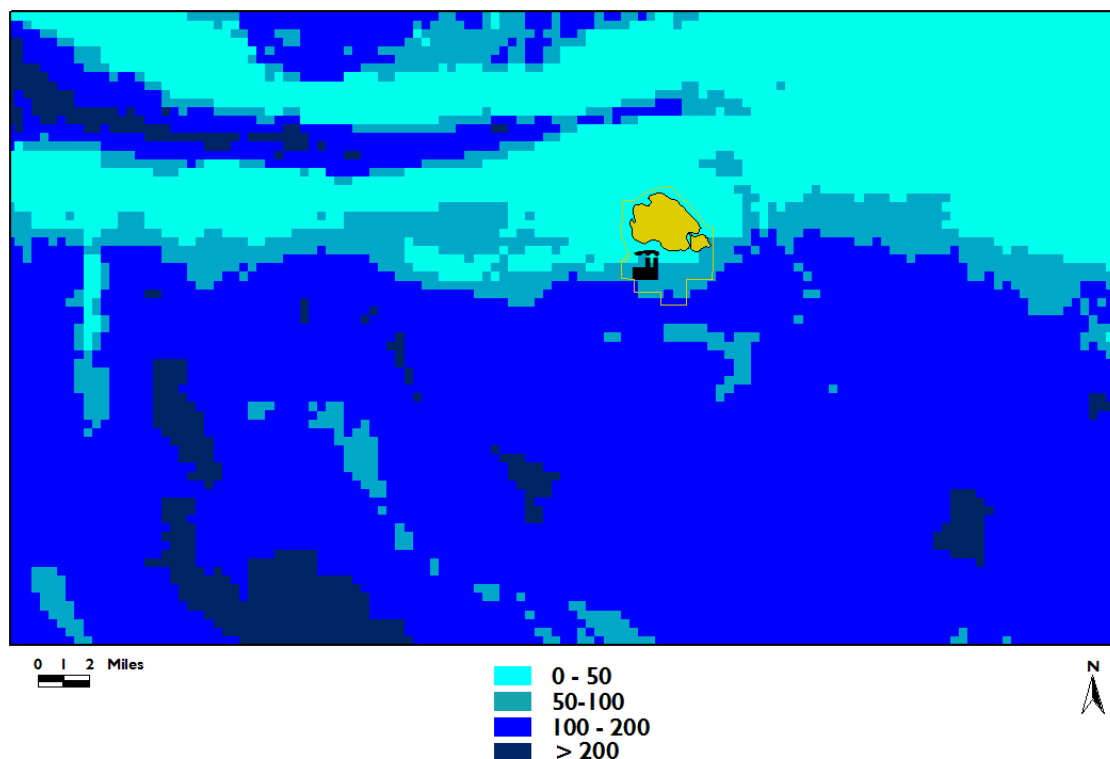


FIGURE 7. Generalized raster map of the study area showing depth to the water table (UNL-CSD, 1996).

Although the water table in the southern two-thirds of the model area is too deep ( $> 100$  ft) for evapotranspiration of groundwater, the water table in the Platte River system valley is shallow ( $< 15$  ft) at many locations and significant amounts of evapotranspiration occurs through riparian woodlands and grasses.

Groundwater flow south of the South Platte River valley in the southwest part of the study area is southwest to northeast. In the eastern half of the study area, the flow gradient is primarily eastward with an apparent flow divide, indicating groundwater moving northeast and southeast on each side of the divide (Figure 8). The southern component of this is oriented towards the Republican River and associated tributaries for discharge. Decades of seepage from Sutherland Reservoir created a mound of groundwater (Figure 9) that alters the regional flow pattern near the lake. The ultimate discharge area of both regional groundwater flow and lake seepage is the Platte River system except for the component of flow south of the groundwater divide in the southeastern portion of the model. In the northeast portion of the study area between the North and South Platte Rivers, the water table is relatively flat and the mapped flow gradient indicates movement of water directly east.

Since the advent of center-pivot agriculture in the 1950s, the High Plains aquifer in the study area has become highly utilized as a source for irrigation water. In the study area alone, over 1,500 irrigation wells tap the aquifer, with several dozen of these wells located in close proximity to the GGS well field.

Although significant declines in water levels in the High Plains aquifer have been well documented in recent years (McGuire, 2007), groundwater levels in the study area have remained relatively stable or had small fluctuations, except for areas near the southern boundary where noticeable declines occurred in the 1970s. Part of this stability is due to the continuous seepage emanating from the Sutherland Reservoir providing a continuous supply of recharge to the aquifer and mitigating the impacts of irrigation pumping over the past several decades. In addition to this seepage, improved irrigation efficiency has also contributed to minimal declines of study-area water levels relative to other areas of Nebraska and High Plains aquifer states. A final factor contributing to minimal water levels declines occurred in 2004 when the Twin Platte Natural Resources District (TPNRD), a local resources management agency that oversees groundwater management in the study area, implemented a drilling moratorium along the Platte

River corridor in an attempt to meet state surface water appropriation limits and Federal requirements for in-stream flows in the Platte River for critical habitat areas for four endangered species (piping plover, least tern, whooping crane, pallid sturgeon) .

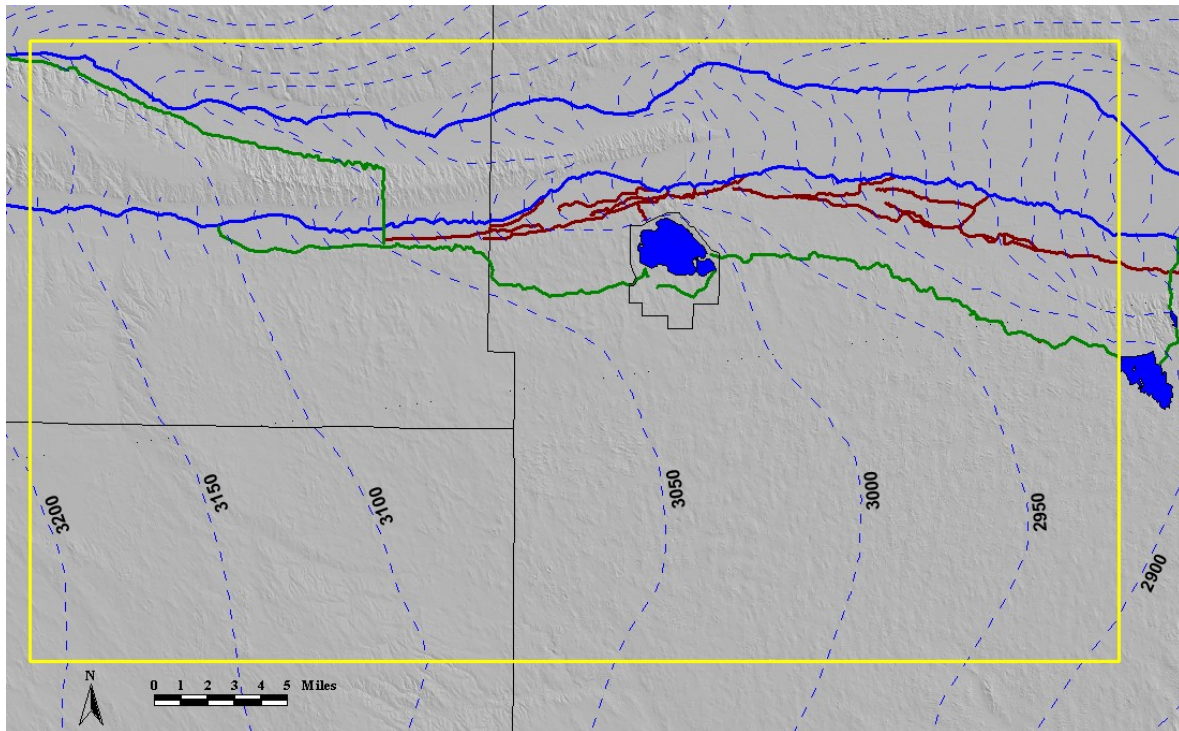


FIGURE 8. 1995 regional water table elevation contours. Contour interval is 50 ft. (UNL-CSD, 1995).

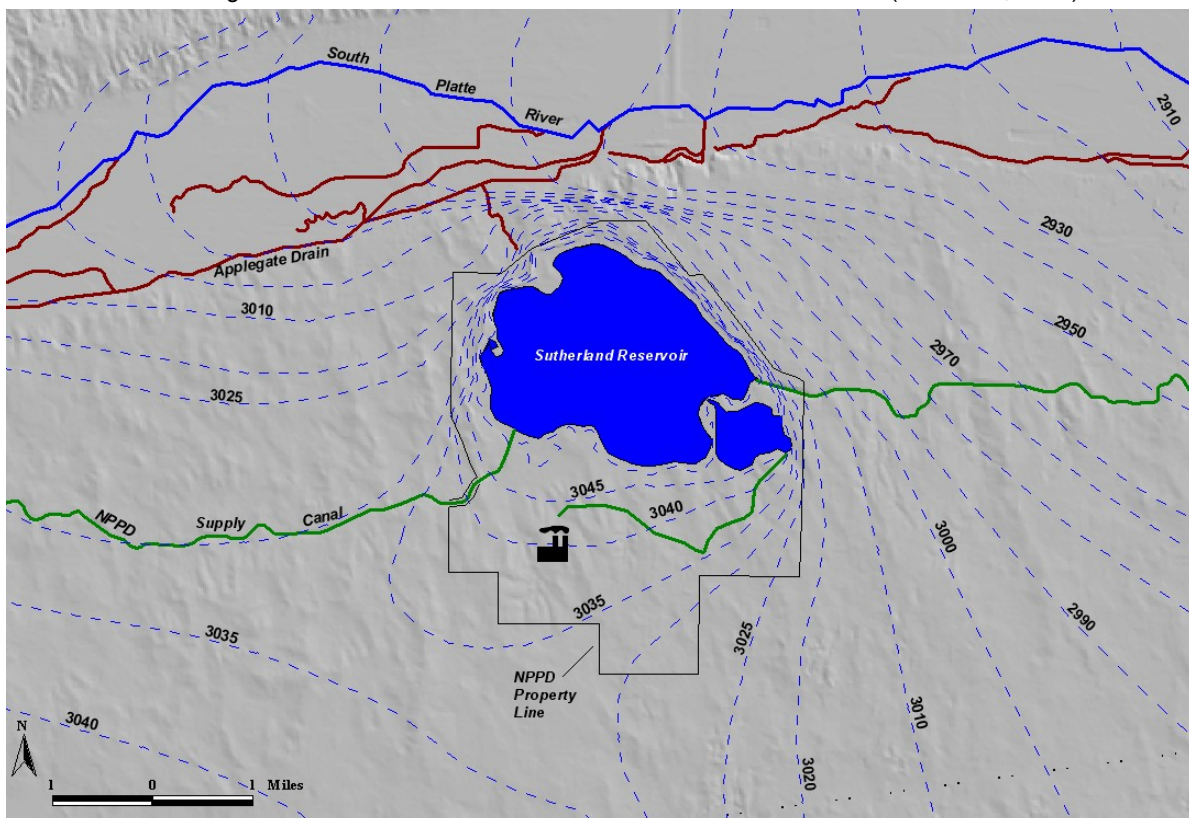


FIGURE 9. Fall 2004 water table elevation in the near-site area. Contour interval is 5 ft. (NPPD unpublished data).



## **Data Acquisition and Analysis**

The most robust modeling studies utilize many different types of data. The weakest groundwater models are calibrated to hydraulic head only, while the strongest studies include observations of fluxes, path-line delineators, water-age/travel-time, temperature, concentration, and geologic features in the calibration data. The installation and monitoring of the GGS well field provided a wealth of geologic and hydrologic data that is ideal for construction of a detailed groundwater flow model.

### ***Geologic Data***

Geologic data, typically in the form of borehole logs, provides the framework for defining layers and boundaries in a groundwater flow model. Fortunately, abundant geologic data were already available from dozens of irrigation well logs in the GGS-SR study area. The COHYST and Republican River models utilized data from NDNR and UNL-CSD databases to develop grid layer boundaries. One limiting factor of the irrigation well logs was that most do not penetrate to the base of the aquifer, resulting in an unknown thickness of the Ogallala Group at many well locations. Within the model area, 92 well logs provide data on the entire thickness of the aquifer.

Within close proximity of Sutherland Reservoir, over 70 boreholes were drilled between 2004 and 2006 for production, testing, water level observation, and geochemical sampling (Image 4). This concentration of boreholes allowed for detailed description of the geologic framework near Sutherland Reservoir. Each borehole and associated electronic log was analyzed with stratigraphic database and visualization software. With the large concentration of data in a small portion of the model (near the reservoir) and a more scattered distribution of boreholes in the rest of the model area, careful consideration ensured that geologic mapping was smooth and consistent between the concentrated area of borehole data and the outer regions of the model domain. For the outer area beyond the well field, geologic unit and model layer elevations were based on data from the COHYST borehole database (Cannia and others, 2006). These formation boundaries were based on information from UNL-CSD borehole logs and geophysical logs. Within the COHYST hydrostratigraphic layer selections, the top of COHYST Ogallala Group (layer 4) was used as the top of Ogallala Group in the outer area of the GGS-SR study area. The top of the COHYST layer 6 corresponded with the basal Tertiary fines hydrostratigraphic unit from the GGS borehole data analysis. In the Quaternary portion of the aquifer, the Quaternary coarse units defined in the GGS-SR study area corresponded with the elevations of hydrostratigraphic unit 2 in the COHYST database. Land surface elevations from the COHYST database were set as the top of the uppermost layer at the 92 well locations used in the GGS-SR study area. The elevations of the hydrostratigraphic unit contacts, as described in the following sections, were interpolated between wells and used as model layer elevations in various conceptualizations of the aquifer system.

### ***Interpretation of Geologic Information***

As previously mentioned, the Miocene-age Ogallala Group is highly heterogeneous both vertically and laterally due to the fluvial environment its sediments were deposited in. Past regional modeling studies have conceptually represented the group as a single aquifer/hydrostratigraphic unit (Luckey and others, 1986; Republican River Compact Administration, 2003; Luckey and Cannia, 2006) while others have attempted to define individual hydrostratigraphic units (and corresponding model layers) within the Group (Cannia and others, 2006).

To evaluate the abundant geologic data (Image 5) found in both the borehole lithologic and the geophysical logs, raw data was entered into the geologic database software package RockWare 2006. All pertinent information was collected in a single digital location, including hole location information, lithologic descriptions for each interval drilled, and notes on unique aspects of the hole as described by the logging geologist or driller. A problem typically encountered when categorizing geologic descriptions from raw field data was the varying range of terminology and descriptors used by drillers or logging geologists who analyzed drill cuttings. Even when attempts were made to use consistent terminology, differences still existed in the lithologic logs, with the most common deviations being the length or detail of description or how a particular material was described. This problem was particularly acute for drill cuttings from the Ogallala Group due to its heterogeneous nature. During the first phase of analysis and database entry, the geologic data were separated into 31 categories based on age/formation, grain size

and sorting, amount of consolidation and cementation, and presence of rootlets or other fossilized organics. One of these categories was the Brule Formation, considered the base of the High Plains aquifer. In all 31 descriptions were first used to define the geology of the material comprising the aquifer.



IMAGE 4. Drill site of geochemical monitoring well nest 6, east of GGS. Drill cuttings from this borehole provided lithologic data from the middle of the well field. Photo taken in May 2006.

IMAGE 5. Drill cutting samples collected from the deep well at geochemical monitoring well nest 5 in May 2006. Samples were archived at the UNL-CSD.



Geophysical well logs were available for nearly all of the boreholes in the near-site area. Each of these logs was visually analyzed to support the selected elevations of major geologic formations noted in the lithologic log descriptions. Analysis of many of the geophysical logs allowed for an improved determination of the elevation of tops of geologic formations as some of the geologic logs described materials over 10 ft intervals, thus did not provide close constraint on the elevation. Evaluation of the geophysical logs also revealed a trend of predominately finer-grained material in the lower 100 to 150 ft of



the Ogallala Group at many locations. The presence of this trend was considered in the creation of the layers for the numerical model.

In order to group the borehole information into hydrostratigraphic units that would serve to delineate both model layers and distinct zones within a model layer, the keyword descriptors shown in the example borehole logs were placed into five categories based on sediment texture/sorting, degree of cementation, and to a lesser degree, depositional history. Five categories were chosen to capture the major characteristics of the deposits that comprise the aquifer and control movement of water both vertically and horizontally, yet limit the number of layers/descriptors for each interval drilled in the boreholes. For example, in the test borehole for operating well 40 (Figure 10) in the GGS well field from the depth 230 to 320 ft, three different keyword descriptors were used to define an interval that likely behaves uniformly in terms of movement of water. Although minor variations in horizontal hydraulic conductivity (Kh) most certainly exist between a silty, fine sandstone and an interval of siltstone with sand seams, it is conceptualized that these types of deposits have a similar influence on the bulk movement of water through the aquifer and that the calibrated value of Kh for a zone comprised of these materials would capture the average bulk Kh within that portion of the aquifer. The keyword descriptors were grouped into the five hydrostratigraphic zones as follows:

**Quaternary Fines-** These include the uppermost stratigraphic intervals of undifferentiated silts, clays, or fine sands. These deposits are unsaturated except in areas adjacent to the lake and in some areas of the Platte River-system valley.

**Quaternary Coarse-** Any interval greater than 10 ft in thickness that exists stratigraphically above the Ogallala Group and is comprised of medium to coarse sand, gravel (any size or sorting) or combination thereof.

**Upper Tertiary Fine-** Any interval within the Ogallala Group that exists above the lower most interval of Tertiary Coarse deposits and is comprised of unconsolidated fine sand, silt, clay, or semi-consolidated to consolidated siltstone, claystone, or fine sandstone.

**Tertiary Coarse-** Any interval greater than 10 ft in thickness that exists within the Ogallala Group and is comprised of medium to coarse sand, gravel (any size or sorting) or combination thereof.

**Basal Tertiary Fine-** This includes material in the interval of the Ogallala Group that exists below the lowermost Tertiary Coarse zone. This unit is typically composed of fine, loose-to-firmly cemented sandstone or siltstone, but can have seams of unconsolidated fine sand, silt, and clay. This zone was prevalent in nearly every borehole in the well field area and typically makes up the lowermost 100-175 feet of the Ogallala Group within the near-site area. Evidence of this interval was visible in several of the geophysical logs from well-field test holes.

Figures 10 and 11 show descriptive comparisons of how raw lithologic data (as described by the on-site field geologist) were assigned one of the 31 keyword descriptors. Also each figure presents a graphical example of how keyword descriptors were used to define the five major hydrostratigraphic zones present at each borehole location. In the OW-40 borehole (Figure 10), two intervals of Tertiary fines are present that are separated by a coarse Tertiary unit of approximately 50 ft in thickness. Categorizing the hydrostratigraphic units into 5 major zones also allows repetition of the zones as indicated in the fence diagram of the near-site well field area in Figure 12. In much of the area within the well field, several alternating intervals of Tertiary coarse and fine zones exist above the basal Tertiary fines. Also, note the presence of an overall greater abundance of both Quaternary and Tertiary coarse material in OW-40 (approximately 100 ft combined), which is located on the north side of the well field and closer to the present day South Platte River valley. The borehole for OW-19, which is located on the southern side of the well field, contains approximately 20 ft of coarse material in the middle of the Ogallala Group. These two end members were chosen as examples to illustrate the greater abundance of coarse sands and gravels in the northern end of the well field near Sutherland Reservoir and disappearance of Quaternary coarse deposits southward in the near-site area. This trend is also apparent in the fence diagram in figure 12.

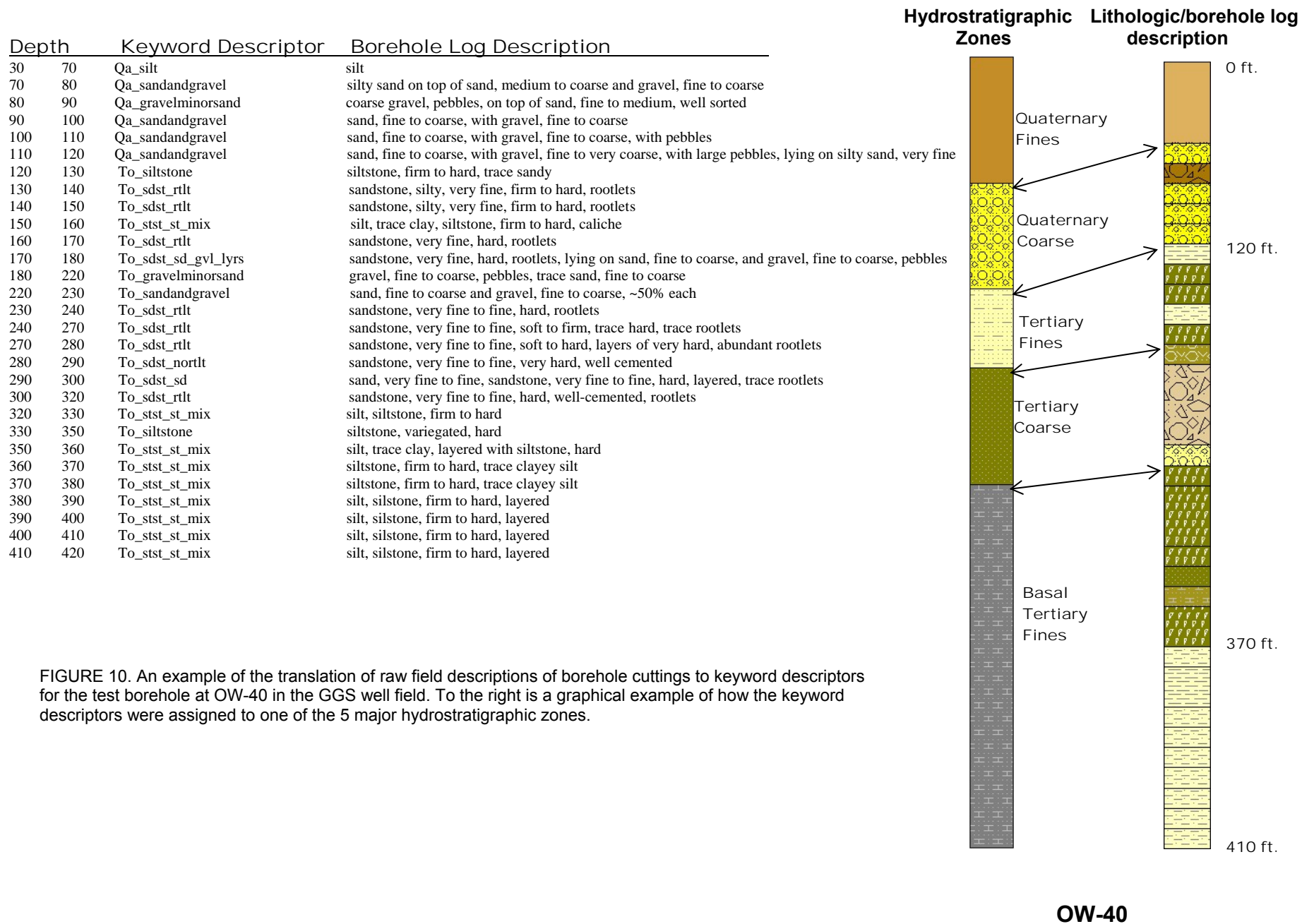


FIGURE 10. An example of the translation of raw field descriptions of borehole cuttings to keyword descriptors for the test borehole at OW-40 in the GGS well field. To the right is a graphical example of how the keyword descriptors were assigned to one of the 5 major hydrostratigraphic zones.

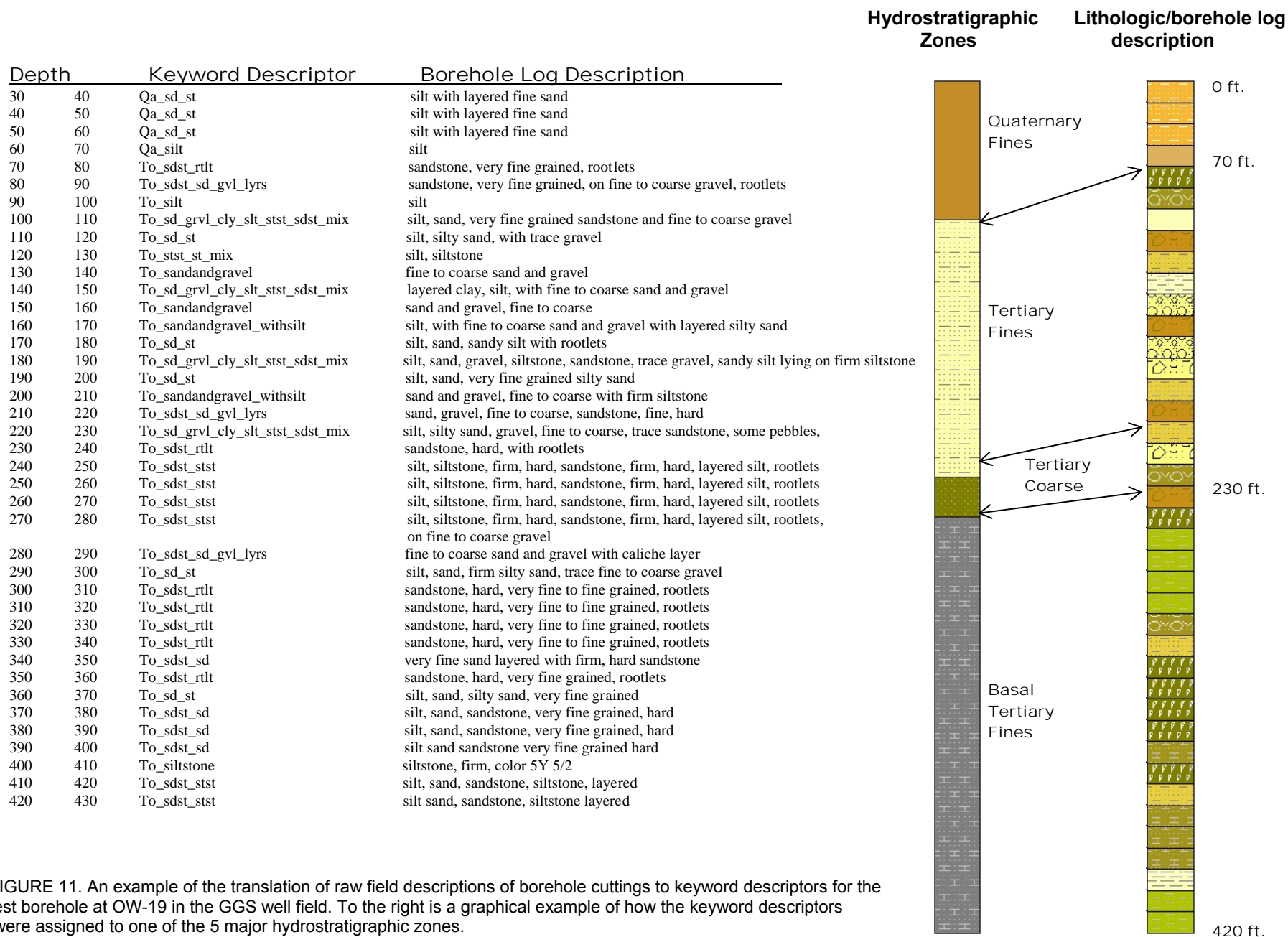


FIGURE 11. An example of the translation of raw field descriptions of borehole cuttings to keyword descriptors for the test borehole at OW-19 in the GGS well field. To the right is a graphical example of how the keyword descriptors were assigned to one of the 5 major hydrostratigraphic zones.

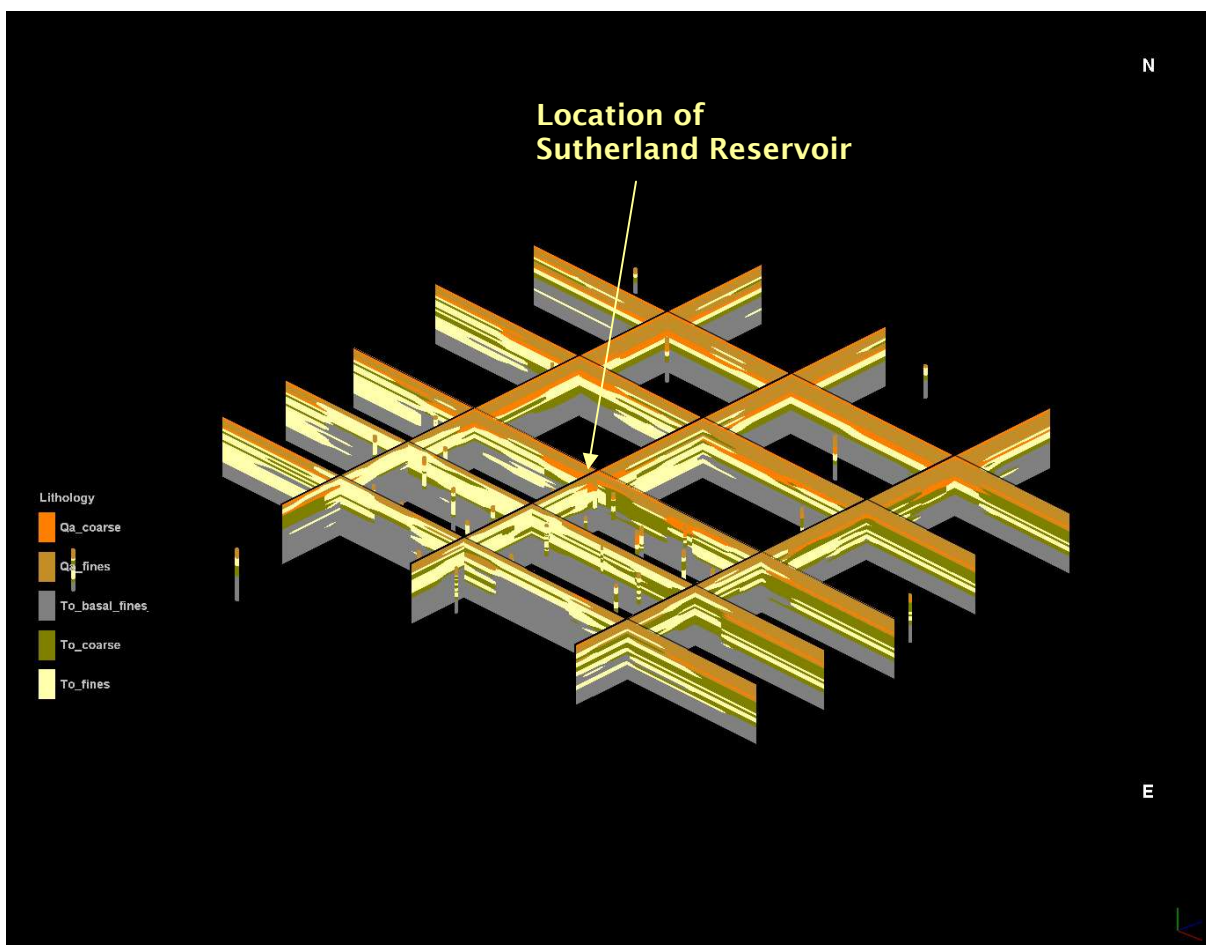


FIGURE 12. A 3-D fence diagram of the near-site area hydrostratigraphy based on the five defined hydrostratigraphic zones from the borehole log keyword descriptors. Borehole locations are also shown to indicate the locations of all boreholes used in the interpolation of the zones to create the fence diagram. The high density of boreholes in the southern portion of the fence diagram is the center of the GGS well field, and the area within the four larger inner squares on the north side of the diagram is the location of Sutherland Reservoir. Vertical exaggeration = 25x.

The five hydrostratigraphic zones provide the basis for both model layers and individual zones that were used for construction of the numerical model grid and material zone arrays characterizing the most prevalent material of distinct areas. The construction of the model grids is described in the following section Model Construction. A complete set of diagrams for hydrostratigraphic zones of all available boreholes from the wellfield are available in Appendix E.

As shown in the fence diagram (Figure 12), even with five major hydrostratigraphic zones, the repetition of Tertiary coarse and fine deposits that vary in both spatial extent and thickness created an opportunity to develop various conceptualizations of the site to best represent the variability in the aquifer. To overcome problems that could arise from an excessive number of model layers to represent distinct intervals in the upper Ogallala Group, areas of similar material texture were aggregated into unique zones in the near-site area. The application of these zones in development of alternative conceptualizations is described in the section on multiple conceptual model development.

### ***Aquifer Characteristics in the Near-Site Area***

As previously mentioned, the GGS well field provided abundant information for characterization of not only the hydrostratigraphic setting, but also hydraulic properties of the aquifer. For each well location (Figure 13), performance tests were conducted to determine the pumping capacities and associated

drawdown at each location. Although these analyses were not long-term aquifer tests, they provided preliminary insight into the behavior and production potential of the aquifer. These data also provided the basis for development of a group of site conceptualizations for the numerical simulations described later in this report.

Average transmissivities based on 24-hour drawdown and 24-hour recovery well tests at each of the production wells provided an initial range of transmissivity in the near-site area (Image 6). Average transmissivities (of both the drawdown and recovery tests) at the 40 well sites ranged from 37,525 gallons per day per foot (gpd/ft) to 316,800 gpd/ft, with a mean value of 116,639 gpd/ft. Although there is a general decreasing trend in transmissivity from north to south with higher values ( $> 100,000$  gpd/ft) in wells on the northeast and northwest sides of the reservoir, some wells on the southern edge of the well field yielded large transmissivities (e.g. OW-30 at 176,000 gpd/ft), and yet other wells near the reservoir yielded transmissivities less than 50,000 gpd/ft (e.g. sites 3 and 36).

Figure 13 shows the average pumping rates of the GGS wells for the summers of 2005, 2006, and 2007. The well field was pumped at various lengths of time each summer to provide colder groundwater to reduce the temperature of outflows from the GGS cooling pond into Sutherland Reservoir. This action was necessary for NPPD to meet Nebraska Department of Environmental quality requirements for discharge water temperatures. Water from the wells was not utilized to maintain the reservoir stage necessary for normal GGS operations, as water supplies in Lake McConaughy remained sufficient to maintain the reservoir levels above the intake of cooling water for GGS during those summers. Even though the wells were not used for this purpose and pumped continuously for projected time spans necessary for maintenance of the reservoir levels, significant drawdowns occurred at the pumping well locations each summer, which provided more in-depth data on aquifer response to several wells operating simultaneously in the well field. Although appreciable drawdown occurred, recovery at each well reached near static pre-pumping rates by the fall of each season. Note that initial well test transmissivity values did not necessarily correspond to the highest average pumping rates of the wells. For example, wells 13 and 12 had initial average (from both drawdown and recovery tests) transmissivity values of 316,800 and 145,200 gpd/ft, respectively. Each of these wells, however, had average pumping rates from these summers in the lowest range of the pumping rates (1,500 to 2,000 gpm) as shown in Figure 13.



IMAGE 6. A view of GGS well field production well 35 located southwest of Sutherland Reservoir.

Wells on the west and northeast sides of Sutherland Reservoir were not installed with pumps as of 2008. NPPD strategy with well field management was not to pump wells adjacent to the lake on the northwest and northeast sides of the reservoir if they had initially high well-test transmissivity in order to minimize induced lake seepage. With this strategy, NPPD relied on wells south of the reservoir to meet cooling needs of GGS discharge water.



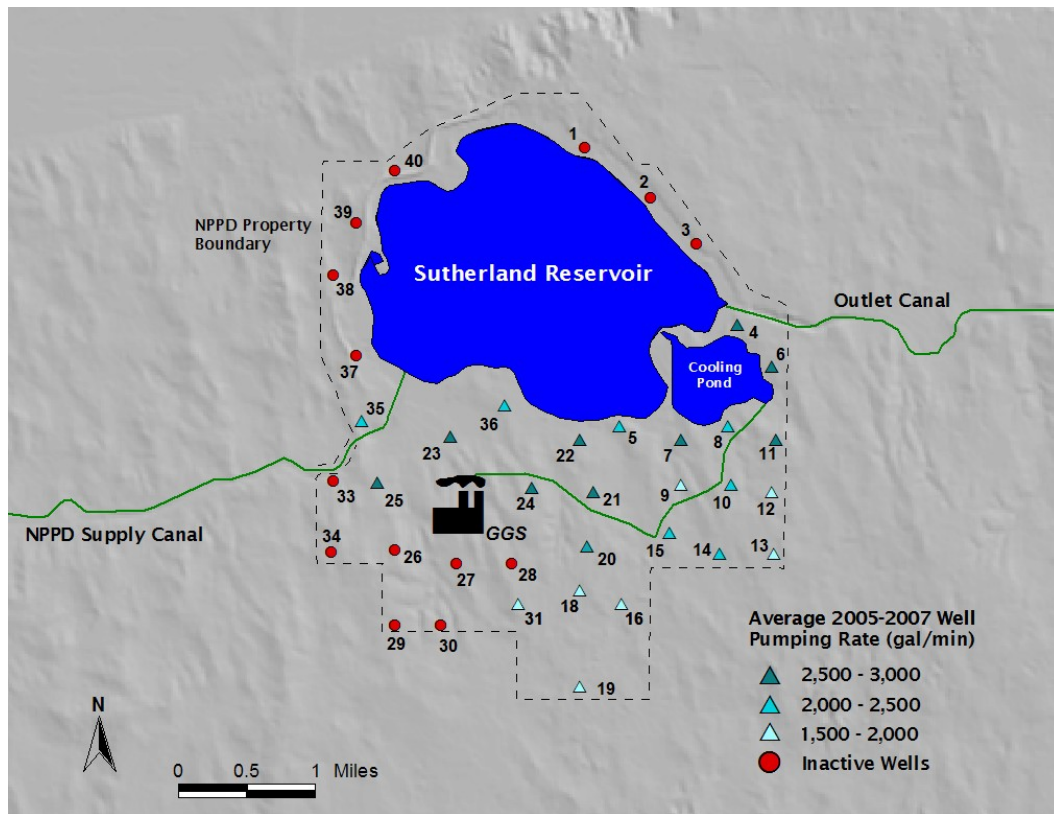


FIGURE 13. GGS well field showing locations of individually numbered wells. Color codes of active wells are the average pumping rates from the summers of 2005 through 2007.

Water table changes were tracked continuously at 8 sites and provided water level observation data for model calibration of the transient period that accounted for the pumping schedules during the summers of 2005, 2006, and 2007. Figure 14 shows examples of monitoring well data from locations Obs-4, Obs-6, and Obs-8 (locations of these wells are shown in Figures 15 and 16). Obs-4 and Obs-8 each have a shallow well with a 15 ft screen at the water table (well B) and a well with a 15 ft screen near the bottom of the aquifer (well A). These 3 observation nests were selected as they represent different areas of the well field and proximity to Sutherland Reservoir. Also, Obs-4 and Obs-6 are located where no saturated Quaternary deposits exist, whereas the aquifer at Obs-8 contains over 40 ft of sand and gravel above the Ogallala Group.

Obs-4, located on the southern edge of the GGS well field west of pumping well 19, shows a drawdown response of nearly 16 ft for the deep well during the 2006 pumping season. The total drawdown at this location was slightly less for 2005 and 2007. Prior to the 2005 pumping season, the water levels from late 2004 appear to show a slight increasing trend, possibly recovering from the previous irrigation season since no NPPD well had pumping prior to that time except for the 24-hr performance tests. Following the 2005 pumping season, in both wells it appeared the water level continued to be recovering after nearly 10 months. The same trend occurs for the 2006 season and the recovery period extending into 2007, although the shallow well (green line) deviates from the deep well recovery by over a foot in the spring of 2007. In the deep well, water levels recovered to within 1 ft of the pre-2005 levels after both the 2005 and 2006 pumping seasons.

Obs-6, located southeast of the GGS well field, exhibited a maximum water level decline slightly over 10 ft in 2006. The water level recovered to within 1 ft of the pre-2005 pumping levels after 3 months, and continued to gradually rise prior to the 2006 pumping season. The water level appeared to take a longer time to recover after the 2006 pumping season, with the recovery levels reaching within 2 ft of pre-NPPD pumping conditions just prior to the start of pumping in 2007.

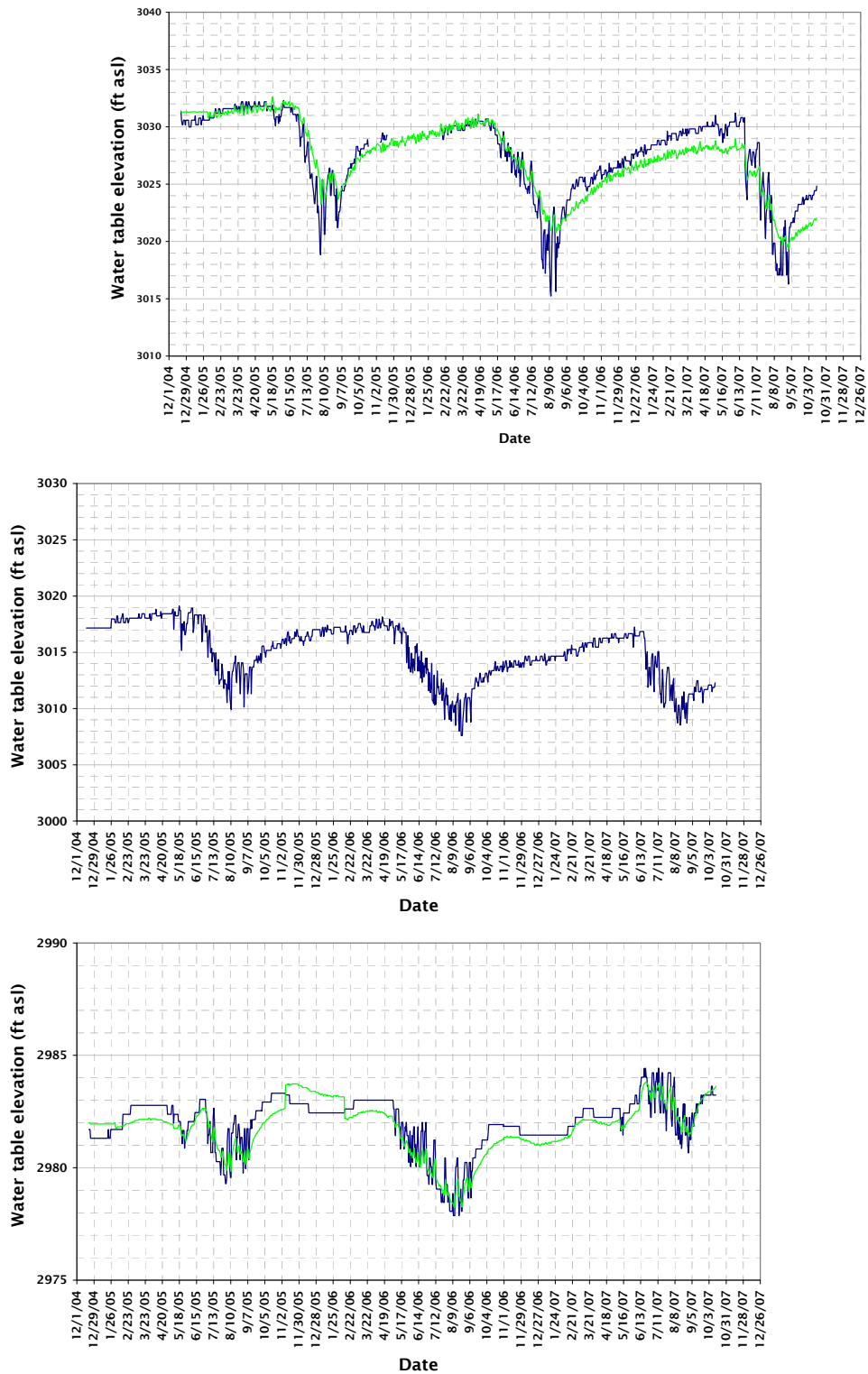


FIGURE 14. Continuously recorded well hydrographs during the pumping seasons 2005, 2006, and 2007 at observation well nests Obs-4 (top), Obs-6 (middle), and Obs-8 (bottom). Locations are shown in Figure 13. The blue line is associated with the deep well and the green line is for the shallow well in Obs-4 and Obs-8. Note different scale on the y-axis.

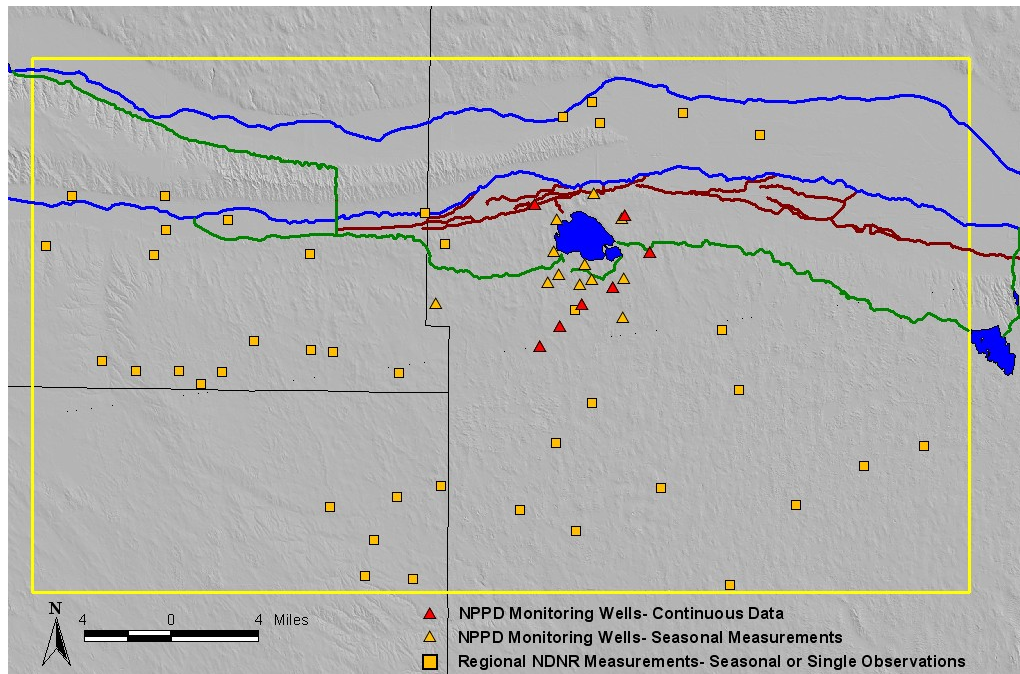


FIGURE 15. Map of study area showing outer-area and near-site locations of ground water level observations. Regional NDNR measurements were also supplemented by data from the TPNRD.

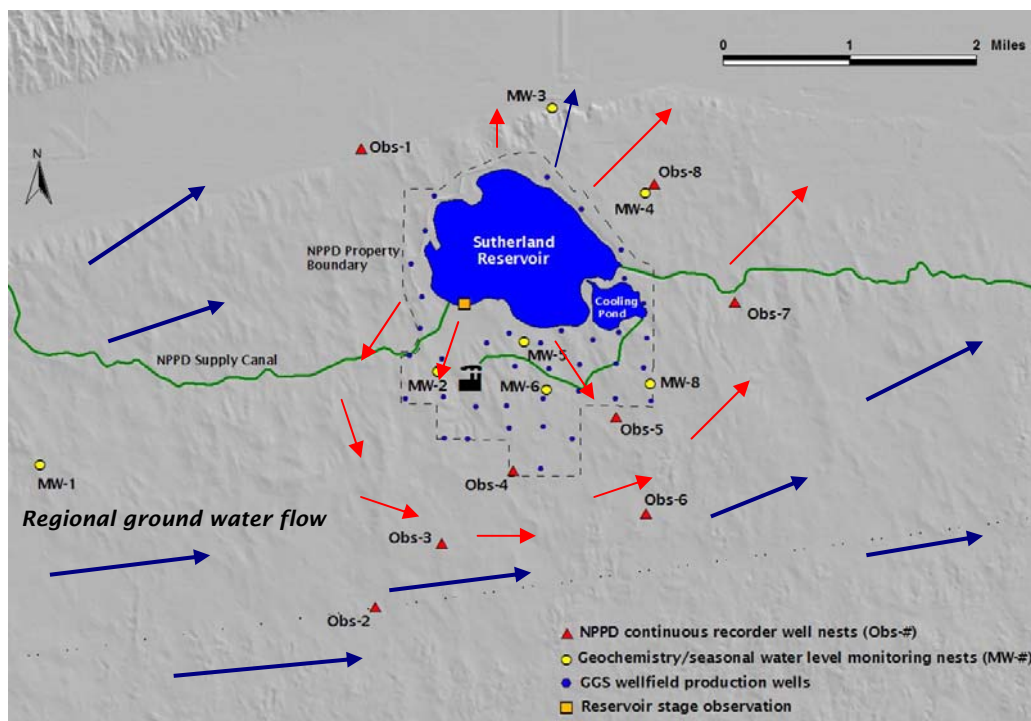


FIGURE 16. Map of continuously recorded water level well nests (red triangles) and geochemistry monitoring well nests (yellow circles) in the near-site area of the model domain. MW-1 was not used as a flowpath age observation location. Red arrows indicate the conceptualized movement of ground water in the near-site area,. Blue arrows indicate direction of deeper regional ground water movement. Regional ground water flow has been detected at depth north of the reservoir in the deep well at monitoring well nest 3.



Obs-8, located northeast of and down-gradient from Sutherland Reservoir, showed different responses for each pumping season. In 2005, the maximum drawdown was just over 3 ft, and rapid fluctuations occurred during the pumping season. Within 2 months, water levels had recovered to pre-pumping levels. In 2006, water level declines reached 5 ft, and water levels recovered to within levels observed prior to the 2005 pumping season within 2 months. However, water levels did not reach pre-2006 groundwater levels until just prior to pumping in 2007. The higher levels observed in 2007 were possibly a result of higher stage in nearby Sutherland Reservoir, less pumping in nearby irrigation wells, or possible equipment error. Water levels in the shallow and deep wells did not deviate more than 2 ft with patterns trending very closely to one another, although the direction of the vertical gradient (e.g. up/down) changed at times for Obs-4 and Obs-8. These three wells were shown to exemplify the observed behavior of the aquifer in response to the stresses induced from GGS well field pumping in the summers of 2005 through 2007. Although over a period of several months for the wells south of the reservoir, these hydrographs indicate the capacity of the aquifer to recover to near pre-pumping levels even after two seasons of withdrawals even when coupled with pumping in surrounding irrigation wells. The rest of the hydrographs from the GGS observation wells are shown in Appendix E.

## ***Hydrologic Data***

The presence of both major surface water features and an abundance of groundwater levels in the highly utilized aquifer in the near-site area allowed for the opportunity to gather a variety of information on the hydrologic system for the development of conceptual models. Available data for surface water and groundwater are described below.

### **Surface Water**

Measurements of surface water flows to determine baseflow (the groundwater contribution to stream or river flow) are critical for calibrating a groundwater model. Flow measurements provide a unique data observation that breaks correlation between typical parameters that are calibrated in groundwater modeling projects. In the GGS-SR study area, sporadic and inconsistent flow data for the South Platte River limited the number of possible flow measurements available to determine baseflow. Problems included data from various gages being available at different time periods as well as data not being available for the transient time period of the models described in this report. In addition to South Platte River flows, several engineered drains exist in the vicinity of Sutherland Reservoir. Only one of those, Applegate Drain, had historic flow records from a staff gage near the mouth of the drain which empties into the South Platte River. This problem was recognized early in the project and to overcome the lack of flow data pertinent to the GGS model, staff gages were installed at 6 locations in the model area in the spring of 2006.

Technicians from the NDNR made monthly discharge measurements at all locations to develop stage-discharge relations. Two gages were installed on the two braided channels of the South Platte River at Sutherland, and 4 gages were installed at various drains across the model area. The NDNR also continued measurements of Applegate Drain, thus providing 5 drain flow locations. The gages on the South Platte River were used with measurements from a downstream USGS gage location at the city of North Platte to determine baseflow for a reach of the river between Sutherland and North Platte. This stretch of the river historically gains flow from the Sutherland Reservoir seepage as noted by comparing flows between the Korty Diversion, Paxton, Sutherland, and North Platte.

In addition to stream flows, Sutherland Reservoir stage elevations are measured daily by NPPD and provide an additional type of observation for the entire transient period simulated by the GGS models.

### **Groundwater**

As described in the previous section on the GGS well field, NPPD installed seven observation well nests within and on the periphery of the production well sites. An additional observation well is an abandoned irrigation well approximately one mile southeast of the well field. Each nest location is equipped with a shallow observation well screen with a 15 ft screen near the water table and a deep well with a 15 ft screen located near the base of the aquifer. Continuous water level recorders were installed in the nested wells. Water levels have been recorded since late 2004 and provide observations for nearly half of the transient period simulated by the GGS models.

In 2005, NPPD and the USGS partnered to install three monitoring well nests in the study area to develop a background suite of geochemical data for the aquifer. Each nest has at least 2 wells with short-interval screens (5 ft) to sample discrete zones within the aquifer. In 2006, four more nests were installed for geochemical sampling. Each of these nests also provides locations for seasonal water level measurements. The Twin Platte NRD measured each nest seasonally in 2005 and 2006, and in the summer of 2007, continuous recorders were installed at several of the nests for automated monitoring.

In addition to these locations for groundwater level observations, several neighboring irrigators voluntarily allowed the Twin Platte NRD to make season water-level measurements at irrigation or stock wells. These measurements provide a third source of near-site water levels used in calibration. In the outer model area, water level measurements were available at 13 scattered locations obtained from the NDNR online databases. Most measurement locations contained seasonal measurements through 2003.

### Geochemistry

Geochemical data collected from the monitoring wells by the USGS were used in the development of multiple conceptual models of groundwater flow and to better calibrate the GGS models. The first phase of the project determined geochemical differences between regional groundwater in the High Plains aquifer, Sutherland Reservoir, and the South Platte River using major ions and stable isotopes of water. Following this initial phase, a preliminary version of the groundwater flow model of the GGS area was used to delineate flow paths originating at the reservoir for selection of locations for well nests installed in 2006. The 2<sup>nd</sup> phase of the project included sampling groundwater and surface water for selected major ions, isotopes of water, and tracers of groundwater age for the purposes of determining groundwater/surface water mixing in the aquifer and travel times in the aquifer of reservoir leakage. The groundwater ages were further used as a unique type of model calibration data. For further details on methodologies and geochemical results, see McMahon and others, in prep.).

### ***Climate Data***

Groundwater recharge is a common parameter adjusted during calibration of groundwater models. Regardless of the methodology used to estimate groundwater recharge, climate patterns (precipitation and evaporation/evapotranspiration) are the fundamental factors when first assessing recharge estimates. Long-term precipitation data are available at several sites surrounding the study area, with the oldest records dating back to 1894. All sites with analogous timeframes of precipitation records within 10 miles of the model boundary were used to interpolate annual precipitation. These data were used as the basis for various recharge conceptualizations discussed later in this document. All precipitation records were acquired from the High Plains Regional Climate Center (<http://www.hprcc.unl.edu>). Appendix B contains the precipitation records at all of the weather stations that were used to interpolate the annual precipitation map for use in determining recharge in the models.

### ***Land Use Influence on Recharge***

Studies of the High Plains aquifer have indicated that land use practices can have substantial influences on rates of groundwater recharge (McMahon and Others, 2006, Dugan and Zelt, 2000, Luckey and Cannia, 2006). To best capture the diversity of land use within the GGS model area, satellite imagery of the region was analyzed using GIS to define zones delineating different land use practices as one conceptualization of recharge distribution to test in the numerical water models. Although the imagery (CALMIT, 2005) identifies 26 crops and/or vegetative areas across Nebraska, only a limited number of crops were present in the 2005 imagery of the GGS-SR study area as indicated by Figure 4 and in the section on agricultural uses of water. This characterization of recharge was not based on the individual crop types, but rather on whether the crops were irrigated or not. With this condition, 3 land use zones were defined based on whether the land was used as irrigated cropping, dryland cropping, or rangeland/pasture. In addition to these 3 agricultural-based categories, 2 additional zones were used to define riparian forest/grasses and urban areas. The zones defined as irrigated in 2005 were predominately corn and soybeans, two crops that have similar crop irrigation requirements throughout the growing season.

The justification for grouping crops in the irrigated areas is based on the fact that typically, corn and soybeans are rotated seasonally. All conditions (soil, precipitation, slope, application of irrigation water) being equal, slight differences in movement of soil water towards the water table likely exist between corn and soybeans based on their crop irrigation requirements and timing of peak consumption rates. Despite these differences, it is assumed that whether corn, soybeans, or other less common crops occupy an area, the rate of infiltration through the unsaturated zone will be distinctly higher under irrigated lands regardless of the crop type when compared to dryland crop areas (Scanlon and others, 2005). This condition occurs because of higher soil moisture content under irrigated lands throughout the growing season, thus creating conditions of higher likelihood of excess soil moisture moving downward when precipitation events occur on the irrigated crop areas (Dugan and Zelt, 2000). Also, as indicated by Figure 4, it is assumed that since 2001, with respect to bulk water movement from the land surface to the water table, the pattern of land use practice in the study area has remained relatively consistent, as the 2001 and 2005 land-use maps show similar cropping practices and overall extent of cropped land. It is expected that these three conditions (irrigated, dryland, rangeland) at the land surface over the last decade have created three distinct zones of recharge. When land is converted from rangeland or dryland cropping to irrigated, farmers will likely continue to irrigate crops on a consistent basis after making the investment in irrigation infrastructure.

Dryland area crops are primarily small grains and summer fallow, although, a small number of dryland corn and alfalfa acres are present in the study area. Based on the relatively consistent pattern of crop types on dryland acres, it is assumed that only small differences exist in potential recharge based on crop types in the dryland zones. Similar to crop rotation under irrigated land, dryland areas where wheat is grown are rotated between fallow and active for maintenance of soil moisture. It is assumed that over time, the average rate of recharge to the water table under dryland acres is relatively consistent even with the alternating pattern of active and fallow acres.

Range/pasture areas are the third of the agriculture-related land use zones. As indicated in Figure 4, a large portion of the southeast quarter of the study area is range/pasture. The use of this land as primarily pasture is based on the sandy soils that persist over much of the area. These sand soils have low soil moisture holding capacities, a condition that is essential for growing crops in this area of the high plains. Short grasses are present in the range/pasture areas, but like the sand hills north of the Platte River system valley, a high recharge potential exists due to the sandy soils. A minor amount of range/pasture land occurs in the southwest quarter of the study area, although these areas have loess-derived soils thus are expected to have lower recharge potential than the range/pasture areas in the sandy areas.

## Use of Diverse Data as Observations

Observations of true field conditions are essential for calibration of any natural system. Often, as the number of observations increases, particularly observations of different system features, the estimates of optimal parameter values are more reliable (Poeter and Hill, 1997). For the GGS-SR study area simulations, 4 different observation types were applied in the calibration process.

Weights are associated with each observation to reflect its uncertainty and to render the residual dimensionless so that residuals from all types of observations can be summed. Some observations are more reliable, whereas others may be less reliable due to uncertainty associated with their measurement. An example of this is a hydraulic head measurement which is determined as land surface elevation, plus casing stick-up minus depth to water. The elevation of the land surface at one location may have been determined from a precision survey, while another may have been estimated from a topographic map with 20 ft contours. The first may be known to  $\pm 0.01$  ft while the latter is on the order of  $\pm 5$  ft. Weighting also creates consistent units for observations of different types of measurements (Hill and Tiedeman, 2007). For example, if measurements of both head (ft) and flow ( $\text{ft}^3/\text{s}$ ) are included in a model, then the squared residuals will have different units of  $(\text{ft})^2$  and  $(\text{ft}^3/\text{s})^2$  so it is not valid to sum the squared residuals. The measurement variance of such observations reflects their uncertainty (larger variance indicates greater uncertainty) and has units of  $(\text{ft})^2$  and  $(\text{ft}^3/\text{s})^2$  respectively. By using the inverse of the measurement variance to weight the squared residuals then measurements with large uncertainty are given small weights and the squared residuals are dimensionless, thus it is valid to sum the weighted

squared residuals. Further discussion of weights is provided later in this report. A description of each of the four types of observations used in the models is provided in the following subsections of this report.

### **Groundwater Levels**

Groundwater levels were available from both near-site and outer model areas. Forty locations in the outer model area (Figure 15) provided seasonal (fall and/or spring) measurements, but no one location had a period of record extending through the entire transient simulation period (2002-spring 2007). For example, in the outer area observations, 15 of the 40 locations had seasonal measurements only for the years of 2002 and 2003. Most of the outer-area observations are south of the Platte River-system valley. Unfortunately, there were large areas where no groundwater level observations were available, particularly in the southwest quarter of the model in Perkins County and between Sutherland Reservoir and the eastern model boundary. The outer-area observations were measured manually either on a seasonal (fall and spring) or annual basis. The lack of surveyed ground surface elevations was factored into the uncertainty associated with these observations.

In the near-site area, an abundance of groundwater level observations were available from 2004 to 2007 at NPPD observation and monitoring well locations. At the observation nests (red triangles in Figures 15 and 16), daily observations from continuous data recorders were available for the observation wells (Figure 15) at both the shallow and deep screened wells. With 2 wells at 7 nests recording groundwater levels on a daily basis for nearly three years, several thousand groundwater level observations were available for use in the calibration. However, it was decided that daily values provide redundant information. In order to create a smaller dataset of observations with intervals short enough to capture changes in groundwater levels, observation values were averaged over 7 days for the deep wells only during the summer months and averaged over one month intervals during the winter months. At the geochemistry monitoring well nests (gold triangles in Figure 15) seasonal manually measured observations were obtained from the TPNRD. In total, 716 individual head observations were used in the transient model calibration process.

### **Surface Water Flows**

Groundwater contributions to surface flows (baseflow) in the South Platte River and drains were used as flow observations for the calibration (Image 7 and Figure 17). Observations were obtained from both historic records and measurements from staff gages installed at accessible locations within the study area in 2006. Applegate Drain (no. 2 on Figure 17) uses a combination of historical NDNR records from 2004 to mid-2005 and monthly stage-discharge observations made by NDNR technicians for the period from June 2006 until April 2007. The South Platte River observations used a combination of NDNR measurements at the cities of North Platte and Roscoe and the Nebraska DNR stage-discharge observations near the city of Sutherland. Measurements were not obtained during the months of December 2006 and January 2007 at all of the sites due to frozen channels or inaccessibility due to poor road conditions. Using both archived data and measurements made during the study, a total of 54 observations of groundwater outflow to drains and 11 observations of groundwater outflow to rivers were applied in the calibration process.

NDNR personnel determined flows at the gage locations using the conventional current-meter method with USGS-approved AA and Pygmy flow meters (Jim Retchless, NDNR, personal communication, 2008). Flows measured at drains were considered to represent the groundwater contribution to flow at each drain above the staff gage location. Because measurements at the gages were made monthly, the possibility that surface runoff influenced the measured flow was evaluated (using local precipitation records) for the week prior to each measurement. If it was determined that a runoff event was likely contributing to a measurement, a lower weight was applied to that observation. For example, the February 2007 measurements on Hershey Slough, Beer Slough, and Fremont Slough all indicated a likely presence of surface water runoff. These higher than normal flows coincided with warmer temperatures following large snowfall events in the area earlier in 2007.

Groundwater contribution to surface flow in the South Platte River was estimated for two separate reaches. Inconsistent dates of flow data between the existing NDNR gages (sites 7 and 8 on Figure 17) in the 2002-2007 timeframe proved to complicate the ability to calculate flow observations for the South Platte River. However, the addition of staff gage locations on the South Platte River near Sutherland

allowed for estimation of baseflow for selected points in time along two separate reaches of the river. The flows during the fall and winter months of 2006-07 at the gages placed near the town of Sutherland



IMAGE 7. Flow measurement location of Fremont Slough (site 3 in Figure 15), looking upstream. Image taken in May 2006.

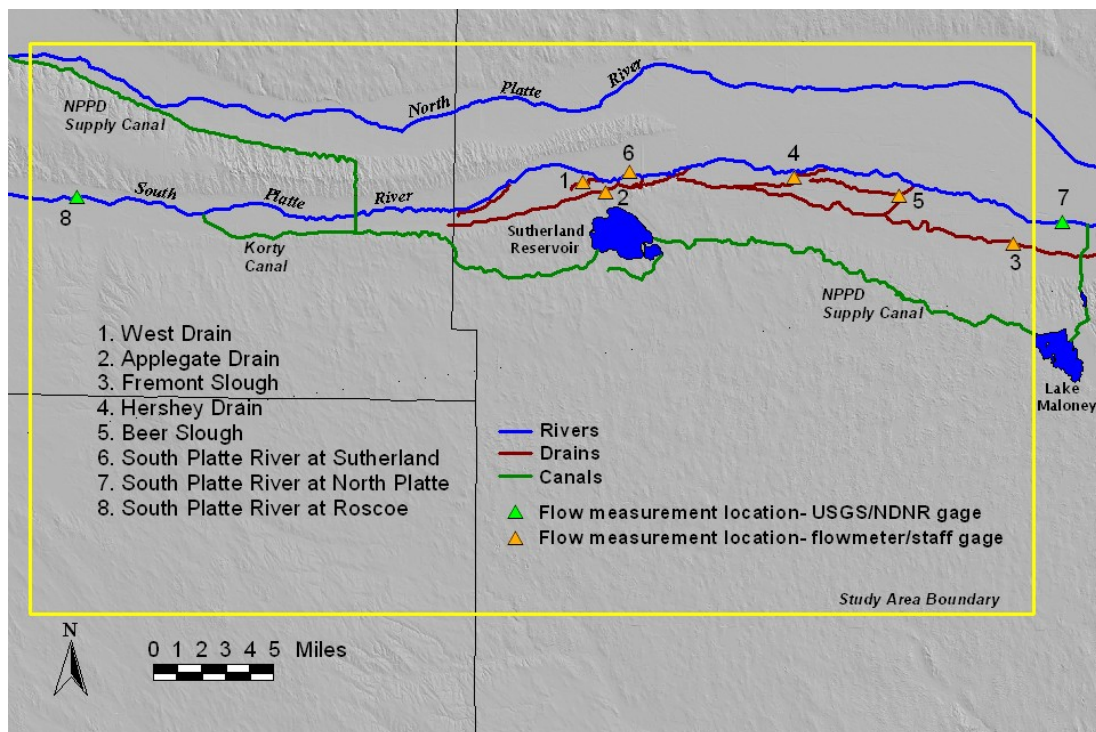


FIGURE 17. Map of study area showing locations of drain and river flow observations. All locations indicate staff gages installed in May of 2006 with the exception of no. 7, which is a NDNR gage station.

(Figure 17, site 6) were considered the baseflow of the river at that time due to few precipitation events occurring in that time period and the lack of runoff from irrigated fields since little to no irrigation occurs during the fall and winter months.

The upstream reach of the South Platte River between the gage near Roscoe (Figure 17, site 8) and Sutherland (Figure 17, site 6) had an observation for seven points in time in 2006 and 2007. This reach was potentially complicated by the presence of the Korty Canal diversion approximately 5 miles downstream of the Roscoe gage. However, due to low flow conditions at Roscoe, diversions were not occurring at Korty Canal during the time of the observations. For 4 of the 7 observation dates, the South

Platte River at Roscoe did not flow, and two other dates had less than 5 ft<sup>3</sup>/s. These conditions allowed simple determination of baseflow for 6 of the 7 observations because the upstream flow was considered zero thus all flow at the Sutherland gage (minus the inflows from Applegate and West Drains) was considered baseflow. For the one observation with flow at the Roscoe gage (April 2007), a smaller weight was assigned to the observation to reduce the influence of a likely surface runoff component present from a relatively significant precipitation event occurring in the two days prior to the NDNR measurement at Sutherland (NWS records indicated 2.84 inches of rain from April 22-24 at the Kingsley Dam station).

The observed baseflow for the downstream reach of the South Platte River (between sites 6 and 7 on Figure 17) was determined using the same method as the upstream reach by subtracting the flow between the NDNR gage at the city of North Platte and the combined north channel and south channel flows measured at Sutherland by NDNR technicians. Tributary inflow from Hershey Slough and Beer Slough was subtracted from the outflow value to ensure only the groundwater contribution to flow was used in the analysis. The NDNR gage at North Platte is approximately 1.5 miles downstream of the eastern model boundary, so it was assumed that this distance was negligible in calculating the overall contribution of groundwater to surface flow over the entire 22 mile reach of the river.

After examining the hydrographs of the measured values at site 6 (Figure 17), it was determined that four dates represented baseflow conditions, three fall flow dates in 2006 and the April 2007 measurement. Two more dates, December of 2006 and January 2007 were likely 100% baseflow as well, but upstream measurements for this reach were not available. Although the surface flow measured at North Platte for this reach is typically much higher than at the upstream gage, subtraction of surface water inflows from drains over this reach indicated an average baseflow of 33.9 ft<sup>3</sup>/s in the fall of 2006 and 60 ft<sup>3</sup>/s in April 2007. Observations on this reach were given a smaller weight due to the fact that several ungaged ditches and an unnamed drain about 1 mile downstream of site 6 empty into this reach of river. This unnamed drain empties into the South Platte at a location that is inaccessible by automobile and is located on private property. A formal method of estimating flow in this drain was not available. However, examination of this area on Google Earth indicated that the stream appeared to have a flow and width similar to that of Hershey or Applegate Drains. Without flow estimates from these drains and ditches, greater uncertainty exists in what portion of the flow measurement at North Platte was contributed by groundwater, thus justifying the application of smaller weights for observations of this reach on the river.

### ***Reservoir Stages***

Daily records of stage of the Sutherland Reservoir managed by NPPD provide a third type of observation for use in the calibration. Daily observations were used for every day that a stage was available, creating 1851 stage observations. Short intervals of missing data existed in the NPPD records during the simulation timeframe. Observations of reservoir stage were assigned small uncertainty because even with potential error from measuring equipment or wind forcing waves to artificially raise the water level near the gage, the true stage was likely to be relatively close to the measured value.

### ***Water Age***

The fourth type of observation utilized for calibration was based on the apparent age of groundwater measured at the geochemistry monitoring well nests (Image 8). The USGS investigation of the geochemistry in the GGS-SR area provided estimates of groundwater ages using the tritium/helium-3 (<sup>3</sup>H/<sup>3</sup>He) method. In order to use groundwater age as an observation, additional information on mixing of water in the subsurface was needed. Fortunately, the USGS study also analyzed groundwater and surface water samples for chloride and sulfate concentrations, as well as stable isotopes of water, which were used to determine mixing ratios of groundwater and surface water within the aquifer (Image 9). Several wells sampled in the monitoring nests contained water that was 100% reservoir water. One hundred percent reservoir water was present at all shallow wells and 2 mid-depth wells in the monitoring nests. Only apparent ages from wells containing 100 % reservoir water were used in the calibration procedure.

To use this information for calibration, it was assumed that the age of the water indicated the average time required for a drop of water to move from the reservoir through the aquifer to the screen of the monitoring well. The process of water movement was simulated using a particle tracking code that is discussed later in this report in the section on model construction.



In all, four types of data were use to calibrate the alternative conceptual models. The data are summarized in Table 1.



IMAGE 8. Geochemistry monitoring well nest 3 (MW-3 on Figure 12). Photo taken in May 2006.

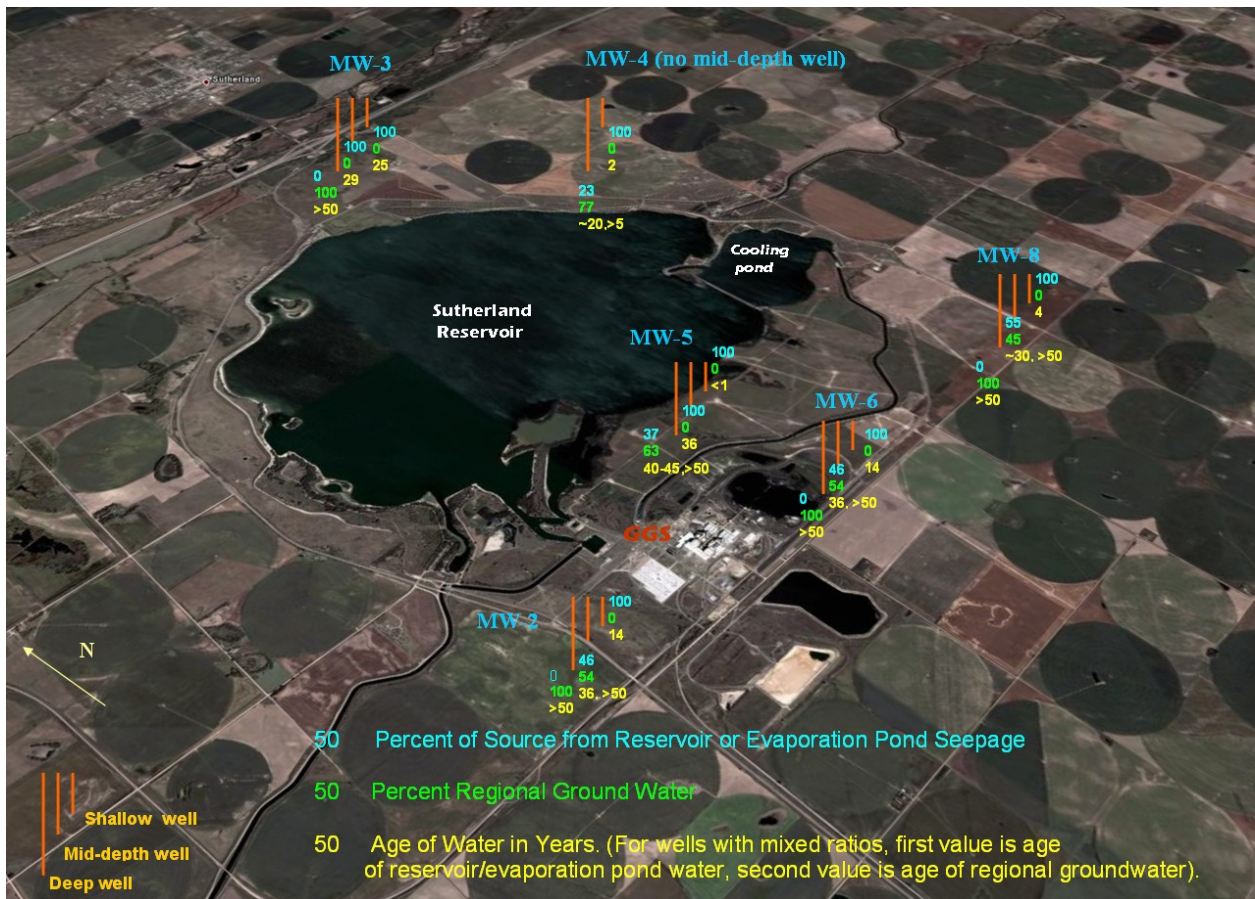


IMAGE 9. Aerial view of geochemistry monitoring well locations in the near-site area with percentage of source water and estimated apparent age of sample at each well nest.

TABLE 1. Summary of observation information used in the calibration of the numerical models of the study area.

Observation Type	Number of Observations	Observation Source
Groundwater levels	657	NPPD continuous pressure transducers, TPNRD manual measurements
Surface flows	59	NDNR surface flow meter measurements
Reservoir stages	1852	NPPD- continuous stage recorder
Apparent groundwater age	6	USGS- geochemistry analysis

## Multiple Conceptual Model Development

This section discusses the conceptual models considered for this project. First generic information on conceptual models is provided. Then the strategy for conceptual model development for the GGS-SR study area is presented. Finally, the alternative models evaluated by this project for the GGS-SR study area are described.

### ***Concepts of Modeling Natural Systems***

Numerical groundwater models are mathematical approximations of true aquifer systems. Simply put, the approximation is an attempt to fit an equation to field observations. One can compare this with an attempt to fit a model (e.g. the equation for a line or a polynomial curve) to data. If there is any error in the measurements or shortcoming in the ability of the equation to represent the system there will be non-zero residuals (a residual is the difference between a measured value and the value calculated using the equation) due to an imperfect fit (Figure 18, box A). If complexity is added to the equation, the model may more accurately fit the observations (Figure 18, box B), but it may be fitting the errors in the measurements rather than the behavior of the system and so may result in larger predictive uncertainty. For groundwater models, the term complexity refers to the number of parameters required to define the model. This condition of simplicity vs. complexity is arguably the most fundamental question that confronts hydrologists when modeling any type of hydrologic system. What is at stake is the predictive capability of the model, as model complexity reaches the threshold where improved model fit worsens the predictive capability of the model (Figure 18, box C), (Hill and Tiedeman, 2007). For example, if the y-axis of Figure 18 represented temperature and the x-axis represented the height of mercury in a thermometer we can see that fitting the data with the complex model would indicate that sometimes the temperature is lower when the height of mercury is larger, but this would be an artifact of over fitting the data.

Due to uncertainty in flow system characteristics such as the heterogeneous nature of geologic materials, an exact representation of an aquifer system can never be attained. As suggested by Hill (2006), *“Models are not built to represent all details of a field site, nor is that possible or even necessarily desirable. Model goals need to be addressed within the context of the data available, the system processes and characteristics about which the data provide information, and the predictions of interest.”* The general consensus in groundwater modeling science as suggested by Hill (2006) is to implement the principle of parsimony, which is a strategy that keeps models as simple as possible, adding only enough complexity to a model to improve the fit to observations without reducing predictive capability. In simple terms, it is the attempt to find the middle ground between a simple and complex model that allows the most accurate predictions.



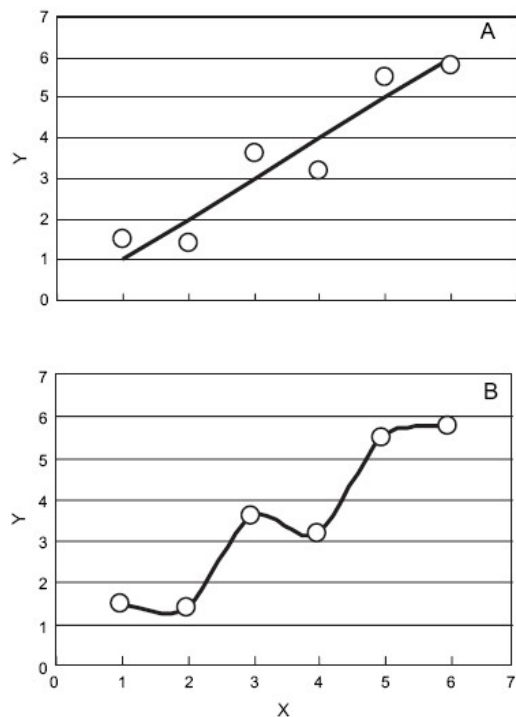
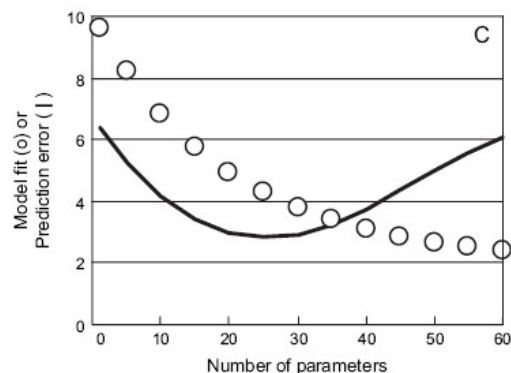


FIGURE 18. Three graphs showing a linear model fit (A), a more complex model (B), and an example of the tradeoff between the accuracy in predictive capability and complexity in a model (C) (from Hill, 2006).



### Conceptual Model Strategy

A conceptual model of a system defines the features (geometry, material properties, boundary conditions, and stresses) of a system that are expected to influence the flow system dynamics. If these features are important in representing flow for the calibration period, they are likely to be important to the simulations used for predictive analyses. Even the simplest aquifer systems that are composed of a relatively uniform material and well defined boundaries can have a great deal of uncertainty due to gaps in data (i.e. lack of observations in critical areas of the system). Given the inherent uncertainty associated with any numerical representation of a system, it is recommended that multiple conceptualizations of a flow system be developed and analyzed before predicting response to future system stresses (Poeter and Anderson, 2005). An *alternative model* is any model that has a different representation of hydrogeologic units, boundary conditions, or parameters. For example, two models of the same site location, one with specified flows on the boundaries that change in time and one with constant water levels maintained at the boundaries throughout the simulation would be considered alternative models.

The applicability of this approach cannot be understated in attempts to reliably model groundwater systems. Often times, managers are dealt large uncertainty with information presented to them from trial-and-error calibrated models, from which the range of uncertainty on parameters and predictions is not known. Given the many possible ways the character of the aquifer materials of the flow system in the GGS-SR and surrounding study area could be represented, their differing character is a prime target for defining multiple conceptual models. For example, management of surface water-groundwater interactions is an issue of great interest in the Platte River basin. The perception of model consumers can be a factor when determining how many layers a model should include in order to accurately simulate exchanges of water between surface features and the aquifer or for predictions of future impacts to river baseflow or aquifer drawdown. A common notion is that more model layers equates to a better model for assessing surface-groundwater interactions for alternative management scenarios. This approach has been explored by others in the past for other HPA-type settings, but not with UCODE\_2005 and associated analysis tools. For example, Sophocleous and Perkins (1993) used an inversely calibrated, two-dimensional model to assess impacts of groundwater pumping on a stream connected to a Pleistocene-age alluvial aquifer in central Kansas. Sophocleous and others (1995) also investigated the influence of grid size and heterogeneity of transmissivity in a numerical model versus the predictions of a homogeneous analytical model on stream depletion estimates in a hypothetical setting. This study ranked

the representation of aquifer heterogeneity as one of the top three factors influencing the rate of stream depletion in a numerical model simulation. However, the study did not explore the impacts of system dynamics on a field system nor did it explore the influence of calibration on parameter estimation and predictive certainty.

One of the primary goals of this investigation is to determine the most suitable models for predicting impacts of future water-use scenarios on the flow system in the study area by using multiple working hypotheses of the system. Thus multiple conceptualizations of the system are considered. Criteria are used to compare and rank the models in terms of the balance between the model complexity and the fit of model simulations to field data. This methodology provides insight for evaluating the appropriate level of model detail. For example, a comparison of five groundwater models of an alluvial aquifer in Switzerland (Foglia and others, 2007) was conducted using some of the criteria applied in this investigation (AICc, BIC, and SSWR as discussed later in the model calibration section). The models contained 1 to 6 parameters for Kh. The criteria demonstrated that the model with three Kh parameters provided the best trade-off between the complexity of the model and the fit to observed data (Figure 19).

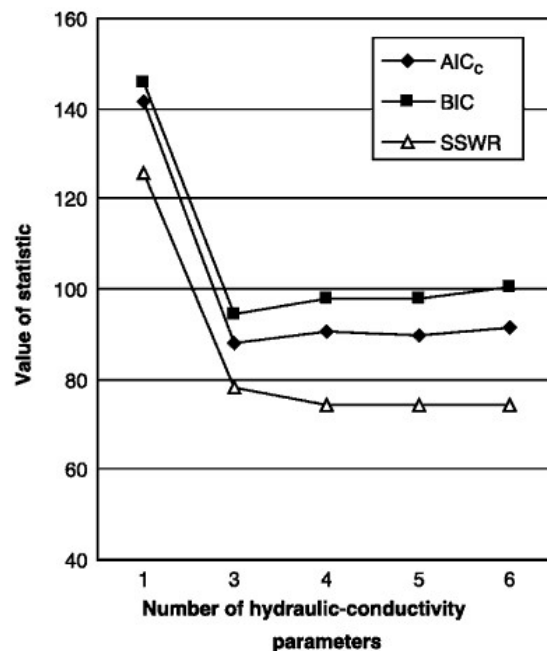


FIGURE 19. Example results from a multi-model comparison of simulations using different numbers of hydraulic conductivity parameters to represent an alluvial aquifer setting in Switzerland (Foglia and others, 2007).

Rankings based on the criteria indicate the “best” model in a suite of alternative conceptualizations. However, since the “best” model may not account for all the uncertainty in a site conceptualization, model parameter estimates and predictions can be averaged from multiple models (Poeter and Anderson, 2005). This is particularly effective when no one model is clearly superior to others in the suite of ranked calibrated models, and an averaged prediction accounts for the uncertainty present in all of the models used to determine the predictive value.

### ***Initial Site Conceptualization***

Characterization of the groundwater flow system within the study area was conducted to identify the major system features, flow patterns, and stresses to provide guidance for developing tractable, well-posed, site models. In general, the major controls on how well the numerical representations of the system match the observations are 1) how much and where water enters and leaves the flow system and

2) the hydrostratigraphic characteristics that control flow and storage of water as it moves through the system. Figures 20 and 21 provide a graphic representation of large-scale processes that are considered to be important to the conceptualization of the system's water budget. The major inflow components of the system are cross-boundary movement into the area from the west, entry of river water into the aquifer in losing reaches of the South Platte River, variable precipitation-based recharge, and recharge from reservoir/canal seepage. Major outflow components of the flow system include cross-boundary movement towards the east, extraction of water from the aquifer to industrial, irrigation, municipal, and domestic wells, movement of groundwater to rivers and drains, and removal of shallow groundwater from the system via evapotranspiration. Each process was accounted for in the numerical representation of the various site conceptualizations by defining each as a specific type of boundary condition.

Given the importance of these controls on system dynamics, the conceptualization of the hydrostratigraphy and groundwater recharge received the most emphasis in the development of each conceptual model. The following sections describe how each of the system characteristics was considered in the process of creating the suite of numerical models of the study area.

### ***Groundwater Movement***

As indicated by Figures 8 and 9, the water table contours indicate groundwater flow in the study area is generally from west/southwest to east/northeast. The contours also indicate a groundwater flow divide in an east-west orientation across the southern portion of the study area. South of this divide, groundwater flow direction is towards the Republican River basin. The west-to-east movement of water is through the unconfined sediments of the Ogallala Group and overlying undifferentiated Quaternary deposits. Groundwater flow exiting the model area occurs primarily across the eastern boundary and groundwater discharge to the South and North Platte Rivers and the engineered drains that exist between the South Platte River and the Sutherland Project canals.

Near the middle of the study area, Sutherland Reservoir plays a significant role in altering the dynamics of the west to east component of groundwater flow. The stage of Sutherland Reservoir is above the regional water table for a radius of more than 5 miles in any direction from the reservoir. This elevated water level has created a groundwater mound with local components of groundwater flow near the reservoir that deviate from the regional flow pattern. To the west of the reservoir, regional groundwater flow is deflected northeast or southeast. Although the flow system in the study area is considered unconfined, local semi-confined conditions may exist due to local occurrences of fine-grained geologic units. Water level observation nest 1 (Figure 16), installed by NPPD in late 2004, had an increase in head of nearly 8 feet between its shallow well screened between 40 to 50 ft below land surface and the deep well screened near the bottom of the aquifer at 250 ft below the land surface. During drilling of the deep piezometer at nest 1, the well flowed at 62 gallons per minute. Of all the wells drilled in for the well field project, this nest was the only location that exhibited artesian conditions.

Relatively steep gradients in hydraulic head emanate from the reservoir in all directions, with the strongest gradients flowing towards the north and northeast. These gradients are further evidence of the strong connection of surface water stored in the reservoir and the underlying aquifer. Southward flow of groundwater from the reservoir moves in an easterly direction about 2 to 3 miles south of the reservoir.

The geochemical survey conducted by the USGS provided further support for the conceptualization of groundwater flow deduced on maps of the piezometric surface including the vertical flow components within the near-site portion of the model. Chemical and isotopic data from water sampled in 2006 (McMahon and others, 2009 in review), indicate that reservoir water is present at all of the shallow and mid-depth monitoring wells within the near-site area, confirming that vertical flow is present beneath the reservoir and outward in the north, northeast, south, and southeast directions. However, reservoir water was present in only two of the 6 deep wells. The deep well at nest 5 (Figure 16) showed that just over one-third of the water sampled near the base of the aquifer originated as reservoir seepage. Nest 5 is less than 1000 ft from the reservoir shore, thus indicating the influence of vertical flow immediately beneath the reservoir. The deep well at monitoring nest 4 also shows a presence of reservoir derived water. This is likely due to the highly permeable sediments in both the Quaternary and upper-Ogallala Group that are in direct connection with the reservoir. These deposits convey water northeasterly with a downward vertical component of flow as the reservoir seepage enters the aquifer and flows towards the South Platte River. The apparent age of water in the deep well of nest 4 is approximately 20 years,

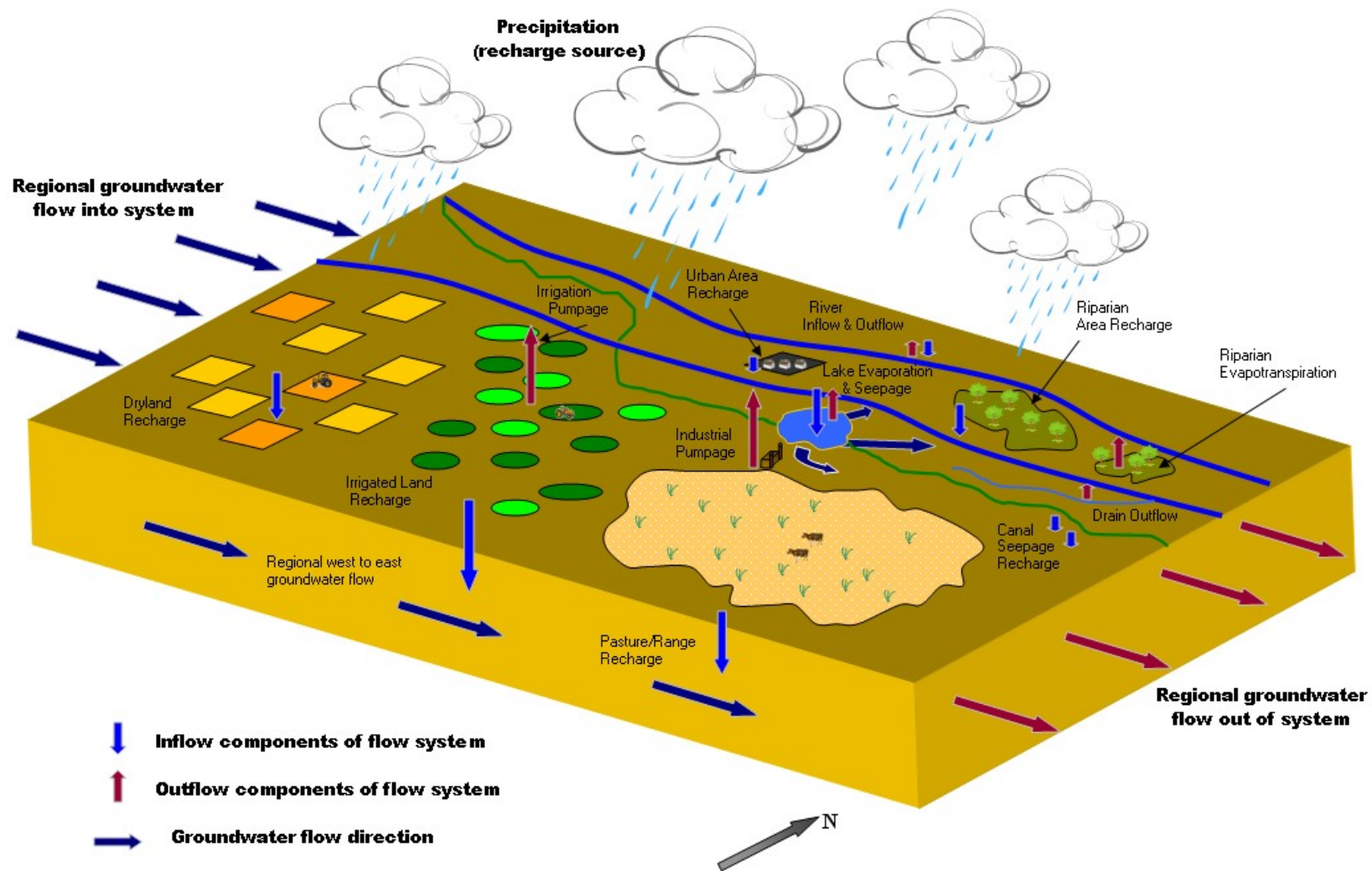


FIGURE 20. A graphic conceptualization of major influences on the movement of water through the GGS-SR study area.

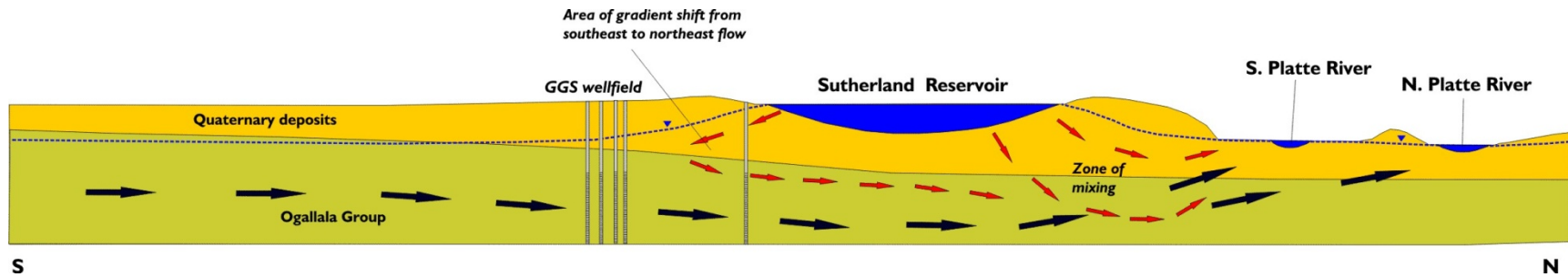
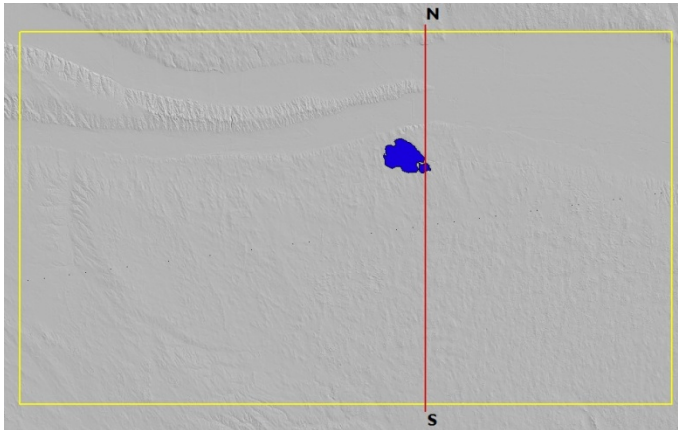


FIGURE 21. North-south cross-section of study area indicating the general direction of lake seepage and ground water flow near Sutherland Reservoir, based on the ground water-level map (Figure 7) and ground water ages shown in Image 9. The area of gradient shift (red arrows on south side of reservoir) is the area southeast of the NPPD property line in Figure.7.



Location of above cross-section relative to Figure 20.



as compared to water that is approximately 2 years in age at the shallow well of nest 4. This difference in age could indicate either different locations of seepage entering the aquifer through the reservoir bed, or different lithologies within the aquifer controlling flow velocity. Of the four deep wells without reservoir-derived water, three are located along a west-to-east transect approximately 1 mile south of the reservoir. In all of these wells, the water source is the regional aquifer and the water is more than 50 years old. The transect of wells is located on the fringe of where the wedge of coarse Quaternary sediments pinches out, as indicated by no Quaternary sediments in nests 6 and 8 and only 12 ft of such sediments in nest 2. In addition to the lack of permeable Quaternary units, thick zones of fine, unconsolidated to semi-consolidated sediment are present at these locations. It is believed that the lack of permeable Quaternary sediments in this portion of the near-site area, impedes reservoir seepage from reaching the base of the aquifer, thus it flows south-southeasterly through coarse zones in the upper-Ogallala Group where the source water in shallow wells is 100% reservoir water. The deep well at nest 3, approximately 1.25 miles north of Sutherland Reservoir and less than 2 miles northwest of nest 4 (which contains mixed-source deep water) also contains 100% regional aquifer water. Located in an area just north of a very steep gradient of groundwater flow north of the reservoir (Figure 9), where the source water would be expected to be primarily reservoir-derived, the presence of regional water only at the deep well suggests that this area is a zone of regional aquifer discharge that feeds the South Platte River. Additional evidence that this area is a regional discharge zone is the upward vertical gradient measured at the three wells of nest 3.

A general north-south cross section of the aquifer near Sutherland Reservoir (Figure 21) shows the general direction of both reservoir-derived (red arrows) and regional groundwater movement (blue arrows) in the vicinity of the reservoir. Flow also occurs toward and away from the viewer of the cross-section. In this area the groundwater ages and mixing ratios indicate regional groundwater discharges to the South and North Platte Rivers.

The distribution of source water components indicates that seepage of reservoir water enters permeable sediments at shallow and mid-depth zones (less than 200 ft below land surface) in the aquifer and develops a more horizontal flow component at these depths. This condition likely exists due to coarse Quaternary and upper Ogallala Group sediments providing preferential horizontal pathways as seepage travels in the north, east, and south directions from the reservoir above tighter, less permeable zones within the lower Ogallala Group.

## ***Recharge***

In many studies of unconfined groundwater flow systems, quantification of recharge to the water table from infiltration through the overlying unsaturated zone is one of the most poorly constrained budget items in the conceptual model. In most systems, uncertainty exists in the rate, timing, and spatial distribution of recharge to the water table. Several factors influence this process, including local precipitation rates, vegetation, land slope, land-use practices, soil texture, and thickness of the unsaturated zone. Conceptually, the primary source of water for recharge across the entire GGS-SR study area is precipitation, but locally areas of higher recharge occur due to seepage from Sutherland Reservoir and the supply canal which contribute large volumes of water to the aquifer in the near site area.

Precipitation rates across the model average from 18 to 20 in/yr (Figure 3). Given this sometimes fluctuating yet relatively consistent water source, it is conceptualized that the processes and conditions at the land surface dictate the potential for precipitation to move past the soil root zone, travel through the unsaturated zone and eventually become groundwater recharge. Although annual precipitation rates vary from year to year and the occurrence of droughts on the High Plains are well documented, the conceptualization of recharge for this study is that although annual pulses of unsaturated zone flow will vary, these fluctuations are overwhelmed by the difference in recharge rates that occur because of different processes occurring at the surface. This assumption removes the uncertainty associated with attempting to simulate the timing of variable rates of unsaturated zone flow that occur through highly variable sediments in the non-saturated Quaternary deposits or upper Ogallala Group.

Based on these controlling processes of recharge to the HPA, various recharge conceptualizations were tested to determine 1) the processes or land uses that are most influential on groundwater flow

system in the study area, and 2) which representation of surface characteristics provides the best match of simulated equivalents and field observations. Five conceptualizations were defined and are described in detail in the following sections. The conceptualizations range from a simple uniform recharge rate assigned to the entire study area to numerous zones based on soil type, land-use practice, and topographic conditions. The zones based on soils, topography, and land use practices are similar to one another in areal extent, but have different levels of spatial detail and complexity. The rate of recharge to any individual zone in any of the recharge conceptualizations was estimated as a percentage of average annual precipitation within the study area.

### Uniform Recharge

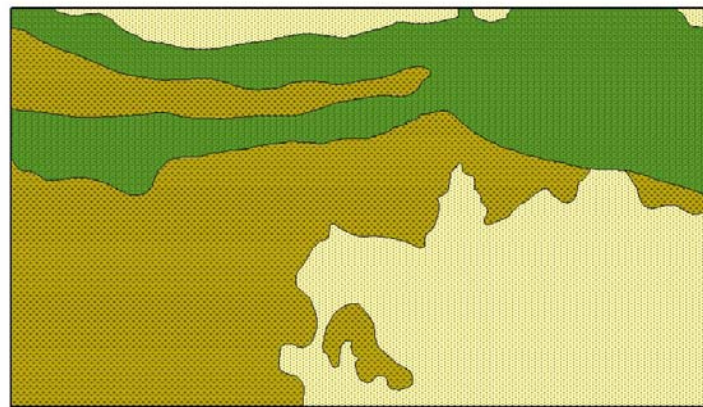
The first and simplest conceptualization is the application of a uniform recharge rate on the entire study area (identified as U in Table 1). Although a consistent rate of recharge on the entire model domain is unlikely, a uniform recharge rate serves as a base case in the process of increasing complexity. The calibrated rate of uniform recharge provides a base comparison to conceptualizations that contain spatial complexity. A water mass-balance investigation by Szilagyi and others (2005) utilizing GIS-based information on land cover, land and water table elevations, base recharge, and recharge potential indicated that most of the study area in this report receives 1.2 in/yr or less (6% or less of annual precipitation) of total recharge, with a small area in the alluvial valley of the Platte River-system receiving potentially 1.9 in/yr (over 10% of annual precipitation) of total groundwater recharge. Although the datasets used for determining these values in their investigation had spatial variability, the results indicated the magnitude of recharge to be relatively uniform in the study area.

### Topographic Regions of Recharge

The second recharge conceptualization is based on topographic regions (UNL-CSD, 1951) within the study area (map A, Figure 22). This configuration adds more complexity compared to a uniform representation, yet is still based on a generalized grouping of topographic characteristics. The three major topographic regions that serve as individual zones for calibration of recharge rates are plains, valleys, and sand hills/sand sheets. Plains are defined as relatively flat, upland areas with loess (silt) derived soils that contain relatively low runoff and allow for moderate infiltration of rainfall and irrigation water. Valleys are areas containing the major surface drainage features in Nebraska that have variable soils due the heterogeneous depositional patterns of the braided Platte River system. Depth to groundwater is relatively shallow in the valley areas and evapotranspiration rates are high considering the large amount of vegetation present in these areas. Sand hills/sand sheets are defined as areas of sand dunes stabilized by grasses. Dunes can vary in shape, size, density of vegetation, and typically have very high infiltration rates of precipitation. Low relief sand hills occupy most of the southeast quarter of the study area and are used primarily for grazing, although irrigated cropping is practiced in limited areas of this topographic region.

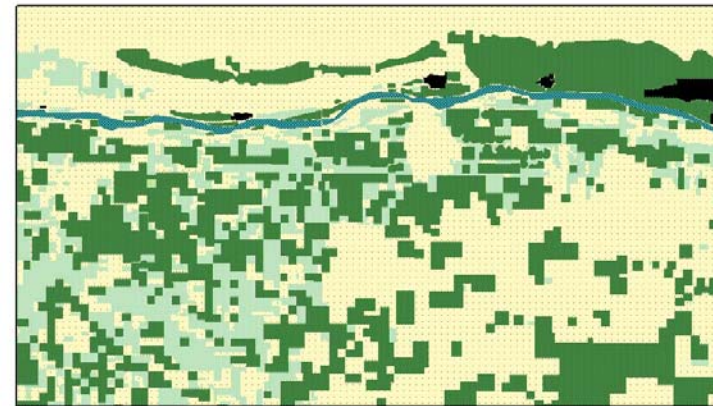
Estimated recharge rates in these areas vary widely depending on the methodology used for determining the rates. As reported in the uniform recharge section, a state-wide water mass-balance GIS investigation indicated rates can vary from 1 to 6 percent of annual precipitation rates. The High Plains RASA investigation (Gutentag and others, 1984) estimated recharge rates of pre-development (prior to widespread irrigated agriculture) rates of 0.06 in/yr (0.3 percent of annual precipitation) for the plains region based on trial-and-error calibration. Rates of 0.15 in/yr (0.8 percent of annual precipitation) were estimated by the COHYST modeling study (available on the Web at [http://cohyst.dnr.ne.gov/cohyst\\_preliminarydata.html](http://cohyst.dnr.ne.gov/cohyst_preliminarydata.html)). The Republican River modeling study applied recharge ranging from 0.97 to 1.29 in/yr (5 to 7 percent of annual precipitation) on the plains area of the model area and used values ranging from 2.68 to 3.25 in/yr (14 to 18 percent of annual precipitation) in the sand dunes portion of the study area (available on the world wide web at [www.republicanrivercompact.org](http://www.republicanrivercompact.org)).

Recharge values in the valley portion of the study area have been estimated to be higher than plains regions, but have greater variability due to vegetation and soil types. The estimated rate from the COHYST trial-and-error calibrated model was 0.9 in/yr (4.8 percent of annual precipitation) for areas defined as valleys.



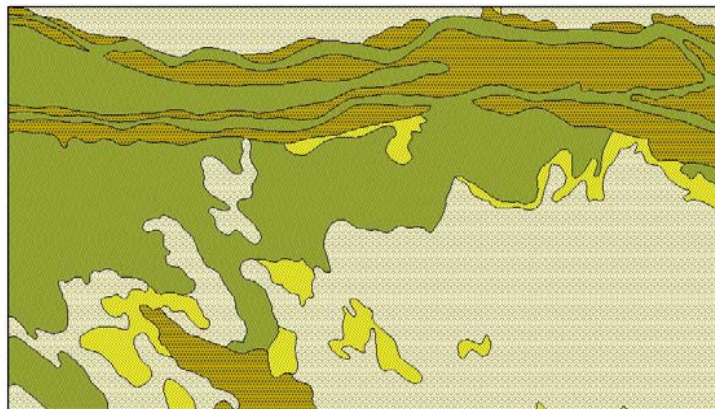
Plains  
Sand hills/dunes  
Alluvial valley

A.



Zone 1 (rangeland/pasture)  
Zone 2 (dryland agriculture)  
Zone 3 (irrigated agriculture)  
Zone 4 (riparian forests/pastures/wetlands)  
Zone 5 (urban areas)

B.



Zone 1 (0.01 - 0.10 in/in)  
Zone 2 (0.10 - 0.15 in/in)  
Zone 3 (0.15 - 0.20 in/in)  
Zone 4 (0.20 - 0.25 in/in)

C.



Dryland cropping on plains  
Rangeland/pasture in alluvial valley  
Irrigated cropping on sand hills  
Dryland cropping in alluvial valley  
Irrigated cropping in alluvial valley  
Riparian woodlands/pasture  
Irrigated cropping on plains  
Rangeland/pasture on plains  
Rangeland/pasture on sand hills  
Urban areas/municipalities

D.

FIGURE 22. Four of the five recharge conceptualizations of the study area: (A) topographic regions (B) major land-use zones (C) aggregate soils based on soil moisture capacity and (D) combined major land-use and topographic regions. Uniform recharge (U) is not shown.

Recharge estimates in sand hill areas have a wider range of variability than either the plains or valley regions. Szilagyi and others (2005), reported ranges of recharge rates in sand hill areas from 6 to 9 percent of annual average precipitation in the study area, although higher rates of recharge are reported in sand hill areas in the eastern portion of the Nebraska Sand Hills. A summary of model analyses reported in the High Plains RASA study indicated recharge rates ranging from 10 to 22 percent of annual precipitation in sand hill areas north of the study area (Gutentag and others, 1984). The model developed by the RASA study applied a rate of 1.07 in/yr (5.7 percent of annual precipitation) in the sand hills portion of the study area. A groundwater model investigation by Chen and Chen (2004) indicated that 13 percent of annual precipitation reaches the aquifer as recharge in the sand hills areas north of the study area. The COHYST simulation for this area applied a pre-development recharge rate of 2.5 in/yr in the sand hills north of the study area (13.5% of annual precipitation) and 1.5 in/yr in the sand hills/sand sheets in the southeastern portion of the study area (8 percent of annual precipitation).

### Land-use Based Recharge

Three major land-use practices exist in the model area (map B Figure 22) on the uplands south of the South Platte River valley that occupy nearly two-thirds of the model area. In this region, dryland cropping, irrigated cropping, and pasture/grassland for grazing livestock are the primary land-uses. It has been noted in several studies that recharge is likely to be influenced by cropping methods in semi-arid environments. Dugan and Zelt (2000) used a regional scale soil-water balance model of the High Plains region that took into account climatic factors, soil type, and vegetation to determine water potentially available as groundwater recharge. At Holyoke, CO (approximately 40 miles southwest of the western study area boundary), deep percolation under irrigated croplands was higher than dryland crop areas by an average of 24 percent for various crop and soil types. In addition to determining the greater potential for recharge on irrigated lands, the soil-water balance model work by Dugan and Zelt also indicated mean annual potential groundwater recharge exceeds two inches on irrigated land in the model area. Sophocleous and others (2002) tested pore water movement using heat-dissipation sensors and tensiometers in thick unsaturated zones in Kansas under both irrigated land and native grassland. Using both pore-water pressure-head gradient and Darcy's Law, recharge flux estimates were made at these sites and rates were found to be higher under irrigated land (0.1 in/yr and 0.02-0.04 in/yr for irrigated land vs. < 0.001 in/yr for grassland). At the same locations, the USGS conducted studies of geochemical tracer movement through the unsaturated zone. Using concentrations of tritium in the unsaturated zone pore water, it was determined that fluxes of water movement under the irrigated land test sites were 4-12 times greater than movement of water under the grassland location (McMahon and others, 2003). The USGS also conducted similar studies at three locations in the northern HPA to compare rates of pore water movement in thick unsaturated zones under irrigated corn fields and native grassland. The two irrigated sites at Perkins County, NE (< 5 miles southeast of the study area) and Yuma County, CO, had calculated water fluxes of 4.0 and 4.4 in/yr, respectively (21 and 22 percent of annual precipitation, respectively). Rates at both of these locations were higher than the rate (2.8 in/yr) calculated at Chase County, NE rangeland test site (McMahon and others, 2006).

In addition to these field studies determining groundwater recharge rates, Peckenpaugh and others (1995) calculated initial recharge rates for a variety of cropping lands from soil-water balance computer programs to apply in a groundwater model of the Upper Republican NRD which in-part occupies approximately one-fourth of the western portion of the study area. Deep percolation values from the soil-moisture balance programs (assumed to become groundwater recharge) varied for different crops under different irrigation conditions. Deep percolation for irrigated corn ranged from 0.62 in/yr (3 percent of annual recharge) on silty/clayey soils to 2.5 in/yr (13.5 percent of annual precipitation) on sandy soils. For irrigated small grains, recharge ranged from 1.5 in/yr (8 percent of annual precipitation) on silt and clay rich soils to 3.9 in/yr (22 percent of annual precipitation) on sandy soils. On dryland farming areas, the soil moisture balance code resulted in a range from 0.94 in/yr (5.1 percent of annual precipitation) on silt and clay rich soils to 2.5 in/yr on sandy soils (13.5 percent of annual precipitation). For small grains on dryland farming areas, deep percolation rates ranged from 0.04 in/yr (0.2 percent of annual precipitation) on silt and clay rich soils to 3.8 in/yr on sandy soils (21 percent of annual precipitation). It should also be noted that non-irrigated native-pasture deep-percolation rates ranged from 0.10 in/yr (0.5 percent of annual precipitation) on silty/clayey soils to 1.5 in/yr on sandy soils (8 percent of annual precipitation). These ranges provide insight into the variable rates that are likely to exist across the study area. Although some



of these rates vary considerably, the differences of recharge under the three major land uses are not expected to vary much by crop type considering the percentage of corn and soybeans planted versus other crops as described earlier in the report.

Conceptually, it is expected that dryland farming recharge rates would be higher than rates under native grasslands/pasture, and that recharge rates under irrigated croplands would be higher than either grasslands or dryland croplands. This condition was observed by Scanlon and others (2005) on the High Plains of Texas. This concept is based on the likely presence of greater soil moisture content in the root zone under irrigated land during summer growing time, thus creating a greater potential for precipitation on these lands to move soil water beyond the soil root zone (Dugan and Zelt, 2000). However, the conceptualization of potential recharge rates increasing with increased level of land use from pasture to irrigated crops could be modified for a large portion of the rangeland in the study area. In the southeast quarter of the model, sparsely vegetated sand dunes and sheets exist that are defined as rangeland. It is possible that large amounts of precipitation can enter the system as groundwater recharge in these areas. Image 10 shows the extent of these dune areas. These three types of major land use classifications were individually zoned for calibration of recharge rate in the numerical models based on 2005 satellite imagery from CALMIT (Figure 4). In the alluvial valley of the South and North Platte Rivers, land use is primarily irrigated or sub-irrigated cropping. The remainder of the land in the valley is riparian woodland/grassland or urban areas.

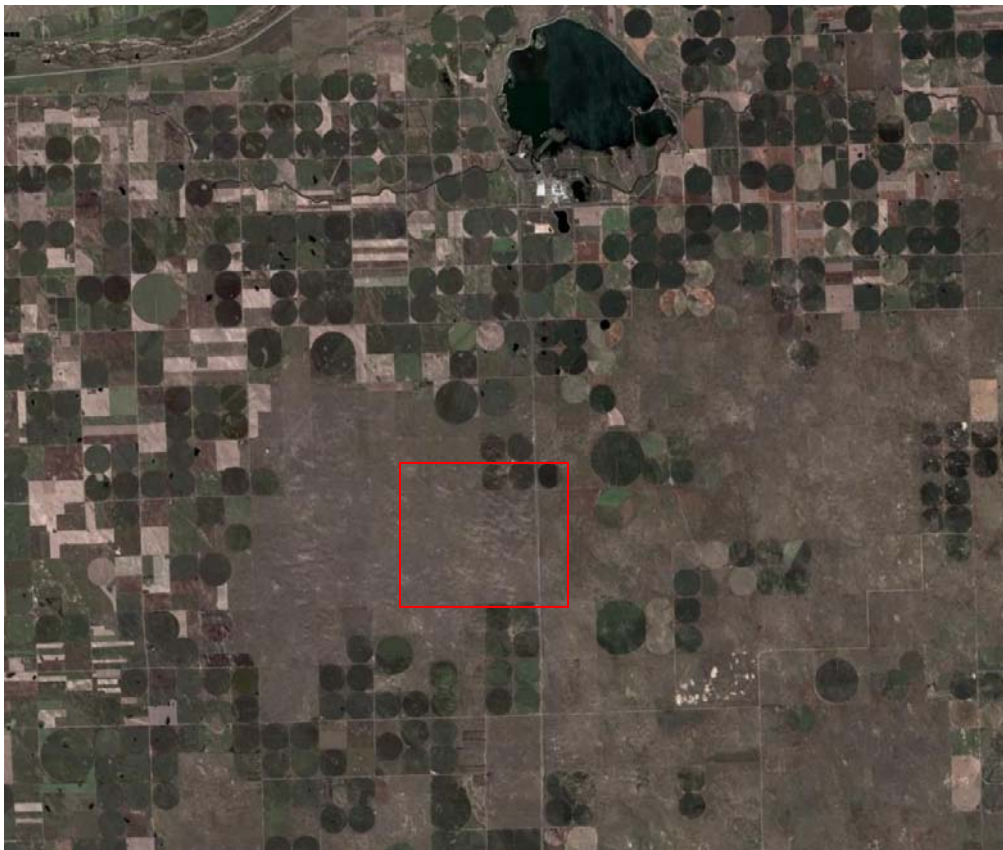


IMAGE 10. Aerial view of the sand dune area south of Sutherland Reservoir sampled from Google Earth. Linear and domal dunes are evident within the red box just south of the center of the image.

### Soil-based Recharge

Soil texture within the model area varies from loam to fine sand. Using GIS, soil zones based on the STATSGO database were grouped by soil moisture holding capacity values (map C Figure 22) and defined as unique zones in which recharge rates would likely be distinct for the particular group of soils relative to other soil types. Peckenpaugh and others (1995) used soil moisture balance calculations to determine that soil type can have strong influence on the amount of deep percolation that occurs under



various cropping types. Four major zones were created based on these groupings. Two dominant zones are present in the upland area, with zone 1 containing soils with the lowest soil moisture holding capacity, and zone 4 having the highest. Also present in the uplands are smaller zones of intermediate soil moisture holding capacities (zones 2 and 3). Zone 3 soils, which range from 0.15 to 0.20 inches per inch holding capacity, comprise most of the soils in the alluvial valley. Although these zones are similar to the topographic regions conceptualization, the zoning of recharge using moisture holding capacities offers more detail in the size and extent of the various zones (for example, low moisture holding capacity soils present in the southwest portion of the area), which are based on quantitative evidence as opposed to a qualitative classification of unique recharge rates as in the topographic regions.

### Combined Land-Use / Topographic Regions Recharge

The most detailed of the hypothesized recharge configurations (map D Figure 22), the combined land use/topographic regions map was defined using GIS tools. Estimation of recharge rates during calibration of this conceptualization of recharge distribution determines whether recharge rates on the major landforms vary by land use practices as well. Land-use was combined with topographic regions instead of soil-types to limit the number of categories that would be produced from a soils-land use combination, thus reducing the chances of defining insensitive recharge parameters. The combination of land-uses and the three major topographic regions resulted in ten unique recharge zones. Conceptually, irrigated land use on coarse soils of the sand dune landscape was expected to have the highest rates of recharge, while rangeland on plains (silty/clayey soils) and within the alluvial valley would have the lowest recharge rates. For the numerical models tested with this recharge conceptualization, four of the major land-use types were adjusted in the model calibration, and the remaining recharge rates were derived as a percentage of the adjusted values due to insensitivity or parameter correlation which are explained later.

### ***Hydrostratigraphy***

One of the more confounding questions when conceptualizing the High Plains aquifer for a groundwater model is how to adequately represent the stratigraphic variability in the model grid. From a regional perspective, the Ogallala Group can be viewed as one aquifer layer, as conceptualized by the High Plains RASA (Gutentag and others, 1984), or the Republican River Compact Administration (2003). Chen and Chen (2004) simulated the High Plains aquifer in the Nebraska Sand Hills (just north of the GGS study area) with two layers, with the Ogallala Group assigned to the bottom layer and all material above the Ogallala Group assigned to the top layer. Still others (Cannia and others, 2006) defined nine regionally mappable geologic units within the High Plains aquifer in Nebraska, although not all nine geologic units were present at any one location in the COHYST study region. Based on these examples, it is clear that numerous strategies can be used to numerically represent an aquifer in settings such as the deposits that comprise the HPA. Options include simplification of the geology/hydrostratigraphy by grouping materials together, or separating geologic units into several model layers based on specified criteria such as the lateral and horizontal extent of the deposit, similar texture/sorting of materials, or depositional history of the geologic deposits. Still another option is to create unique zones based on areas consisting of geologic deposits with similar hydraulic properties and assigning these zones to either simplified or detailed layer representations.

The multiple working hypotheses approach to this investigation provides the opportunity to explore these alternative methods for representing the HPA in a numerical simulation. Statistical criteria used in this study evaluate the balance between the level of complexity used to represent the hydrostratigraphy and the fit of simulated equivalents to field observations. Several representations of the aquifer were created based on the five hydrostratigraphic zones described in the section on Geologic Data. The representations range from simplistic homogeneous models with one hydrostratigraphic layer to heterogeneous three-dimensional (multiple hydrostratigraphic layers) configurations. The number and thickness of model layers and the presence of heterogeneity were evaluated.

### Outer Study Area Transmissivity Zones

Heterogeneity in the outer study area was based on aquifer information from the High Plains RASA study (Gutentag and others, 1984). Three zones were defined as illustrated in Figure 23.

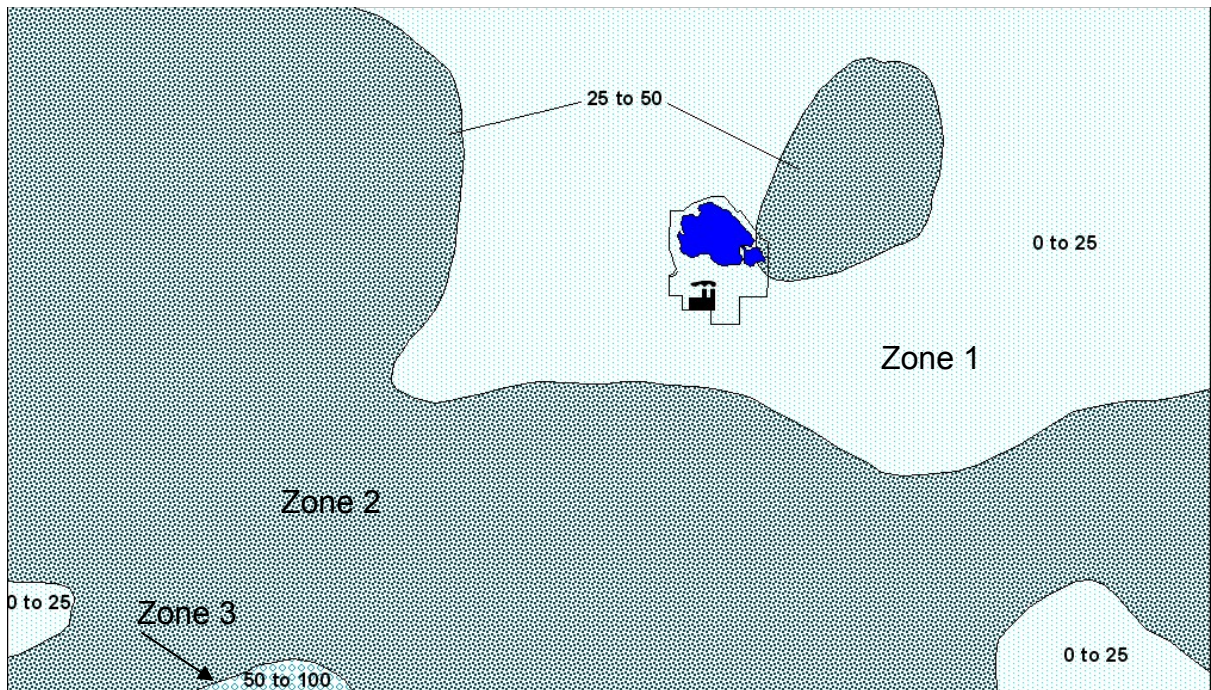


FIGURE 23. Hydraulic conductivity distribution from the High Plains RASA. The labeled zones refer to zones of homogeneous hydraulic conductivity to be estimated during calibration of models using this conceptualization. The two smaller zones with hydraulic conductivity ranging from 0 to 25 ft/d are parameterized as zone 1. The upper value of each range was used as the starting value for calibration of hydraulic conductivity (ft/d) when implementing this hydraulic conductivity representation.

### Near-site Transmissivity Zones

As described previously, the study area contains an abundant number of boreholes with detailed geologic information. Most of these boreholes are located in a small area in the vicinity of Sutherland Reservoir. Each borehole was analyzed in detail to identify major hydrostratigraphic zones in the near-site area of the model (Figures 24 and 25). Despite the significant variability in grain size, sorting, and cementation of the Ogallala Group both vertically and horizontally, continuous deposits of coarse, unconsolidated sediments (any material described in the lithologic logs as medium sand or greater in grain size or any sand/gravel combination) are present in the upper 200 feet of the group in the near-site area. These deposits are inter-layered with finer or semi-consolidated sediments in many boreholes, but vertically continuous zones of unconsolidated sands/gravels in the upper Ogallala with thickness greater than 40 ft were present in nearly all boreholes in the near-site area. It is assumed that these locations have higher transmissivity than areas where these extensive thicknesses of coarse deposits were not present. Within the upper Ogallala, two zones were delineated based on vertically continuous zones of coarse deposits: one zone with vertically continuous thickness of sands/gravels ranging from 0 to 40 ft, and a second zone with vertically continuous thickness of sands/gravels of 40 ft or greater. Some boreholes near the west side of the reservoir contained vertically continuous zones of coarse deposits of more than 140 ft within the Ogallala Group. Similarly, two separate zones were defined in the coarse Quaternary deposits based on vertically continuous thicknesses of sands/gravels above the Ogallala Group. These zones were mapped using GIS software and their associated value of Kh was estimated during calibration. These zones were applied to each type of grid described above. For two layer grid models, the Quaternary and Ogallala Group coarse zones are assigned to grid layers 1 and 2, respectively. For grids in which 2 layers are used to define the Ogallala Group, the Ogallala Group coarse zone is always assigned to the upper layer. For grids with 2 layers defining the Quaternary stratigraphy, the coarse zones were assigned to layer 2. For single layer grid models, only the Ogallala Group zones were assigned to the layer since the thickness of the Ogallala Group coarse zones are significantly thicker than the Quaternary deposits in the near-site area.



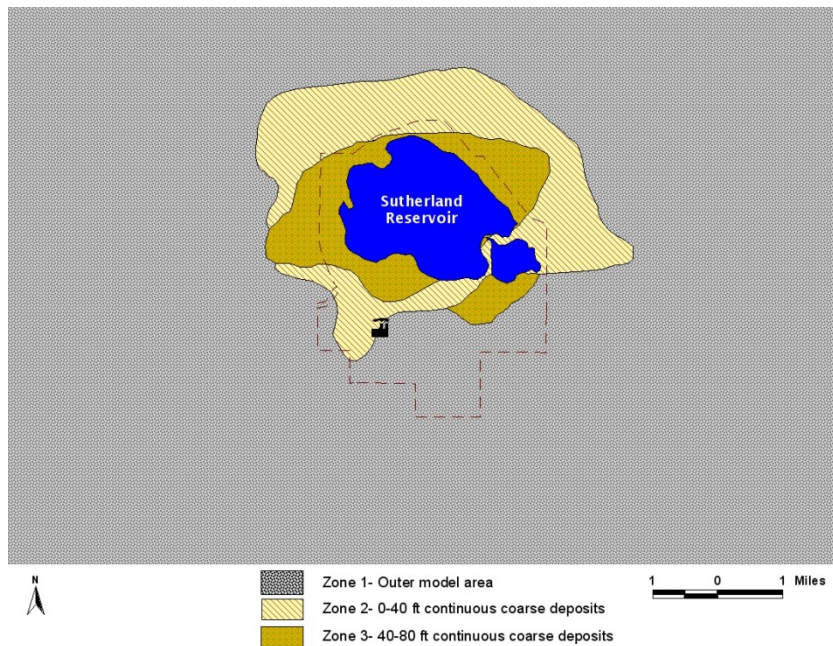


FIGURE 24. Unique hydraulic conductivity zones of the near-site area based on thicknesses of vertically continuous Quaternary-age coarse deposits. The dashed line is the NPPD property boundary.

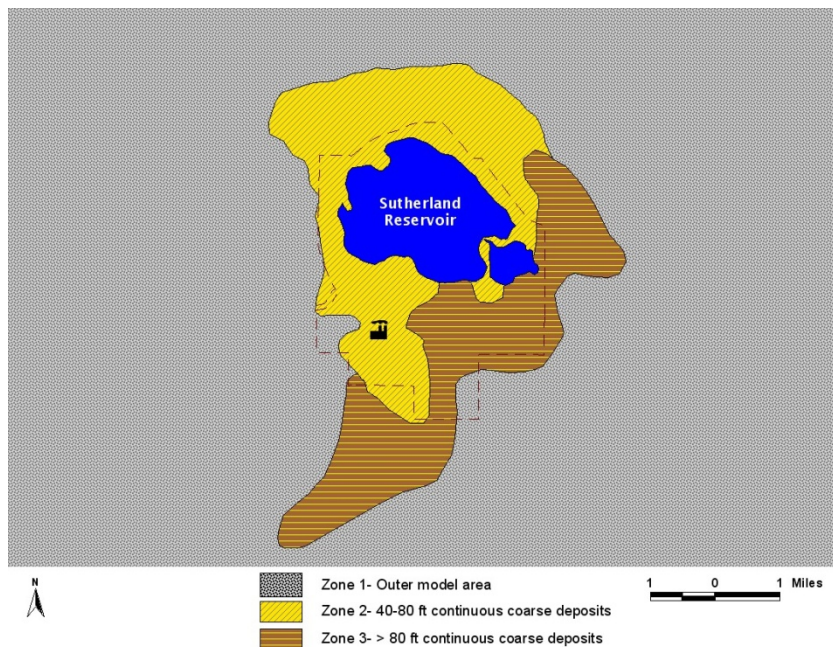


FIGURE 25. Unique hydraulic conductivity zones of the near-site area based on thicknesses of vertically continuous coarse deposits in the upper Ogallala Group. The dashed line is the NPPD property boundary.

### Initial Aquifer Transmissivities

Although model calibration provides optimal estimates of parameter values such as transmissivity, which is the product of  $Kh$  and thickness, starting values need to be input for  $Kh$  as a function of space and reasonable ranges of values need to be estimated to evaluate the validity of the optimized values. On a regional basis, Ogallala Group  $Kh$  values have been estimated to range from 0 to 100 ft/d in west central Nebraska. Locally, values of Quaternary alluvial units considered part of the High Plains aquifer range from 250 to 300 ft/d (Gutentag and others, 1984). For conceptual models with uniform  $Kh$  values

applied to the entire grid (2D models) or uniform values within entire layers, initial Kh values were based on average estimates of Kh from the High Plains RASA. These initial values were modified during the calibration process which is discussed later in this report. Estimates of aquifer Kh from tests of each well in the GGS well field were used to create an initial model input dataset with variable Kh values for the more heterogeneous alternative conceptual models. Transmissivities and storage coefficients were estimated from the aquifer tests using both the Jacob straight-line method (Fetter, 2001) for drawdown and recovery as well as curve-matching techniques based on the Theis method (Fetter, 2001) (personal communication with Hemenway Groundwater Engineering, 2/2/2007). Values from the Jacob method were generally higher than the estimated values from the Theis method. Therefore, average values were calculated for each well location as an estimated starting value for transmissivity and storage coefficient at that location.

Although each well in the NPPD well field is screened in the bottom 200 ft of the aquifer, the transmissivity at each well was divided by the total saturated thickness of the aquifer to determine the composite Kh at that location. These values were then interpolated from each well to the model grid to calculate initial Kh values at each model cell. However, given the concentration of data near Sutherland Reservoir and the limited amount of data in the outer study area, an alternate technique was applied to provide initial estimates of hydraulic conductivities in the outer-area of the model.

For the outer model area, few data existed for estimation of the spatial distribution of Kh with the exception of regional maps indicating generally uniform values as shown in the High Plains RASA study. The range of values of Kh in the outer area was estimated using well information from the NDNR registered well database (cohyst.dnr.ne.gov) as the quotient of transmissivity and thickness. Transmissivity was calculated from specific capacity (the quotient of sustained pumping rate and corresponding drawdown,  $Q/s_w$ ) as suggested by Driscoll (1986):

$$T = 1500 (Q/s_w) \quad (\text{equation 1})$$

T = aquifer transmissivity (gal/d/ft)

Q = constant discharge rate of well (gal/min)

$s_w$  = drawdown (ft) in well after 1 day of pumping at rate Q

The data-fields “gpm” and “pwaterlev” from the NDNR database were used for the Q and  $s_w$  terms, respectively. To obtain transmissivity values in units suited for calculation of initial Kh values at the irrigation wells, the values from the equation above were converted to units of ft<sup>2</sup>/d. Average transmissivity for over 1,200 wells in the study area was 11,410 ft<sup>2</sup>/d with a maximum of 250,688 ft<sup>2</sup>/d and a minimum of just under 1,000 ft<sup>2</sup>/d. Translated to Kh (by dividing the T term by the saturated thickness at the well location), the average Kh was 38 ft/d, with a maximum of 835 ft/d and a minimum of 5 ft/d.

These values for the outer model area were combined with values from the near-site well tests in the GGS well field to provide a complete set of points for interpolation of Kh values (Figure 26) to the model grid for some of the heterogeneous conceptual models. These serve as starting values for the calibration if the Kh is estimated or as fixed input values for Kh for simulations in which Kh was not adjusted.

### ***Conceptual Models of the Groundwater Flow System***

Based on the components of recharge and hydrostratigraphy described in the previous section and the characteristics of the groundwater flow system in the GGS-SR study area, a suite of models was developed based on various combinations of recharge conceptualizations A through E and hydrostratigraphic hypotheses 1 through 13 (Figure 27). The approach to developing these conceptual models follows the recommended process of parsimony (Poeter and Anderson, 2005, Hill, 2006). A range of models were created, from simplistic conceptualizations that incorporated a single hydrostratigraphic layer with uniform recharge to 4 hydrostratigraphic layer models with heterogeneous zones of hydraulic conductivity and recharge based on land-use on various topographic regions. For each conceptual model, all recharge components and individual Kh terms, as well as 5 conductance terms (three assigned to engineered drains and two separate reaches of the South Platte River), and the lake leakance that



controls the exchange of water between Sutherland Reservoir and the underlying aquifer were estimated in the calibration process.

Considering the combinations of the various recharge and hydrostratigraphic scenarios, along with different model layering and other fixed-parameter conceptualizations, 42 numerical models were created for parameter estimation and multi-model ranking. Table 2 lists each model, named CM-# (**C**onceptual **M**odel). A grouping of models is also assigned in table 2, since many of the models have various recharge configurations tested on the same hydrostratigraphic conceptualization. This categorization was added for ease of tracking how models of identical hydrostratigraphy compare with different recharge definitions. In addition to the several groupings of model types, several “miscellaneous” models were created that differed by boundary conditions or assigned parameters. A fixed hydraulic conductivity field based on field measurements was tested on a group of three models with various recharge configurations. This conceptualization was developed to test whether raw field data interpolated to the grid could reach an optimal solution and high model rank without adjustment in the calibration and to determine the optimal values of other parameters such as recharge in an optimization with fixed hydraulic conductivities. Also, a group of three models with a fixed head on the southern boundary of the model were tested on a single layer, a two layer, and a four layer model. This was done to test whether the no-flow boundary on the south border of the model influenced the groundwater flow field in the vicinity of the GGS wellfield.

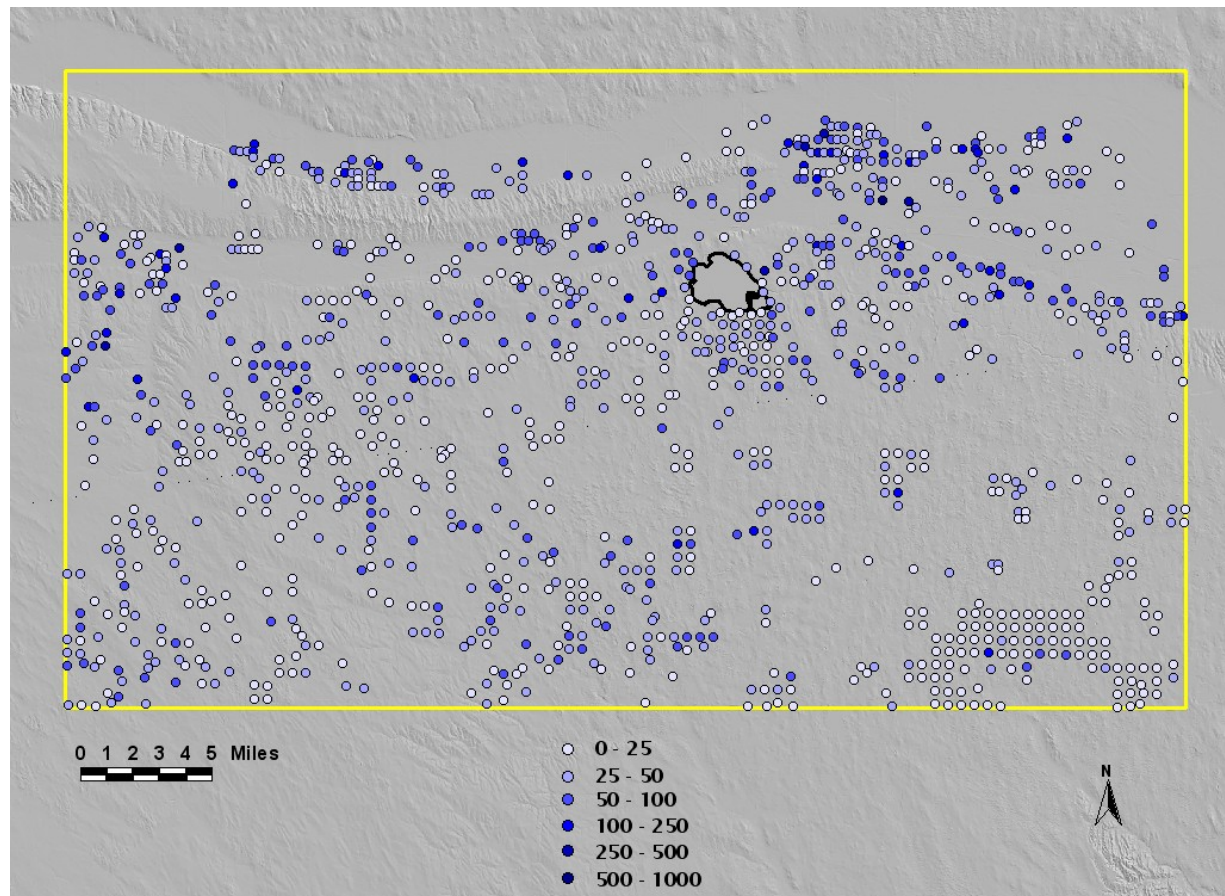
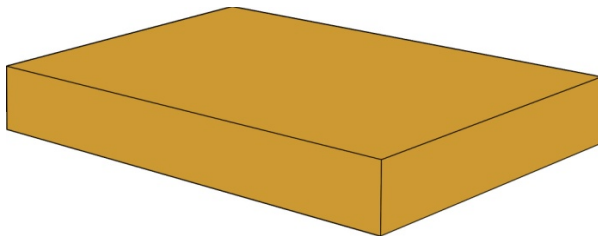
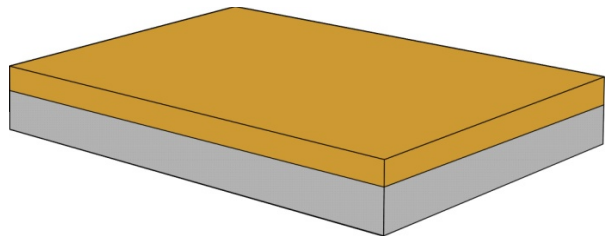


FIGURE 26. Map of hydraulic conductivity values (ft/d) at all irrigation wells and GGS well field test locations.

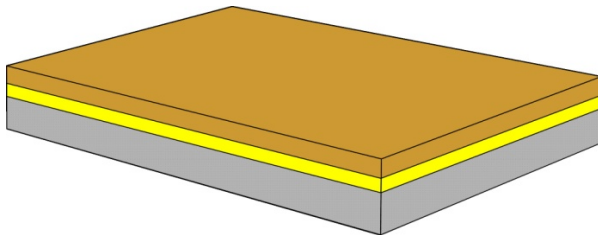




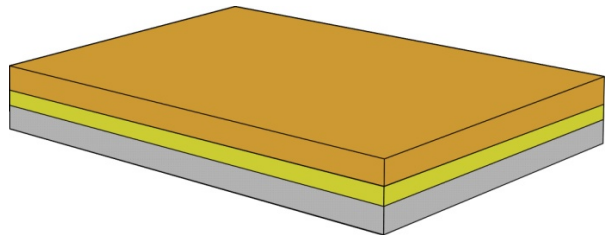
**Hypothesis 1** - Single-layer (two-dimensional) grid representation of the aquifer.



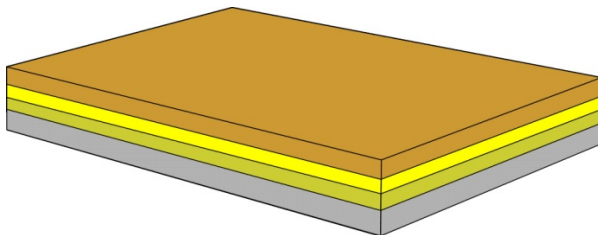
**Hypothesis 2** - 2-layer aquifer representation. Top layer all Quaternary units, bottom layer all Tertiary units.



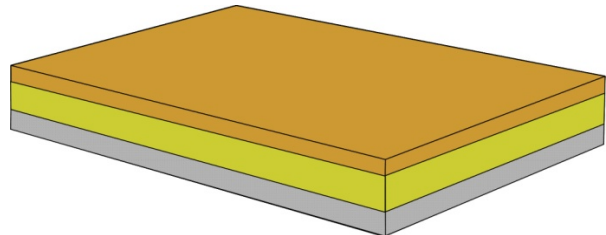
**Hypothesis 3** - 3-layer aquifer representation. Top layer is all Quaternary fines, layer 2 all Quaternary coarse material, third layer represents all of the Ogallala Group.



**Hypothesis 4** - 3-layer aquifer representation. Top layer all Quaternary materials, 2<sup>nd</sup> layer all Ogallala Group above Tertiary basal fines (bottom layer).



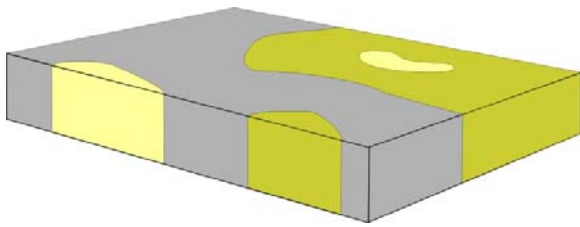
**Hypothesis 5** - 4-layer aquifer representation. Top layer is all Quaternary fines, layer 2 all Quaternary coarse material, third layer all Ogallala Group coarse and fine units above the Tertiary basal fines (bottom layer).



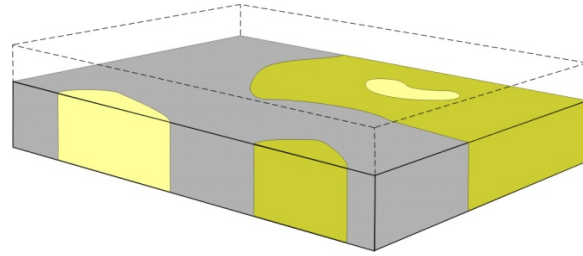
**Hypothesis 6** - 3-layer aquifer representation. Top layer is all Quaternary fines, layer 2 all Quaternary coarse and upper Tertiary deposits above the basal Tertiary fines (bottom layer).

FIGURE 27. Block diagrams and descriptions of the alternative hydrostratigraphic hypotheses considered in the multiple conceptual models of the High Plains aquifer in the study area. Each layer shown in the diagram corresponds to a numerical model layer.

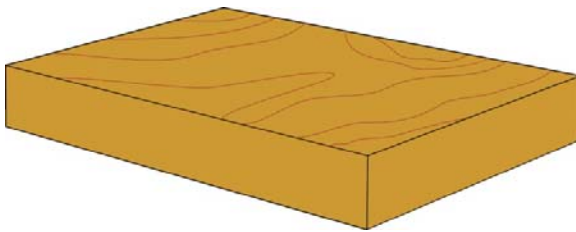
*continued on next page*



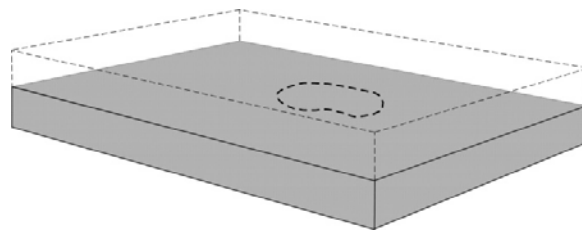
**Hypothesis 7** - Single layer representation of the aquifer. Separate zones of hydraulic conductivity based on USGS High Plains RASA data.



**Hypothesis 8** - 2-layer aquifer representation with the top representing all Quaternary deposits, bottom layer contains separate zones based on USGS High Plains RASA data. (Upper layer left transparent to show the variable zones of hydraulic conductivity in layer 2).



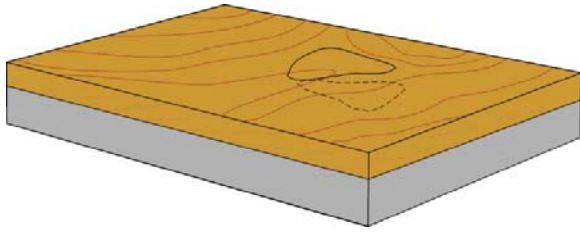
**Hypothesis 9** - Single layer aquifer representation. Interpolated hydraulic conductivity from well test and specific capacity data assigned to entire 2D grid.



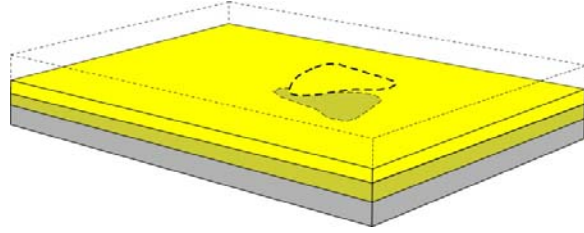
**Hypothesis 10** - 2-layer aquifer representation. Top layer represents all Quaternary deposits and is assigned a uniform hydraulic conductivity. Layer 2 represents all Ogallala Group deposits, with unique values of hydraulic conductivity estimated for separate zones based on near-site area thicknesses of coarse Ogallala Group materials.

*continuation of Figure 27* - Block diagrams and descriptions of the alternative hydrostratigraphic hypotheses considered in the multiple conceptual models of the High Plains aquifer in the study area. Each layer shown in the diagram corresponds to a numerical model layer.

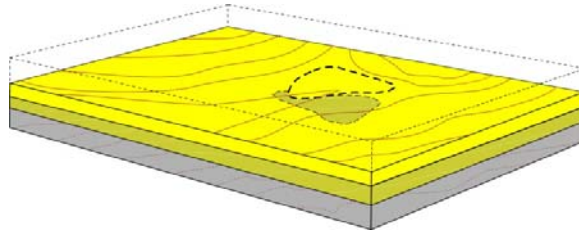
*continued on next page*



**Hypothesis 11**- 2-layer aquifer representation. Interpolated hydraulic conductivity assigned to both layers, with zones assigned to both layers based on mapped thicknesses of coarse deposits in both the Quaternary deposits and within the Ogallala Group.



**Hypothesis 12** - 4-layer aquifer representation. Top layer represents Quaternary fines. Layer 2 all Quaternary coarse material, with separate zones for presence of coarse deposits. Layer 3 represents all Ogallala Group deposits above the Tertiary basal fines (bottom layer) with unique zones in the near-site area that represent presence of coarse deposits in the upper portion



**Hypothesis 13** - 4-layer aquifer representation. Interpolated hydraulic conductivity assigned to layers 2, 3, and 4. Top layer represents Quaternary fine deposits. Layer 2 represents all Quaternary coarse deposits with unique zones. Layer 3 represents the upper portion of the Ogallala Group with unique zones of coarse deposits within that interval of the group. Bottom layer represents basal Tertiary fines.

*continuation of Figure 27* - Block diagrams and descriptions of the alternative hydrostratigraphic hypotheses considered in the multiple conceptual models of the High Plains aquifer in the study area. Each layer shown in the diagram corresponds to a numerical model layer.

TABLE 2. List of 42 conceptual models for the study area evaluated for the multi-model analysis and ranking. Abbreviations for parameters are: hydraulic conductivity (Kh), recharge (rch), lakebed leakance (leak), drain conductance (drncon), and river conductance (rivcon). Parameters with more than one representation are followed by a parenthesis indicating the number of terms estimated for that parameter.

Conceptual Model Group	Conceptual Model ID	Hydrostratigraphic Hypothesis	Recharge Conceptualization	No. of Parameters Estimated	Parameters Estimated
1	CM-1	1	U	6	Kh, leak, rivcon, drncon (2), rch
	CM-2	1	A	8	Kh, leak, rivcon, drncon (2), rch (3)
	CM-3	1	B	8	Kh, leak, rivcon, drncon (2), rch (3)
2	CM-5	2	U	7	Kh (2), leak, rivcon, drncon (2), rch
	CM-6	2	A	9	Kh (2), leak, rivcon, drncon (2), rch (3)
	CM-7	2	B	10	Kh (2), leak, rivcon, drncon (2), rch (4)
3	CM-9	3	U	8	Kh (3), leak, rivcon, drncon (2), rch
	CM-10	3	A	11	Kh (3), leak, rivcon, drncon (2), rch (3)
	CM-11	3	B	11	Kh (3), leak, rivcon, drncon (2), rch (4)
	CM-12	3	D	10	Kh (3), leak, rivcon, drncon (2), rch (3)
	CM-12s	3	C	10	Kh (3), leak, rivcon, drncon (2), rch (3)
4	CM-13	4	U	8	Kh (3), leak, rivcon, drncon (2), rch
	CM-14	4	A	10	Kh (3), leak, rivcon, drncon (2), rch (3)
	CM-15	4	B	11	Kh (3), leak, rivcon, drncon (2), rch (4)
	CM-16s	4	C	11	Kh (3), leak, rivcon, drncon (2), rch (4)
	CM-16	4	D	10	Kh (3), leak, rivcon, drncon (2), rch (3)
5	CM-17	5	U	9	Kh (4), leak, rivcon, drncon (2), rch
	CM-18	5	A	10	Kh (4), leak, rivcon, drncon (2), rch (2)
	CM-19	5	B	11	Kh (4), leak, rivcon, drncon (2), rch (3)
	CM-20	5	D	11	Kh (4), leak, rivcon, drncon (2), rch(3)
6	CM-21	7	U	7	Kh (2), leak, rivcon, drncon (2), rch
	CM-22	8	U	9	Kh (4), leak, rivcon, drncon (2), rch
	CM-23	7	A	10	Kh (3), leak, rivcon, drncon (2), rch (3)
	CM-24	7	B	8	Kh (2), leak, rivcon, drncon (2), rch (3)
	CM-25	8	A	11	Kh (4), leak, rivcon, drncon (2), rch (3)
	CM-26	8	B	10	Kh (3), leak, rivcon, drncon (2), rch (3)
	CM-27s	8	C	11	Kh (4), leak, rivcon, drncon (2), rch (3)
	CM-27	8	D	11	Kh (4), leak, rivcon, drncon (2), rch (3)
7	CM-28	9	U	6	Kh, leak, rivcon, drncon (2), rch
	CM-29	9	A	8	Kh, leak, rivcon, drncon (2), rch (3)
	CM-30	9	B	8	Kh, leak, rivcon, drncon (2), rch (3)
Misc.	CM-31	6	A	10	Kh (3), leak, rivcon, drncon (2), rch (3)
	CM-32	10	B	12	Kh (4), leak, rivcon, drncon (2), rch (4)
	CM-33	12	U	13	Kh (8), leak, rivcon, drncon (2), rch
	CM-34	13	B	15	Kh (8), leak, rivcon, drncon (2), rch (3)
	CM-35	9	B	7	leak, rivcon, drncon (2), rch (3)
	CM-36	9	D	6	rivcon, drncon (2), rch (3)
	CM-7fKh	2	B	8	Leak, rivcon, drncon (2), rch (4)
	CM-19fKh	5	B	7	Leak, rivcon, drncon (2), rch (3)
	CM-7 chd_south	2	B	9	Kh (2), leak, rivcon, drncon (2), rch (4)
	CM-18 chd_south	5	A	10	Kh (4), leak, rivcon, drncon (2), rch (2)
	CM-23 chd_south	7	A	10	Kh (3), leak, rivcon, drncon (2), rch (3)

# Numerical Model of Study Area

## ***Numerical Modeling Concepts***

A numerical model is a mathematical representation of a complex system. A numerical groundwater model represents aquifers and their interactions with external stresses using the groundwater flow equations that combine Darcy's Law with conservation of mass. The numerical model is a simplified representation of the system yet maintains the influential stresses that are important to the predictions of interest. This simplification process is necessary due to uncertainty regarding the exact nature of a flow system in time and space. Several assumptions are made for the model described in this report:

1. Groundwater flow is through porous sedimentary media and obeys Darcy's Law over the extent of the study area.
2. Horizontal conductivity is isotropic. Vertical hydraulic conductivity is anisotropic and the magnitude of vertical anisotropy is adjusted during model calibration for some of the conceptual models.
3. Model parameters are uniform within each grid cell. To account for system heterogeneity in the area of interest, the numerical model grid has a fine spacing in the area encompassing Sutherland Reservoir and the GGS well field (Figure 28).
4. On average, the groundwater flow system is in a relatively steady condition from 1997 through 2001. Although minor seasonal fluctuations occur during this time, no major trends in water levels and flow rates are detected for this timeframe. Average system stresses during this time period serve as model inputs for the steady state model of the system.
5. The groundwater flow system within the near-site area is stable during the steady state period, including the gradient of groundwater flow surrounding Sutherland Reservoir. Because of this condition, groundwater flow paths and travel times are relatively constant.

## ***Model Construction***

### Software

The groundwater models of the GGS-SR study area were developed using a combination of GIS software, stratigraphic modeling and visualization software, groundwater model graphical user interfaces (GUIs), and data-formatting codes. The numerical groundwater flow code MODFLOW-2000 (Harbaugh and others, 2000; Hill and others, 2000; [water.usgs.gov/nrp/gwsoftware/modflow2000/modflow2000.html](http://water.usgs.gov/nrp/gwsoftware/modflow2000/modflow2000.html)) was used to simulate the flow system. MODFLOW 2000 is a block-centered, finite difference code that solves the three-dimensional, partial-differential, groundwater-flow equations that describe porous media flow. MODFLOW assigns one uniform value of model each applicable model property to each cell. Internal and external boundary stresses are represented with individual packages or "modules" within MODFLOW that account for various components of the flow system such as rivers, lakes, or lake seepage. MODFLOW calculates head and flow at all grid cells for each step in time. Groundwater Modeling System (GMS), a graphical user interface for groundwater modeling (Aquaveo, 2002, [www.aquaveo.com/gms](http://www.aquaveo.com/gms)) was used for the initial construction of the MODFLOW packages, although modifications were made to these files using text editors throughout the modeling process so the files are no longer functional within GMS. The contouring software Surfer ([www.goldensoftware.com](http://www.goldensoftware.com)) and GMS were used to construct various stratigraphic models that were eventually transferred to MODFLOW grids. The USGS code MODPATH (Pollock, 1994; [water.usgs.gov/nrp/gwsoftware/modpath5/modpath5.html](http://water.usgs.gov/nrp/gwsoftware/modpath5/modpath5.html)) is an advective flow tracking package that uses output from MODFLOW to track the path and rate of groundwater movement. UCODE\_2005 (Poeter and others, 2005; [igwmc.mines.edu/freeware/ucode/](http://igwmc.mines.edu/freeware/ucode/)), a code that performs calibration by nonlinear regression and related analysis including predictive uncertainty evaluation was utilized to calibrate each of the study area models and evaluate their predictions and associated uncertainty. For comparison of the various models of the GGS-SR study area, a multi-model analysis (MMA, Poeter and Hill, 2007; [igwmc.mines.edu/freeware/mma/](http://igwmc.mines.edu/freeware/mma/)) and ranking code was used to determine which model(s) provided the best predictive capabilities. The USGS program GW\_Chart (Winston, 2000; [water.usgs.gov/nrp/gwsoftware/GW\\_Chart/GW\\_Chart.html](http://water.usgs.gov/nrp/gwsoftware/GW_Chart/GW_Chart.html)) was used to visualize output from UCODE\_2005.



### Grid Definition

The GGS-SR study area was discretized using a finite difference grid. The rectangular model grid for the GGS-SR study area extends 46 and 24 miles in the east-west and north-south directions, respectively, for a total area of approximately 1,125 square miles. The large area was selected to minimize influence of external boundary conditions on the cone of depression created by GGS well field operations. A model of the well field created using data from the COHYST model in 2004 with a southern boundary just over 2 miles beyond the NPPD property line indicated that external boundaries, whether specified head or no-flow, could influence the depth and extent of the cone of depression from long-term GGS well field pumping.

The grid is 121 rows and 190 columns, with smaller cell sizes providing detail in the well field and reservoir area (Figure 28). The largest cells near the edge of the model were 1309 ft x 1301 ft, and the smallest cells in the well field area were 493 ft x 376 ft. The location of Sutherland Reservoir (white line Figure 28) and NPPD property (orange line Figure 28) are the focus the refined grid cells just northeast of the center of the grid. All areas north of the North Platte River (red cells Figure 28) were set as inactive for each simulation. Each model used the same horizontal grid arrangement shown in Figure 28, but the number of layers differs among the conceptual models (Figure 27).

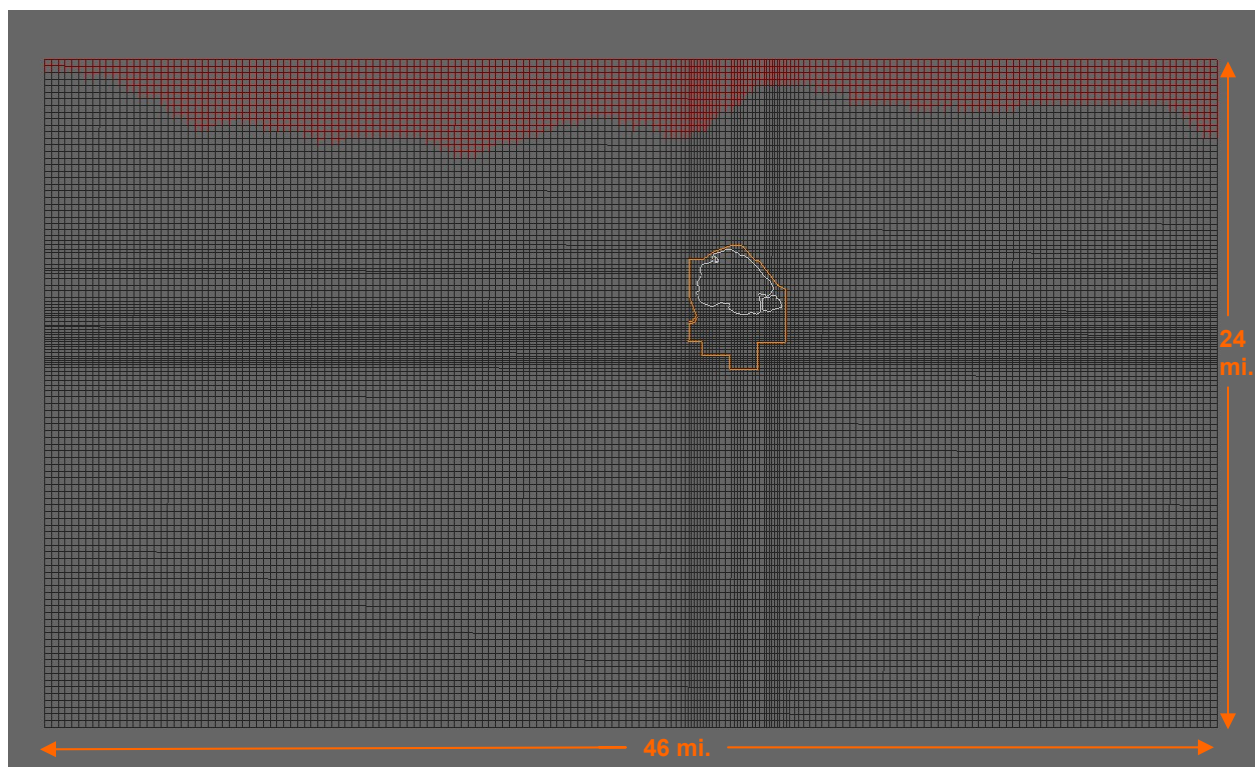


FIGURE 28. Finite-difference model grid of the GGS-SR study area. The orange line indicates the extent of the NPPD well field and the white lines show the area of Sutherland Reservoir and the GGS cooling pond. The red cells on the north side of the grid indicate inactive cells north of the North Platte River.

### Timeframe of Simulations

For most groundwater modeling projects it is necessary to simulate steady state conditions of a flow system in order to establish initial conditions for a transient simulation. This steady state simulation needs to represent a period of time with relatively constant average water levels and flows. A steady state simulation of the site was developed to represent conditions from 1997 to 2001. Climatically, precipitation

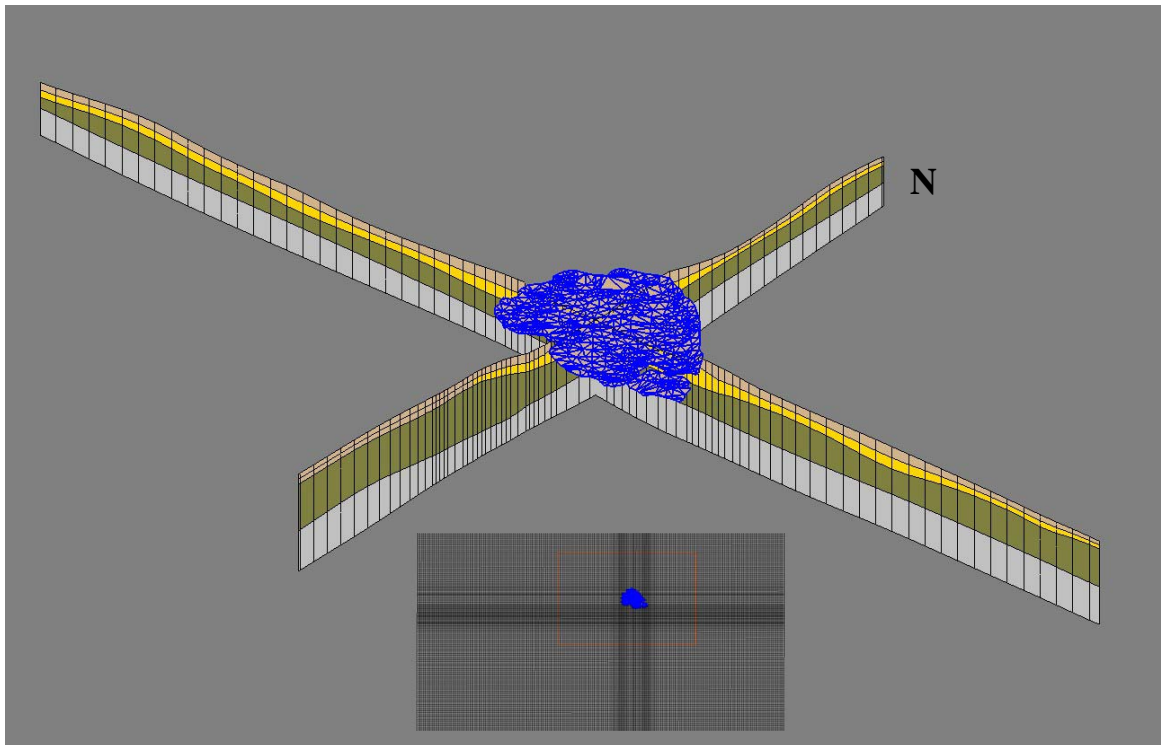


FIGURE 29. Cross-section of the MODFLOW 4-layer model grid and the TIN model used to define Sutherland Reservoir. The orange outline on the index map shows the extent of the grid cross sections.

was near long-term average rates for this timeframe and available groundwater level observations showed relatively small to no overall changes other than the typical seasonal fluctuations. Hydrologic conditions within the study area have been altered by land use practices over the last 50 years as well as from construction of the Sutherland Project. Over the last several decades, the flow system has reached a new state of quasi-equilibrium with the groundwater mound created by Sutherland Project seepage. Although minor fluctuations have occurred in the system due to varying weather conditions, the strategy for model development was to consider a timeframe after the stabilization of the groundwater mound as a period of “steady state.” This strategy was efficient in contrast to simulating pre-anthropogenic conditions and simulating all the new stresses that occurred over the past century, which would have required substantial computation time and involved large uncertainty given the minimal information on the stresses over that long period and the lack of observations.

Transient conditions were simulated for five years from 2002 to the spring of 2007, a time period in which the GGS well field was pumped during two summers (2005 and 2006) for mitigation of temperatures of water released from GGS into Sutherland Reservoir. Stress periods in the transient model vary in length from a week to several months (Table 3). The part of the year when little to no irrigation pumping occurs is termed the non-pumping season. This period usually extends from October through April. Each non-pumping season was represented with one stress period and daily time steps. During the years prior to construction and operation of the GGS well field (2002-04), each pumping season (May-September) used stress periods of one month in length with daily time steps. In the 2005 and 2006 pumping seasons when the GGS well field was in operation, the simulation used 7-day stress periods and 1-day time steps, starting on the first day of substantial withdrawals for each season. Each year several wells were tested by pumping for less than one hour. These tests were not included in the simulations. The stress periods were shortened to a week in length during the times of well field pumping to more accurately simulate the influence of the pumping on the flow system.

TABLE 3. Timeframe of transient simulation with: length of each stress period; number of time steps per stress period; corresponding calendar time; and status of well pumping for both irrigation and GGS well field wells for each stress period.

Stress Period	Length (d)	No. of time steps	Timeframe	Pumping status
1	73	73	Jan –March 2002	
2	48	48	March – May 2002	
3	31	31	May 2002	Irrigation pumping active
4	30	30	June 2002	Irrigation pumping active
5	31	31	July 2002	Irrigation pumping active
6	31	31	Aug 2002	Irrigation pumping active
7	30	30	Sept 2002	Irrigation pumping active
8	165	165	Oct 2002 –15 March 2003	
9	47	47	15 March 2003 to May 2003	
10	31	31	May 2003	Irrigation pumping active
11	30	30	June 2003	Irrigation pumping active
12	31	31	July 2003	Irrigation pumping active
13	31	31	Aug 2003	Irrigation pumping active
14	30	30	Sept 2003	Irrigation pumping active
15	166	166	Oct 2003 to 15 March 2004	
16	47	47	15 March 2004 to May 1, 2004	
17	31	31	May 2004	Irrigation pumping active
18	30	30	June 2004	Irrigation pumping active
19	31	31	July 2004	Irrigation pumping active
20	31	31	Aug 2004	Irrigation pumping active
21	30	30	Sept 2004	Irrigation pumping active
22	165	165	Oct 2004 – 14 March 2005	
23	47	47	15 March 2005 – May 1 2005	
24	9	9	May 1 2005 – May 10 2005	Irrigation pumping active
25	7	7	May 10 – May 17	Irrigation pumping active
26	7	7	May 17 – May 24	Irrigation pumping active
27	7	7	May 24 – May 31	Irrigation pumping active
28	7	7	May 31 – June 7	Irrigation pumping active
29	7	7	June 7 – June 14	Irrigation pumping active
30	7	7	June 14 – June 21	Irrigation pumping active
31	7	7	June 21 – June 28	Irrigation pumping active
32	7	7	June 28 – July 5	Irrigation pumping active
33	7	7	July 5 – July 12	Irrigation & GGS pumping active
34	7	7	July 12 – July 19	Irrigation & GGS pumping active
35	7	7	July 19 – July 26	Irrigation & GGS pumping active
36	7	7	July 26 – August 2	Irrigation & GGS pumping active
37	7	7	Aug 2 – Aug 9	Irrigation & GGS pumping active
38	7	7	Aug 9 – Aug 16	Irrigation & GGS pumping active

Table 3 continued

TABLE 3. Timeframe of transient simulation with: length of each stress period; number of time steps per stress period; corresponding calendar time; and status of well pumping for both irrigation and GGS well field wells for each stress period.

Stress Period	Length (d)	No. of time steps	Timeframe	Pumping status
39	7	7	Aug 16 – Aug 23	Irrigation & GGS pumping active
40	7	7	Aug 23 – Aug 30	Irrigation & GGS pumping active
41	7	7	Aug 30 – Sept 6	Irrigation & GGS pumping active
42	7	7	Sept 6 – Sept 13	Irrigation & GGS pumping active
43	7	7	Sept 13 – Sept 20	Irrigation pumping active
44	7	7	Sept 20 – Sept 27	Irrigation pumping active
45	7	7	Sept 27 – Oct 4	
46	7	7	Oct 4 – Oct 11	
47	7	7	Oct 11 – Oct 18	GGS pumping active
48	148	148	Oct 18 – Oct 25	GGS pumping active
49	47	47	Oct 25, 2005 – May 1, 2006	
50	10	10	May 1 – May 11	Irrigation pumping active
51	14	14	May 11 – May 25	Irrigation pumping active
52	7	7	May 25 – June 1	Irrigation & GGS pumping active
53	7	7	June 1 – June 8	Irrigation & GGS pumping active
54	7	7	June 8 – June 15	Irrigation & GGS pumping active
55	7	7	June 15 – June 22	Irrigation & GGS pumping active
56	7	7	June 22 – June 29	Irrigation & GGS pumping active
57	7	7	June 29 – July 6	Irrigation & GGS pumping active
58	7	7	July 6 – July 13	Irrigation & GGS pumping active
59	7	7	July 13 – July 20	Irrigation & GGS pumping active
60	7	7	July 20 – July 27	Irrigation & GGS pumping active
61	7	7	July 27 – Aug 3	Irrigation & GGS pumping active
62	7	7	Aug 3 – Aug 10	Irrigation & GGS pumping active
63	7	7	Aug 10 – Aug 17	Irrigation & GGS pumping active
64	7	7	Aug 17 – Aug 24	Irrigation & GGS pumping active
65	7	7	Aug 24 – Aug 31	Irrigation & GGS pumping active
66	7	7	Aug 31 – Sept 7	Irrigation & GGS pumping
67	21	21	Sept 7 – Sept 28	Irrigation pumping active
68	182	182	Sept 28, 2006 – March 15,	
69	47	47	March 15 – May 1, 2007	

### Boundary Conditions as Defined with MODFLOW Packages

The western and eastern sides of the model were defined to have changing head boundaries which were represented using the CHD package in MODFLOW. An analysis of groundwater levels at all available observation points within 10 miles of the east and west boundaries indicated that water levels changed slightly during the period from 2002 to 2007. Thus, observed groundwater levels at all available locations were interpolated to the model cells in the westernmost and easternmost columns of the model grid for each year between 2002 and 2007. It was assumed that there were no extreme changes in water levels between the times when measurements were taken thus values for heads at times when data were not available were determined by linear interpolation.

The North Platte River serves as the northern boundary of the active model grid. The North Platte was chosen rather than the South Platte River because flow observations were available on stretches of the South Platte River so it was necessary to simulate groundwater seepage from both sides of the river in order to obtain simulated flows equivalent to observed flows. Although the North Platte River flows on a perennial basis and is the ultimate groundwater discharge location for flow from the north, groundwater discharge to the North Platte River was not used as an observation for calibration.

On the southern edge of the model, a no-flow boundary was specified along the entire length of the boundary. The boundary is more than 13 miles south of the GGS well field. A no-flow boundary was chosen because the boundary is assumed to approximately parallel a groundwater flow line. It was expected that the boundary was far enough from the well field that the flow line would not be significantly deflected as a result of pumping.

### Surface Water Stresses

Three major types of surface features are present within the study area and were simulated with three different MODFLOW packages. The South Platte and North Platte Rivers were represented with the River package. The River package is a head-dependent boundary that allows exchange of water to or from the river and the aquifer. The direction of flow is dependent on the difference between the water level in the aquifer and the stage of the river. River stages were based on USGS stream gage elevations and readings from USGS 1:24,000 topographic maps. The river bottom was set 2 ft below the stage. Riverbed conductance is parameter that defines the volumetric rate of exchange of water between the river and the aquifer under a hydraulic gradient of one. This term considers the width, length, bed thickness and vertical Kh of the reach. Although the North and South Platte Rivers are extensively braided, the main flowing channels defined by NDNR in the 1990s served as the mapped extent of the live channels flowing presently.

Engineered drains and ditches in the model were represented with the MODFLOW Drain package. The Drain package behaves similarly to the River package in terms of exchange of water between the surface feature and the aquifer, however, flow is allowed only from the aquifer to the drain feature and “stage” of a drain is specified as the drain elevation. Elevations for the drains were based on USGS 1:24,000 topographic maps. Drain conductance for these channel features is calculated the same as the river conductance term. The conductance terms for both the River and Drain packages were estimated with the inverse calibration process.

Sutherland Reservoir was represented with the MODFLOW Lake Package (LAK3). The Lake Package is a more robust method for representing natural or engineered surface water storage features as compared to using a constant or general head boundary because it allows the stage to change in response to water flowing into or out of the lake. The lakebed was defined using a triangulation-irregular-network (TIN) based on a contoured bathymetric map of lake bottom elevations provided by NPPD. The package requires inputs for precipitation, evaporation, and stream/runoff flow into the lake, as well as outflow from the lake. Movement of water between the lake and the aquifer is controlled with a user-defined lakebed leakance term. Each iteration of MODFLOW produces a budget and stage for the lake which changes with time due to varying inflows and outflows. The relative values of lake stage and aquifer head determine whether the lake receives water from, or loses water to, the aquifer, or whether the lake is a flow-through system. After convergence of the lake budget calculation (typically 1 or 2 iterations), the simulation proceeds forward with the next iteration using the updated lake stage. This process can significantly lengthen the computational time for a MODFLOW simulation, but allows for a more realistic representation of a lake with the opportunity to use lake stage as an observation for calibration. For Sutherland Reservoir, the inflow and outflow simulated in the Lake package is from and to the Sutherland Supply Canal. Steady state model inflow/outflow values were averaged over the 1997-2001 period. For the transient period, the inflow/outflow components of the lake budget were averaged for the length of each individual stress period in the model. Precipitation and evaporation rates were averaged in a similar manner using climate data from the High Plains Climate Center.

### Wells

The Well package in MODFLOW was used to simulate both volumetric inflow and outflow of water in the aquifer. In terms of inflow, the well package was utilized to simulate seepage of flow from the NPPD



Supply Canal (including Korty Canal) into the aquifer. Estimates of seepage were based on an engineering report from the early 1990s (Harza, 1993) that evaluated system efficiency and seepage rates for the entire length of the canal. One well was applied to each cell containing the canal. The inflow for each cell was calculated based on estimated seepage rates for the stretch of the canal containing that model cell.

The Well package was also used to simulate extraction of water from the aquifer for both irrigation wells and the NPPD production wells. The irrigation wells were simulated seasonally with pumping rates based on the area of land served by the well and a net irrigation requirement for the crop grown that season. The net irrigation requirement was calculated as the deficit in crop water use demands not met by precipitation each summer from 2002 to 2006. The total volume of pumpage required for each crop to make up the difference in growing-season precipitation and crop water use was calculated for each growing season and divided over the summer stress period based on the trends in average daily evapotranspiration of corn and soybeans shown in Figure 30. As indicated by this figure, corn reaches its maximum evapotranspiration rate nearly a month before soybeans. This trend was reflected in the pumping rates of wells associated with each of these types of crops. Crops associated with a well were based on 2005 land use data from CALMIT. No satellite imagery data exists over the model area for the years 2002-04 and 2006. However, cropping patterns in this area of Nebraska remain fairly consistent (see 2001 vs. 2005 land use patterns in Figure 4) and it was assumed that no large changes in amount of land or crop type likely occurred between the 2002 and 2006 growing seasons. Irrigation wells were assigned to model grid layer 2 in 2-layer model representations, to layer 2 in 3-layer model representations, and to layer 3 in 4-layer model representations. This assignment was based on a qualitative evaluation of drill logs of irrigation wells in the outer-model area typically having wells screened in the upper portion of the Ogallala Group.

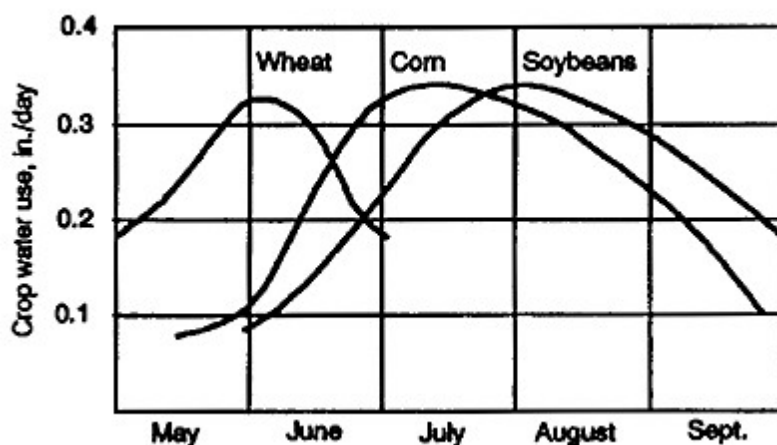


FIGURE 30. Average daily crop evapotranspiration for the summer growing season in Nebraska (Klocke and others, 1999).

Pumpage of the GGS wellfield was also represented with the Well package. Pumping rates during the summers of 2005 and 2006 were calculated as the total volume of water pumped for each well during a specified stress period length to determine an average rate in  $\text{ft}^3/\text{d}$  for each stress period during which a well was active. GGS wells were assigned to model grid layer 2 in 2-layer model representations, and to the bottom layer in the 3- and 4-layer grid representations.

### Layer Representation

The model layer information was processed in MODFLOW using the layer-property flow package (LPF). This package controls the  $K_h$  and  $K_v$  (vertical hydraulic conductivity) values, storage terms, and rewetting behavior. The rewetting option was utilized for all of the models, as early test simulations revealed that many thin cells in the Platte River system valley as well as those on the edge of Sutherland Reservoir were prone to going dry. This problem was alleviated by implementing the rewetting option,

allowing drying and rewetting of such cells. The inputs for this option were determined by experimentation and were not assessed using inverse calibration. The storage terms in the model were set at 0.2 for specific yield and  $1 \times 10^{-5}$  for the specific storage. Preliminary evaluations indicated the models were insensitive to these terms and thus they were set at values typical of geologic materials found in the HPA.

### Sequence of Model Execution and Travel Time Simulation

Following the steady state simulation of average conditions during the 1997 to 2001 time period, a transient simulation of the period from January 1<sup>st</sup>, 2002 to May 1, 2007 was conducted using the steady state heads as initial conditions. Particles were tracked backward from the geochemical monitoring well nests having 100% reservoir water to the reservoir using MODPATH using the steady state flow field because the travel times for some of the samples were greater than the duration of the transient period (2002-2007). Although the steady state period uses average conditions from 1997 to 2001 for climatic inputs, water levels near the reservoir where the monitoring wells are located have remained stable for over a decade, thus the use of the steady state flow field was reasonable for estimating travel times on the order of 1 to 15 years. Although it is likely that a vertical component of flow exists near the reservoir the termination zone was defined as the area of projection of the lake to the layer containing the starting location for the particle in multi-layered models. This was done because early tests prior to calibration indicated that vertical travel time across layers were clearly erroneous (this problem with vertical travel times in thick MODFLOW layers has been recognized as a problem by analytical element modelers, (personal communication, Igor Jankovic, 2001)). Tracking particles to the projection of the lake resulted in pre-calibration travel times to within two orders of magnitude of measured travel times.

After each set of code executions, an evaluation program, Sim\_Adjust (Poeter and Hill, 2008; [igwmc.mines.edu/freeware/sim\\_adjust/](http://igwmc.mines.edu/freeware/sim_adjust/)), examined all of the output information used by the inverse calibration code to ensure the proper number of simulated equivalent values existed in the output files. This precaution was added to the simulation after some simulations early in the model calibration process experienced drying of cells that contained an observation, which eliminated that cell from simulation if it did not rewet. When this condition occurred, Sim\_Adjust added a user-defined default value for the missing observation.

## **Calibration and Quality of Calibration and Prediction**

### ***Calibration Methodology***

Calibration is the process of adjusting parameter values, boundary conditions, model conceptualization, and/or model construction until the model simulation matches field observations. This activity is necessary because the field measurements are not accurate reflections of the model scale properties. Calibration of a model allows for adjustment of model parameters to accommodate an integrated interpretation of the system.

The calibration process for each of the conceptual models was undertaken using UCODE\_2005 (Poeter et al., 2005). UCODE\_2005 and associated codes perform sensitivity analyses, calibration using nonlinear regression, predictions, data need assessments, and uncertainty analysis of parameters and predictions. UCODE\_2005 automates the calibration process using the modified Gauss-Newton (G-N) method of nonlinear regression, a technique that minimizes a least-squares objective function using the normal equations. UCODE\_2005 is based on the pioneering work of Cooley and Naff (1990) and Hill (1992, 1994) in applying nonlinear regression to groundwater problems. Nonlinear regression theory is described by Seber and Wild (1989).

The primary goal of calibration is minimization of an objective function, which for this work is calculated as:

$$S(b) = \sum_{i=1}^{ND} \omega_i [y_i - y_i'(b)]^2 \quad (\text{equation 2})$$

where:

**ND** is the number of observations

$\mathbf{b}$  is a vector of parameter values of size NP

NP is the number of parameters

$y_i$  is an observed value

$y'_i(\mathbf{b})$  is a simulated equivalent to  $y_i$  as calculated by the model for parameters  $\mathbf{b}$

$y_i - y'_i(\mathbf{b})$  is a residual (observed minus simulated value)

$\omega_i$  is a weight reflecting uncertainty associated with observation  $y_i$

In matrix form, this equation becomes

$$S(\mathbf{b}) = [\mathbf{y} - \mathbf{y}'(\mathbf{b})]^T \boldsymbol{\omega} [\mathbf{y} - \mathbf{y}'(\mathbf{b})] \quad (\text{equation 3})$$

$\mathbf{y}$  is a vector of observed values of size ND

$\mathbf{y}'(\mathbf{b})$  is a vector of simulated equivalents of size ND

$\mathbf{y} - \mathbf{y}'(\mathbf{b})$  is a vector of residuals (observed minus simulated values)

$\boldsymbol{\omega}$  is a ND × ND weight matrix reflecting uncertainty associated with the observations with off-diagonal terms reflecting uncertainty associated with correlated observations

The observations can include any output of the model that is dependent on the input parameters to be adjusted during calibration. The weights reflect not only the certainty associated with the observation but also render the weighted squared residuals dimensionless so the residuals associated with different types of observations can be summed.

The calibration process is also called *optimization* or *parameter estimation*. To minimize the objective function,  $S(\mathbf{b})$ , the G-N method proceeds through an iterative process of updating parameters to reduce residuals by assuming a linear relationship. First the *sensitivity* of simulated equivalents to each parameter is determined. Sensitivity is the amount of change in a simulated equivalent divided by the change in an individual parameter value. Given the residuals and the sensitivities, each adjustable parameter is modified, resulting in a new and ideally smaller objective function value. However the relationship is nonlinear so the objective function is not minimized after one adjustment of the parameters and additional iterations are required until minimal change in the parameter values (defined as a fractional value by the modeler) occurs between iterations. At that point the parameter estimation process is said to converge. Parameters are selected to represent physical features or quantities of the groundwater system, such as aquifer transmissivity, riverbed conductance, or evaporation. Generally in groundwater modeling, not all parameters are adjusted during calibration. Some parameters may be “fixed” (i.e. not adjustable).

The sensitivity term is a derivative ( $\Delta y_i / \Delta b_j$ ) of an observation with respect to a parameter. It is the engine that guides the magnitude and direction of change of the parameter value during optimization. Scaled sensitivities provide valuable insight on the information contained in the observations with respect to the parameter values. Scaled sensitivities are dimensionless. Two of the most useful outputs from UCODE are dimensionless-scaled sensitivities (**DSS**) and composite-scaled sensitivities (**CSS**). The DSS are calculated for each parameter-observation pair, and indicate the relative importance of different observations on the estimation of an individual parameter. The CSS indicate the total amount of information all observations provide in the estimation of a single parameter. Parameters with large CSS (e.g. >1) and those with large CSS relative to other parameters are more likely to be estimated with greater confidence in a regression. For parameters with small CSS (e.g. <1, or with relative values <1% of the largest CSS) the observations do not provide enough information to estimate the parameter value. For parameters with this condition, values are often pre-set prior to calibration and are not adjusted during the regression, or are tied by a function to parameters that are estimated (Hill and Tiedeman, 2007).

## Observation Weighting

The weight term,  $\omega$ , in equations 2 and 3 serves two purposes in the calculation of optimal parameters in non-linear regression. First, observations need to be weighted to eliminate units associated with observations, which may be different when dealing with diverse types of data. For example, weighting eliminates the issue of summing residuals between simulated and observed values from head and flow observations. Secondly, weights are needed to control the influence of observations that are less accurately measured relative to those observations that are considered to be measured with greater confidence. An example of this condition would be a groundwater level observation determined with a land surface datum derived from a high quality land survey compared to a groundwater level observation determined with a land-surface datum based on a topographic map with 20-ft contours. In this situation, the observations based on the survey data would be given a larger weight than those based on the latter example. Error in measurements should also be accounted for in observation weights, regardless of the type of observation used (Hill and Tiedeman, 2007). The weight term in equation 2 is calculated as:

$$\omega = 1/\sigma^2 \quad (\text{equation 4})$$

Where  $\sigma^2$  is the variance associated with the measurement. This value can also be assigned as the often better-understood standard deviation associated with the measurement (UCODE\_2005 automatically determines the weight from the user-assigned uncertainty statistic). Weights used in this investigation were calculated by estimating a range in which the modeler was 95% certain would include the true value, then calculating a standard deviation assuming the measurement error was normally distributed. For example, the modeler may estimate there is a 95 percent chance that the true value of the water level elevation at observation well nest 3 is within 1.25 ft of the observed value. A 95% confidence is equivalent to 1.96 standard deviations. The confidence interval (C.I.) of this value would be determined as follows:

$$\text{C.I.} = y_i \pm 1.96 \sigma_i \quad (\text{equation 5})$$

Rearranging these values to solving for standard deviation  $\sigma_i$ :

$$1.96 \sigma_i = 1.25 \text{ ft}$$

$$\sigma_i = 1.58 \text{ ft}$$

The variance is the square of the standard deviation:

$$\sigma_i^2 = (\sigma_i)^2 = 2.48 \text{ ft}^2$$

thus the weight is:

$$1/\sigma^2 = 0.4 \text{ ft}^{-2}$$

Based on the level of presumed accuracy on the observation measurements used in this investigation, observations were weighted differently not only for the four types of observations, but also within each type of observation. Groundwater level observations were assigned different weights based on the data source for the measurements. The near-site water level measurements from the NPPD monitoring wells were given a larger weight ( $\sigma = 1.25 \text{ ft}$ ) than the regional observations ( $\sigma = 4 \text{ ft}$ ) provided by the TPNRD. The NPPD data were continuously recorded with pressure transducers that were monitored closely and check against manual measurements on GPS-surveyed wells, whereas the outer-area wells had little information about the measurements.

Flow measurements were assigned weights based on the type of drainage feature, measurement method, and time of year of the observation. As explained earlier in previous sections, flow observations were based on a combination of staff-gage and flow relationships, manual flow meter measurements for cross-sections of the waterway, and NDNR gage measurements. Weights on drain observations were calculated assuming a 95 percent expectation that the true flow would be within  $\pm 40$  percent of the measurement. The interval was wide because a component of the flow in the drain may not be groundwater discharge, but rather could be runoff from irrigation or precipitation events. Measurements were made once a month on the drains, making it difficult to determine trends in the flows. Weights on river baseflow observations differed for the upper and lower reaches of the South Platte River and with the time of the year. For the upper reach of the South Platte River (from Roscoe to Sutherland), weights

varied from an assumed 95 percent confidence of the measurement being within  $\pm 30$  percent to  $\pm 75$  percent of the observed difference between these two gages. The upstream observation of this reach was based on a USGS gage measurement, whereas the downstream location for this reach was a manual cross-sectional flow-meter measurement from the NDNR. The 75 percent range was applied to three summer measurements, a time when the upper extent of this reach can be dry downstream of the Kory Diversion canal. The lower South Platte River reach, from the flow meter measurement location at Sutherland to the NDNR gage at North Platte, was assigned weights based on an assumed 95 percent confidence of the true flow being within  $\pm 40$  percent of the observed difference between the downstream and upstream locations (minus flow from surface tributaries within this reach). One observation for this reach was assigned a weight based with the confidence of the measured value being within  $\pm 50$  percent of the observed difference of these gages due to apparent surface runoff component of unknown magnitude in the South Platte River gage at North Platte.

Weights for Sutherland Reservoir stage observations were calculated based on a 95 percent confidence of the true stage being within  $\pm 1.0$  ft for all 1,852 daily stage observations. The relatively narrow range was expected to encompass any effect of wave action on windy days that could potentially cause error in the measurement.

Weights for the travel time measurements were based on laboratory equipment precision values provided by the USGS. The individual weights were calculated with a 95 percent confidence that the true value was within 1.5 to 2 times the precision error reported by the USGS, with the larger weights applied to the well nests closest to the reservoir because there is less chance of multiple water sources near the reservoir. The observation at nest 3 was given a smaller weight due to the fact that the well is located in a regional discharge zone and although the water sample was analyzed to be 100% reservoir water its greater distance from the reservoir and location in a regional discharge area renders that assumption less certain.

### ***Confidence Intervals on Optimal Parameters***

If we assume the following then we can calculate reliable confidence intervals on the estimated parameter values: 1) the true errors in the observations are normally distributed; 2) the model is approximately linear near the estimated parameter values; and 3) the model represents the major features of the system so that uncertainty is due only to the parameter estimates (Poeter and Hill, 1997). The linear confidence intervals are calculated using the calculated error variance (CEV), sensitivities, and observation weights. CEV indicates the quality of fit between simulated equivalents and observations:

$$CEV = \frac{S(b)}{ND - NP} \quad (\text{equation 6})$$

Values of CEV near 1.0 indicate the fit of the model to the observed values is consistent with the uncertainty ascribed to the observations. Values less than 1.0 indicate the model fits the observations better than the uncertainty associated with the observations, and a CEV greater than 1.0 signals that the model fit is not as good as would be expected given the confidence the modeler ascribed to the observations.

The variance of the  $i^{\text{th}}$  estimated parameter, which may be for example a hydraulic conductivity thus  $\sigma^2(K)$  is the  $i^{\text{th}}$  diagonal element of the parameter variance-covariance matrix which is determined as:

$$VAR = CEV(\underline{X}^T \omega \underline{X})^{-1} \quad (\text{equation 7})$$

where  $\underline{X}$  is sensitivity matrix,  $\underline{X}^T$  is its transform and other terms have been defined earlier in this report.

The sensitivity matrix is ND x NP in size and is comprised of all the sensitivities of each simulated equivalent to each parameter adjusted in the parameter estimation. VAR is an NP x NP matrix with the diagonals being the variance for each estimated parameter and off-diagonals being the parameter covariances.



The 95-percent confidence interval on an estimated (optimal) parameter value encompasses a range of  $\pm$  approximately 2 standard deviations (more precisely 1.96). For example, the variance on  $Kh_1$  (horizontal K of layer 1) in the case where it is the third parameter in the list of estimated parameters would be:

$$\sigma_{Kh_1}^2 = CEV \left( \underline{\underline{X^T \omega X}} \right)_{3,3}^{-1} \quad (\text{equation 8})$$

where the 3,3 indicates the value in the third row and third column of the matrix. The 95-percent confidence interval on  $Kh_1$  would be:

$$Kh_1 \pm 1.96 \sqrt{\sigma_{Kh_1}^2} \quad (\text{equation 9})$$

The confidence intervals indicate the range of values that have a 95% chance of containing the true unknown parameter value given the observation data and the model. Large confidence intervals suggest that the model is a poor representation of the system and/or the data do not provide much information on the parameters selected for estimation (Hill and Tiedeman, 2007). The latter may be due to insensitivity or to parameter correlation. Parameter correlation is the situation where the combined value of two or more estimated parameters controls the simulated equivalents to the observations. For example if the simulated equivalents are only dependent on the product, quotient, or sum of two parameters then we can estimate that combined value but we cannot estimate independent values for those parameters.

As noted, the confidence interval described above is related to the quality of fit and sensitivity of simulated equivalents to parameters for one model. If alternative models are considered, their confidence intervals may differ and in some cases the range described by the confidence intervals from two models may not overlap. In such a case model-averaging of alternative conceptual models is appropriate.

### **Parameter Correlation**

One problem that can plague groundwater modeling efforts is correlation of parameters. This condition occurs when different combinations of values of two or more parameters produce the same model output. For example, in a two parameter model (recharge and K) and only water level observations, if recharge and Kh are both doubled the resulting water levels will be the same. In that case the available water level data cannot distinguish between independent values of recharge and K, they can only identify the ratio of the two values, so recharge and K are completely correlated (correlation coefficient of 1.0). Parameters can also be negatively correlated. In that an increase in one parameter and a decrease in another will yield the same results. UCODE\_2005 output from a regression reports the parameter correlation coefficient (pcc) for every pair of estimated parameter values. PCC is the normalized covariance between any parameters. Values of correlation can range from -1.0 to 1.0. Values above 0.98 indicate potentially high correlation, suggesting that the regression may not be able to uniquely estimate the two parameters (Poeter and Hill, 1997). Parameters with correlation values between -0.98 and +0.98 can typically be estimated uniquely. Lack of correlation is critical to the optimization process, as correlated parameters can lead to non-convergence of a solution or a misleading solution. Sometimes parameters with pcc close to -1.0 or 1.0 can be independently estimated. The only way to be sure is to begin the regression with different starting values and find that the same optimal values are obtained (where "same" is within one standard deviation of the optimal value).

### **Alternative Approach to Minimizing Objective Function**

Within UCODE\_2005, an option is available for minimizing the non-linear based objective function using alternative methods to the Gauss-Newton approach. Mehl and Hill (2003) demonstrated that the double-dogleg trust region approach could reduce the computational time for minimizing the non-linear objective function for complex problems. The standard Gauss-Newton approach was utilized in initial calibrations of the conceptual models. However, when calibrating the same models using the trust-region approach computation time was reduced and the final objective function values were smaller. Further information on the double-dogleg trust region method is available in Dennis and Schnabel (1996).

## Prediction

Not only can the statistics from nonlinear regression produce confidence intervals on optimal parameter values, they can also be used to calculate uncertainty associated with model predictions made by imposing new stresses on the calibrated model. Individual or simultaneous intervals can be determined on model predictions. The difference results from the critical value used to determine the confidence interval. Simultaneous intervals are wider than individual prediction intervals, but simultaneous intervals allow a user to determine the confidence on multiple predictions of system behavior.

The standard deviation of a prediction is calculated as (Hill and Tiedeman, 2007):

$$s_{z_k} = \left[ \sum_{i=1}^{NP} \sum_{j=1}^{NP} \left( \frac{\partial z_k}{\partial b_j} \right) V(b_{i,j}) \left( \frac{\partial z_k}{\partial b_i} \right) \right]^{\frac{1}{2}} \quad (\text{equation 10})$$

where:

$s_{z_k}$  is the standard deviation of the  $k^{\text{th}}$  prediction

$\frac{\partial z_k}{\partial b_j}$  is the sensitivity of the  $k^{\text{th}}$  prediction with respect to the  $j^{\text{th}}$  estimated parameter

$V(b_{i,j})$  is the  $i,j^{\text{th}}$  element of the parameter variance-covariance matrix.

The confidence interval is then:

$$z_k \pm (\text{critical value})_{z_k} s_{z_k} \quad (\text{equation 11})$$

where the critical value is determined from a Student-t distribution for individual confidence intervals and from the smaller of the Bonferroni or Scheffe distribution for simultaneous intervals.

## Quality of the Calibration

The goodness of fit of simulated equivalents to the observations is a key measure of the quality of the calibration, as are the distributions of residuals and parameter sensitivities and correlations. Several other items output by UCODE provide further insight. Three statistics provide information on the importance of the observations to the regression. First, the *leverage statistic* is calculated for each observation to determine the potential impact the observation could have on the results of the regression. Two additional statistics, Cook's D and DFBETAS, reflect the actual effect of the observations on the regression. The Cook's D statistic indicates how parameter estimates from a regression would differ with the omission of a particular observation, relative to the estimates given an entire set of observations. DFBETAS measures the influence of each observation on each parameter.

Model linearity based on the modified Beale's measure can also be calculated using auxiliary codes and output from UCODE\_2005. Extreme nonlinearity of a model indicates that the linear confidence intervals may not be accurate. If nonlinearity is significant UCODE can be used to calculate nonlinear confidence intervals on the parameter and predicted values. However the equivalent computation of a full and challenging regression is required for each upper and lower confidence interval for each parameter or prediction for which the nonlinear intervals are desired.

## Multi-Model Analysis

As described previously in the Multiple Conceptual Model Strategy section, uncertainty in characteristics of natural systems creates the plausibility of alternative models. The objective of this study is to determine the most suitable model(s) of the flow system in the vicinity of Sutherland Reservoir for predictive analysis. Often more than one calibrated model of a system produces similar calibration statistics. To first determine which alternative conceptualization within a suite of models are most likely, each model is analyzed using a model selection criterion. The Akaike Information Criterion (AICc) was used in this study because alternative methods (Ye et al., 2008; Poeter and Hill, 2007, Neuman and Wierenga, 2003; Neuman, 2003) such as AIC (Aikake's Information Criterion), BIC (Bayesian Information Criterion), and KIC (Kashyap's Criterion) provided essentially identical results. AICc is based on the Kullback-Leibler (K-L) information theory (Kullback and Leibler 1951). AICc estimates the K-L information loss using information for the calibration process including the weighted sum-of-squared residuals, the number of observations ( $n$ ), and the number of parameters ( $k$ ) used in the calibration:

$$AICc = ND \log(S(b)) + 2(NP + 1) + \left( \frac{2(NP + 1)((NP + 1) + 1)}{ND - (NP + 1) - 1} \right) \quad (\text{equation 12})$$

AICc is calculated for each of the models that are being compared. The AICc for each model are ordered from smallest to largest, with the models having the smallest values considered the best or most likely. Model quality is considered to decrease as the ranked AICc values increase. The delta value between models and resulting posterior probability are calculated from AICc. The delta value ( $\Delta_i$ ) of each model is the difference in the AICc relative to the minimum AICc computed for the group of models considered. The delta value indicates the amount of K-L information loss of model  $i$  relative to the lowest ranked ("best") model.

The posterior probability (also called Akaike weight) indicates the likelihood of that model being the best model in terms of minimizing K-L loss. The posterior probability of model  $i$  calculated as: (Poeter and Hill, 2007):

$$p_i = \frac{\exp^{-0.5\Delta_i}}{\sum_{j=1}^R \exp^{-0.5\Delta_j}} \quad (\text{equation 13})$$

where  $R$  is the number of models being considered. The  $p_i$  is used to model-average the predictions:

$$\bar{z}_k = \sum_{i=1}^R p_i z_{k_i} \quad (\text{equation 14})$$

and to determine the model-averaged standard deviation for the prediction:

$$s(\bar{z}_k) = \sum_{i=1}^R p_i \left[ (s(z_k))^2 + (z_i - \bar{z}_k)^2 \right]^{\frac{1}{2}} \quad (\text{equation 15})$$

where the first term in the brackets is the standard deviation of equation 10 (the within model variance) and the second term is the difference between each model prediction and the model-averaged prediction (the between model variance). This standard deviation can be used to determine confidence intervals on the predictions in the same manner as described for calculating confidence intervals on the parameters.

An evidence ratio is calculated as the quotient of the best model posterior probability relative to alternative models. The best model of a group always has an evidence ratio of 1, and all other models will have values greater than 1. For example, if an individual model from a group of simulations is compared to the best model and has an evidence ratio of 16.4, it can be stated that "there is 16.4 times more evidence that the best model represents the true system than the individual model in question" (Poeter and Anderson, 2005).

## Multi-Model Analysis Results

It is not unusual to find that the model selection criteria indicate that one or two of the conceptual models are much more probable than the alternatives even though the sum-of-squared-weighted-residuals is similar. That was the case for this suite of 42 models using AICc or any of the other commonly used criteria (AIC, BIC, KIC). Only 40 of the 42 models converged to the point at which all estimated parameters changed less than one percent for the last iteration of the calibration process. The 40 converged models were evaluated using AICc for this study because: 1) similar model rankings were obtained with AICc and KIC and 2) by derivation AICc seeks to weight models based on predictive ability.

All converged models were considered in the multi-model analysis, even though some models resulted in unreasonable parameter estimates. These models were included to determine how models with unlikely parameters would rank among the entire group of models. Six of the top ten models (Table 4) were either single layer or two layer grid representations of the hydrologic system (CM-23, CM-25, CM-2, CM-3, CM-24, CM-27s). The top two models (CM-23 with a probability of nearly 0.999 and CM-25 with a probability of  $2.8427 \times 10^{-4}$ ) both utilized a regional Kh representation with three zones based on the USGS High Plains RASA data and recharge based on topographic regions. The number of estimated parameter values in the 40 models ranged from 6 to 15. Ten parameter values were estimated for CM-23 and this representation accounts for 99.9 percent of the posterior model probability. It should be noted that the conceptualizations of the top three models (CM-23, CM-25, and CM-18) with a fixed-head boundary on the southern border of the model domain (replacing the no-flow boundary) did not reduce the SSWR of any of the three models and were nearly identical to the parent representations with a no-flow southern boundary. Because of this identical nature of these results, the models with the modified fixed head southern boundary were not considered as alternative representations and thus were not included in the multi-model ranking.

TABLE 4. Ranking of the top ten GGS-SR models.

Model Rank	AICc	$\Delta_i$	Probability	Evidence Ratio	SSWR	No. of Parameters
1. <b>CM-23</b>	7562.2	--	0.999	1.0	48,318	10
2. CM-25	7578.5	16.3	$2.8427 \times 10^{-4}$	$3.5 \times 10^{+3}$	48,626	11
3. CM-18	7579.3	17.2	$1.8848 \times 10^{-4}$	$5.3 \times 10^{+3}$	48,641	10
4. CM-2	7583.2	21.0	$2.7978 \times 10^{-5}$	$3.6 \times 10^{+4}$	48,790	8
5. CM-31	7584.7	22.5	$1.3276 \times 10^{-5}$	$7.5 \times 10^{+4}$	48,742	10
6. CM-3	7585.6	23.4	$8.2353 \times 10^{-6}$	$1.2 \times 10^{+5}$	48,837	8
7. CM-19	7588.1	25.9	$2.3942 \times 10^{-6}$	$4.2 \times 10^{+5}$	48,769	11
8. CM-10	7588.9	26.7	$1.5754 \times 10^{-6}$	$6.3 \times 10^{+5}$	48,823	11
9. CM-24	7595.4	33.3	$5.9245 \times 10^{-8}$	$1.7 \times 10^{+7}$	49,024	8
10. CM-27s	7612.8	50.6	$1.0366 \times 10^{-11}$	$9.6 \times 10^{+10}$	49,278	11

The delta term in the third column, which is the difference between the AICc for each term and the AICc of the top-ranked model, has been used by researchers to describe the quality of a particular model. Burnham and Anderson (2002) determined that models with  $\Delta_i$  less than 2 are very good models and models with  $\Delta_i$  between 4 and 7 have less empirical support. Models with  $\Delta_i$  greater than 10 should not be considered for further use. Based on these criteria only the top model can be classified as “very good”.

The top 10 models have very similar sum-of-squared-weighted-residuals (SOSWR), with the top ranked and tenth ranked models differing by only 515 (a dimensionless term) which is about 1% of the minimum SOSWR. The strong bias toward the model with the lowest SOSWR is common in groundwater modeling and may be a shortcoming of the model selection criteria but that issue is beyond the scope of this report. However, considering this similarity of SOSWR, the top three ranked conceptualizations which have different types of hydrologic system representations (hypotheses 7, 8, and 5 of Figure 27 respectively with ranking 1, 2, and 3) are presented in detail in this report and are included in the predictive analysis.

Although several conceptualizations estimated fewer parameters than the 3 top-ranked models, the top-ranked conceptualizations were generally less complex with respect to aquifer structure, using regional zones of Kh instead of defining hydrostratigraphic units into separate model layers, and recharge distribution based on topographic regions without consideration of land-use or soil moisture capacity. Ten parameters were estimated in the highest ranked multi-layer conceptualization with more than two aquifer layers (CM-18, ranked 3<sup>rd</sup>), although the Kh terms estimated in this model did not include lateral variations that were included in the 1<sup>st</sup> and 2<sup>nd</sup> ranked models. A common theme is evident in the recharge conceptualizations, as 5 of the top 10 models implemented recharge based on topographic regions.

## Calibration Results

As mentioned earlier, 40 of the 42 models converged with a tolerance of 0.01 (that is, all estimated parameters changed less than one percent for the last iteration of the calibration process). Although 40 models were analyzed, it would be impractical to report model results for each conceptualization tested, so calibration results are reported for the top three models which reflect the three different types of conceptualizations in the top five models. This provides a comparison between the most probable model CM-23, which is a single aquifer with no vertical variation although it is represented by 2 numerical model layers, and the next two most probable models: the highest ranked 2-aquifer model (CM-25), and the highest ranked 4-aquifer model (CM-18). The latter model is of particular interest because its conceptual structure is significantly different from CM-23, and a comparison of results between a multi-layered aquifer structure and a single aquifer provides insight into the question of adequacy of a single aquifer model to predict future conditions.

### Model Fit Information

The calculated error variance (CEV) and the standard error, as previously described, provide insight into the relative fit of the model based on the level of confidence assigned in the weighting of observations. These statistics and their 95 percent confidence intervals indicate the three models have similar model fit, despite the difference in conceptualized hydrostratigraphy and recharge. Ideally, these measures should be near 1.0 and their confidence intervals should include 1.0 if the model fit is consistent with the weighting. In these cases too much confidence (weight) was placed in the measurements. Values greater than 1.0 are often encountered in modeling field systems, as assigned weighting reflects only measurement error, whereas the weighted residuals are also affected by model error. The presence of model error does not indicate a poor model as long as weighted residuals display a random nature (Poeter and Hill, 1997).

TABLE 5. The CEV and standard error values for CM-23, CM-25, and CM-18.

Model	95% C.I. Lower Value	CEV	95% C.I. Upper Value	95% C.I. Lower Value	Standard Error	95% C.I. Upper Value
CM-23	17.9	18.9	20.0	4.2	4.3	4.5
CM-25	18.0	19.0	20.1	4.2	4.4	4.5
CM-18	18.0	19.0	20.1	4.2	4.4	4.5



## ***Parameter Correlation***

None of the parameters in the three models were correlated beyond  $\pm 0.95$ . Consequently, there is reasonable confidence that the parameters estimated in the three models are unique, since all of these values fall below the critical level of  $\pm 0.98$  as suggested by Poeter and Hill (1997) and Hill and Tiedeman (2007).

## ***Weighted Residuals and Simulated Values***

The graph of weighted residuals versus simulated values provides insight into the presence of model error. Ideally, the graph should have a narrow, random distribution of points above and below the zero residual line. The graph is similar for each of the three models (Figure 31). The graphs shown on the left of those figures include all observations. However, the flows are in units of cubic-feet per day so subsets of the observations are shown to capture the details related to groundwater levels, travel times, and reservoir stages. The distribution of residuals is fairly well balanced for all of the models.

Each model exhibits a cluster of flow observations in the central portion of the graph ( $x \sim -4,000,000$  ft<sup>3</sup>/d) that are above the zero residual line. These points are observations of discharge to Applegate drain. This condition was more pronounced in early model tests and prompted the definition of a separate drain conductance parameter and two drain parameters derived from that parameter. The remainder of the flow observations that are closer to zero on the x-axis have a slight negative bias, although these values are more random than the of Applegate drain residuals. Two points to the right of zero on the x-axis are observations on the upper South Platte River reach at times when the model simulated losing conditions, while in fact a slight gain in flow was observed. Each model showed a relatively even distribution around zero for the travel time observations.

## ***Observed and Simulated Values***

Graphs of unweighted observed versus unweighted simulated values for each of the three simulations is shown in Figure 32. Ideally, the data would fall along a 1-to-1 line indicating an exact match between observed and simulated values. However, given the uncertainty in the measurements a one to one match is not reasonable or expected. Rather, the weighted observed versus weighted simulated values provide a better representation of the 1-to-1 relationship Figure 33. The overall relationship of observations and simulated equivalent pairs (Figure 32) again indicate that simulated flows to Applegate drain exceed observed flows as indicated in the previous graphs. A more detailed view of the stage and groundwater level values is provided on a separate graph (shown by the small box in the graph for all data) (Figure 32). A few outliers occur for each of the models with the groundwater levels, as expected given the 761 observations of varying quality taken from many sources.

## ***Evaluation of the Statistical Distribution of Residuals***

The validity of statistics resulting from nonlinear regression depends on the errors being random, normally distributed, and independent. We will never know the true errors, so we assume these criteria are met if the weighted residuals exhibit these properties. If weighted residuals are independent and normally distributed, they should form an approximately straight line on a normal probability graph. Figure 34 shows the normal probability graphs for the three models along with 95% confidence intervals on the expected range of synthetic normally distributed residuals with the same statistical properties as the model residuals. CM-23 and CM-25 show that several reservoir stage and groundwater level observations are beyond the 95 percent confidence intervals, indicating the presence of some model bias. The correlation between weighted residuals and the means of synthetic residuals should be close to 1.0 (Poeter and others, 2005). The reported values for CM-23, CM-25, and CM-18 are 0.9973, 0.9974, and 0.997, respectively. Considering that many of the residuals for CM-23 and CM-25 that fall outside of the theoretical ranges in Figure 34 are related to reservoir stages, it is expected that averaged inflow and outflow data used in the lake package may be the source of this error. This is further addressed in the discussion and conclusions section. For CM-18, the values all fit within the theoretical confidence intervals, thus indicating the weighted residuals satisfy the requirements for application of nonlinear regression to optimize the model parameters.

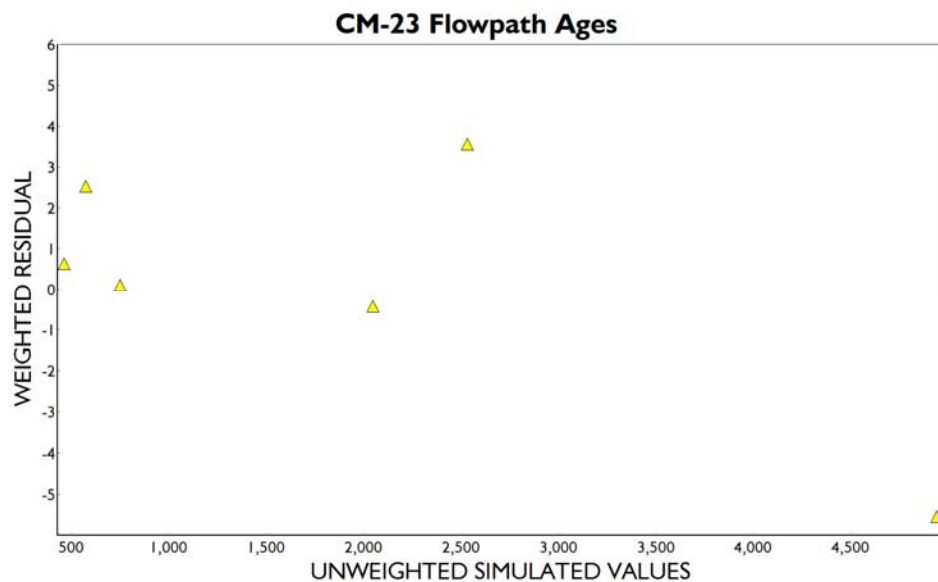
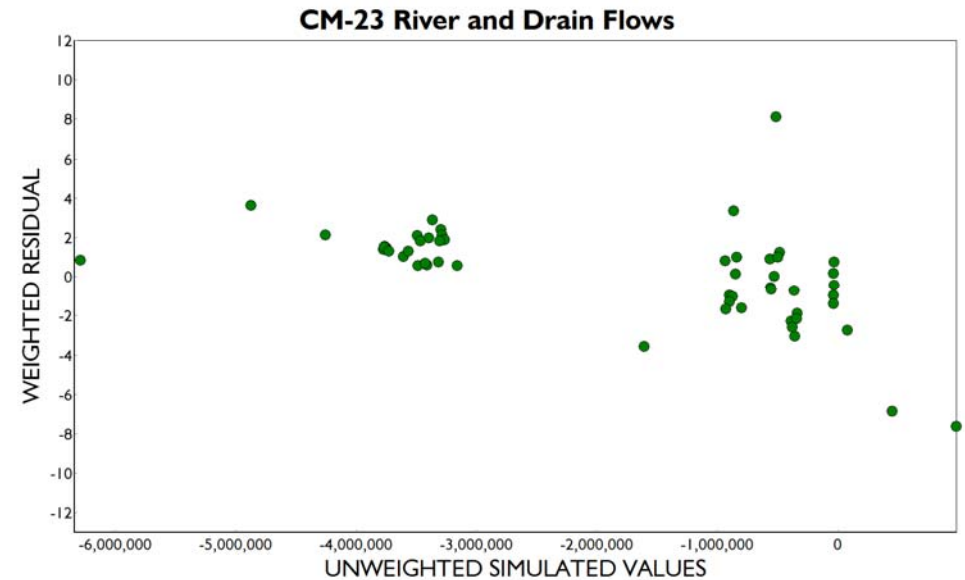
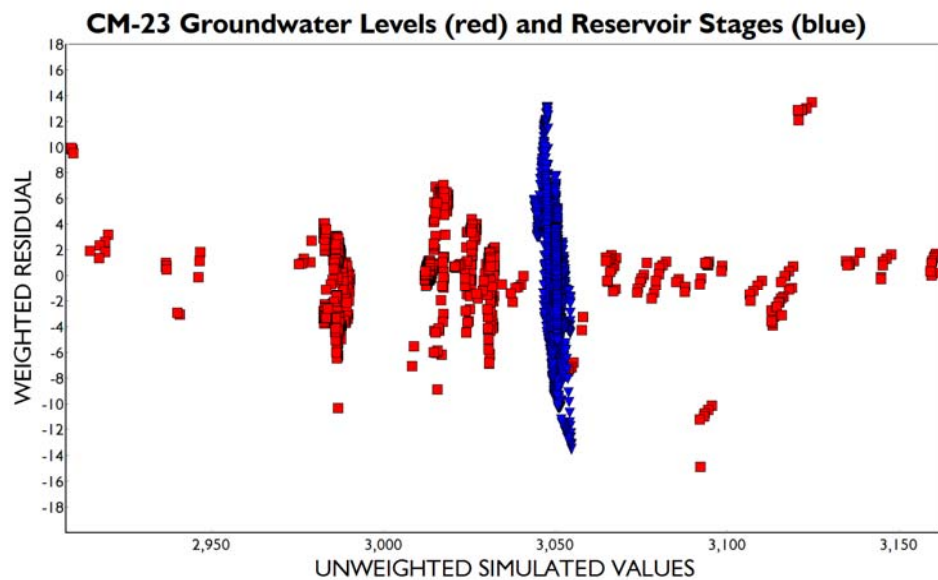


FIGURE 31. Weighted residuals versus simulated equivalents for CM-23 (this page), CM-25 (next page), and CM-18 (subsequent page). Weighted vs. simulated residuals are shown individually for flowpath ages and groundwater contribution to river and drain flows. Weighted residuals for groundwater flows and reservoir stages are displayed on the same graph.

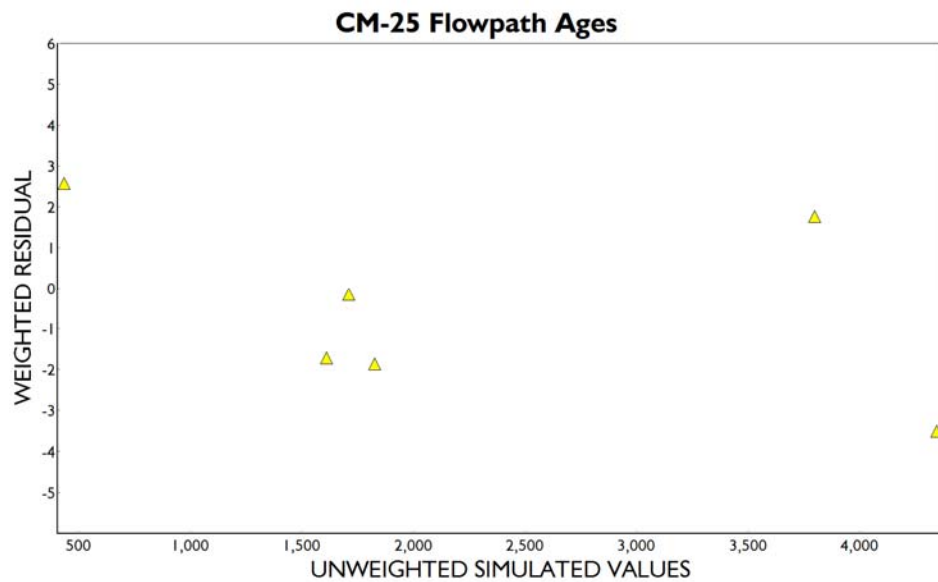
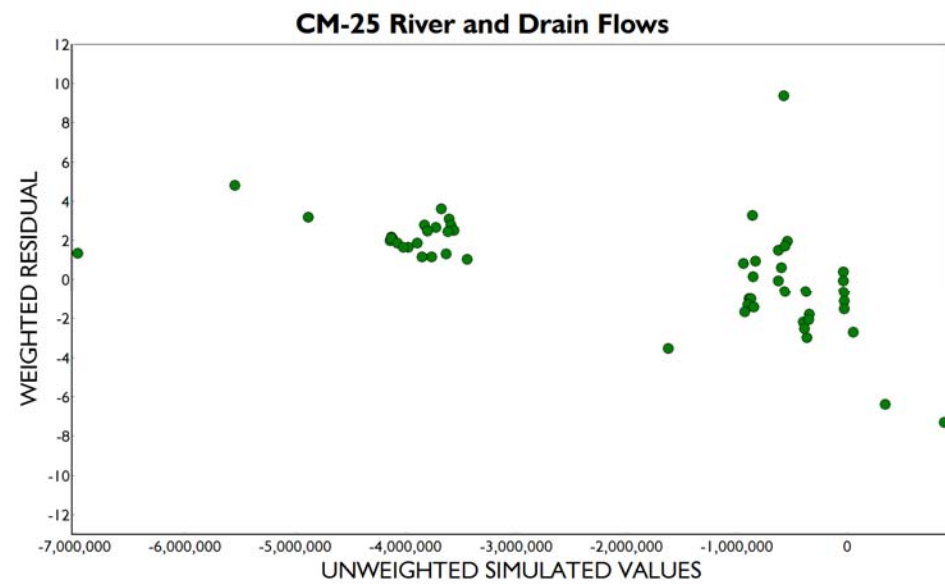
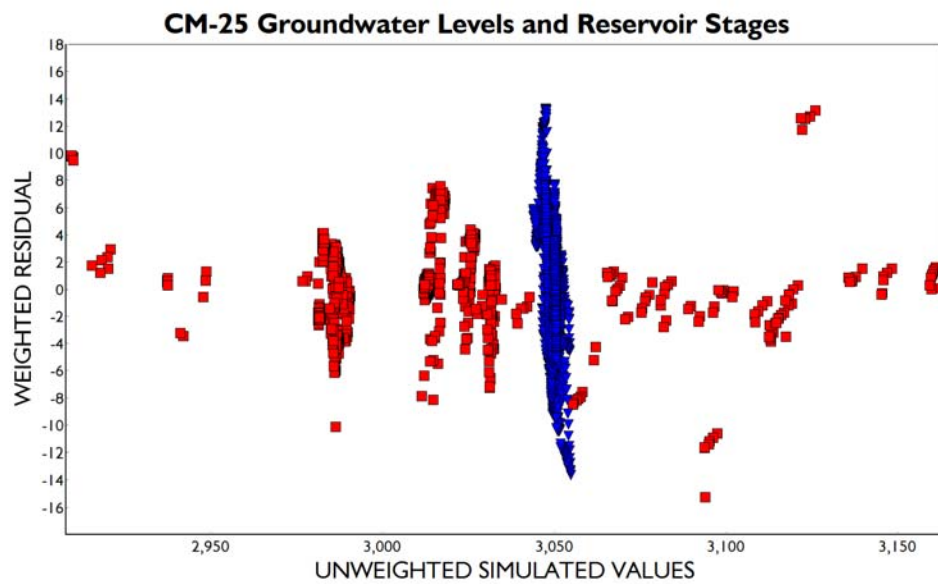


FIGURE 31. (cont.)

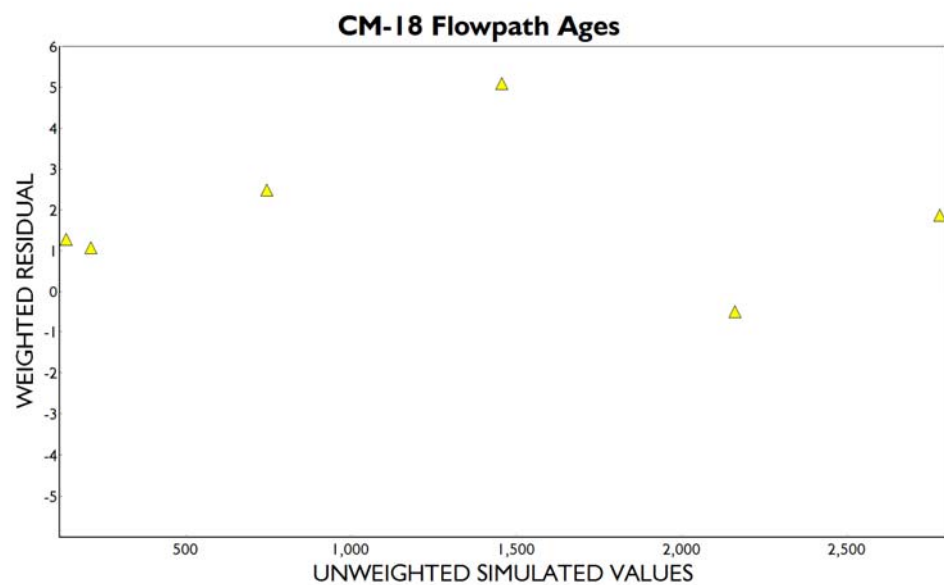
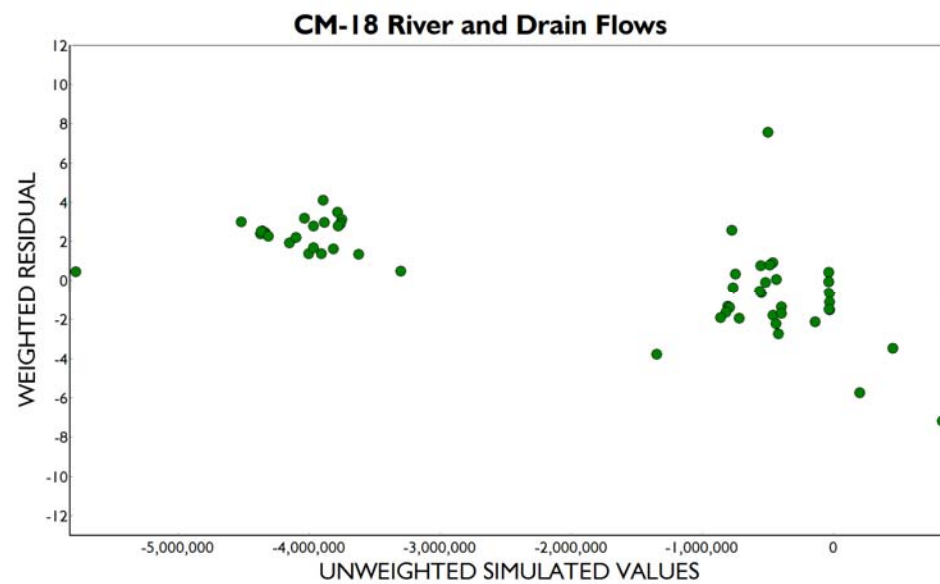
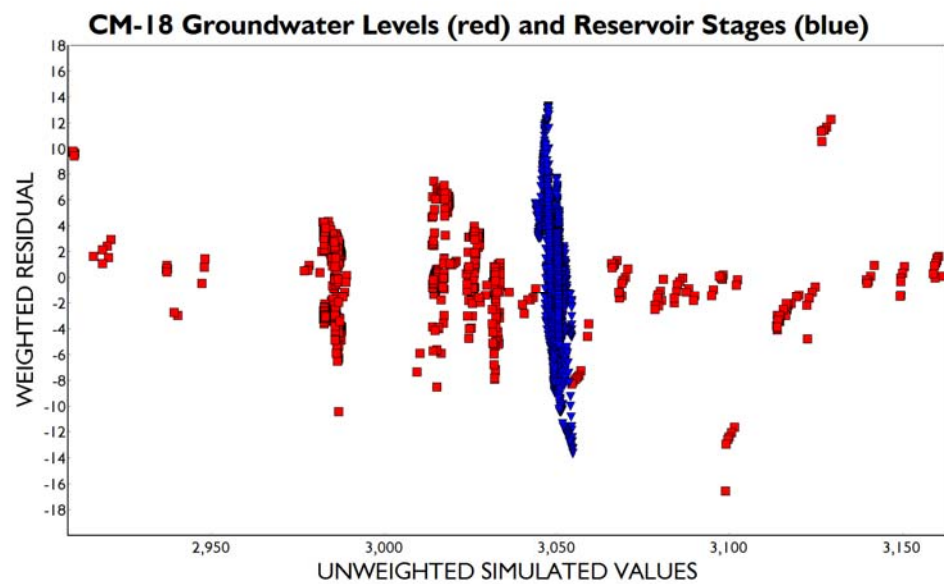


FIGURE 31. (cont.)

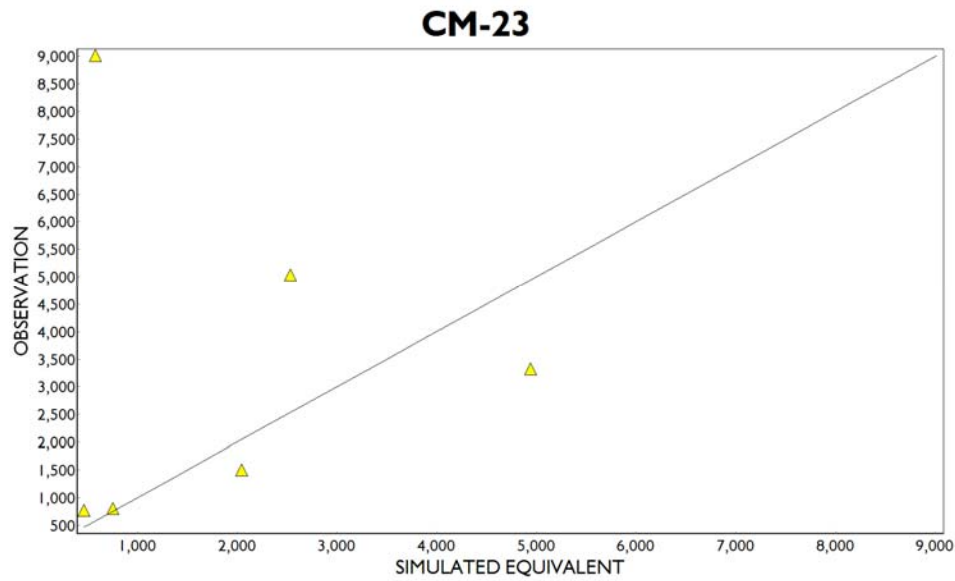
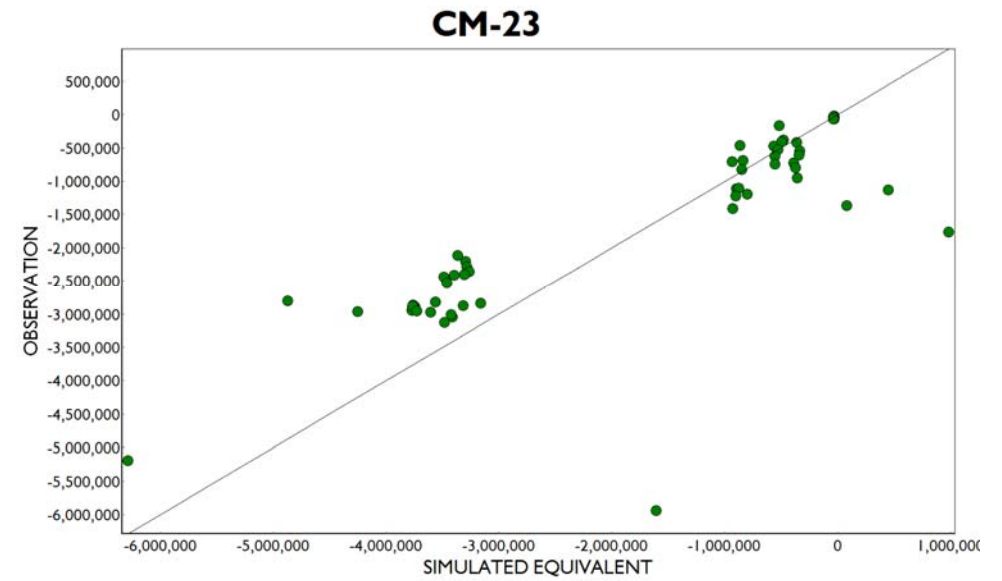
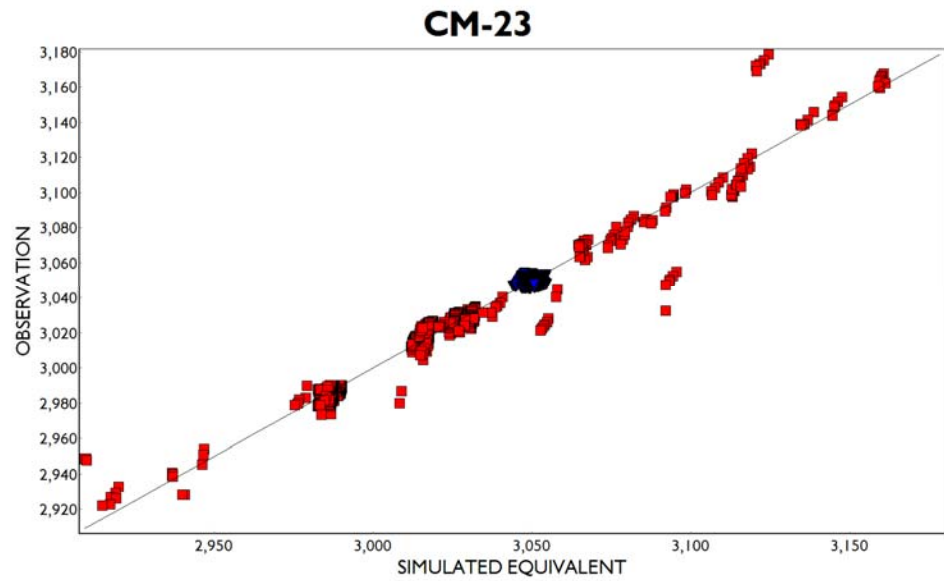


FIGURE 32. Unweighted observed values vs. unweighted simulated values. Groundwater levels (red squares) and reservoir stages are on the upper left chart, river and drain flows are shown above and groundwater flowpath ages are to the left. Plots for CM-25 and CM-18 are displayed on the next two pages.



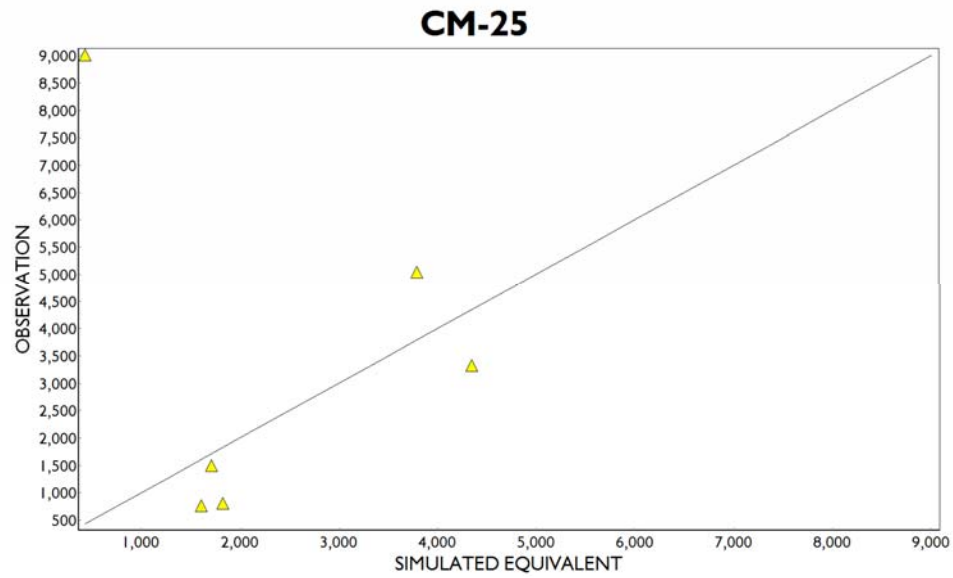
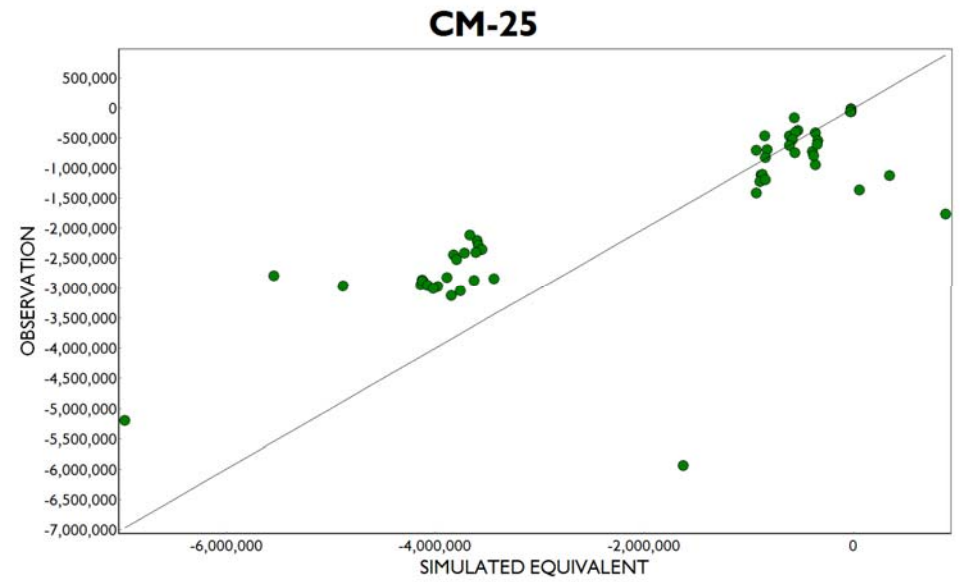
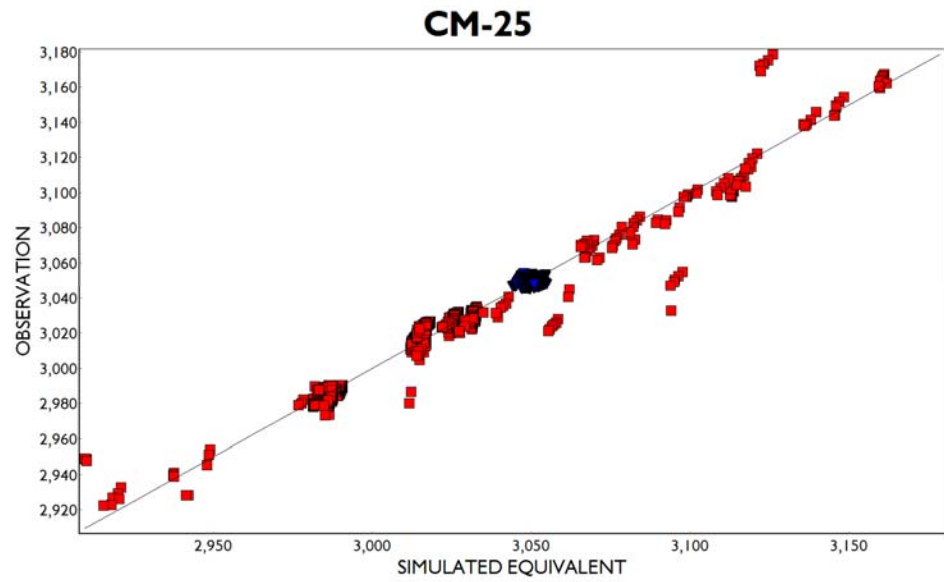


FIGURE 32. (cont.)

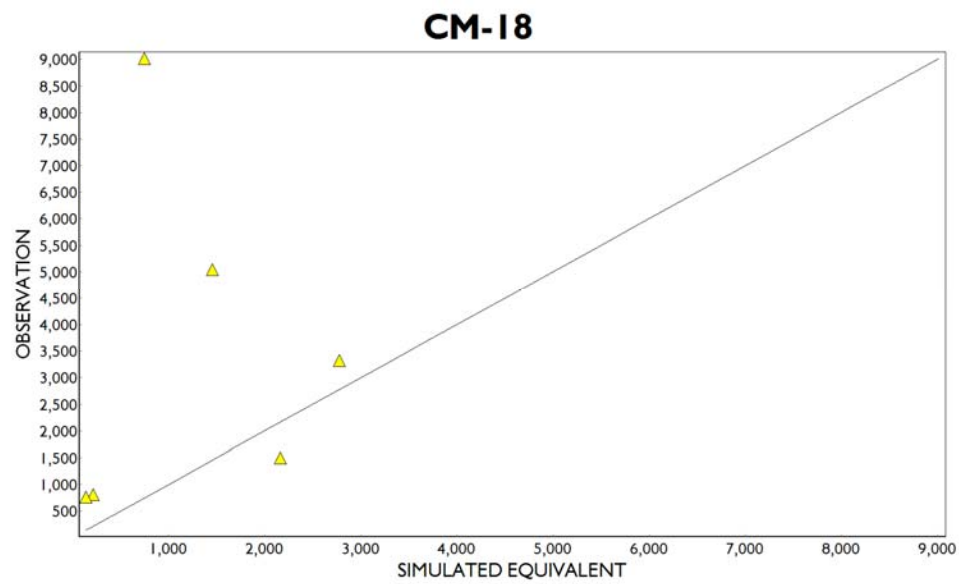
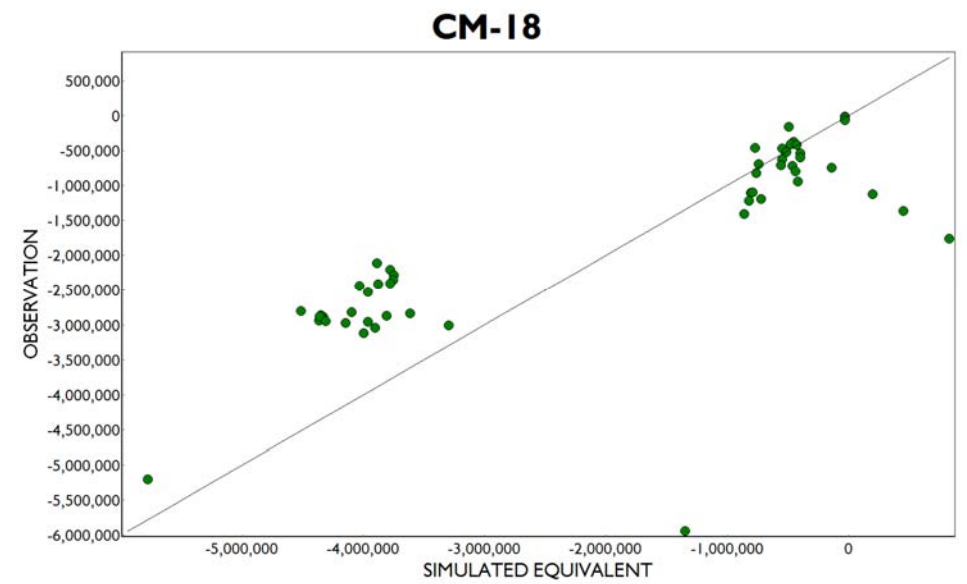
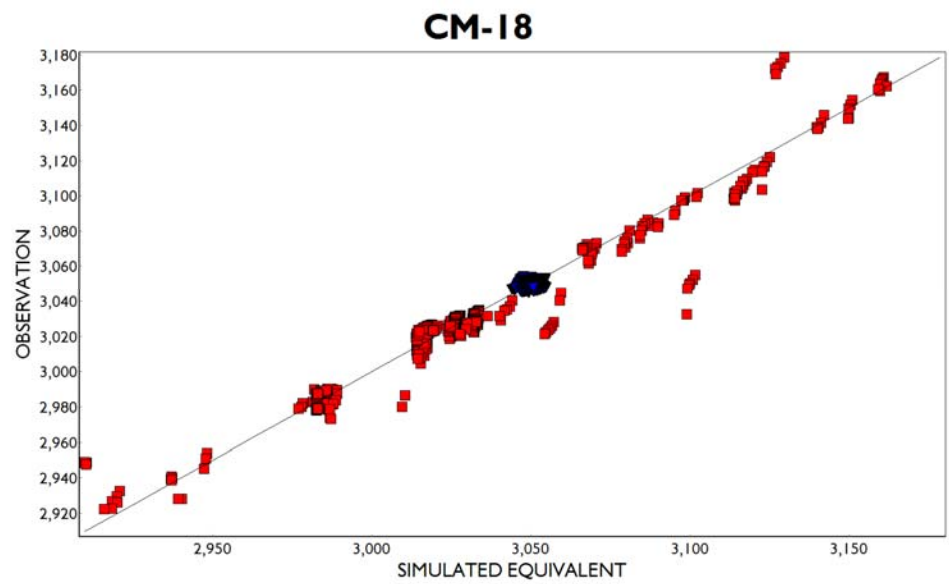


FIGURE 32. (cont.)

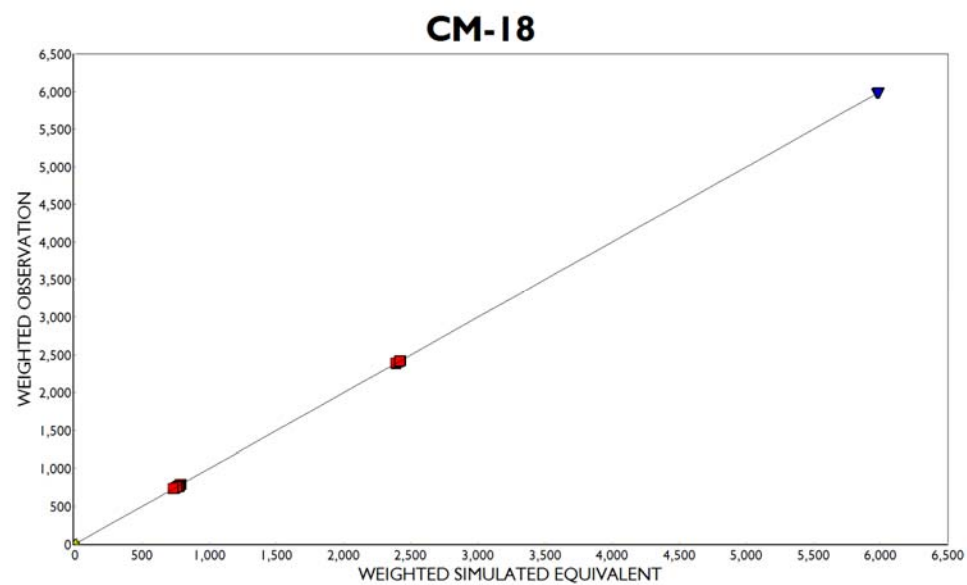
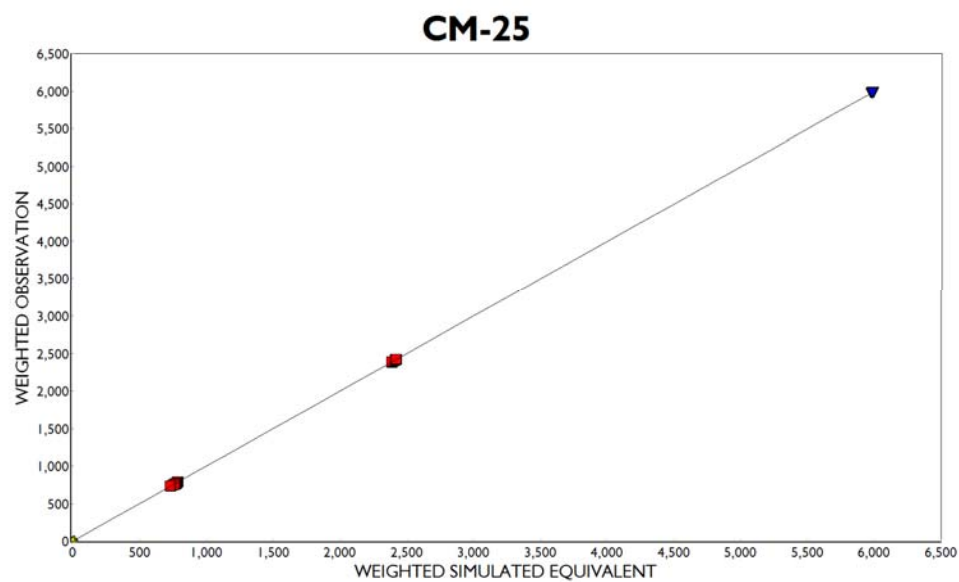
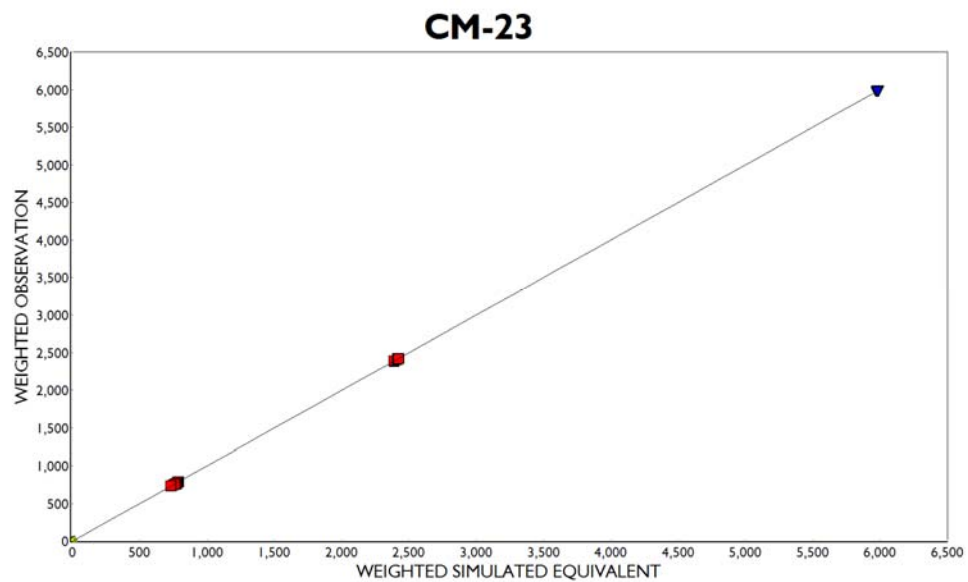


FIGURE 33. Weighted observed vs. weighted simulated values for CM-23, CM-25, and CM-18. The color code for symbols is the same as in Figure 29.

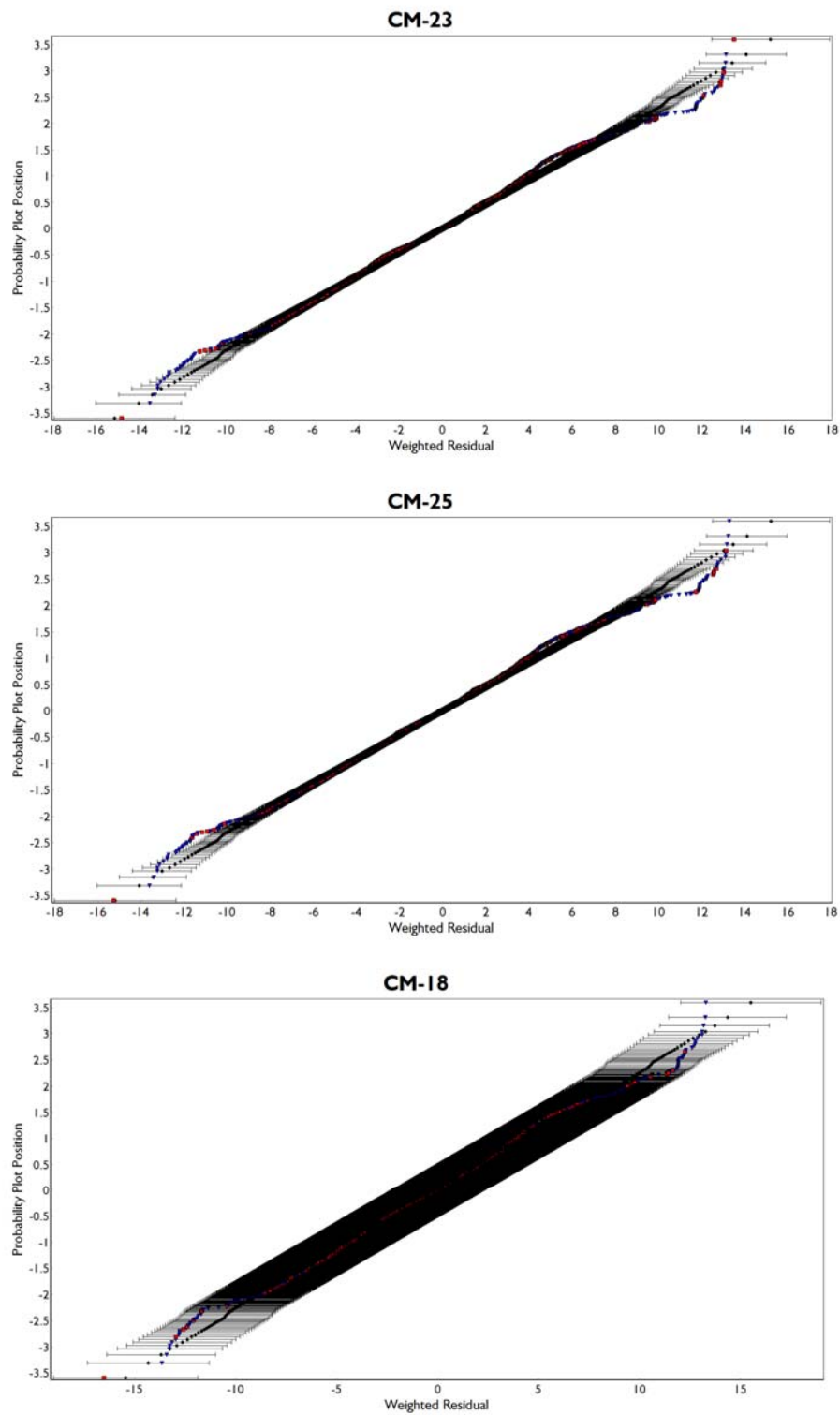


FIGURE 34. Normal probability graphs for CM-23, CM-25, and CM-18 plotted with 95% confidence intervals on normally distributed synthetic residuals with the same statistical characteristics as the model residuals

## Optimized Parameter Information

The optimized model parameters are presented in Table 6 and Figure 35. Note that the each of the Kh (HK#) parameters, despite having the same names, do not relate to the same zone or layer in each of the three models, therefore comparisons between Kh values between models should not be made. However, HK1, HK2, and HK3 in CM-23 represent the same zones as CM-25's HK-2, HK-3, and HK-4, respectively. HK-1, 2, 3, and 4 for CM-18 represent the Kh values uniformly distributed in layers 1 through 4, respectively. Other parameters represent the same model feature in all three models, and so can be compared. Note that Rch3 was not estimated for CM-25 nor CM-18 as preliminary optimizations of these models indicated very little sensitivity to this parameter. It was assigned a rate of 5 percent of annual precipitation (0.95 in/yr) in those models.

TABLE 6. Optimal parameter information from the top 3 conceptual models. Units for parameters are shown in the top row of the table and apply to all other occurrences of the term in other rows. In many cases values in the same column have some equivalence between models (the related text elaborates on this).

CM-23			HK1 ft/d	HK2 ft/d	HK3 ft/d	Leakance ft/d/ft	Riv Cond ft/d/ft	West Cond ft/d/ft	East Cond ft/d/ft	Rch1 in/yr	Rch2 in/yr	Rch3 in/yr
Upper 95% C.I.			220	174	127	$6.9 \times 10^{-3}$	143	24	0.63	3.6	14.4	1.9
Optimal Value			204	156	24	$6.6 \times 10^{-3}$	67	19	0.44	2.9	12.9	0.49
Lower 95% C.I.			189	140	5	$6.2 \times 10^{-3}$	31	14	0.31	2.2	11.8	0.11
CM-25		HK1	HK2	HK3	HK4	Leakance	Riv Cond	West Cond	East Cond	Rch1	Rch2	Rch3 not est.
Upper 95% C.I.		102	263	198	406	$7.0 \times 10^{-3}$	87	36	0.57	3.8	16.7	
Optimal Value		63	243	177	118	$6.7 \times 10^{-3}$	37	27	0.40	3.0	15.0	0.95
Lower 95% C.I.		39	225	159	35	$0.4 \times 10^{-3}$	16	20	0.29	2.5	13.7	
CM-18	HK1	HK2	HK3	HK4		Leakance	Riv Cond	West Cond	East Cond	Rch1	Rch2	Rch3 not est.
Upper 95% C.I.	310	668	174	174		$7.1 \times 10^{-3}$	4.1	34	0.61	3.4	13.3	
Optimal Value	163	511.	149	146		$6.8 \times 10^{-3}$	2.4	25	0.41	2.3	11.8	0.95
Lower 95% C.I.	85	391	127	122		$6.5 \times 10^{-3}$	1.5	18	0.28	1.5	10.3	



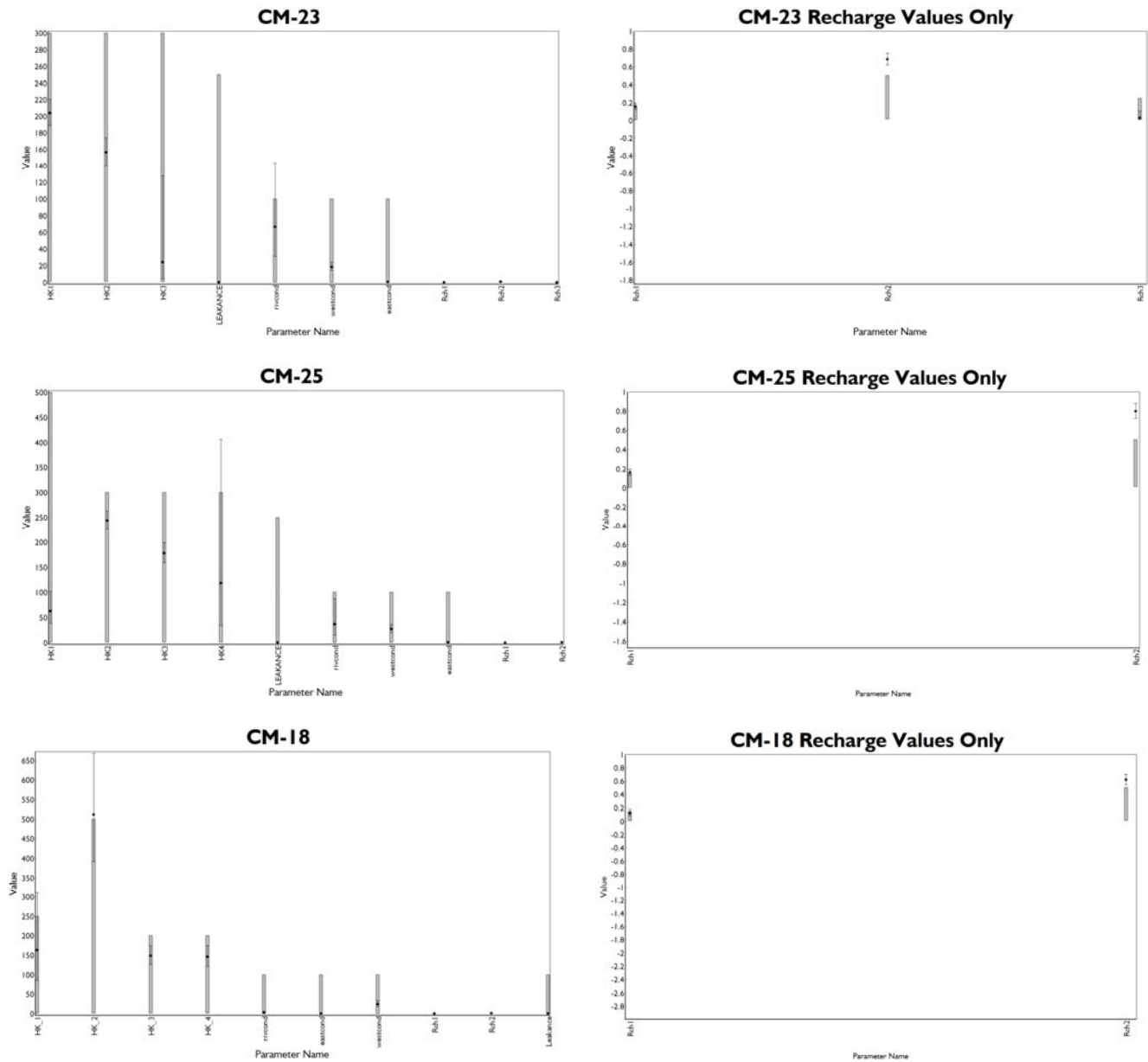


FIGURE 35. Optimal parameter values along with confidence intervals (error bars) and reasonable ranges (gray bars) for the top 3 conceptual models. Units for the values are indicated in Table 6. Recharge values are shown separately as well because the range of their values is smaller.

The optimized parameter values show interesting trends. For Kh, most of the optimized terms that represent Ogallala Group deposits are higher than the average values that have been documented in previous studies, although most of the values are within the expected ranges reported in studies of the HPA. The model optimizations resulted in similar values for the two models using regionally based zones for Kh, most notably with HK1 and HK2 in CM-23 and HK2 and HK3 in CM-25. Although the optimized values for CM-23 are slightly higher than reported Kh values for the Ogallala Group, this model is a single layer encompassing the overlying coarser Quaternary deposits so the Kh term is a composite Ogallala and Quaternary Kh values. In CM-25 HK1 represents Kh of Quaternary deposits throughout layer 1 of the 2-layer representation. The Quaternary deposits are likely to have a wide range of Kh values, and the final value of 63 ft/d closely matches documented values of HPA deposits. HK3 in CM-23 and HK4 in CM-25 represent zones of limited areal extent and more different between the models than any other Kh term. The broad confidence intervals for these two parameters indicate the low sensitivity simulated equivalents to these parameters.

The 4-layer structure of CM-18 is considerably different than CM-23 and CM-25, yet the Kh values are similar for those parameters representing similar areas. However, the models differ greatly in their representation of the Kh of the Quaternary deposits. HK1 represents all surficial Quaternary deposits and is assigned over all of layer 1 in the 4 layer model. The resulting value of 163 ft/d for Kh is higher than would be expected for the fine deposits found at this interval. However, because layer 1 is thin in this model it is inactive throughout much of the grid except in the area surrounding Sutherland Reservoir and the Platte River alluvium, thus the high estimated value only represents local conditions near the reservoir and the river. In addition, the Lake Package of MODFLOW is in direct lateral connection with layer 1 and sits directly above layer 2. Layer 2, a layer conceptualized to contain only coarse deposits in CM-18 might be too thin or have insufficient connection with the lake to produce enough seepage for the regression to match the reservoir stages, thus the regression compensates with a high value of HK1.

The optimal value of HK2, which represents Kh for layer 2 in CM-18, falls within the range of reported values of typical alluvial deposits. As with layer 1, layer 2 of the 4 layer grid is also inactive throughout much of the study area except near Sutherland Reservoir and areas underlying the Platte River-system valley. HK3 and HK4 represent all of layer 3 and 4, respectively, which together encompass all of the Ogallala Group, with HK3 representing approximately the upper half of the group and HK4 the lower half. The two layers comprise over 80 percent of the aquifer thickness even where layer 2 is active as seen in Figures 12 and 29. Since these two layers form the majority of the aquifer in the GGS-SR study area and are uniform throughout the entire layer, they can be compared in a general sense with HK1 and HK2 in CM-23 and HK2 and HK3 in CM-25. The Kh values of layer 3 and 4 in CM-18 are similar to those resulting from the optimization of the single and 2-layer models. Although HK3 is relatively close to HK4, it was conceptualized that HK3 would have higher rates due to the presence of coarse deposits in the near-site area in the Upper Ogallala Group. However, the optimization resulted in a higher value for HK4. This may be a result of the regression responding to conditions in the outer-model area.

Recharge is the other major conceptual difference in the suite of models, and the top six ranked models all used the topographic regions recharge scenario, thus the topographic regions recharge scenario applies to all three of the models discussed in detail. This is not entirely unexpected, as the land-use, soils, and combined topographic regions-land use conceptualizations are a modified version of the general topographic regions map with more detail related to a process or condition. The land-use conceptualization has two dominant land use practices (dryland and irrigated land) in the plains topographic region, and one dominant land-use (rangeland) in the sand hills area. The model ranks indicate that breaking down spatial areas based on these practices or conditions did not improve the fit between simulated and observed values, nor did basing recharge rates on soil-moisture holding capacity in soils. Since the topographic regions cover relatively large areas, the optimizations for the top models indicate that a regionally-based average rate will yield a model fit to observations as well if not better than the more detailed conceptualizations.

Rch3, representing the Platte River Valley, was only optimized for CM-23 because there was low sensitivity in CM-18 and CM-25, thus it was set as a fixed rate of 5 percent of annual precipitation (0.95 in/yr) in the latter two models. When recharge was adjustable, it was estimated as a percentage of annual precipitation which was interpolated between data locations for each cell. The values reported in Table 6 were converted to a rate in inches per year. Rch1 represents recharge on the plains area, which includes the near-site area. Optimized values of Rch1 range from 1.5 to 3.0 in/yr. These rates are consistent with rates reported by Peckenpaugh et al. (1995) for corn and small grains in both irrigated and dryland areas. Because the conceptualization of recharge in the plains area does not discriminate between irrigated and non-irrigated areas, the optimized rates in CM-23 and CM-25 are likely high due to the extensive occurrence of irrigated areas in the plains region. As shown in Figure 15, there are few groundwater level observations in the southwest corner of the model area where a mix of both irrigated and dryland practices are present. The optimized value of Rch2, which represents all of the sand hills/dunes in the study area, is significantly higher than previously reported rates in settings with grass-mantled sandy soils. Recharge rates for this region range from 11.8 to 15.0 in/yr in the sand hills area, or 62 to 79 percent of annual precipitation. These calibrated rates are based on annual precipitation, even though a portion of the recharge in the field is derived from irrigation in the clusters of center-pivot areas within the sand hills areas (figure 4). Another possible cause for the high calibrated rates of recharge relative to those documented in previous studies could be the presence of bare-dunes with very little vegetation (see Image 10). This area is poorly drained by surface features and runoff would likely enter the soil rapidly in the sandy areas. Another potential cause of the higher value of Rch2 may be that the southern boundary wasn't suitably represented as a no-flow condition. This condition was the inspiration for evaluating alternative models of CM-23, CM-25, and CM-18 (CM-23\_chd\_south, CM-25\_chd\_south, and CM-18\_chd\_south). However, the change to a fixed-head boundary did not improve the model fit for CM-23 and only slightly improved the fit for CM-18 so they were not considered further.

The remaining parameters optimized in the models were conductance terms for the South Platte River and drains in the model area, and the leakance term for Sutherland Reservoir. Optimized values for all of these terms were similar in the top three models, with the exception of the river conductance term in CM-18. The value optimized for river conductance in the 4-layer model was more than an order-of-magnitude lower than the optimized values for CM-23 and CM-25 and may be related to the high value of layer 1 Kh in CM-18. The optimized value of lake-leakance was similar for all three models and each had relatively narrow confidence intervals resulting from strong sensitivity to changes in lake-leakance.

After the following overview of other diagnostics of the three models, further discussion of the optimal parameters from all of the model conceptualizations is presented.

### ***Composite Scaled Sensitivities***

Composite scaled sensitivities (CSS) provide insight into the amount of information contained in all of the model observations for the estimation of individual parameters in an optimization. A few trends are apparent in the sensitivities for the three models (Figure 36). The leakance term that controls flow into and out of Sutherland Reservoir has large CSS in all of the models. This may reflect the use of daily reservoir stages as observations. The Kh and recharge parameters that apply to large areas also are sensitive in all models. CM25 showed nearly identical trends in parameter CSS as CM-23 (HK 1, 2, and 3 in CM-23 represent the same zones as CM-25's HK 2, 3, and 4). CM-18 showed more sensitivity to the uniform Kh values representing the Ogallala Group than the overlying Quaternary units, suggesting these units are more important in characterization of the flow system than the overlying deposits, which are much thinner and less extensive than the Ogallala Group. All models showed little sensitivity to the conductance terms, suggesting that perhaps these terms could have been assigned a value rather than estimated in the calibration process.

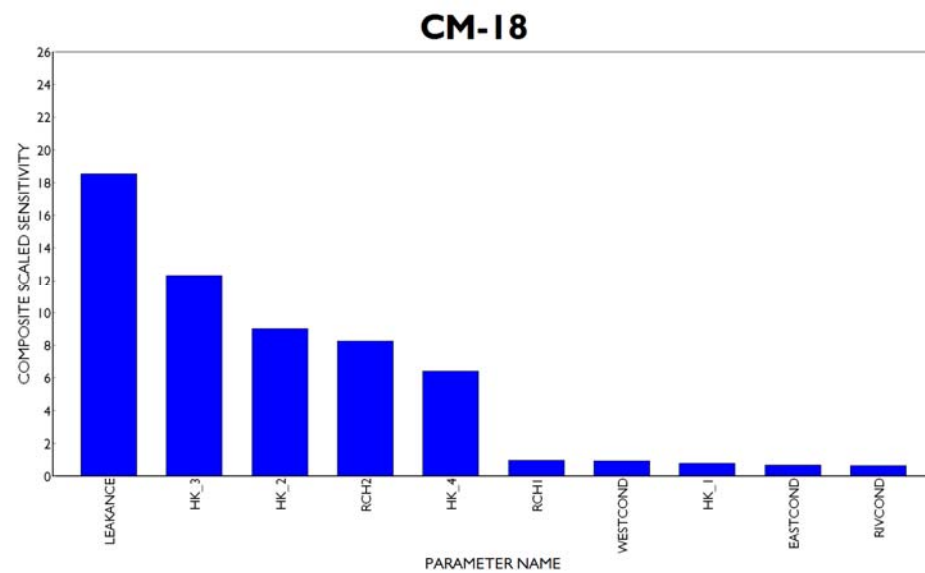
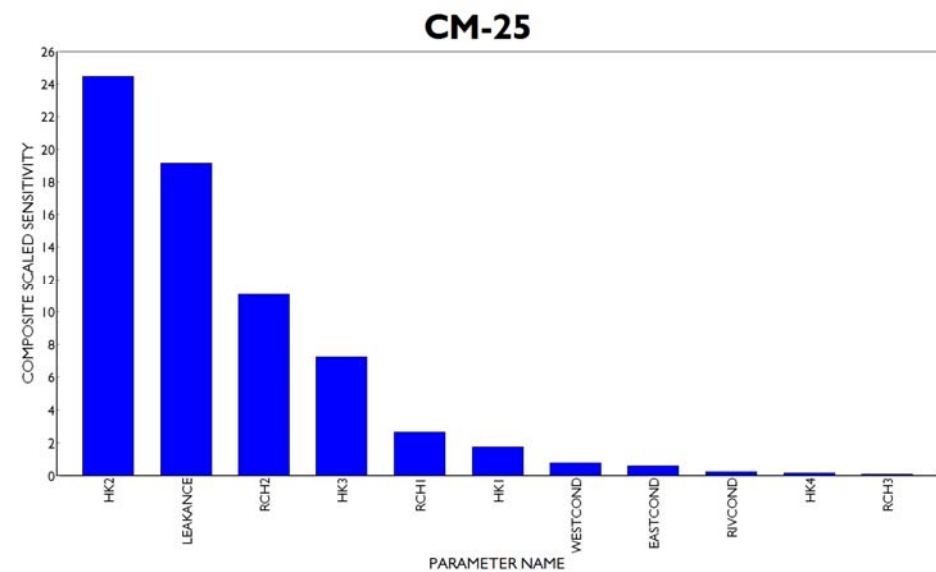
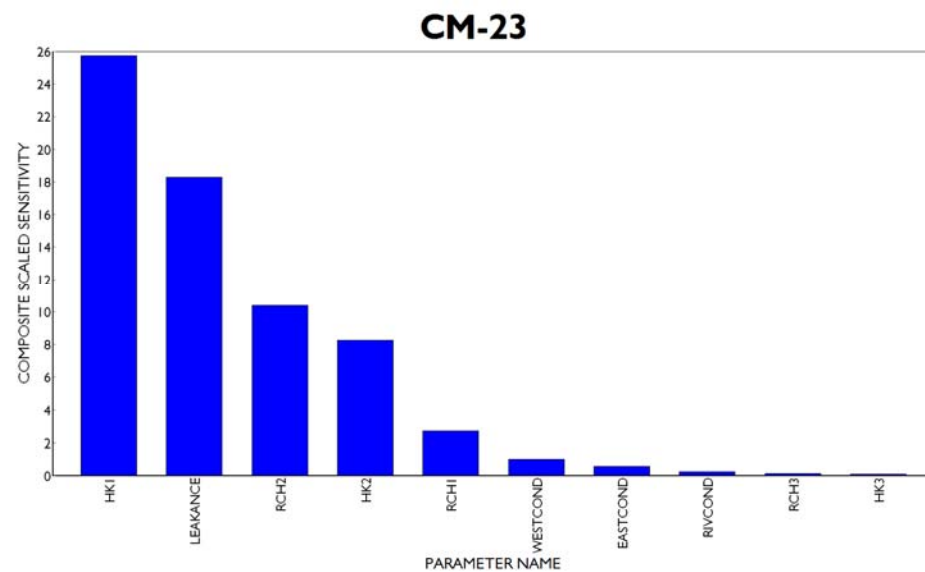


FIGURE 36. Composite scaled sensitivities for CM-23, CM-25, and CM-18.

## ***Analysis of Influence of Individual Observations on the Regression***

Evaluation of the influence of the observations on parameter estimation provides insight on useful endeavors for future field work regarding the types, locations and timing of observations that will be most valuable to future modeling tasks. Leverage statistics indicate the potential for an observation to have bearing on the regression, whereas influence statistics indicate not only their potential importance, but quantify the actual impact the observation has on the regression. The Cook's D statistic indicates how much a set of parameter estimates may change with omission of an observation. A critical value is calculated, and Cook's D values exceeding the critical value are considered influential in the regression. Hill and Tiedeman suggest Rawlins (1988) calculation of the critical value as  $4/ND$ . Using Rawlins' criteria for the models evaluated in this study, the critical value is 0.0016, thus observations that exceed this level are considered influential to the calibration of these models.

Cook's D values are shown in Figure 37 for the 30 most influential observations in the three models discussed in this section. Nearly 100 observations exceed the critical value for all of the models. Although most of the influential observations are heads and reservoir stages, they include at least one of each of the four types of observations used in the calibration for all three models. The numerous influential stage observations indicate the value of stage measurements. Groundwater levels are more influential than stage for the four aquifer model, probably because of the more limited connectivity of the lake to model layers in the 4-layer model. The most influential groundwater level observations were seasonal observations from the outer model area southwest of the GGS well field. Flows from the July 2006 measurement of Beer Slough (Beer2) and measurements made on the upper reach of the South Platte River (upperplt2 and upperplt3) are the most influential flow observations for all of the models. The only flow age observation showing critical influence on all three models was MW-2sh, located on the west side of the GGS well field. However, for model CM-25 the travel time observation MW-6sh was the 9<sup>th</sup> most influential observation in the regression. MW-5sh also had critical influence on CM-25. The variation of influential observations between models indicates that one cannot use just one model conceptualization to draw conclusions about the most valuable types, locations, and time of measurements. However the critical influence of the same observations in many models is useful for planning future field work.

The DFBETAS statistic, relates the relative importance of one observation to one parameter. It would be impractical to report the influence of all 2,570 observations on each of the 10 parameters. Consequently DFBETAS are shown for travel time observations because the travel times are a unique type of observation and are rather expensive so their influence is of particular interest (Figure 38). The critical value for the DFBETAS statistic is calculated as  $2/(ND)^{1/2}$  (Belsley and others, 1980), so it is 0.039 for the models considered here. Several travel time observations are important to select parameters in the optimizations of the three models. The optimization of CM-25 benefited the most from the travel time observations, as 6 of the 10 estimated parameters were influenced by travel time observations with DFBETAS above the critical level. For CM-25, MW-6sh exhibited the most influence on the estimation of any of the observations, with a value beyond the critical limit for four different parameters, including three Kh terms, a recharge estimate, and the leakance estimate. The calibration of CM-18 was less influenced by travel time observations, although MW-2sh influenced estimation of four parameters, including HK3, the Kh assigned to the upper Ogallala Group layer, as well as the Rch2 term, which represented recharge in the sand hills zone. Calibration of CM-23 was least influenced by travel time observations, although MW-2sh was again influential on the estimation of three parameters, including the recharge term for the sand hills zone and the lakebed leakance term. It is clear that travel time observations are indeed useful for calibration of several key parameters (Figure 38).

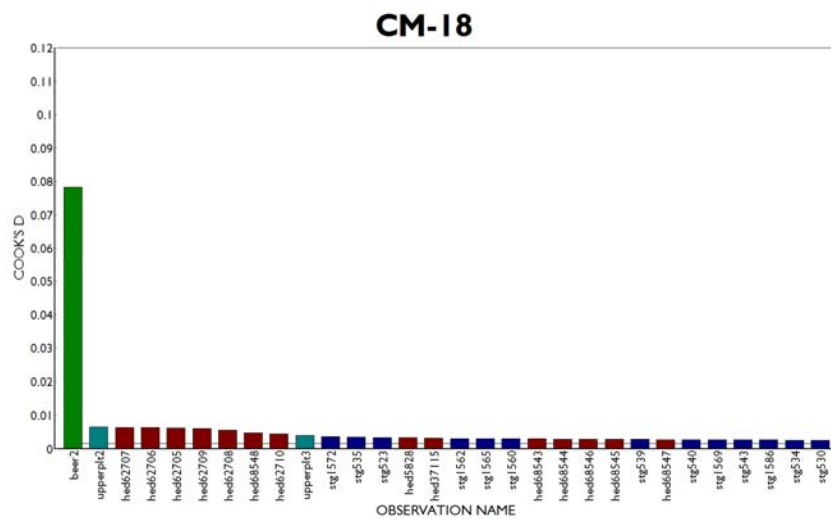
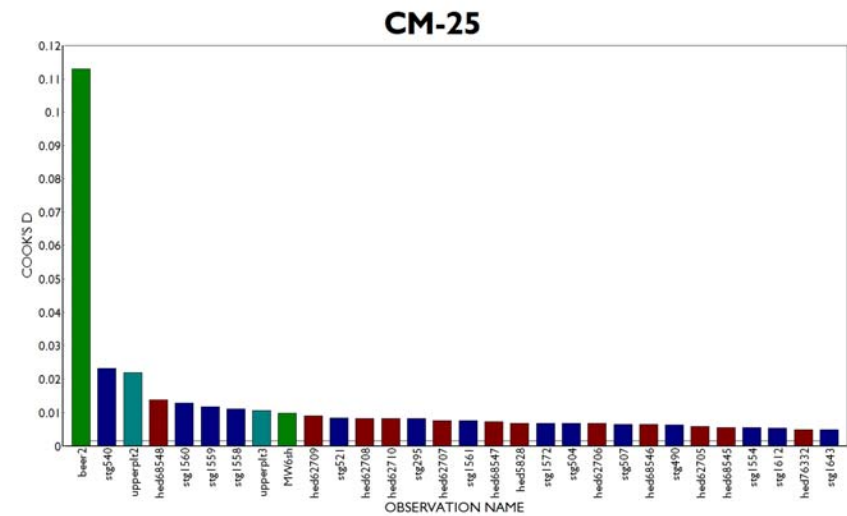
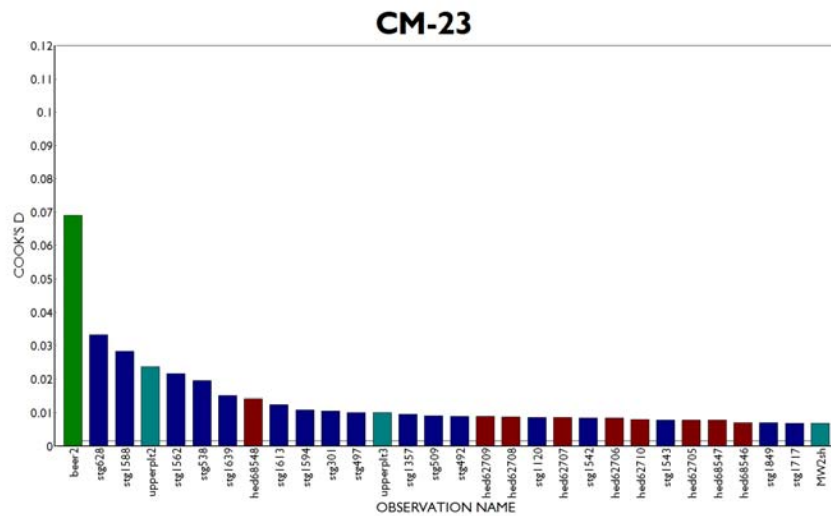


FIGURE 37. Cook's D for CM-23, CM-25, and CM-18 for the 30 most influential observations. Dark blue bars are reservoir stages, maroon bars are groundwater level observations, and various shades of green represent flow and flowpath age observations.



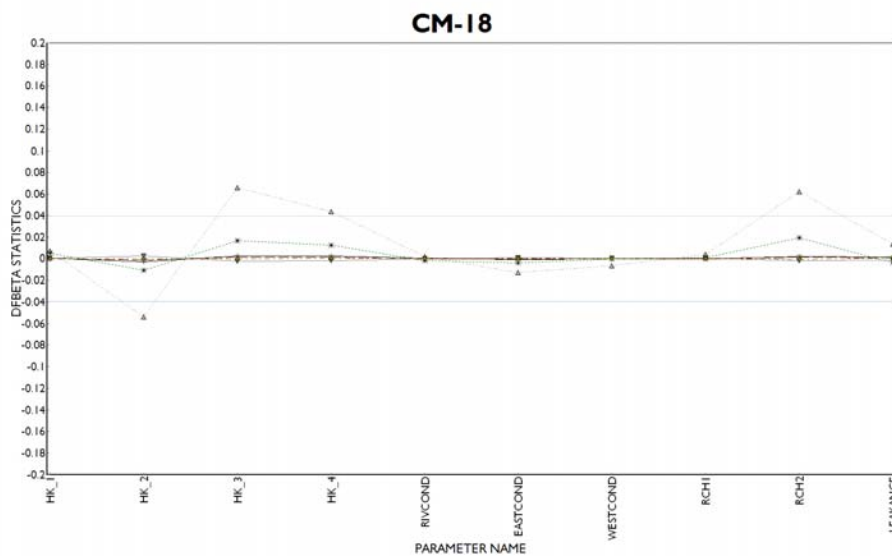
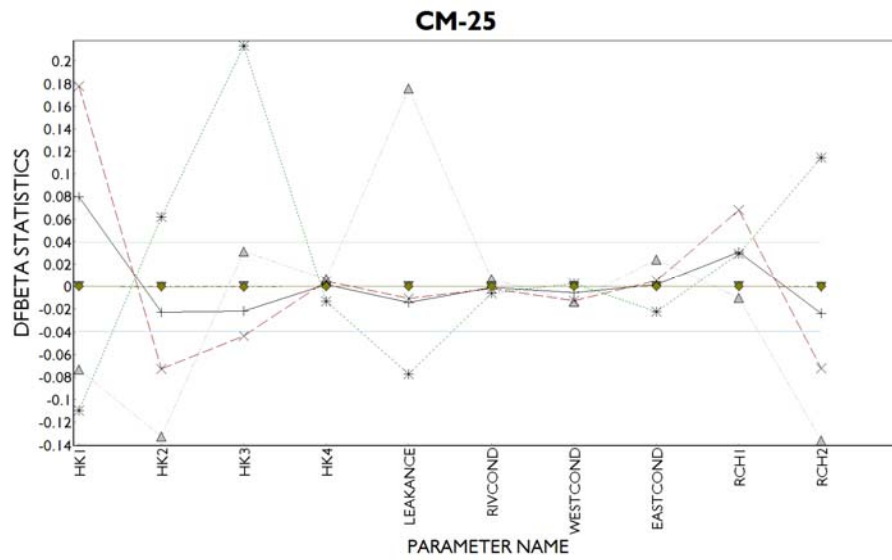
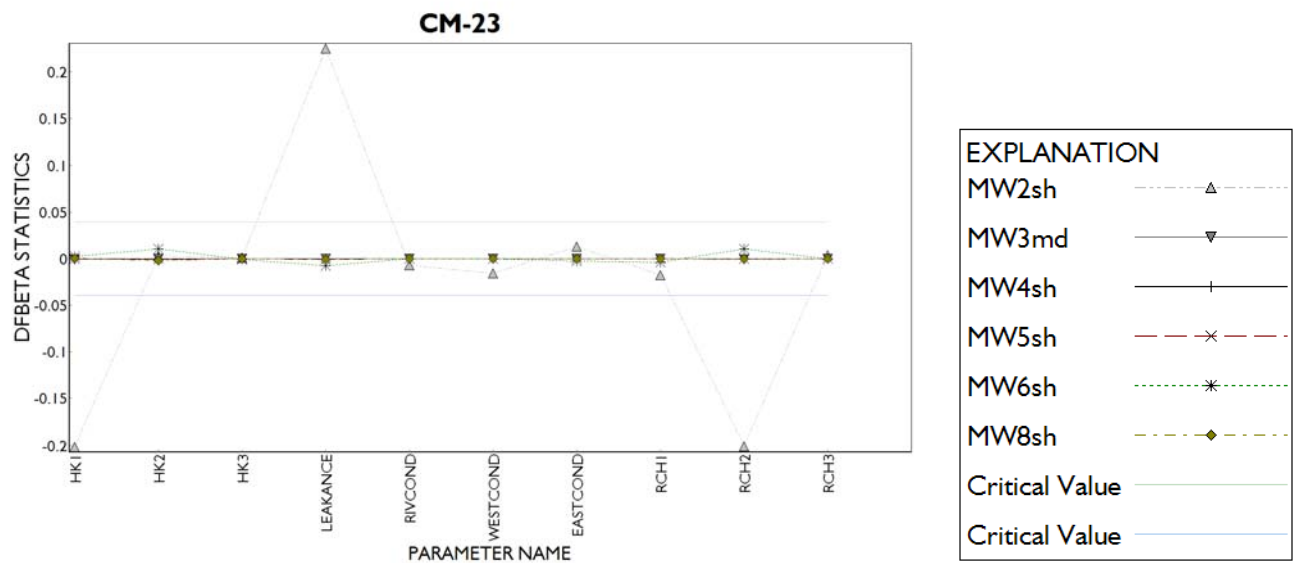


FIGURE 38. DFBETAS for travel-time observations.

## Spatial Trends in Weighted Residuals

Figure 39 exhibits the variability of weighted residuals from optimization of CM-23. Transparent bubbles within smaller or larger bubbles indicate the presence of multiple observations from the same locale, such as where transient groundwater level observations are made. Where colors are solid, only one weighted residual value exists. Ideally, residual maps have a random distribution of size and sign. The map for CM-23 displays an acceptable level of randomness, although there may be a trend towards negative residuals in the southern of the outer study area. Residuals near Sutherland Reservoir and the GGS well field indicate a random distribution of large and small as well as positive and negative residuals. The spatial distribution of residuals is similar for all three models, so only one map is included.

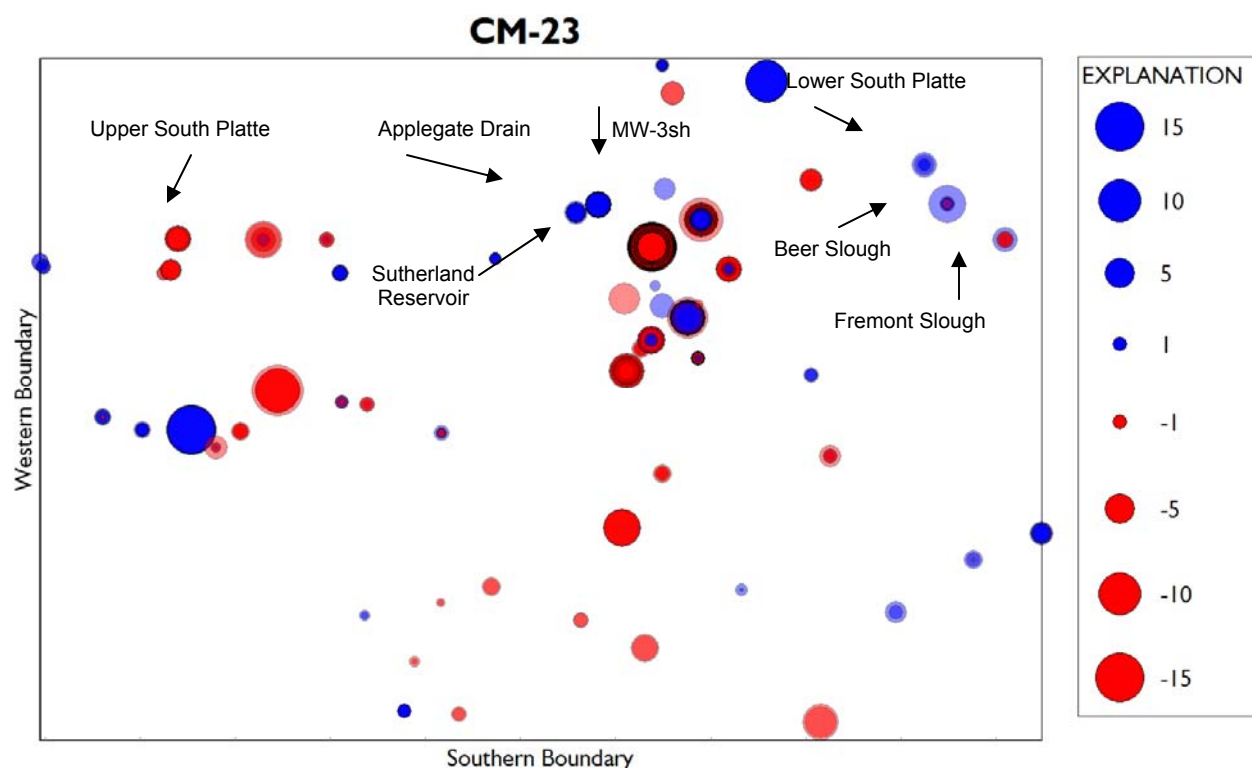


FIGURE 39. Spatial distribution of relative magnitude of weighted residuals (in the model domain). Blue bubbles indicate positive residuals (simulated values < observed values) and red bubbles indicate negative residuals, simulated levels values > than observed values). Points are slightly transparent to show the variability in residuals at locations with multiple observations such as those near Sutherland Reservoir. Select observation names are highlighted. The weighted residuals are dimensionless.

## Discussion of Calibration Results

The information obtained by using UCODE to calibrate models provides insight into model characteristics beyond the information typically gleaned from a trial-and-error calibration. The output indicates influential observations, parameter correlations, and provides confidence levels on estimated parameter values and subsequent predictions. These tools, coupled with the information provided by the MMA analysis allows the user to discriminate the quality of calibrated models in a suite of potential conceptual models of a site.

The graphics and statistics also provide insight into model weaknesses that are easily overlooked when using trial-and-error calibration. Two of the three models had similar distributions of Kh (CM-23 and CM-25) while CM-18 was notably different in representing the hydrostratigraphic units with 4 aquifer

layers. However all of the top-ranked models used a regional-scale, general recharge configuration. Although CM-23 was ranked as the top model by MMA and contained significantly more evidence supporting its calibration as compared to CM-25 and CM-18, the uncertainty in a few estimated parameters as well as the deviation from some of the weighted residuals from theoretical intervals of a normal distribution lends support for averaging model predictions. CM-23 and CM-25 exhibited these deviations, whereas CM-18 did not. The weighted residuals most problematic in the advanced residual analysis plots were primarily reservoir stages and to a lesser degree, groundwater levels. Considering that over 1,900 daily reservoir stage observations were used in the regressions, inaccuracies in the inflow or outflow terms defined for the MODFLOW Lake package could result in larger variations of simulated reservoir stage than what occurs in the field. Averaging predictions based on models that have different hydrostratigraphy can be advantageous as system characteristics present in one model but not others may influence predictions.

The ranking of the optimized models by MMA shed light on the question of the level of complexity necessary to reach the best calibration of the system. In the top 10 models, half had three or more hydrostratigraphic layers, whereas the remaining five models were composed of either a single layer or two layers. None of the top 10 models were conceptualizations with Kh based on the presence of coarse deposits in the near-site area, nor were there any conceptualizations with spatially varying Kh. Although it is common to consider more complex models with spatial variability to be “better” models, the variability present in the Kh field from the interpolation of information from the GGS well field and irrigation wells did not capture variability of aquifer permeability that allowed for improved calibration beyond the quality of a model with uniform hydraulic conductivities. Although Kh variability within the GGS well field existed as indicated by the transmissivity values for GGS wells in Appendix D, the values did not typically differ by more than a factor of 4. Thus, this variability in permeability in the near-site area where hundreds of groundwater level and reservoir stage observations were available did not result in a better fit of simulated to observed values than could be attained using a uniform or zoned Kh distribution.

The use of zones for delineating variation of Kh is sometimes viewed as being too simplistic and not representative of geologic field conditions, however neither the inclusion of unique zones nor smooth spatial variation of Kh in the near-site area based on thicknesses of sand and gravel units resulted in optimizations superior to the representations with uniform values.

In addition to alternative conceptualizations of Kh based on discrete zones and smooth spatial variation, other models were tested that assumed the spatial distribution of Kh values was in fact the true field distribution and the values of Kh were not adjusted during the regression. Unadjusted, spatially variable Kh values were tested on two model hypotheses, CM-7 (2-layers) and CM-19 (4-layers). This exercise was conducted to test the quality of a model with no adjustment of K values, and to determine the optimal values of other parameters when K values were not adjusted. These models performed poorly (CM7fKh and CM19fKh) compared to other conceptualizations for which the optimized values of Kh were typically higher than the fixed Kh values which were based on 24-hour aquifer tests and specific capacity data.

## Predictions

Following optimization of the 42 conceptual models of the site and the multi-model ranking, a predictive scenario was tested on the top 3 ranked simulations from the multi-model analysis. The predictive analysis evaluates the impact of pumping the GGS well field and statistics that reveal information pertaining to parameters that are influential to the predictions, which in-turn provides insight into observations that are important to the predictions. Although MMA showed strong evidence towards CM-23, predictions were evaluated for the top 3 models because they had substantially different hydrostratigraphic structures. If predictions based on the 1-, 2-, and 4-hydrostratigraphic-layer models differed substantially, further variations of the multi-layered alternatives that might provide better quality calibrations would be worth exploring. These would give water-resource managers a stronger sense of the potential extent of impact from long-term pumping of the wellfield.

## Prediction Scenario

Several predictive scenarios are of interest for the GGS well field. The goal is to find a scenario that ensures the aquifer will meet both industrial and agricultural needs over the long-term. First, considering the severity of the drought in the early 2000s, the long-term capacity of the well field under drought conditions is of primary interest to NPPD and surrounding landowners. An example of such a scenario is used in this study to evaluate the predictive capability of the model. The scenario involves pumping the well field for 4 summer months annually for 5 consecutive years. The impacts of interest are: 1) groundwater levels at the end of each pumping season, 2) groundwater levels at the end of each annual recovery period, 3) groundwater levels at the end of the 5 year predictive timeframe, and 4) groundwater discharge to Hershey Slough. Hershey Slough was chosen because of its location between Sutherland Reservoir and the South Platte River. Of particular interest is whether long-term pumping from the well field on the south side of the reservoir reduces lake seepage to the north. Four locations were used to determine the impacts of pumping on the groundwater levels, with three locations beyond the NPPD property line to the west, south, and east, and one location in the center of the GGS well field. Locations for predicting changes in groundwater levels are shown in Figure 40.

For this scenario, each GGS well that was active in 2007 was pumped continuously from July through September for the years 2008 through 2012, with decreasing rates occurring throughout the pumping period each year due to decreased water levels influencing transmissivity. Declining pumping rates were observed in the active wells during the years of 2005, 2006, and 2007. The average rates of decline were used to estimate pumping rates for the future years. The 2007 pumping scenario was included in the simulation to extend the calibration simulation to the start of the prediction period. Actual pumping rates and times provided by NPPD were used for the 2007 summer stress periods.

Because water level declines occur seasonally due to irrigation pumping in the near-site area outside of the NPPD boundary, simply calculating drawdowns of a long term pumping scenario does not determine the impact of the GGS well field. To determine this impact, the difference of heads and flows resulting from a simulation of the 5 year period without the GGS wells pumping and the same simulation with the GGS wells is calculated. All other stresses were held constant at the values that were applied in the transient calibration models. For Sutherland Reservoir represented with the Lake Package, inflows and outflows were constant at the flow values that occurred in the spring of 2007.

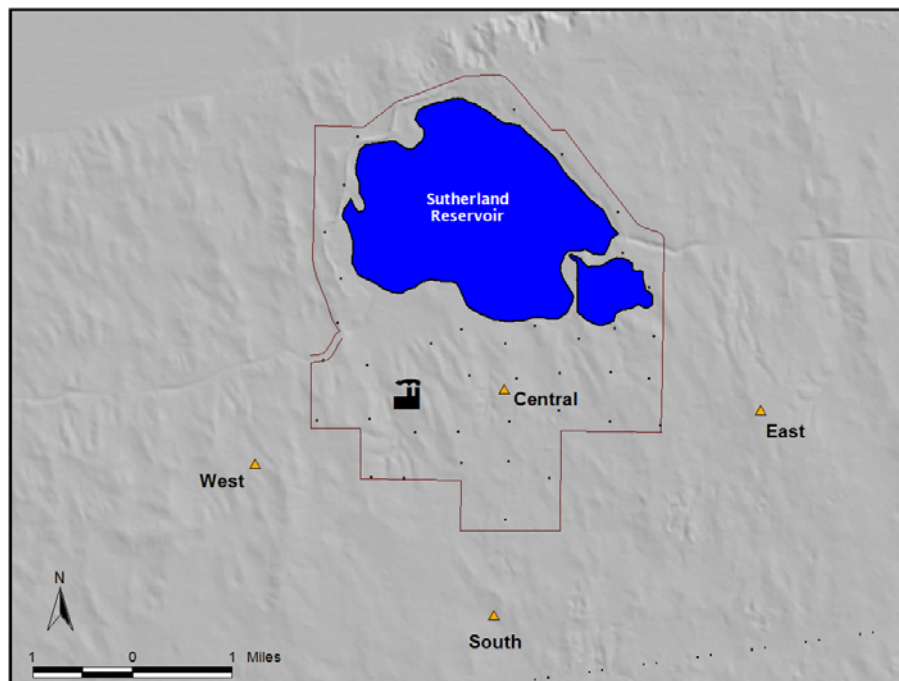


FIGURE 40. Locations of groundwater level prediction points for five-year extreme summer pumping scenario example. Small dots represent pumping wells. Yellow triangles are prediction locations.

## ***Prediction Modeling Tools***

The structure of the extraction capabilities of UCODE\_2005 allow prediction of the impacts of a long-term stress (pumping) on two different system features (groundwater levels and flows) from the same simulation, and calculation of 95-percent confidence intervals on the predictions. The water level declines were not explicitly extracted from the MODFLOW output, but rather determined through a derived equation applied in the UCODE\_2005 input instructions that subtracts the groundwater level at defined times during the pumping period from the spring 2008 base water level values. Once these water level changes were determined, the differences in the declines were determined simply by subtraction of the water level declines from the two different scenarios. As previously described, the capability to average model predictions in MMA allows the user to account for uncertainty associated with the ranked models. In this case predictions from the top 3 ranked models were averaged. The averaging of predictions is determined from equation 13. MMA also can average parameters, but these are not considered here because the Kh parameters in each model did not represent the same layers or zones in the top three models.

In addition to averaging the model predictions, two other important tools allow for insight into assessing the importance of parameters and observations to determining predictions. This capability is one of the most powerful aspects of the statistical data provided when conducting inverse modeling. The prediction scale sensitivity (pss), which is the amount of change a prediction would undergo relative to a fixed change in a parameter, provides information about the importance a particular parameter has on a prediction. To compare the relative difference between the parameters, the sensitivities need to be scaled. For the pss reported in this section, the sensitivities were scaled by multiplying the sensitivity by the standard deviation of the parameter divided by 100, and is expressed as a percentage of a reference value caused by changing the parameter value by an amount equal to one-percent of the parameter standard deviation (Hill and Tiedeman, 2007).

Along with providing insight into important parameters and observations on predictions, MMA also provides confidence intervals on predictions. Such intervals indicate a range that contains the true predicted value, if the model is correct. Confidence intervals reported in Table 7 are simultaneous intervals. These types of intervals have the specified probability of containing the values of all predictions simultaneously. These types of intervals are normally wider than an interval on only one prediction was assessed for a predictive scenario. Simultaneous intervals are ideally suited for the type of predictive analysis of long-term pumping that has numerous prediction locations and types of predictions (groundwater levels and flows).

## ***Prediction Analysis Results***

Model-averaged predictions for the difference in groundwater level declines and changes in groundwater contribution to Hershey Slough flow over the 5 year test period from CM-23, CM-25, and CM-18 are presented in Table 7. The difference in declines (bolded) is reported at the end of the pumping season (October 31) for the first, third, and fifth years of the predictive test. Simultaneous confidence intervals are also tabulated. As expected, the central test well prediction location showed the greatest difference in water table declines, and showed less recovery in the following spring than the test prediction locations on the periphery of the well field. For most of the predictions, the simultaneous confidence intervals are narrow indicating a relatively small uncertainty range for the predicted values. The accuracy of the predictions and their uncertainty depends on the accuracy of the conceptual model. The confidence interval for the central test well, located in the center of the GGS well field, in spring 2009 shows a range of residual decline from 5 to 6 ft. Observed drawdown data is available and showed a remaining decline of 0.2 ft, but this comparison is not appropriate for comparing predictions to observed values as there was minimal pumpage in the GGS wellfield in the summer of 2008. Without pumping the wellfield for a comparable rate and time, validation of the prediction results is not possible at this time. This discrepancy may be reduced if storage parameters were included in the calibration. Storage parameters were not included because of insensitivity to these terms in early calibration tests and to keep the number of estimated parameters within reason to allow for timely completion of the optimization runs.

For the groundwater contribution to Hershey Slough, little change is indicated after the first year of the 5 year pumping scenario, but over the 5 year period, a detectable change in groundwater flow to the drain is apparent. After five years, the decrease in discharge due to the GGS well field pumping is 0.52 (ft<sup>3</sup>/s), which equates to 376 ac-ft per year.

TABLE 7. Model-averaged water level decline differences (in bold) between a scenario with and without the GGS well field pumping for 4 months annually for the summers of 2008 through 2012 from CM-23, CM-25 and CM-18. Along with the averaged water level declines are 95% simultaneous confidence intervals. The change in groundwater contribution to Hershey Slough is also reported for the end of the pumping seasons. The first, third, and final pumping season results are presented, as well as the levels after 6 months of recovery in 2013. (95% Low C.I. = 95% lower confidence interval; Avg Incr DD = average increase in drawdown due to pumping of the GGS well field; Avg Decr Flow = average decrease in groundwater discharge due to pumping of the GGS well field; 95% Upr C.I. = 95% upper confidence interval)

	West test well (ft)			South test well (ft)			Central test well (ft)			East test well (ft)			Groundwater contribution to Hershey Slough (ft <sup>3</sup> /s)		
	95% Low C.I.	Avg Incr DD	95% Upr C.I.	95% Low C.I.	Avg Incr DD	95% Upr C.I.	95% Low C.I.	Avg Incr DD	95% Upr C.I.	95% Low C.I.	Avg Incr DD	95% Upr C.I.	95% Low C.I.	Avg Decr Flow	95% Upr C.I.
Fall 2008	1.8	<b>2.0</b>	2.2	2.1	<b>2.5</b>	2.9	19.4	<b>21.0</b>	22.7	3.6	<b>3.9</b>	4.2	-0.01	<b>0.02</b>	0.05
Spring 2009	2.7	<b>2.9</b>	3.0	2.8	<b>3.2</b>	3.7	5.0	<b>5.4</b>	5.8	3.4	<b>3.6</b>	3.8			
Fall 2010	5.3	<b>5.5</b>	5.7	6.1	<b>6.2</b>	6.4	23.1	<b>25.0</b>	27.0	7.4	<b>7.6</b>	7.8	0.11	<b>0.37</b>	0.64
Spring 2011	5.1	<b>5.5</b>	6.0	5.7	<b>6.2</b>	6.7	7.7	<b>8.7</b>	9.7	6.0	<b>6.4</b>	6.9			
Fall 2012	6.4	<b>6.7</b>	7.0	7.4	<b>7.7</b>	8.0	23.1	<b>25.5</b>	27.9	8.5	<b>8.8</b>	9.0	0.16	<b>0.52</b>	0.88
Spring 2013	6.0	<b>6.6</b>	7.1	6.8	<b>7.4</b>	7.9	8.8	<b>9.6</b>	10.4	7.0	<b>7.4</b>	7.9			

The predicted difference in drawdowns and discharge to Hershey Slough with and without continuous pumping of the GGS well field for 4 months each summer using CM\_25 (2<sup>nd</sup> ranked model) and CM\_18 (3<sup>rd</sup> ranked model) are generally similar to the model averaged predictions as illustrated in Figure 41. The most significant deviations occur when using CM\_18 and predicting the difference in drawdown in the center of the well field.

Locations for the predictions were chosen to represent locations beyond the NPPD property where irrigated agriculture occurs and long-term GGS well field pumping may impact static and pumping levels for irrigation wells. The results in Table 7 indicate that, based on the confidence intervals, the maximum level of decline after 5 years of pumping by GGS pumping at any of the three outer test locations would approach 10 feet (east test location). At the west and south locations, the recovery of the water table appears to be relatively slow when the GGS well field is pumped concurrently with the area irrigation wells, as the spring 2013 declines are still close to the maximum level of decline from the previous fall, although the east well shows the predicted decline recovers by almost 50%.



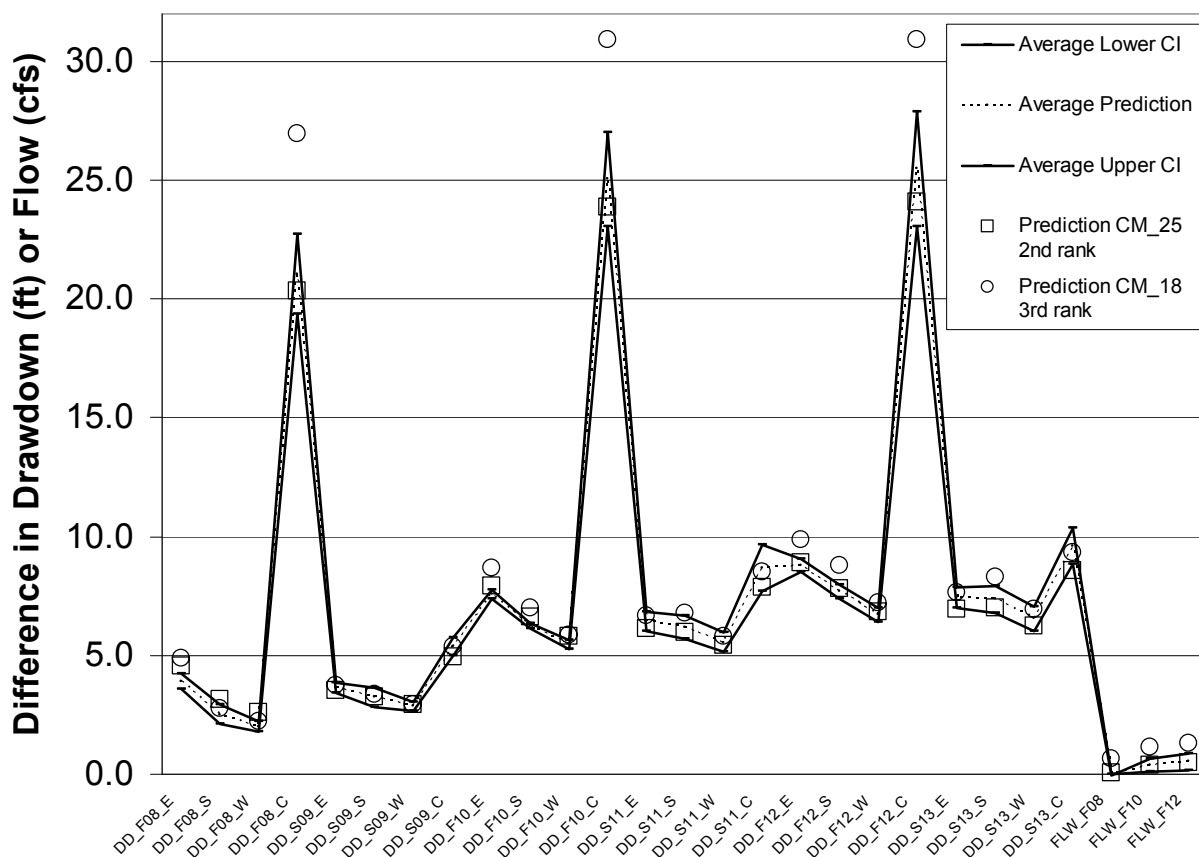


FIGURE 41. Model averaged predictions and their confidence intervals for predictions listed in Table 7 along with individual predictions for the 2<sup>nd</sup> and 3<sup>rd</sup> ranked models. DD = drawdown, FLW = groundwater discharge, F = fall, S = spring, ## = year, E S W C = east, south, west, and central prediction locations respectively.

Differences in water level declines between the 5-year predictive scenario with and without the GGS well field pumping at the end of the fifth year of pumping for model CM-23 are shown in Figure 42. The declines are most pronounced within the NPPD property, with a broader zone of lesser decline (15 ft or less) extending over two miles beyond the NPPD property boundary to the southwest, south, and east. The map indicates declines on the east and west sides of Sutherland Reservoir, a condition that was not observed in early models of the site that represented the reservoir using a constant head boundary. Instead of holding the lake stage constant with a constant head boundary, the Lake package boundary allows for fluctuating lake levels thus water levels in layers under the lake vary more when gradients are induced by pumping. Two of the highest capacity wells (wells 4 and 6) are located north of the cooling pond, a location which could influence declines simulated northeast of the reservoir. Pumping well 35, to the southwest of Sutherland Reservoir would have the most influence on declines to the west of the reservoir. Model CM-23 was constructed with 2 numerical model layers but had the same Kh zones applied to each layer and a vertical hydraulic conductivity term set to equal the horizontal value, thus representing a single homogeneous isotropic aquifer, a condition that would allow for water levels to be influenced by pumping in the layer beneath or adjacent to the lake.

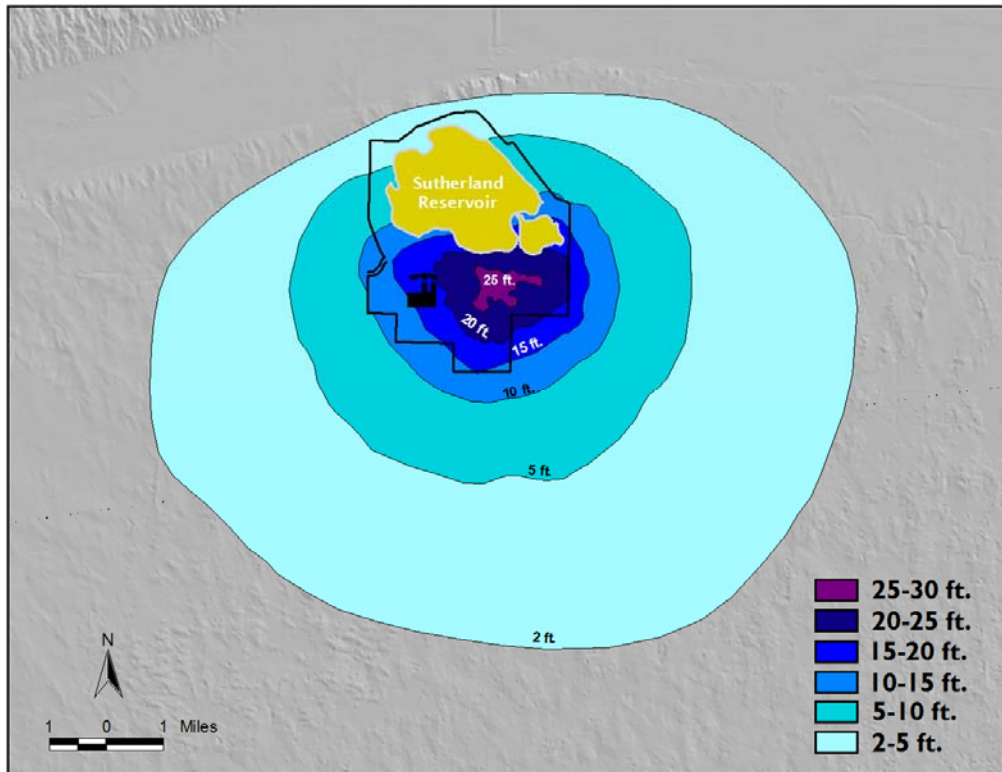


FIGURE 42. The difference in water table decline between scenarios with and without the GGS well field pumping approaches 30 feet in the well field. The contours represent the water table declines at the end of 5 consecutive years with 4-months of pumping the GGS well field each summer using the optimized CM-23 conceptualization.

### ***Important Information for Predictions***

Prediction scaled sensitivities ( $pss = \text{prediction-sensitivity} \times \text{parameter-standard-deviation} / \text{predicted-value}$ ) for the 33 predictions listed in Table 7 are presented in Figure 43. The x-axis shows the parameters optimized in CM-23. This relationship provides insight as to which parameters are most important in determining predictions with this model. The sensitivities indicate that the zone 2 and zone 3 Kh parameters, the river conductance term, the conductance term on the east drains, and the Rch3 term had the most influence on the determination of groundwater level differences between the two scenarios. Note that for CM-23, the HK3 and Rch3 terms showed little sensitivity in the optimizations, but had notable influence on the predictions. Such a situation suggests that it is important to collect more data that will improve the sensitivity to these parameters for future calibration. The types of observations most important to determining the predictions can be identified by coupling this information with composite scaled sensitivities (CSS) and DFBETAS which were described in the previous section. For example, figure 43 shows that the predictions were slightly sensitive to the HK1 term. Although the DFBETAS values are presented only for the flowpath age observations (Figure 38), identifying that HK1 showed the strongest sensitivity in the CSS plot (Figure 36), and that the flowpath observation MW-2sh was one of the few flowpath observations exhibiting importance to the determination of HK1 indicates that the flowpath age measurement at this well was important to the prediction scenario. To support this further, MW-2sh was also one of the top 30 (out of 2,570) observations having influence on the calibration of all the parameters as a whole. The same trend appears for MW-2sh and the conductance term for the east drains, although this parameter wasn't as sensitive in the optimization of CM-23 as HK1. This inferential approach to assessing prediction-parameter-observation relationships can be of great value in determining the type and location of observations important to predictions. Further examination of the

results can be conducted for all parameters and observations, but for brevity sake and to prevent redundancy, only the examples with the flowpath observations are described here.

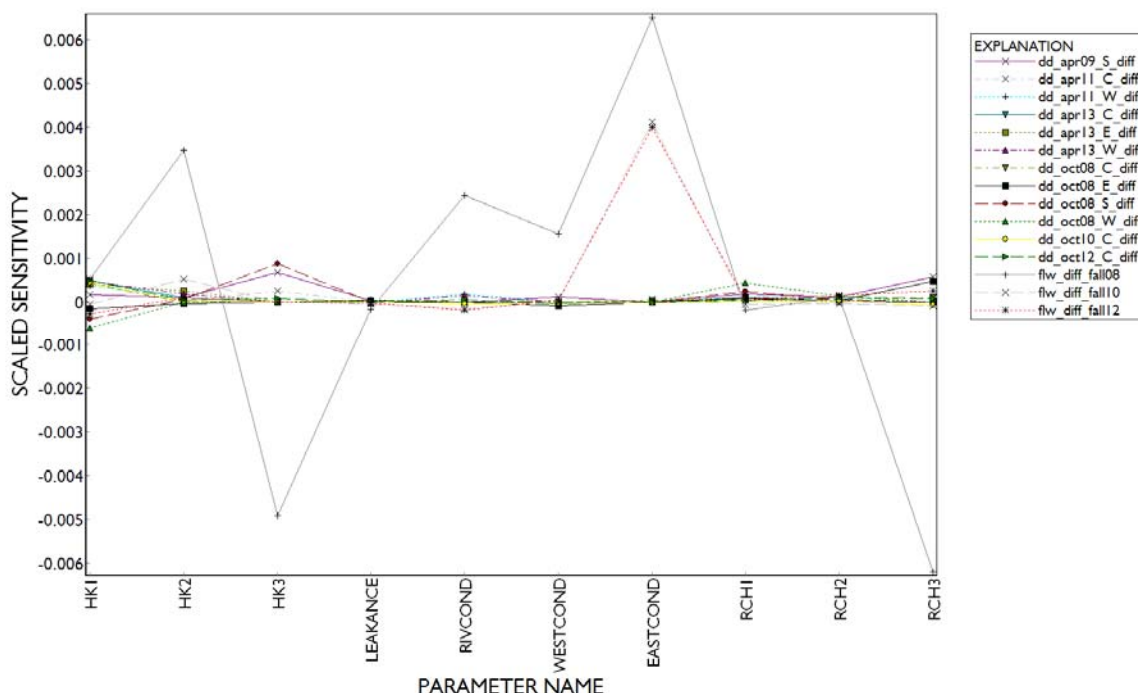


FIGURE 43. Results from the prediction scaled sensitivity analysis of CM-23, showing the sensitivity of predictions to the optimized parameters in the simulation.

## Discussion

This report presents an explorative exercise into application of not just a calibration method, but an overall approach to groundwater modeling. Methodologies, applications, and strategies in groundwater modeling science, along with computer processing capabilities have evolved to a point where valuable information can be extracted from results of multiple conceptual models.

### ***Further Discussion of Model Calibrations***

As previously described, 40 of the 42 calibrations of conceptual models considered in this investigation, converged to a tolerance of less than 1% change of parameter values between regression iterations. Multi-model analysis indicated that the top model CM-23 was far more probable than the other candidate models, thus the “best” representation of the groundwater system in the study area. This result is counterintuitive to the notion that the more complex models are better. CM-23 utilized a relatively simple hydrostratigraphic representation, yet the regression found a set of values for the parameters that provided the best fit to the observations. One of the most common questions in numerical groundwater modeling, especially in the HPA, is how many hydrostratigraphic layers are suitable to best represent the system. This investigation reveals that the best fit to observations is achieved with a model that uses regionally-based, vertically-homogeneous zones of mapped hydraulic conductivity, not 3 or 4 hydrostratigraphic layers, nor interpolated Kh values, nor specified, local zones of unique Kh values. What does this say about representing the hydrostratigraphy in the HPA? Models with regional to sub-regional dimensions (recall the model extent in this report is over 1,100 square miles) can fit observations with uniform Kh values applied to regionally based zones as well as or better than complex and/or multi-layered conceptualizations. Optimized parameters for the Kh terms in CM-23 and the 2<sup>nd</sup> ranked and also simple model, CM-25, were within the range of values noted to exist in the HPA, although they tended to be in the upper range of documented values (Gutentag et al., 1984). It is thought that the higher ranging

values for these models resulted from the regression compensating for higher Kh values in the upper Ogallala Group and Quaternary units in the near-site area, which combined with the lower Ogallala Group, resulted in a composite Kh for the 1- and 2-stratigraphic-layer models that was closer to an average Kh for all of the units as opposed to just Ogallala Group materials. For CM-18, the 3<sup>rd</sup> ranked model and the highest ranked multi-hydrostratigraphic-layer model, the modeled Kh values were reasonable although the Kh applied to layer 1 was higher than would be expected for that layer. It is possible that although it was considered to represent fine/silty deposits, zones within the interval picked during construction of the model included coarse materials, especially in the alluvium of the Platte River system. It is also possible that the higher Kh term for layer 1 account for local conditions near the reservoir that move seepage water away from the reservoir.

In terms of groundwater recharge, relatively simplistic representations and assumptions were used in the various schemes defined in the conceptualization. This strategy was chosen to provide insight into major controls on recharge, although the basis for defining characteristics of certain representations, such as irrigated versus dryland agriculture, were from observations at local-scale site studies (McMahon and others, 2003). The top three models all used recharge based on generalized aggregate maps of topographic regions instead of more detailed representations, indicating that such coarse representations of recharge in these regions capture the general processes and patterns of recharge. This is not to say that, for example, a detailed, coupled saturated-vadose zone model is inferior to the representation used to optimize the top ranked models in this report, but that a generalized landscape representation using average climatic conditions provided the best model fits compared to the alternative conceptualizations.

The optimized recharge values from the top three models which varied recharge based on topographic region were reasonable for 2 of the 3 zones, with the one exception being the sand hills areas. The values from the regressions indicated that 62 to 79 percent of annual average precipitation infiltrated in the sand hills area. Such rates are considerably higher than rates reported in previous studies. Although this rate is high, (66% of annual average precipitation is slightly over 12 inches), the optimized value is total recharge, which includes return irrigation drainage in center pivot areas. Recharge rates are expected to be relatively high in the sand hills areas due to the presence of sandy soils. Despite the fact that much of this area is used for grazing, over 200 center pivots irrigate thousands of acres in the sand hills; thus, high localized rates of recharge are expected. In addition, sand dune blowouts, areas of open sand on dunes where no grasses are present, are common in these areas and infiltration is likely to be higher in unvegetated sand than vegetated sand. Again, in these areas recharge rates are expected to be relatively high. The sand hills areas had some of the smallest residuals in the optimized models, as shown in Figure 39. The significantly higher recharge values for the sand hills area in the top ranked models relative to previously estimated rates provide a catalyst for further investigation into recharge rates in this area, especially in the zones where intensive irrigation occurs on sandy soils.

### ***Use of Unique Observation Data***

As indicated in preceding sections of this report, four types of observations were utilized in the model optimizations. Although groundwater levels and flow observations are traditionally used as observations, two unique observation types were available for these calibrations, reservoir stages and groundwater flowpath ages. Given the four types of observations a total of 2,570 observations were used for calibration. As described in the sections on optimization results and predictions, each of the four types of observations was important in the estimation of parameters. For two of the top three models one of the most influential observations was a drain flow measurement on Beer Slough, which was obtained using relatively inexpensive equipment and was a data source that did not exist prior to the investigation. This investigation provides evidence that using many diverse types of observation data for calibration of a groundwater model and using preliminary model investigations to guide data collection is an effective strategy.

### ***Sequence of Modeling Process***

It has been recommended that groundwater model investigations should follow a sequence of 1) initially developing a model to guide data collection, 2) gathering field data, 3) updating the models, and 4) repeating the process as necessary, yet it is often difficult to systematically follow this cyclical process. Budget constraints, project deadlines, and lack of field access are just a few of the possible roadblocks in

the process of any modeling study. For the investigation presented here, preliminary residual and sensitivity analyses of non-optimized simulations of the system at the onset of the project were utilized to provide insight and guidance for locating monitoring well nests for the geochemical study component of the project, an effort that eventually provided the necessary information to create flowpath observations that were beneficial to the calibration of the models. Because flow observations have been identified in many modeling studies as important observations, a strategy was defined to identify as many surface flow observations as possible. This speculative approach proved beneficial as several surface flow observations proved to be important in the estimation of parameters in the models discussed in the results section. These data also proved beneficial during initial phases of modeling in the project, as observed values provided ranges of discharge expected for the surface features. When model results showed highly erroneous output, it was determined that a few of the input files were incorrectly structured and these were rectified early in the modeling process.

It is also beneficial to continuously check the inputs of observations and model features throughout the modeling process. For example, during an exercise of reviewing input files defining the drains and rivers in the models and their respective observations, perusal of the study area in Google Earth revealed a feature in which significant flow was present in the study area but that was not represented in the models. This drain was inaccessible by road and hence could not serve as an observation, but by noticing the presence of the drain that appeared to have a flow comparable to Applegate Drain and adding it to the models, simulated equivalents to groundwater flow to the area of drains north of Sutherland Reservoir, as well as the downstream reach of the South Platte River improved significantly. Despite the potential for obstacles in the process of using investigative models to guide data collection that eventually improve models, this process should be implemented whenever possible in modeling investigations, even if only one cycle of modeling/data-collection/revised-modeling is feasible. It is also strongly recommended that data sets be continuously checked throughout modeling investigations, and simple, inexpensive tools such as staff gages and mapping tools such as Google Earth be utilized to supplement the diversity in observation data.

## Conclusions

The intent of this investigation was to develop a management tool with predictive assessment capabilities for the area near Sutherland Reservoir and Gerald Gentleman Station in west central Nebraska. Emerging strategies in groundwater modeling were implemented to develop a groundwater model for managing groundwater in an area with competing uses of groundwater. Several questions regarding groundwater models for this region were explored, and the impacts of an extreme scenario where the GGS well field would be utilized at maximum capacity for several consecutive summers. From this investigation, the following results and conditions were determined regarding:

### ***Multi-Model Analysis***

- Testing of alternative hypotheses of the GGS-SR groundwater system revealed that one model clearly stood above the rest in the model rankings. This model was not the most simplistic representation nor was it the most complex of the suite of models considered. This finding could be summed up best by the statement in Hill (2006) that "It is noted that neither very simple nor very complex models are likely to provide the most accurate predictions and that finding the best level of complexities is an ill-defined process."
- The second-ranked model was quite similar, but the model evaluation criteria indicate it is 3500 times less likely to represent the system than the top ranked model. Although beyond the scope of this project, this drastic difference in likelihood given such a similar fit suggests that the application of model evaluation criteria to groundwater models requires further study.
- The third-ranked model was significantly different in model structure and was more complex than the top 2 models. It is recommended to the users of these models that predictions continue to be explored with each of the top three models, because their fit to the data is quite similar yet the model select criterion strongly penalizes slight differences. If the predictions are similar for all

models as they were in the scenario evaluated here, the top ranked model could be used exclusively, but if the impacts are significantly different then accounting for the uncertainties in the system using the different models can help provide conservative estimates of predictions that account for conditions found in the various conceptualizations. The range of model testing does not need to be limited to the top 3 models as shown in the results section of this report.

- Most optimized parameter values were similar to values commonly observed in the field or estimated for other investigations, with the exception of the hydraulic conductivity of layer 1 in CM-18 (third-ranked model), and recharge estimated for the sand hills topographic region for all models. In order to evaluate the estimated value of Kh, future refinements of this model could explore the nature of deposits in the uppermost portion of the Platte River system valley alluvium and refinement of layer elevations. The estimated value of recharge in the sand hills region accounts for water entering the system from both precipitation-based recharge and irrigation return flow, not just native pastureland recharge. Although the optimized values are likely higher than the actual recharge rates, these results indicate that current estimates of recharge in the sand hills areas are perhaps too low, especially considering the sandy nature of the soil, the existence of bare sand exposures, and the presence of clustered center pivot irrigation in many areas of the sand hills.
- The prediction scenario described in the model shows that pumping of the GGS well field has an extensive range of influence after 5 years of pumping the well field for four months each summer. However, the largest drawdowns occur within the NPPD property boundary. The cone of depression indicates a transmissive system, as the difference in drawdown with and without GGS pumping is small (2-5 ft) over much of the area of influence beyond the NPPD property boundary. Although the coarse grid of the model cannot indicate drawdown in individual production wells, the fact that the upper range of maximum drawdown predicted at the end of the 5<sup>th</sup> year was about 28 ft in any cell indicates that the well field remains viable even under high stress conditions. This decline is less than 10 percent of the saturated thickness of the aquifer in the area of the well field.
- The simulated difference in water table declines, as indicated in the previous bullet item, has more of a conical shape as compared to early modeling investigations of the site that applied a constant head boundary just 2 miles south of the southernmost portion of the NPPD property boundary and used a constant head boundary to represent Sutherland Reservoir. Although adequate for preliminary tests for the impacts of pumping and aquifer viability, the models presented in this report eliminate the issues of boundary effects to the south of the well field and allow for exploration of the behavior of groundwater levels adjacent to and underneath Sutherland Reservoir.

## **Observations**

- The utilization of numerous types of observations proved to be beneficial in the calibration of the models, as indicated by the variety of observation types that were influential in the estimation of model parameters. As shown in plots of Cook's D and DFBETAS statistics, flowpath age and reservoir stage observations were influential in estimating parameters that were most sensitive in the optimizations.

## **Representation of the HPA**

- The question of how a groundwater model should represent the HPA continues to be debated in Nebraska modeling studies. This study determined that a model with 1 stratigraphic layer and regionally defined zones of Kh provides a fit to observations better than models utilizing four stratigraphic layers to represent the HPA. It may be that improved spatial distribution of Kh within the layers would reverse this finding, but data to accomplish this are not available at this time.
- Sub-regional scale models such as the ones constructed for this report are best optimized with regionally characterized parameters. The localized detail in the vicinity of the GGS well field, which is a relatively small portion of the model area, had little influence on improving the fit to field observations. This may indicate that the available detailed localized data were insufficient to



correctly define the interconnections of units in the complex framework resulting in incorrect connections that led to the slightly degraded fit to field observations.

- Despite the better fit of simple rather than complex representations, the effort of characterizing the near-site hydrostratigraphy should not be considered an unimportant endeavor, because these data further understanding of the system and would be beneficial in localized, contaminant transport models in the vicinity of GGS.
- The multi-layered model CM-18 indicated that the simulated equivalents to the observations were more sensitive to parameters representing Kh in the Ogallala Group than the parameter representing the coarse Quaternary deposits. Although the expected higher permeability in the Quaternary deposits was assigned to layer 2 in CM-18, the Ogallala Group deposits comprise more than 90 percent of the saturated thickness of the aquifer in the near-site area and have the most influence on the groundwater flow system.
- The fact that the single stratigraphic-layer representations provided better fit than the four-stratigraphic-layer models is beneficial, in that they require less computer execution time than the four-stratigraphic-layer models for both optimization and predictive analysis.

### ***Geochemical Analysis***

- The geochemical analysis of the site conducted by the U.S. Geological Survey from 2005 to 2007 was beneficial to the calibration of the models, as two observations in particular, MW-2sh and MW6-sh were important in parameter estimation for the top three models. Since the flowpath ages exist exclusively in the near-site area within the well field, the fact that these observations were important in the determination of the regionally zoned Kh values underscores the importance of these observations in estimating a regionally assigned Kh term that provides the best fit to observations within the near-site area.
- In addition to providing useful observations for the model optimizations, the background suite of geochemical data resulting from the study provided a useful baseline for non-modeling questions that NPPD may face in the future regarding water quality in the region, as well as determining, if the question arises, the source of water in the aquifer (regional HPA water vs. surface water seepage). Considering that fresh water is a shared resource in the semi-arid study area, having a baseline of geochemical conditions as well as glimpses into how the geochemistry changed after two years of GGS well field pumping may be valuable information for future management decisions. Further information regarding the geochemical analysis is provided in McMahon and others (2009).

### ***Further Exploration and Recommendations***

All hydrologic investigations are modeling investigations, whether the “model” is a sketch of a flow system on a pad of paper or a detailed numerical model processed with a cluster of computers. All models of natural systems, regardless of their type, are simple approximations of true conditions. Because of this imperfect capacity of humans and computers to represent natural systems, models should be updated continuously with new information and re-evaluated, including modification of current conceptualizations and/or development of new conceptualizations.

Despite the advanced approach to calibration of multiple conceptual models in this report, this modeling effort is no exception to the statements in the previous paragraph. Different conceptualizations or modifications of the current conceptualizations should continue to be explored. Often modeling investigations that attempt to address certain questions raise new questions about the system, as is the case with this study. Although the models presented in this report are fully capable of predictive analysis, following are key recommendations for further enhancement of the models.

- Use the current optimized models and test different ways of representing Sutherland Reservoir, such as using a general head or a transient constant head boundary instead of a lake package in layer 1. This will eliminate the use of lake stage as observations, but some of the largest mismatches in simulated and observed conditions involved the stages, so it may be better to use the stage data as input rather than as observations.

- Attempt to improve the match with the 1,852 stage observations by using daily stress periods, which could potentially reduce the larger residuals by eliminating the use of average inflow and outflow conditions of the Supply Canal over stress periods that were several weeks or months in length. Although this would create much larger input and output files, continued advances in computer processing speed may make this a feasible option. Inflows and outflows to the reservoir changed frequently in the field, and these rapid changes may be the cause of the mismatch between simulated and observed stages that may be better captured by the models with daily inflow and outflow terms. Alternatively, smaller weights might be placed on the stage observations, since the standard error for the models indicate that the model fit was not as good as indicated by the weights assigned to the observations.
- Evaluate the use of the MODFLOW stream package for representing the South Platte River because the current model simulates losing conditions in the upper reach of the river. With the stream package, that reach of the river would be allowed to go dry once the volume of water in the streambed either flows out of the reach or seeps into the subsurface, thus reducing the error simulated for that reach with a few of the summertime observations for the transient period.
- Conduct field work to improve estimates of groundwater recharge in sand dunes, particularly those stabilized by grasses. The optimized values of total groundwater recharge in the sand hills are high even compared to the wide range of recharge values estimated for these landscapes from previous studies.
- Network clusters of computers to expedite the optimization process. This is recommended for any project involving a suite of models with thousands of cells.
- Continue to collect surface water information in the study area because the inexpensive flow observations were valuable to optimization of the models. They are of importance not only for the purpose of local investigations, but also to understanding of the system in a regional context. Over three years of observation data from local drains and the South Platte River have been collected for this study, and this data will benefit future modeling projects and studies. As long term droughts are known to persist on the High Plains, such data are important in helping predict the behavior of the hydrologic system in the region under different climatic conditions. As the common phrase goes, "you cannot manage what you do not measure."

## References

- Aquaveo, 2002. Distributors of the software Groundwater Modeling System version 6.0. Available on the world wide web at [www.aquaveo.com](http://www.aquaveo.com)
- Belsley, D.A., Kuh, E. and R.E. Welsch. 1980. *Regression diagnostics, indentifying influential data and source of collinearity*. Hoboken, NJ, Wiley Publishing.
- Bjorklund, L.J. and R.F. Brown. 1957. *Geology and ground-water resources of the lower South Platte River valley between Hardin, Colorado and Paxton, Nebraska, with a section on Chemical quality of the ground water by H.A. Swenson*. U.S. Geological Survey Water-Supply Paper 1378. 431 p.
- Burnham, K.P. and D.R. Anderson. 2002. *Model selection and multi-model inference- A practical information-theoretical approach*. New York, NY, Springer-Verlag. 488 p.
- CALMIT. 2005. Center for Advanced Land Management Information Technologies. *2005 Land Use Mapping*. Accessed on the world wide web at <http://www.calmit.unl.edu/2005landuse/index.shtml>.
- Cannia, J.C., Woodward, D. and L.D. Cast. 2006. *Cooperative Hydrology Study (COHYST) Hydrostratigraphic Units and Aquifer Characterization Report*. Accessed on the world wide web at [http://cohyst.dnr.ne.gov/document/dc012hydro\\_aquifer\\_022406.pdf](http://cohyst.dnr.ne.gov/document/dc012hydro_aquifer_022406.pdf)
- Chen, Xunhong and Xi Chen. 2004. *Simulating the effects of reduced precipitation on ground water and streamflow in the Nebraska Sand Hills*. Journal of the American Water Resources Association. Paper No. 03076.
- COHYST, 2004. *Overview of the Objectives, Processes, and Products of the COHYST Project, Technical Committee Report* available on the world wide web at [http://cohyst.dnr.ne.gov/cohyst\\_preliminarydata.html](http://cohyst.dnr.ne.gov/cohyst_preliminarydata.html)
- Condra, G.E. 1907, *Geology and water resources of the Republican River valley and adjacent areas, Nebraska*. U.S. Geological Survey Water-Supply Paper 216, 71 p.
- Cooley, R.L., and R.L. Naff. 1990. *Regression modeling of groundwater flow*. U.S. Geological Survey techniques in water-resources investigations. Book 3, chapter B4.
- D'Agnese, F.A., O'Brien, G.M., Faunt, C.C., Belcher, W.R., and C. San Juan. 2002. *A three-dimensional numerical model of predevelopment conditions in the Death Valley regional groundwater flow system, Nevada and California*. U.S. Geological Survey Water-Resources Investigation Report, 02-4102.
- Darton, N.H. 1905. *Preliminary report on the geology and underground water resources of the central Great Plains*. U.S. Geological Survey Professional Paper 32, 433 p.
- Dennis, J.E. and R.B. Schnabel. 1996. *Numerical methods for unconstrained optimization and nonlinear equations*. Philadelphia, PA, Society for Industrial and Applied Mathematics. 378 p.
- Driscoll, F.G. 1986. *Groundwater and Wells*. Second Edition. Published by Johnson Filtration Systems Inc.
- Dugan, J.T. and R.B. Zelt. 2000. *Simulation and Analysis of Soil-Water Conditions in the Great Plains and Adjacent Areas, Central United States, 1951-80*. U.S. Geological Survey Water Supply Paper 2427, 81 p.
- Fetter, C.W. 2001. *Applied Hydrogeology*. 4th Edition. MacMillan College Publishing Company.

Foglia, L., Mehl, S.W., Hill, M.C., Perona, P., and P. Burlando. 2007. *Testing alternative groundwater models using cross-validation and other methods*. Ground Water, vol.45, no. 5. p. 627-641.

Goeke, J.W., Peckenpaugh, J.M., Cady, R.E., and J.T. Dugan. 1992. *Hydrogeology of parts of the Twin Platte and Middle Republican Natural Resources Districts, southwestern Nebraska*. Nebraska Water Survey Paper no. 70, 89 p.

Gutentag, E.D., Heimes, F.J., Krothe, N.C., Luckey, R.R., and J.B. Weeks. 1984. *Geohydrology of the High Plains aquifer in parts of Colorado, Kansas, Nebraska, New Mexico, Oklahoma, South Dakota, Texas, and Wyoming*. U.S. Geological Survey Professional Paper 1400-B, 63 p.

Harbaugh, J.W., Banta, E.R., Hill, M.C., and McDonald, M.G. 2000. MODFLOW-2000, The U.S. Geological Survey's modular groundwater flow model—User guide to modularization concepts and the groundwater flow process: U.S. Geological Survey Open-File Report 00–92, 121 p.

Harza. 1993. *Water Utilization Study for the Sutherland Project, FERC Project No. 1835, Volume.1*. Unpublished project report prepared for the Nebraska Public Power District.

Courtney Hemenway, 2007, personal communication, chemenway1@msn.com

High Plains Regional Climate Center. 2008. Precipitation database accessed on the world wide web at [www.hprcc.unl.edu](http://www.hprcc.unl.edu), October 2008.

Hill, M.C. 1992. *A computer program (MODFLOWP) for estimating parameters of a transient, three-dimensional, ground water flow model using nonlinear regression*. U.S. Geological Survey Open-File Report 91-484.

Hill, M.C. 1994. *Five computer programs for testing weighted residuals and calculating linear confidence and prediction intervals on results from the ground water parameter-estimation computer program MODFLOWP*. U.S. Geological Survey Open-File Report 93-481.

Hill, M.C., Banta, E.R., Harbaugh, A.W., and E.R. Anderman. 2000. *MODFLOW-2000, The U.S. Geological Survey's modular groundwater flow model—User guide to the observation, sensitivity, and parameter-estimation procedures and three post-processing programs*. U.S. Geological Survey Open-File Report 00–184, 209 p.

Hill, M.C. 2006. *The practical use of simplicity in developing groundwater models*. Ground Water, vol. 44, no. 6, p. 775-781.

Hill, M.C. and C.R. Tiedeman. 2007. *Effective Groundwater Model Calibration*. Hoboken, NJ, Wiley Interscience.

Hunt, R.J., Feinstein, D.T., Pint, C.D., and M.P. Anderson. 2006. *The importance of diverse data types to calibrate a watershed model of the Trout Lake Basin, Northern Wisconsin, USA*. Journal of Hydrology, volume 321, p. 386-296.

Igor Jankovic, 2001, personal communication, [ijankovi@eng.buffalo.edu](mailto:ijankovi@eng.buffalo.edu)

Klocke, N.L., Hubbard, K.G., Kranz, W.L., and D.G. Watts. 1999. *Evapotranspiration and Crop Water Use*. University of Nebraska-Lincoln Institute of Agriculture and Natural Resources NebGuide online publication. Accessed on the world wide web at <http://www.p2pays.org/ref/20/19769.htm>

Ed Kouma, 2008, personal communication, [ekouma@gp.usbr.gov](mailto:ekouma@gp.usbr.gov)

Kullback, S. and R.A. Leibler. 1951. *On information and sufficiency*. Annals and Mathematical Statistics 22. 79-86.

Frank Kwapnioski, personal communication, fskwapn@nppd.com

Lappala, E.G. 1978. *Quantitative hydrogeology of the Upper Republican Natural Resources District, Southwest Nebraska*. U.S. Geological Survey Water-Resources Investigations Report 78-38. 200 p.

Luckey, R.R. and J.C. Cannia. 2006. *Groundwater Flow Model of the Western Model Unit of the Nebraska Cooperative Hydrology Study (COHYST) Area*. Accessed on the world wide web at [http://cohyst.dnr.ne.gov/adobe/dc012WMU\\_GFMR\\_060519.pdf](http://cohyst.dnr.ne.gov/adobe/dc012WMU_GFMR_060519.pdf).

Luckey, R.R., Gutentag, E.D., Heimes, F.J., and J.B. Weeks. 1986. *Digital simulation of groundwater flow in the High Plains aquifer in parts of Colorado, Kansas, Nebraska, New Mexico, Oklahoma, South Dakota, Texas, and Wyoming*. U.S. Geological Survey Professional Paper 1400-D, 57 p.

Luckey, R.R., Gutentag, E.D., Heimes, F.J., and J.B. Weeks. 1988. *Effects of future ground-water pumpage on the High Plains aquifer in parts of Colorado, Kansas, Nebraska, New Mexico, Oklahoma, South Dakota, Texas, and Wyoming*. U.S. Geological Survey Professional Paper 1400-E, 44 p.

Lugn, A.L. and L.K. Wenzel. 1938. *Geology and ground-water resources of south-central Nebraska- with special reference to the Platte River valley between Chapman and Gothenburg*. U.S. Geological Survey Water-Supply Paper 779. 242 p.

McGuire, V.L. 2007. *Water-level changes in the High Plains Aquifer, Predevelopment to 2003, and 2003 to 2005*. U.S. Geological Survey Scientific Investigations Report 2006-5324.

McMahon, P. B., Dennehy, K.F., Bruce, B.W., Bohlke, J.K., Michel, R.L., Gurdak, J.J., and D. B. Hurlbut. 2006. *Storage and transit time of chemicals in thick unsaturated zones under rangeland and irrigated cropland, High Plains, United States*. Water Resources Research, vol. 42, W03413.

McMahon, P. B., K. F. Dennehy, R. L. Michel, M. A. Sophocleous, K. M Ellett, and D. B. Hurlbut. 2003. *Water movement through thick unsaturated zones overlying the central High Plains aquifer, southwestern Kansas, 2000– 2001*. U.S. Geological Survey Water Resources. Investigations Report, 03–4171, 32 p.

McMahon, P.B., C.P. Carney, E.P. Poeter, and S.M. Peterson, in prep. *Geochemical evaluation of competing water uses for agriculture and energy production, northern High Plains aquifer, USA*. To be submitted to Applied Geochemistry.

Mehl, S.W. and M.C. Hill. 2003. *Locally refined block-centered finite-difference groundwater models, Evaluation of parameter sensitivity and the consequences for inverse modeling and predictions*. IAHS Publication 277, p. 227-232.

Missouri River Basin Commission. 1975. *Stream-aquifer hydrology, technical paper, Platte River Basin, Nebraska*. Level B Study, Missouri River Basin Commission, 67 p.

Missouri Basin State Association. 1982a. *Technical Paper, Ground Water Depletion, Platte and Kansas River Basins, Colorado-Kansas-Nebraska-Wyoming*. Appendix II of Ground Water Depletions Technical Paper; Omaha, Nebr., Missouri River Basin hydrology study, 71 p.

Missouri Basin State Association. 1982b. *Transmissivity and stream depletion factor maps; Platte and Kansas River Basins, Colorado-Kansas-Nebraska-Wyoming*. Appendix II of Ground Water Depletions Technical Paper; Omaha, Nebr., Missouri River Basin hydrology study, 16 pls.

Nebraska Department of Environmental Quality. 1981. Title 124, Chapter 18- *Lagoons, Site Location and Evaluation*. Design. Figure 18.3.

Nebraska Department of Natural Resources. 1998. *Estimated Water Use in Nebraska, 1995*. Accessed on the world wide web at [www.dnr.ne.gov/misc/report95.pdf](http://www.dnr.ne.gov/misc/report95.pdf).

Neuman, S.P. 2003. *Maximum likelihood Bayesian averaging of uncertain model predictions*. Stochastic Environmental Research and Risk Assessment, v. 17, p. 291–305.

Neuman, S.P. and P.J. Wierenga. 2003. *A comprehensive strategy of hydrogeologic modeling and uncertainty analysis for nuclear facilities and sites*. U.S. Nuclear Regulatory Commission NUREG/CR-6805, 236 p.

Peckenpaugh, J.M., Kern, R.A., Dugan, J.T., and J.M. Kilpatrick. 1995. *Simulated response of the High Plains aquifer to groundwater withdrawals in the Upper Republican Natural Resources District, Nebraska*. U.S. Geological Survey Water-Resources Investigations Report 95-4014.

Pettijohn, R.A., and H.H. Chen. 1983a. *Geohydrology of the High Plains aquifer system in Nebraska*. U.S. Geological Survey Water-Resources Investigations Report 82-502, map, scale 1:175,000, 3 sheets.

Pettijohn, R.A., and H.H. Chen. 1983b. *Hydraulic conductivity, specific yield, and pumpage—High Plains aquifer system, Nebraska*. U.S. Geological Survey Water-Resources Investigations Report 82-4014, map, scale 1:175,000, 3 sheets.

Pollock, D.W. 1994. *User's guide for MODPATH/MODPATH-PLOT, Version 3: A particle tracking post-processing package for MODFLOW, the U.S. Geological Survey finite-difference groundwater flow model*. U.S. Geological Survey Open-File Report 94-464, 249 p.

Poeter, E.P. and M.C. Hill. 1997. *Inverse Models, A Necessary Step in Groundwater Modeling*. Ground Water. Vol. 35, no. 2. p. 250-260.

Poeter, E.P., Hill, M.C., Banta, E.R., Mehl, S., and S. Christensen. 2005. *UCODE\_2005 and six other computer codes for universal sensitivity analysis, calibration, and uncertainty evaluation*. U.S. Geological Survey Techniques and Methods report 6-A11. Revised version released on 2 February 2008.

Poeter, E.P. and D.R. Anderson. 2005. *Multimodel Ranking and Inference in Groundwater Modeling*. Ground Water. Vol. 43, no. 4. p. 597-605.

Poeter, E.P. and M.C. Hill. 2007. *MMA, A Computer Code for Multi-Model Analysis*. U.S. Geological Survey Techniques and Methods 6-E3. Available online at [http://water.usgs.gov/software/lists/ground\\_water/](http://water.usgs.gov/software/lists/ground_water/)

Poeter, E.P. and M.C. Hill. 2008. *SIM\_ADJUST -- A Computer Code that Adjusts Simulated Equivalents for Observations or Predictions*. International Ground Water Modeling Center Report GWMI 2008-01, 28p.

Rawlins, J.O. 1988. *Applied Regression Analysis*. Pacific Grove, CA. Wadsworth and Brooks.



Republican River Compact Administration. 2003. *Groundwater Model Documentation*. Accessed on the world wide web at <http://www.republicanrivercompact.org/v12p/RRCAModelDocumentation.pdf>.

Jim Retchess, 2008, personal communication. [James.reтчless@nebraska.gov](mailto:James.reтчless@nebraska.gov)

Scanlon, B.R., Reedy, R.C., Stonestrom, D.A., and D.E. Prudic. 2005. *Impact of land use and land cover change on groundwater recharge and quantity in the southwestern USA*. *Global Change Biology*, no. 11, p. 1577-1593. Available on the world wide web at [http://www.beg.utexas.edu/staffinfo/Scanlon\\_pdf/ScanlonGCB05.pdf](http://www.beg.utexas.edu/staffinfo/Scanlon_pdf/ScanlonGCB05.pdf)

Seber, G.F. and C.J. Wild. 1989. *Nonlinear Regression*. Wiley Interscience.

Sophocleous, M.A., and S.P. Perkins. 1993. *Calibrated models as management tools for stream-aquifer systems: the case of central Kansas, USA*. *Journal of Hydrology*, 152(1-4): 31-56.

Sophocleous, M.A., Koussis, A., Martin, J.L. and S.P. Perkins. 1995. *Evaluation of simplified stream-aquifer depletion models for water rights administration*. *Ground Water*, 33(4): 579-588.

Sophocleous, M.A., Kluitenberg, G.J., and J. Healey. 2002. *Southwestern Kansas High Plains deep vadose zone pilot study to estimate Darcian-based groundwater recharge at three instrumental sites*. Kansas Geological Survey Open-File Report 2001-11, KGS, Wichita, KS. 120 p.

Szilagyi, J., Harvey, F.E., and J.F. Ayers. 2005. *Regional estimation of total recharge to ground water in Nebraska*. *Ground Water*, vol. 43, no. 1, 63-69.

Tiedeman, C.P., Kernodle, J.M., and D.P. McAda. 1998b. *Application of non-linear regression methods to a groundwater flow model of the Albuquerque Basin, New Mexico*. U.S. Geological Survey Water-Resources Investigations Report 98-4172.

University of Nebraska-Lincoln Conservation and Survey Division. 1951. *Topographic Regions of Nebraska*. Accessed on the worldwide web at the Platte River Cooperative Hydrology Study databank, [http://cohyst.dnr.ne.gov/cohyst\\_preliminarydata.html](http://cohyst.dnr.ne.gov/cohyst_preliminarydata.html)

University of Nebraska-Lincoln Conservation and Survey Division. 1996. *Generalized depth-to-water map*. Accessed on the worldwide web at <http://snr.unl.edu/data/geographygis/NebrGISwater.asp>

University of Nebraska-Lincoln Conservation and Survey Division. 1995. *Configuration of the water table map, 1995*. Accessed on the worldwide web at <http://snr.unl.edu/data/geographygis/NebrGISwater.asp>

United States Census Bureau. 2000. Accessed online at [quickfacts.census.gov](http://quickfacts.census.gov) in October 2007.

Weeks, J.B., Gutentag, E.D., Heimes, F.J., and R.R. Luckey. 1988. *Summary of the High Plains Regional Aquifer-System Analysis in Parts of Colorado, Kansas, Nebraska, New Mexico, Oklahoma, South Dakota, Texas, and Wyoming*. U.S. Geological Survey Professional Paper 1400-A.

Wenzel, L.K. and H.A. Waite. 1941. *Ground Water in Keith County, Nebraska*. U.S. Geological Survey Water-Supply Paper 848. 68 p.

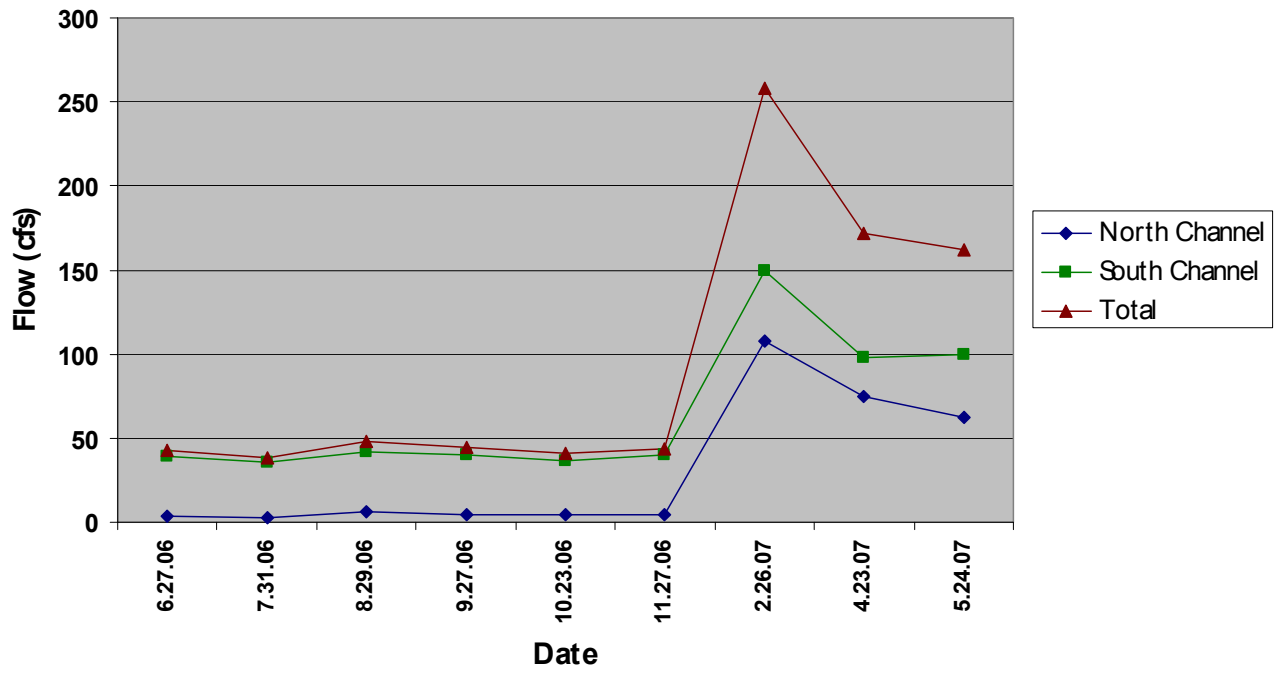
Winston, R.B. 2000. *Graphical user interface for MODFLOW*. Version 4. Current version is 1.21. U.S. Geological Survey open-file report 00-315.

Ye, M., Meyer, P.D., and S. P. Neuman. 2008. *On model selection criteria in multimodel analysis*. Water Resources Research. Vol. 44, doi:10.1029/2008WR006803.

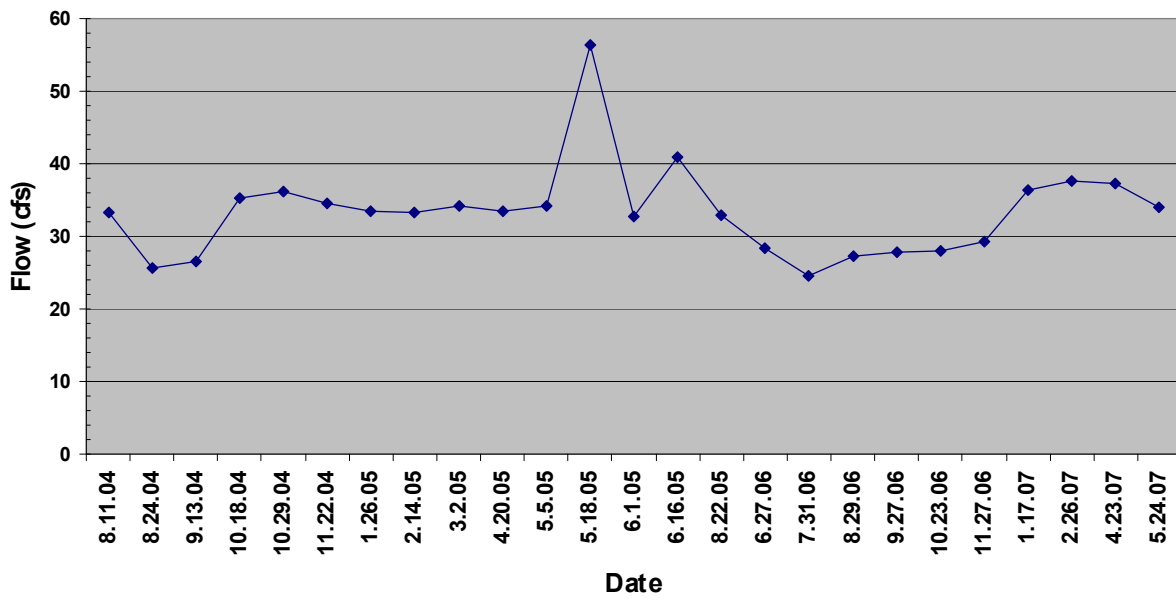
## **APPENDIX A**

***Measured Monthly Flow Data at River and Drain Flow Observation  
Locations and Sutherland Reservoir stage hydrograph for  
transient period from which daily observations were obtained***

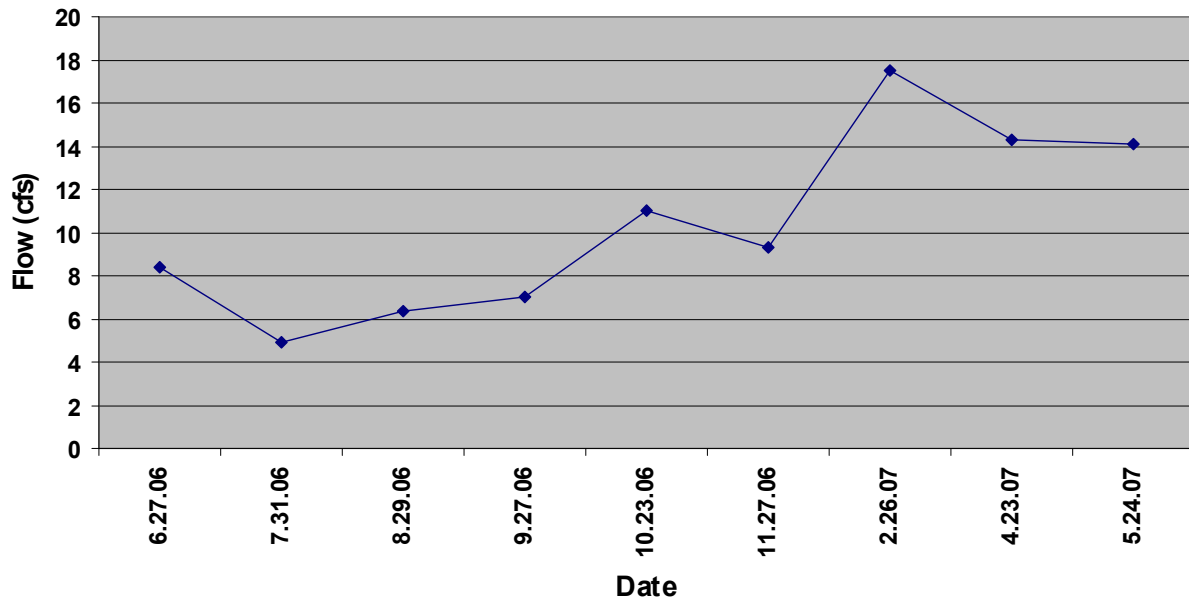
### South Platte River



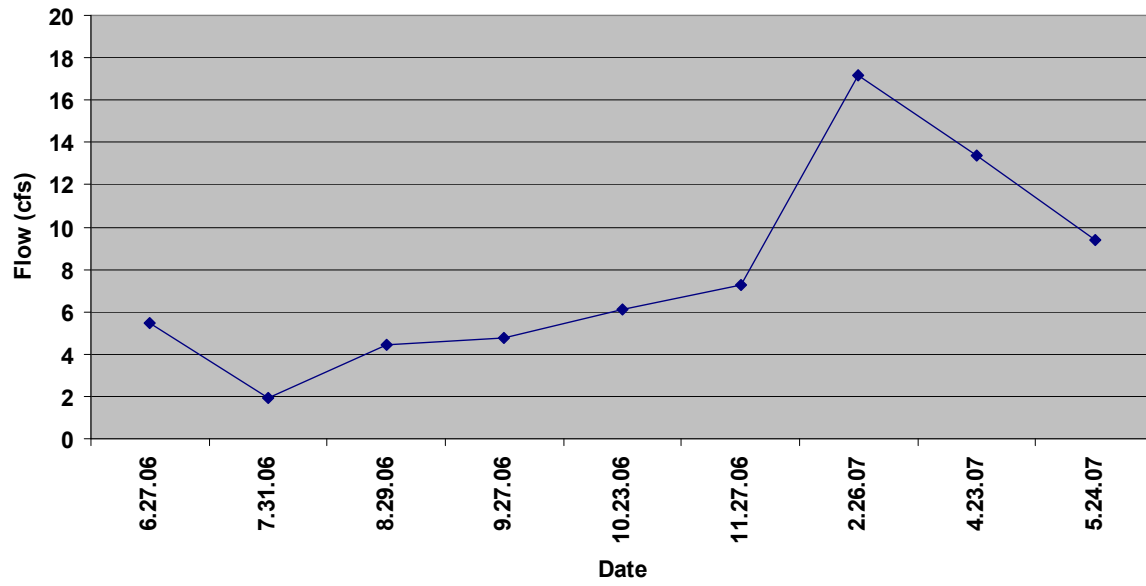
### Applegate Drain



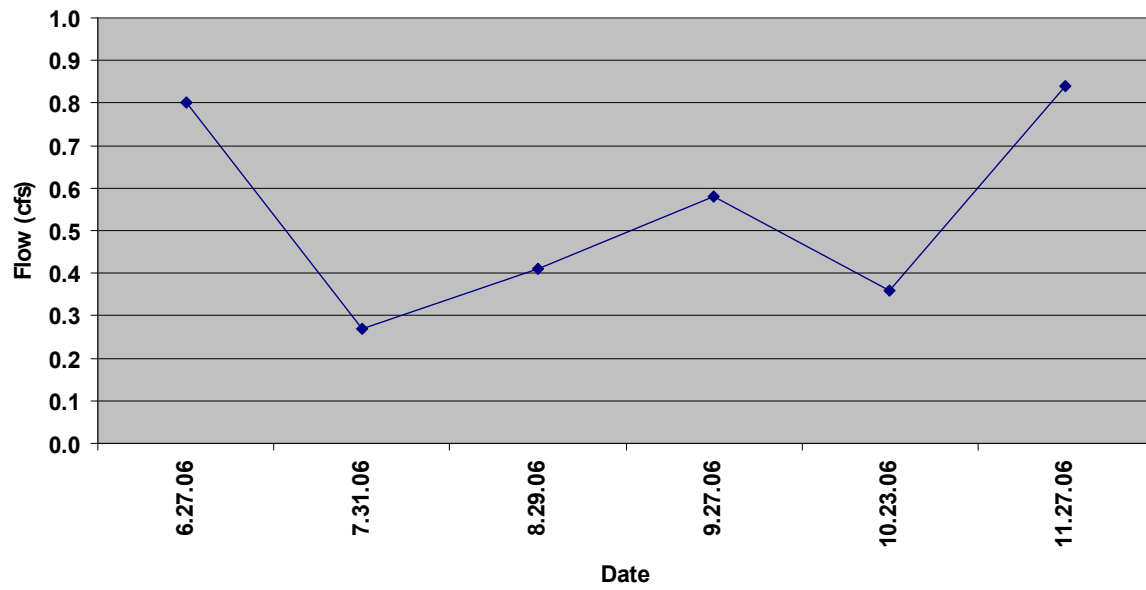
### Hershey Slough



**Beer Slough**

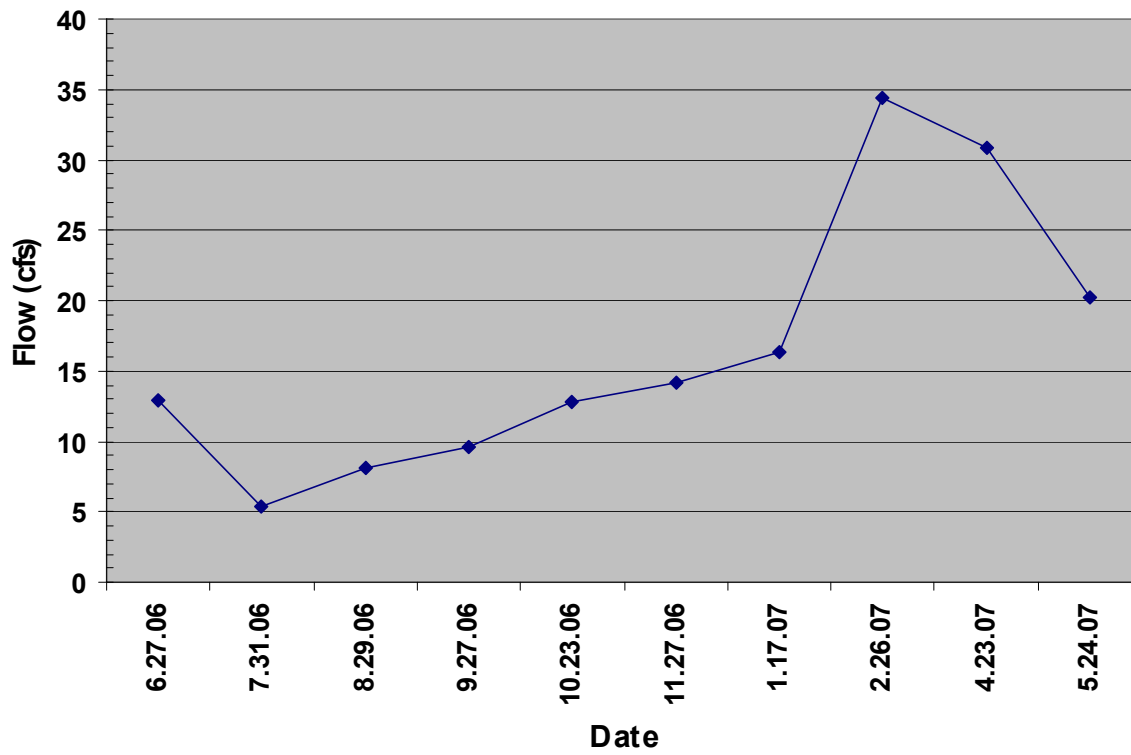


**West Drain**

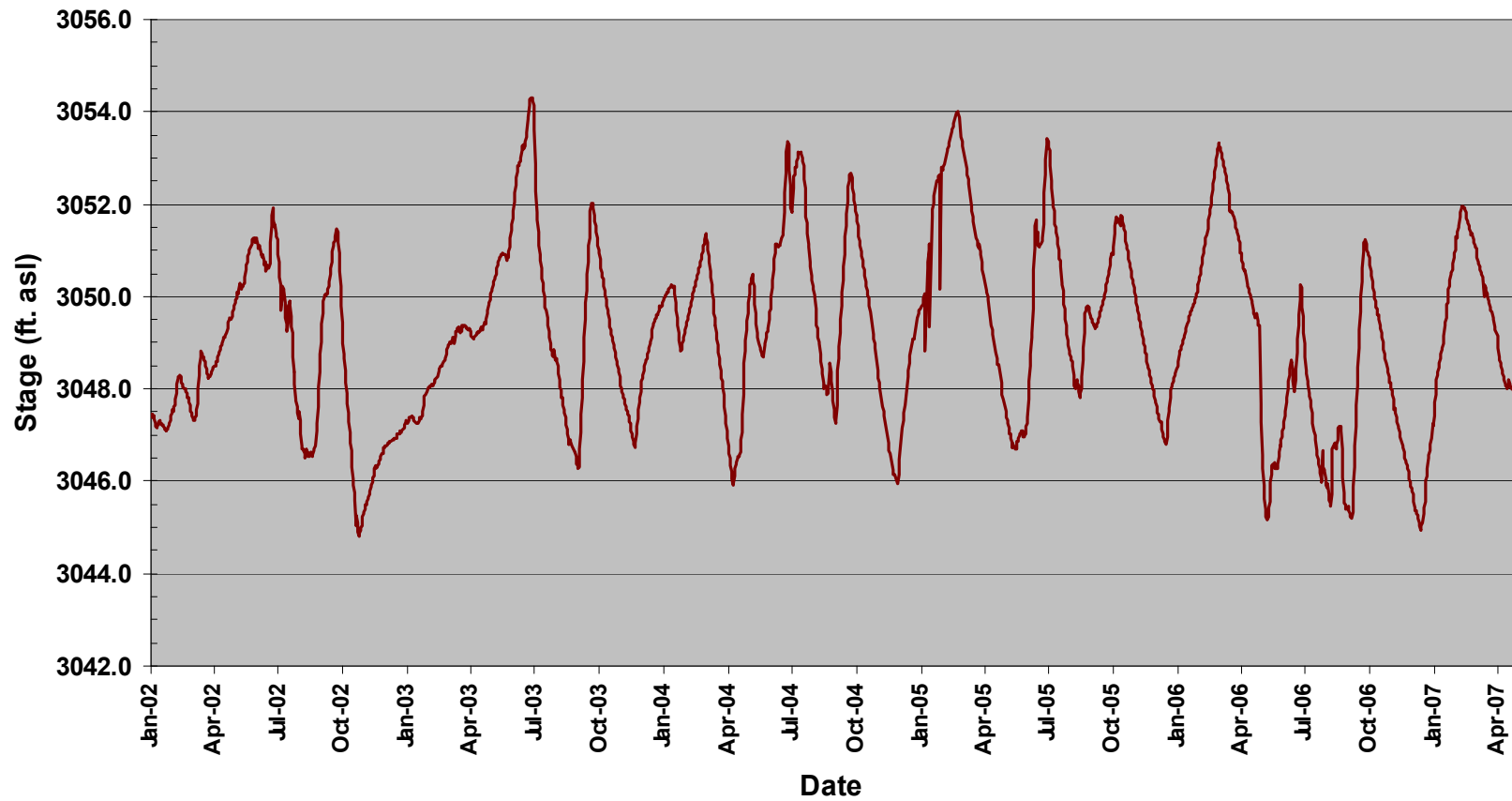




## Fremont Slough



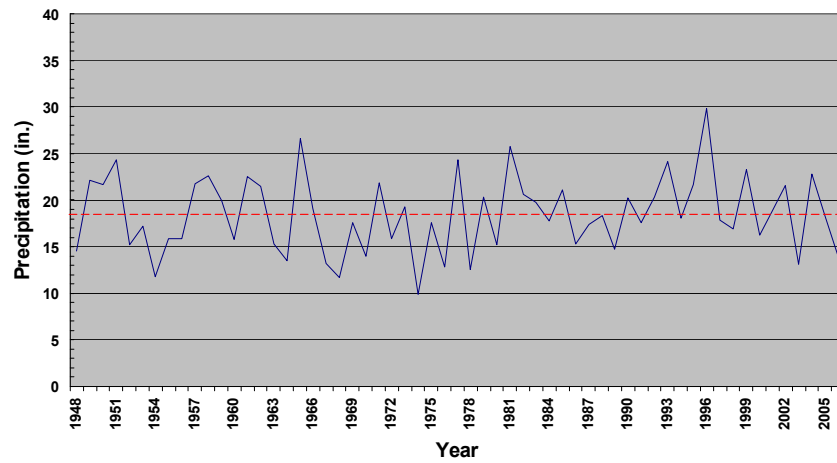
**Sutherland Reservoir Stage January 1, 2002 to May 1, 2007**



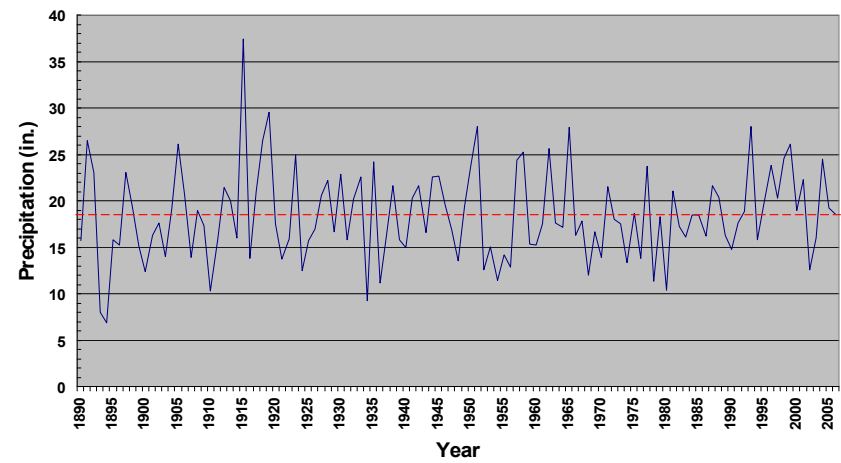
## **APPENDIX B**

***Precipitation records for all stations used to create interpolated map  
of average annual precipitation that served as basis for recharge  
multiplier array***

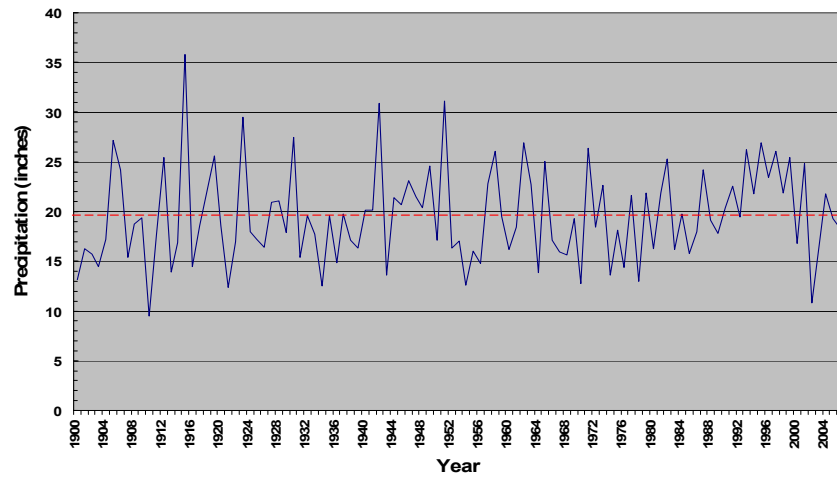
**Ogallala 1948-2006**



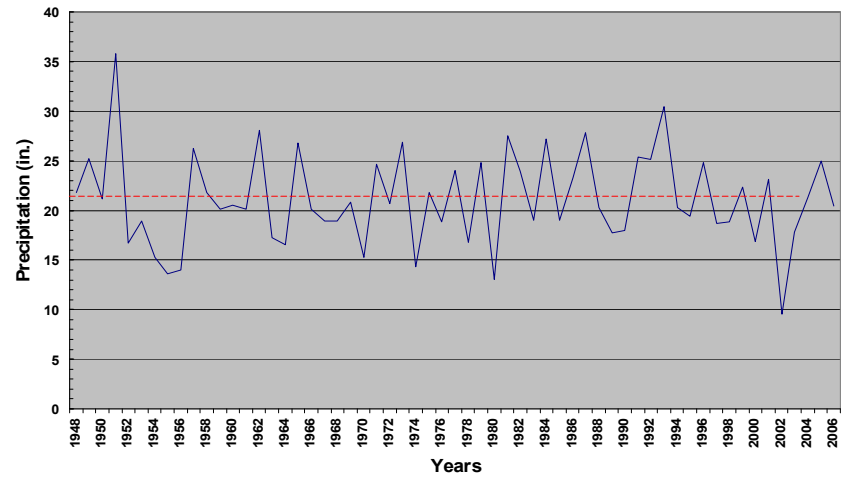
**Paxton 1890-2006**



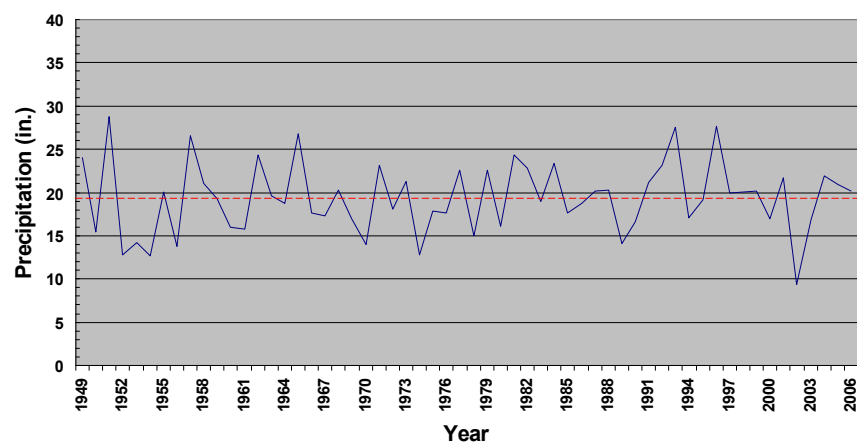
**Madrid 1900-2006**



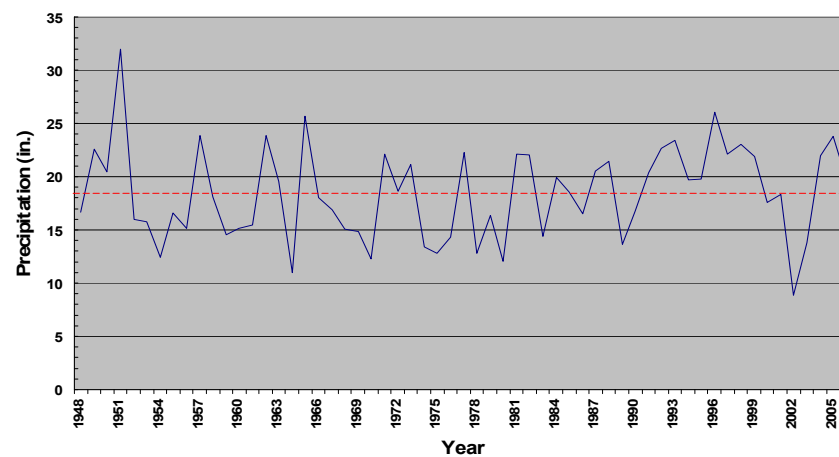
**Wellfleet 1948-2006**



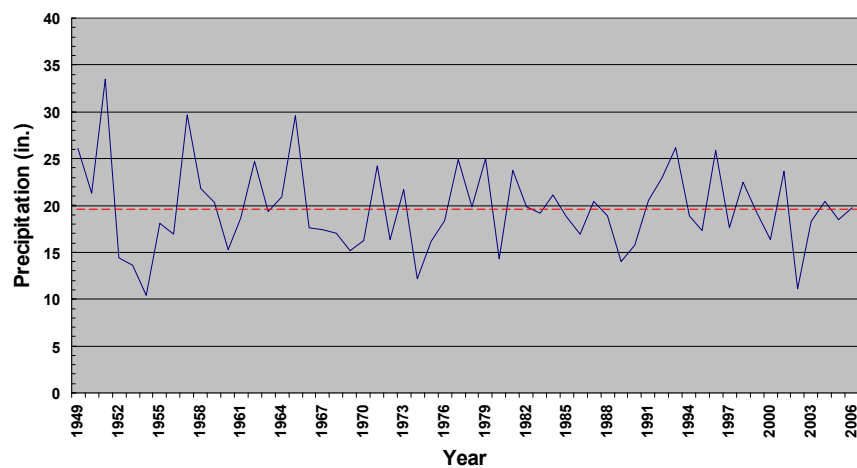
**North Platte Experimental Farm 1949-2006**



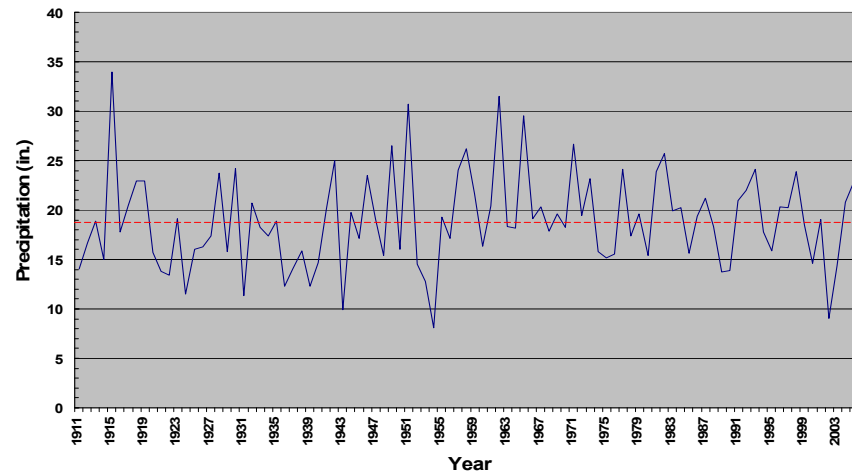
**Wallace 1948-2006**

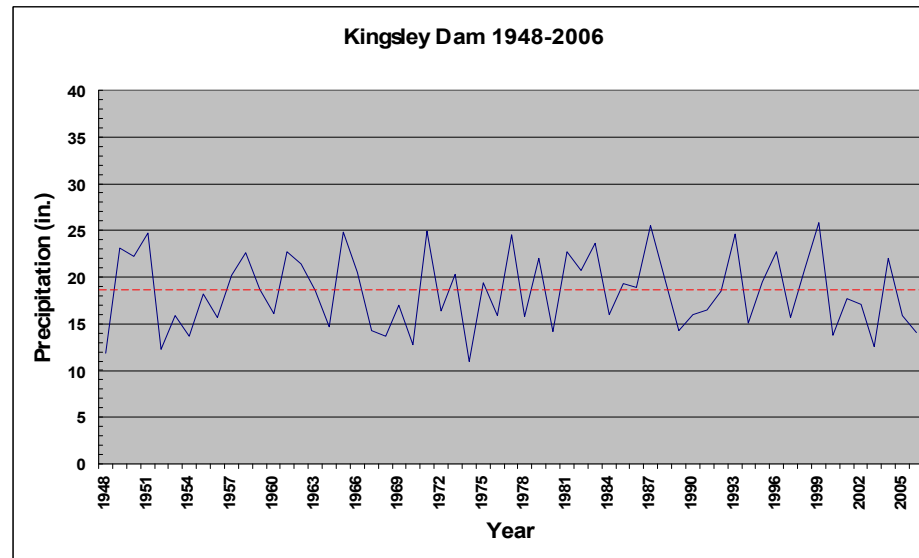


**North Platte Airport 1949-2006**



**Hershey 1911-2006**







## **APPENDIX C**

***Weights for surface flow and flowpath age observations***

		1	2	3
Model Observation Name		Observed flow		STATISTIC
			first term % of flow in column 1	standard deviation used in UCODE_2005 (% of flow in column 2)/1.96
		(cu ft/d)	(cu ft/d)	(cu ft/d)
Beer Slough	beer1	-474336.0	95% Certain flow is within 30% of measured -142300.8	-72602.4
	beer2	-167616.0	95% Certain flow is within 50% of measured -83808.0	-42759.2
	beer3	-382752.0	95% Certain flow is within 30% of measured -114825.6	-58584.5
	beer4	-412128.0	95% Certain flow is within 30% of measured -123638.4	-63080.8
	beer5	-526176.0	95% Certain flow is within 30% of measured -157852.8	-80537.1
	beer6	-628992.0	95% Certain flow is within 30% of measured -188697.6	-96274.3
Applegate Drain	apple1	-2877120.0	95% Certain flow is within 30% of measured -863136.0	-440375.5
	apple2	-2211840.0	95% Certain flow is within 30% of measured -663552.0	-338546.9
	apple3	-2289600.0	95% Certain flow is within 30% of measured -686880.0	-350449.0
	apple4	-3049920.0	95% Certain flow is within 30% of measured -914976.0	-466824.5

apple5	-3127680.0	95% Certain flow is within 30% of measured -938304.0	-478726.5
apple6	-2980800.0	95% Certain flow is within 30% of measured -894240.0	-456244.9
apple7	-2894400.0	95% Certain flow is within 30% of measured -868320.0	-443020.4
apple8	-2868480.0	95% Certain flow is within 30% of measured -860544.0	-439053.1
apple9	-2946240.0	95% Certain flow is within 30% of measured -883872.0	-450955.1
apple10	-2885760.0	95% Certain flow is within 30% of measured -865728.0	-441698.0
apple11	-2954880.0	95% Certain flow is within 30% of measured -886464.0	-452277.6
app12	-2825280.0	95% Certain flow is within 30% of measured -847584.0	-432440.8
apple13	-2842560.0	95% Certain flow is within 30% of measured -852768.0	-435085.7
apple14	-2445120.0	95% Certain flow is within 30% of measured -733536.0	-374253.1
apple15	-2116800.0	95% Certain flow is within 30% of measured -635040.0	-324000.0
apple16	-2358720.0	95% Certain flow is within 30% of measured -707616.0	-361028.6
apple17	-2410560.0	95% Certain flow is within 30% of measured -723168.0	-368963.3

<b>Hershey Slough</b>	apple18	-2419200.0	95% Certain flow is within 30% of measured -725760.0	-370285.7
	apple19	-2531520.0	95% Certain flow is within 30% of measured -759456.0	-387477.6
	hrshy1	-726624.0	95% Certain flow is within 30% of measured -217987.2	-111218.0
	hrshy2	-423360.0	95% Certain flow is within 30% of measured -127008.0	-64800.0
	hrshy3	-547776.0	95% Certain flow is within 30% of measured -164332.8	-83843.3
	hrshy4	-608256.0	95% Certain flow is within 30% of measured -182476.8	-93100.4
	hrshy5	-950400.0	95% Certain flow is within 30% of measured -285120.0	-145469.4
	hrshy6	-802656.0	95% Certain flow is within 30% of measured -240796.8	-122855.5
	west1	-69120.0	95% Certain flow is within 50% of measured -34560.0	-17632.7
	west2	-23328.0	95% Certain flow is within 50% of measured -11664.0	-5951.0
<b>West Drain</b>	west3	-35424.0	95% Certain flow is within 50% of measured -17712.0	-9036.7
	west4	-50112.0	95% Certain flow is within 50% of measured -25056.0	-12783.7

<b>Fremont Slough</b>	west5	-31104.0	95% Certain flow is within 50% of measured -15552.0	-7934.7
	west6	-72576.0	95% Certain flow is within 50% of measured -36288.0	-18514.3
	frmnt1	-1114560.0	95% Certain flow is within 30% of measured -334368.0	-170595.9
	frmnt2	-465696.0	95% Certain flow is within 50% of measured -232848.0	-118800.0
	frmnt3	-696384.0	95% Certain flow is within 40% of measured -278553.6	-142119.2
	frmnt4	-825120.0	95% Certain flow is within 30% of measured -247536.0	-126293.9
	frmnt5	-1105920.0	95% Certain flow is within 30% of measured -331776.0	-169273.5
	frmnt6	-1226880.0	95% Certain flow is within 30% of measured -368064.0	-187787.8
	frmnt7	-1416960.0	95% Certain flow is within 30% of measured -425088.0	-216881.6
	upperplt1	-1196640.0	95% Certain flow is within 30% of measured -358992.0	-183159.2
	upperplt2	-1130976.0	95% Certain flow is within 30% of measured -339292.8	-173108.6
	upperplt3	-1767744.0	95% Certain flow is within 30% of measured -530323.2	-270573.1
	upperplt4	-1372032.0	95% Certain flow is within 30% of measured -411609.6	-210004.9
<b>South Platte Reaches</b>				

upperplt5	-747360.0	95% Certain flow is within 30% of measured -224208.0	-114391.8
upperplt6	-713664.0	95% Certain flow is within 30% of measured -214099.2	-109234.3
upperplt7	-5944320.0	95% Certain flow is within 40% of measured -1783296.0	-909844.9
lwrplt1	-3008448.0	95% Certain flow is within 40% of measured -1203379.2	-613969.0
lwrplt2	-2963520.0	95% Certain flow is within 40% of measured -1185408.0	-604800.0
lwrplt3	-2801952.0	95% Certain flow is within 40% of measured -1120780.8	-571826.9
lwrplt4	-5201280.0	95% Certain flow is within 40% of measured -2080512.0	-1061485.7

**Flowpath age +/- % certainty and calculated standard deviations (s)  
(weight = 1/(standard deviation)<sup>2</sup>)**

MW2sh 9.1 yrs, 95% certain +/- 1.56 yrs	1.56 yrs = 572 d. s = 572 d./1.96 = 292 d
*MW3mid 29 yrs, 90% certain +/- 15 yrs	15 yrs = 5475 d. s = 5475 d./1.64 = 3338 d
MW4sh 2.2 yrs, 95% certain +/- 3 yrs	3 yrs = 1074 d. s = 1074 d./1.96 = 548 d
MW5sh 2.2 yrs, 95% certain +/- 2.6 yrs	2.6 yrs = 964 d. s = 964 d./1.96 = 492 d
MW6sh 13.8 yrs, 95% certain +/- 3.8 yrs	3.8 yrs = 1378 d. s = 1378 d./1.96 = 703 d
MW8sh 4.1 yrs, 95% certain +/- 7.1 yrs	7.1 yrs = 2575 d. s = 2575 d./1.96 = 1314 d

\*For MW3mid, a 90% confidence interval was declared due to the potential for mixing in this area of the aquifer.

Site Name	Apparent Age (yrs)	Precision (yrs)	
MW-1 shallow	>50		
MW-1 deep	>50		
MW-2 shallow	9.1	0.4	The range of ages for confidence intervals initially were based on precision listed to the right. The values were increased for each of the wells due to uncertainty beyond the laboratory precision, such as the sighting of screened intervals in wells in mixing zones where the age of the sample could be altered from the specified age of the seeped reservoir water.
MW-2 deep	>50		
MW-3 shallow	24.7	0.4	
MW-3 middle	29.5	1.2	
MW-3 deep	>50		
MW-4 shallow	2.2	1.0	
MW-4 deep	>50		
MW-5 shallow	2.1	0.9	
MW-5 middle	36.3	0.7	
MW-5 deep	31.0	1.4	
MW-6 shallow	13.8	1.1	
MW-6 deep	>50		
MW-8 shallow	4.1	1.8	
MW-8 deep	> 50		



## **APPENDIX D**

*Well field construction information including well performance test design and resulting transmissivity values and well construction specifications provided by Hemenway Groundwater Engineering, Inc.*

Appendix D Table 1. Results from 24 hour pumping and recovery tests with average transmissivity for each well.

<b>Well Number</b>	<b>24 hr Pumping Test Transmissivity 1 (gpd/ft)</b>	<b>24 hr Pumping Test Transmissivity 2 (gpd/ft)</b>	<b>24hr Test Recovery Transmissivity 1 (gpd/ft)</b>	<b>24hr Test Recovery Transmissivity 2 (gpd/ft)</b>	<b>Average Transmissivity (gpd/ft)</b>
OW-1	92,400		123,200		107,800
OW-2	158,400		132,000		145,200
OW-3	50,769		44,000		47,385
OW-4	105,600		88,000	121,846	105,149
OW-5	79,200		72,000		75,600
OW-6	88,000		NA		88,000
OW-7	99,000		60,923		79,962
OW-8	56,571	99,000	49,500	99,000	76,018
OW-9	47,143	73,333	44,000		54,825
OW-10	127,600		127,600		127,600
OW-11	259,600		222,514		241,057
OW-12	132,000		158,400		145,200
OW-13	316,800		316,800		316,800
OW-14	99,000	99,000	158,400		118,800
OW-15	145,200		96,800		121,000
OW-16	66,000		36,414		51,207
OW-18	99,000		105,600		102,300
OW-19	82,500		110,000		96,250
OW-20	91,384	118,000	237,600		148,995
OW-21	99,000		121,846		110,423
OW-22	67,200		67,200		67,200
OW-23	99,000		121,846		110,423
OW-24	52,800		56,571		54,686
OW-25	83,368		88,000	132,000	101,123
OW-26	73,333		88,000		80,667
OW-27	77,647		82,500	132,000	97,382
OW-28	132,000		99,000		115,500
OW-29	49,280		147,840		98,560
OW-30	176,000		176,000		176,000
OW-31	110,000		120,000		115,000
OW-33	42,240		58,666	40,615	47,174
OW-34	110,000		120,000		115,000
OW-35	123,200		73,920		98,560
OW-36	40,615		34,435		37,525
OW-37	83,368		66,000	158,400	102,589
OW-38	113,143		158,400		135,772
OW-39	316,800		176,000		246,400
OW-40	396,000		226,285		311,143

Appendix D Table 2. Specifications for well performance tests at each well during construction of the GGS well field.

Well	Bailing	Pump Development	Step Test	Step Test Rates	Step Test Length	Constant- Rate Test Start Date	Constant- Rate Test (gpm)	Static Water Level (feet)	Pumping Water @24hrs (feet)	Drawdown at 24 Hours (feet)	Specific Capacity (gpm/ft)	Length of Constant- Rate (hours)	Length of Recovery (hours)
Number	(Hours)	(Hours)	Date	(gpm)	(hours)	Date	(gpm)	(feet)	(feet)	(feet)	(gpm/ft)	(hours)	(hours)
OW-1	1	3	6/14/2004	1800/2500/3000	3.5	6/15/2004	2500	80.96	145.54	64.58	38.7	19	24
OW-2	1	1	6/13/2004	2000/2500/3000	3.5	6/14/2004	3000	68.3	131.65	63.35	47.4	24	24
OW-3	1	3	6/12/2004	1750/2250/2750	3.5	6/13/2004	2500	56.1	154.45	98.35	25.4	12	24
OW-4	1	2	6/11/2004	1800/2600/3000	3.5	6/12/2004	3000	44.90	112.71	67.81	44.2	24	24
OW-5	1	1	6/22/2004	1900/2500/3000	3.5	6/23/2004	3000	27.1	128.36	101.26	29.6	24	24
OW-6	1	3	6/6/2004	2000/2500/3000	3.5	6/7/2004	3000	44.97	123.13	78.16	38.4	24	24
OW-7	1	3	5/16/2004	2000/2500/3000	3.5	5/17/2004	3000	32.68	126.3	93.62	32.0	24	24
OW-8	1	3	5/15/2004	2000/2500/3000	3.5	5/16/2004	3000	43.71	177.44	133.73	22.4	24	24
OW-9	1	3	5/12/2004	1500/2000/2500	3.5	5/13/2004	2500	52.85	198.39	145.54	17.2	24	24
OW-10	1	2	5/21/2004	2000/2500/2900	3.5	5/22/2004	2900	93.15	136.875	43.73	66.3	21.1	24
OW-11	1	3	6/10/2004	2000/2500/2950	3.5	6/11/2004	2800	97.15	138.91	41.76	67.0	24	24
OW-12	1	3	6/9/2004	2000/2500/3000	3.5	6/10/2004	2800	108.15	167.45	59.30	47.2	24	24
OW-13	1	3	6/8/2004	1800/2500/3000	3.5	6/9/2004	3000	123.72	157.8	34.08	88.0	24	24
OW-14	1	3	5/25/2004	2000/2500/3000	3.5	5/26/2004	3000	78.97	144.07	65.10	46.1	24	24
OW-15	1	3	5/19/2004	1750/2250/2750	3.5	5/20/2004	2750	72.20	151.07	78.87	34.9	24	24
OW-16	1	3	6/5/2004	1000/1600/2200	3.5	6/8/2004	2000	83.60	230.64	147.04	13.6	24	24
OW-18	1	3	5/26/2004	2000/2500/3000	3.5	5/27/2004	3000	89.81	148.78	58.97	50.9	24	24
OW-19	1	3	6/3/2004	1600/2200/2800	3.5	6/4/2004	2500	108.97	181.75	72.78	34.4	24	24
OW-20	1	3	4/30/2004	1750/2000/2250	3.5	4/30/2004	2250	89.30	141.63	52.33	43.0	23	23
OW-21	1	3	5/7/2004	2000/2500/3000	3.5	5/10/2004	3000	62.40	124.09	61.69	48.6	24	24
OW-22	1	3	5/13/2004	1600/2200/2800	3.5	5/14/2004	2800	51.51	119.74	68.23	41.0	24	24
OW-23	1	3	5/4/2004	2000/2500/3000	3.5	5/5/2004	3000	30.83	91.94	61.11	49.1	24	24
OW-24	1	1	6/21/2004	2000/2500/3000	3.5	6/21/2004	3000	71.32	117.89	46.57	64.4	24	24
OW-25	1	3	6/4/2004	2000/2500/3000	3.5	6/5/2004	3000	42.85	128.96	86.11	34.8	21	24
OW-26	1	3	5/22/2004	1500/2000/2500	3.5	5/23/2004	2400	132.18	221.27	89.09	26.9	24	24
OW-27	1	3	5/2/2004	1750/2000/2500	3.5	5/3/2004	2500	91.55	170.62	79.07	31.6	24	24
OW-28	1	3	6/2/2004	1500/2000/2400	3.5	6/3/2004	2250	108.49	188.22	79.73	28.2	24	24
OW-29	3	3	5/17/2004	2000/2500/2900	3.5	5/18/2004	2800	132.34	204.93	72.59	38.6	24	24
OW-30	1	3	5/19/2004	2000/2500/3000	3.5	5/22/2004	3000	115.03	172.551	57.52	52.2	24	24
OW-31	1	3	5/25/2004	1500/2000/2500	3.5	5/25/2004	2250	116.12	204.43	88.31	25.5	24	24

Well	Bailing	Pump Development	Step Test	Step Test Rates	Step Test Length	Constant- Rate Test Start Date	Constant- Rate Test (gpm)	Static Water Level (feet)	Pumping Water @24hrs (feet)	Drawdown at 24 Hours (feet)	Specific Capacity (gpm/ft)	Length of Constant- Rate (hours)	Length of Recovery (hours)
Number	(Hours)	(Hours)	Date	(gpm)	(hours)	Date	(gpm)	(feet)	(feet)	(feet)	(gpm/ft)	(hours)	(hours)
OW-33	1	2	6/25/2004	1500/2000/2500	3.5	6/26/2004	2000	64.58	220.73	156.15	12.8	24	24
OW-34	1	2	6/25/2004	1800/2300/2800	3.5	6/25/2004	2500	126.87	182.63	55.76	44.8	16	24
OW-35	1	1	6/20/2004	2000/2500/2950	3.5	6/20/2004	2800	50.52	168.51	117.99	23.7	12	24
OW-36	1	1	6/23/2004	1900/2500/3000	3.5	6/24/2004	3000	24.37	195.63	171.26	17.5	24	24
OW-37	1	1	6/19/2004	2000/2500/2850	3.5	6/19/2004	2500	45.11	175.37	130.26	19.2	24	24
OW-38	1	1	6/18/2004	1950/2500/3000	3.5	6/18/2004	3000	53.3	109.88	56.58	53.0	24	24
OW-39	1	1	6/16/2004	2000/2500/3000	3.5	6/17/2004	3000	40.3	81.87	41.57	72.2	24	24
OW-40	1	1	6/15/2004	2000/2500/3000	3.5	6/16/2004	3000	31.6	74.375	42.78	70.1	24	24

Appendix D Table 3. Kh determined from two methods of estimating transmissivity values at each well during the construction of the well field. The average Kh values were used to interpolate a variable Kh dataset to the GGS model grids to test the conceptualization of variable Kh versus uniform values of Kh applied to model layers. Note that the transmissivity values (T) were converted from gallons per day/ft to ft<sup>2</sup> per day. Source: Hemenway Groundwater Engineering, Inc.

T from drawdown during pumping				T from recovery data				Average Kh (ft/d) from two methods
Well	T (sq.ft/d)	Sat Thk	Kh	Well	T (sq.ft/d)	Sat Thk	Kh	
OW-1	7,620.3	335.0	22.7	OW-1	14,411.8	335.0	43.0	32.9
OW-2	8,689.8	335.0	25.9	OW-2	19,411.8	335.0	57.9	41.9
OW-3	4,211.2	329.0	12.8	OW-3	6,334.8	329.0	19.3	16.0
OW-4	7,754.0	338.0	22.9	OW-4	14,057.3	338.0	41.6	32.3
OW-5	5,280.7	343.0	15.4	OW-5	10,107.0	343.0	29.5	22.4
OW-6	6,550.8	328.0	20.0	OW-6	11,764.7	328.0	35.9	27.9
OW-7	5,748.7	340.0	16.9	OW-7	10,690.0	340.0	31.4	24.2
OW-8	3,917.1	334.0	11.7	OW-8	10,162.8	334.0	30.4	21.1
OW-9	2,927.8	333.0	8.8	OW-9	7,329.6	333.0	22.0	15.4
OW-10	12,032.1	327.0	36.8	OW-10	17,058.8	327.0	52.2	44.5
OW-11	12,139.0	321.0	37.8	OW-11	32,226.9	321.0	100.4	69.1
OW-12	8,917.1	319.0	28.0	OW-12	19,411.8	319.0	60.9	44.4
OW-13	16,310.2	317.0	51.5	OW-13	42,352.9	317.0	133.6	92.5
OW-14	8,021.4	325.0	24.7	OW-14	15,882.4	325.0	48.9	36.8
OW-15	5,929.1	334.0	17.8	OW-15	16,176.5	334.0	48.4	33.1
OW-16	2,259.4	332.0	6.8	OW-16	6,845.9	332.0	20.6	13.7
OW-18	8,970.6	334.0	26.9	OW-18	13,676.5	334.0	40.9	33.9
OW-19	6,243.3	333.0	18.7	OW-19	12,867.6	333.0	38.6	28.7
OW-20	7,954.5	337.0	23.6	OW-20	19,919.1	337.0	59.1	41.4
OW-21	8,542.8	337.0	25.3	OW-21	14,762.4	337.0	43.8	34.6
OW-22	7,098.9	342.0	20.8	OW-22	8,984.0	342.0	26.3	23.5
OW-23	8,636.4	344.0	25.1	OW-23	14,762.4	344.0	42.9	34.0
OW-24	11,631.0	340.0	34.2	OW-24	7,310.9	340.0	21.5	27.9
OW-25	6,336.9	340.0	18.6	OW-25	13,519.1	340.0	39.8	29.2
OW-26	4,786.1	336.0	14.2	OW-26	10,784.3	336.0	32.1	23.2
OW-27	5,320.9	337.0	15.8	OW-27	13,019.0	337.0	38.6	27.2
OW-28	5,026.7	337.0	14.9	OW-28	15,441.2	337.0	45.8	30.4
OW-29	6,631.0	336.0	19.7	OW-29	13,176.5	336.0	39.2	29.5
OW-30	9,238.0	336.0	27.5	OW-30	23,529.4	336.0	70.0	48.8
OW-31	4,197.9	335.0	12.5	OW-31	15,374.3	335.0	45.9	29.2
OW-33	2,112.3	337.0	6.3	OW-33	6,306.6	337.0	18.7	12.5
OW-34	8,034.8	336.0	23.9	OW-34	15,374.3	336.0	45.8	34.8
OW-35	3,883.7	341.0	11.4	OW-35	13,176.5	341.0	38.6	25.0
OW-36	2,981.3	345.0	8.6	OW-36	5,016.7	345.0	14.5	11.6
OW-37	3,070.9	343.0	9.0	OW-37	13,715.2	343.0	40.0	24.5
OW-38	9,385.0	336.0	27.9	OW-38	18,151.3	336.0	54.0	41.0
OW-39	13,155.1	341.0	38.6	OW-39	32,941.2	341.0	96.6	67.6
OW-40	12,754.0	329.0	38.8	OW-40	41,596.6	329.0	126.4	82.6
AVERAGE			21.7				47.2	34.4

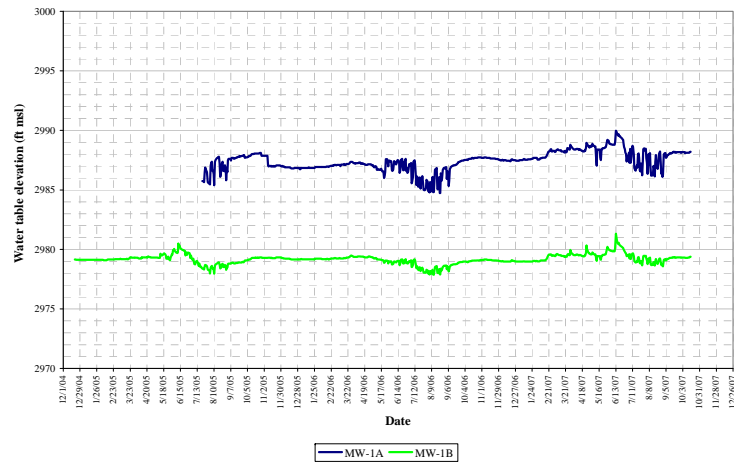
## **APPENDIX E**

*Hydrographs for NPPD observation well nests in the near-site area of the GGS well field not shown in the main body of the report. Nest locations are shown in Figure 16.*

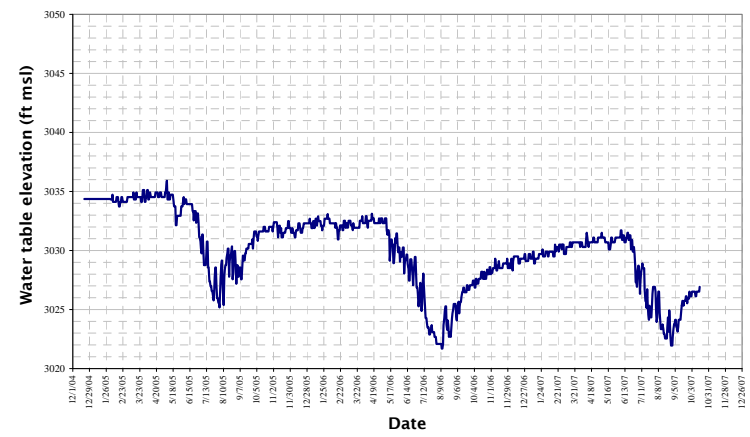
*Hydrographs include the summer pumping seasons of 2005, 2006, and 2007.*

*Observed water levels presented in these charts provided transient water level observations used in the model optimizations. No chart is shown for the Obs-2 nest location as the continuous-measurement equipment provided erroneous data during the 2005 pumping season.*

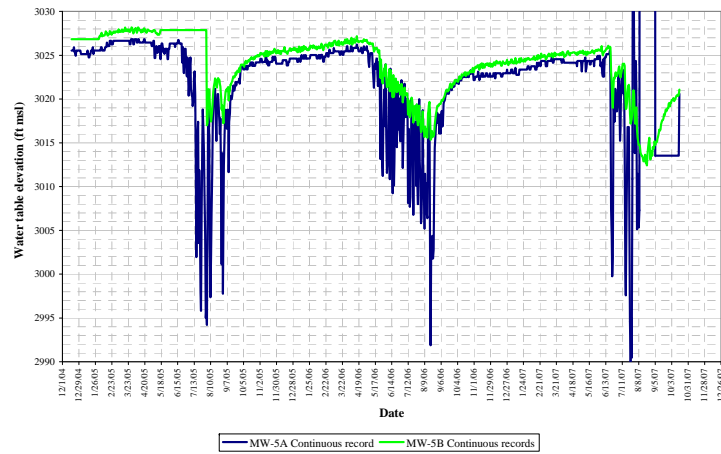
Obs-1



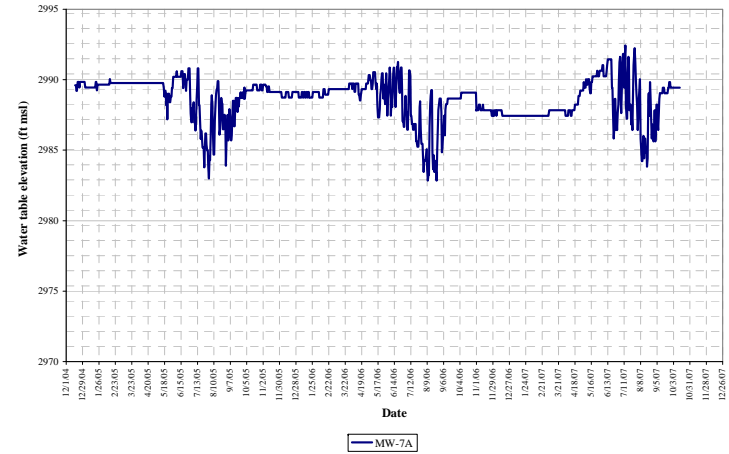
Obs-3



Obs-5



Obs-7



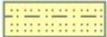


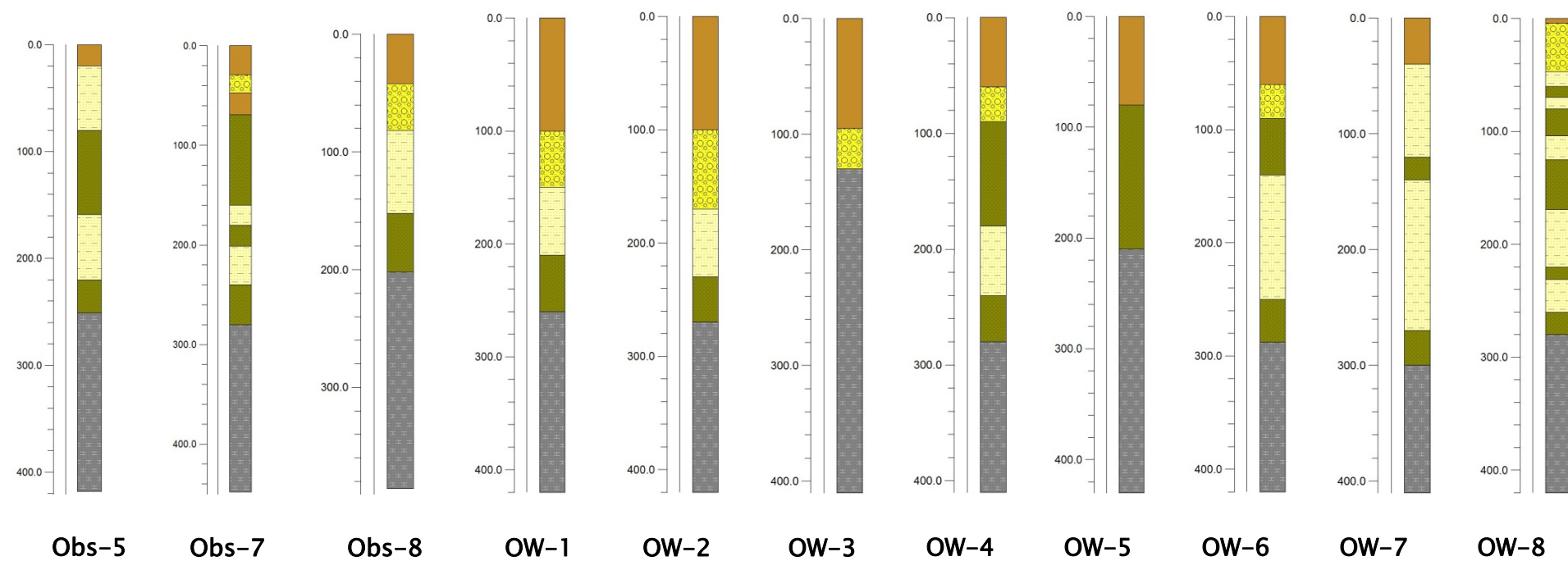
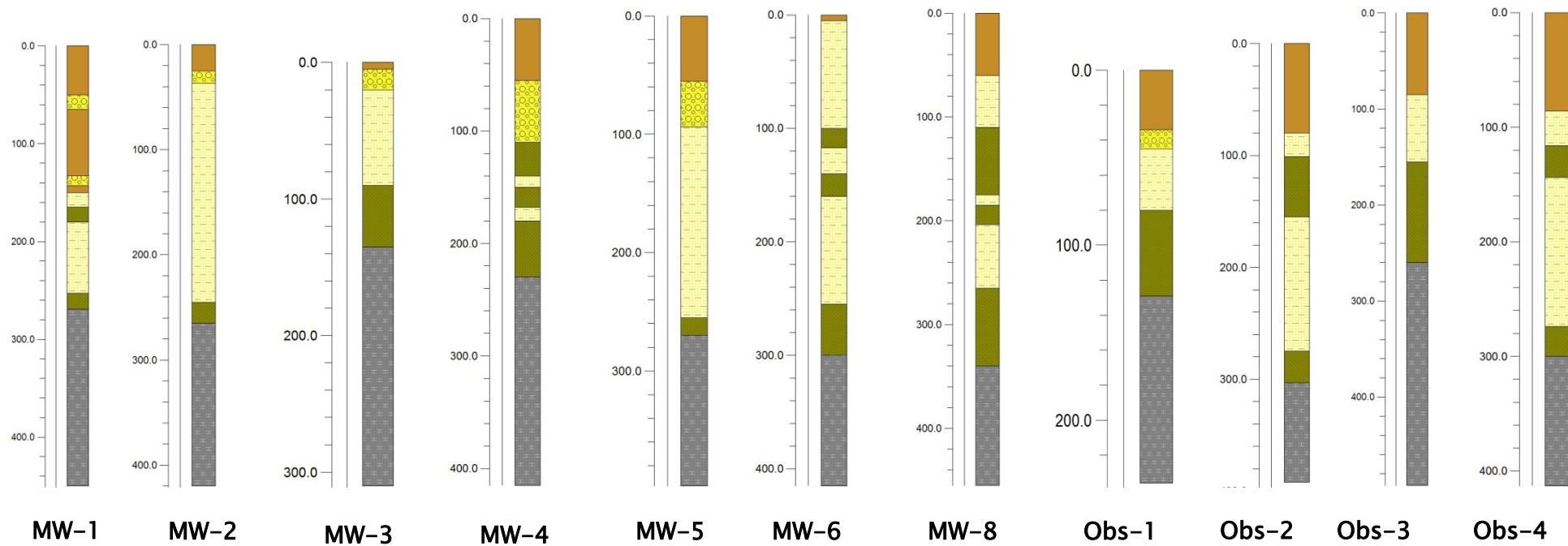


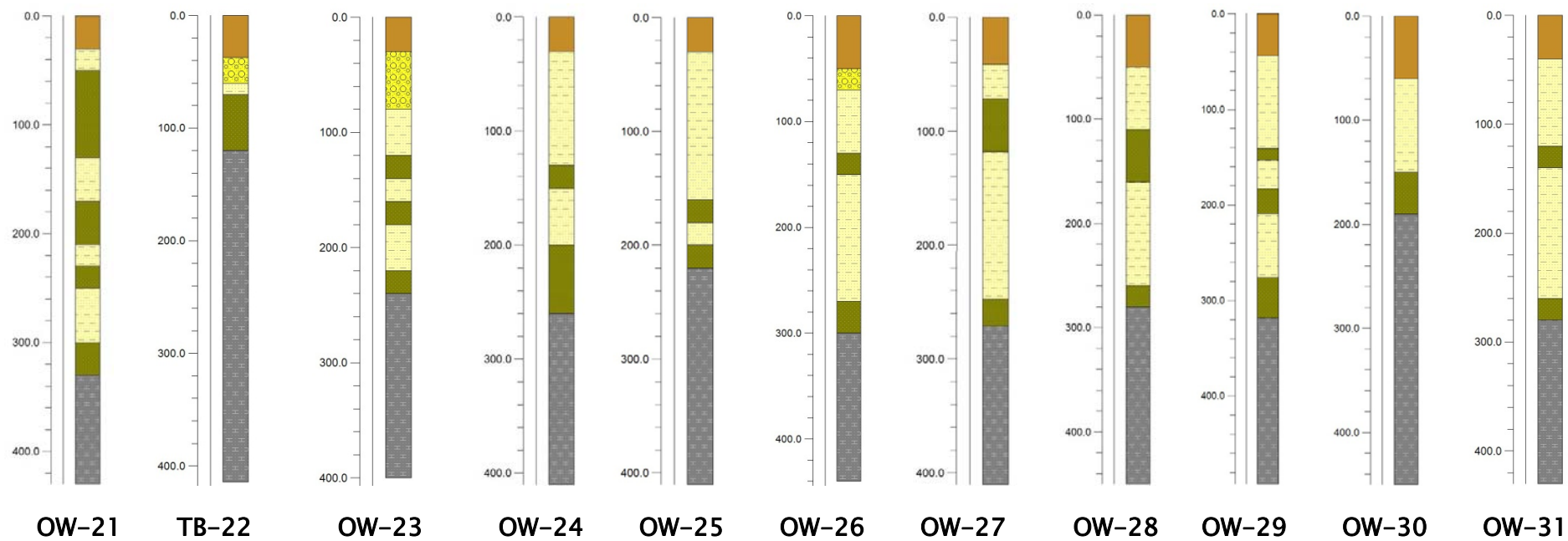
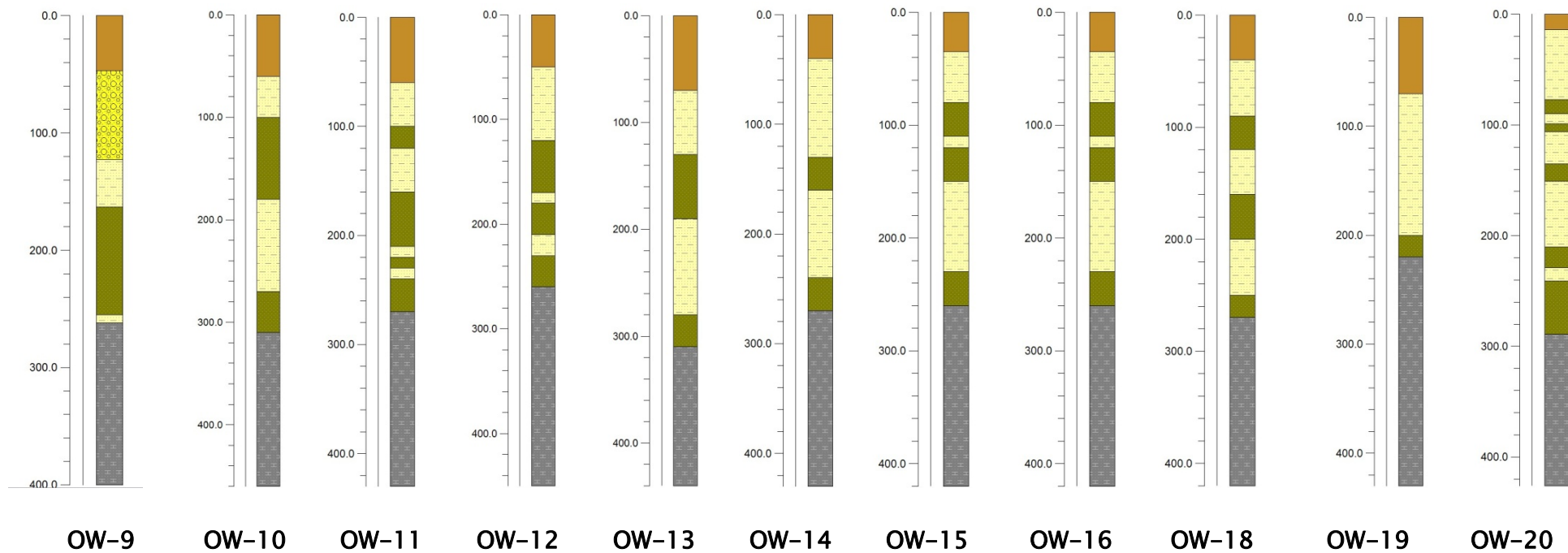
**APPENDIX F**

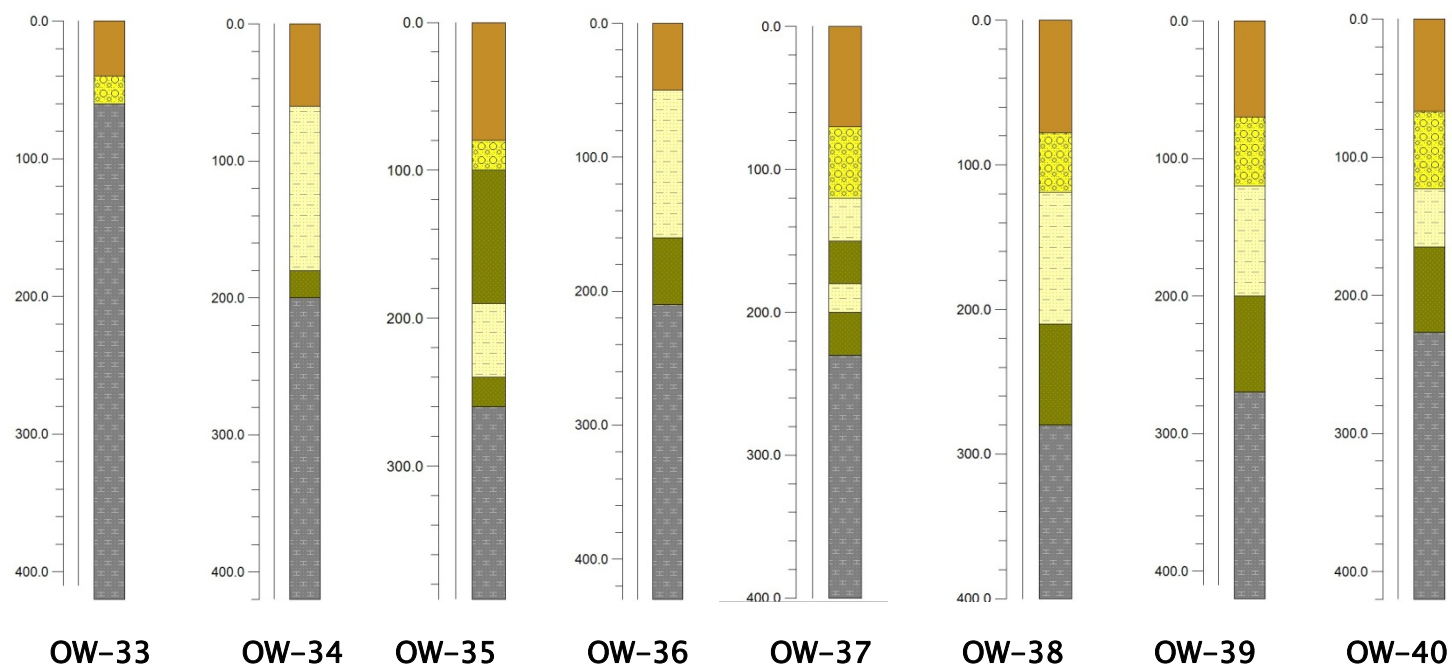
*Geologic borehole diagrams of all GGS well field test holes showing elevations based on the 5 hydrostratigraphic zones defined in the Geologic Data section*

**Pattern Key**

				
Quaternary Fines	Quaternary Coarse	Tertiary Fines	Tertiary Coarse	Tertiary Basal Fines







### Pattern Key



## **APPENDIX G**

***Complete list of optimized model rankings based on the AICc criteria***

Model	AICc	$\Delta_i$	Probability	Evidence Ratio	SOSWR	No. Parameters
CM-23	7,562.2	0.0	0.999	1.0	48,318	10
CM-25	7578.5	16.3	$2.843 \times 10^{-4}$	$3.5 \times 10^3$	48,626	11
CM-18	7579.3	17.2	$1.885 \times 10^{-4}$	$5.3 \times 10^3$	48,641	10
CM-2	7583.2	21.0	$2.798 \times 10^{-5}$	$3.6 \times 10^4$	48,790	8
CM-31	7584.7	22.5	$1.328 \times 10^{-5}$	$7.5 \times 10^4$	48,742	13
CM-3	7585.6	23.4	$8.235 \times 10^{-6}$	$1.2 \times 10^5$	48,837	8
CM-19	7588.1	25.9	$2.394 \times 10^{-6}$	$4.2 \times 10^5$	48,769	11
CM-10	7588.9	26.7	$1.575 \times 10^{-6}$	$6.3 \times 10^5$	48,823	11
CM-24	7595.4	33.3	$5.925 \times 10^{-8}$	$1.7 \times 10^7$	49,024	8
CM-27s	7612.8	50.6	$1.037 \times 10^{-11}$	$9.6 \times 10^{10}$	49,278	11
CM-7	7,630.5	68.28	$1.13 \times 10^{-13}$	$6.6980 \times 10^{14}$	49,619	10
CM-6	7,646.1	83.91	$4.57 \times 10^{-17}$	$1.6625 \times 10^{18}$	49,961	9
CM-26	7,678.0	115.8	5.48E-24	$1.3852 \times 10^{25}$	50,544	10
CM-9	7,679.2	117.0	$2.92 \times 10^{-24}$	$2.6000 \times 10^{25}$	50,648	8
CM-21	7,680.3	118.1	$1.75 \times 10^{-24}$	$4.3314 \times 10^{25}$	50,708	7
CM-5	7,684.7	122.5	$1.93 \times 10^{-25}$	$3.9306 \times 10^{26}$	50,795	7
CM-17	7,701.4	139.2	$4.59 \times 10^{-29}$	$1.6534 \times 10^{30}$	51,046	9
CM-1	7,707.1	144.9	$2.58 \times 10^{-30}$	$2.9480 \times 10^{31}$	51,281	6
CM-13	7,722.3	160.1	$1.29 \times 10^{-33}$	$5.8835 \times 10^{34}$	51,505	8
CM-34	7,782.9	220.7	$9.14 \times 10^{-47}$	$8.3130 \times 10^{47}$	52,443	15
CM-27	7,860.5	298.3	$1.28 \times 10^{-63}$	$5.9207 \times 10^{64}$	54,222	11
CM-29	7,945.1	382.9	0.0	$1.4269 \times 10^{83}$	56,169	8
CM-32	7,957.0	394.8	0.0	$5.3408 \times 10^{85}$	56,252	12
CM-28	8,029.7	467.5	0.0	$3.2860 \times 10^{101}$	58,139	6
CM-30	8,275.3	713.1	0.0	$7.06 \times 10^{154}$	63,869	8
CM-35	8,703.4	1,411.1	0.0	$6.3598 \times 10^{247}$	75,504	7
CM-16s	8,840.5	1,278.3	0.0	$3.8127 \times 10^{277}$	79,393	11
CM-12	8,842.9	1,280.7	0.0	$1.2755 \times 10^{278}$	79,530	10

CM-7fkh	8,864.6	1,302.3	0.0	$6.4112 \times 10^{282}$	80,329	8
CM-11	8,897.5	1,335.3	0.0	$9.1689 \times 10^{289}$	81,174	11
CM-15	9,100.9	1,538.7	0.0	0.0	87,857	11
CM-14	9,659.9	2,097.7	0.0	0.0	109,290	10
CM-36	9,963.5	2,401.3	0.0	0.0	123,380	6
CM-33	10,055.5	2,493.3	0.0	0.0	127,180	13
CM-16	12,239.3	4,677.1	0.0	0.0	298,180	10
CM-20	15,273.8	7,711.6	0.0	0.0	970,330	11
CM-19fkh	21,974.6	14,412.3	0.0	0.0	1.32E+07	7